Alma Mater Studiorum – Università di Bologna

DOTTORATO DI RICERCA IN

BIODIVERSITA' ED EVOLUZIONE

Ciclo XXVIII

Settore Concorsuale di afferenza: 05/B1 – ZOOLOGIA E ANTROPOLOGIA (Prevalente)

Settore Scientifico disciplinare: BIO/05 – ZOOLOGIA (Prevalente)

Settore Concorsuale di afferenza: 05/C1 – ECOLOGIA

Settore Scientifico disciplinare: BIO/07 – ECOLOGIA

TITOLO TESI

REPRODUCTION, GROWTH AND BIOMINERALIZATION OF CALCIFYING MARINE ORGANISMS AND THEIR RELATIONSHIPS WITH ENVIRONMENTAL PARAMETERS

Presentata da: Dott.ssa Francesca Gizzi

Coordinatore Dottorato

Prof.ssa Barbara Mantovani

Relatore

Dott. Stefano Goffredo

Correlatori

Prof. Giuseppe Falini

Prof. Christian R. Voolstra

Esame finale anno 2016

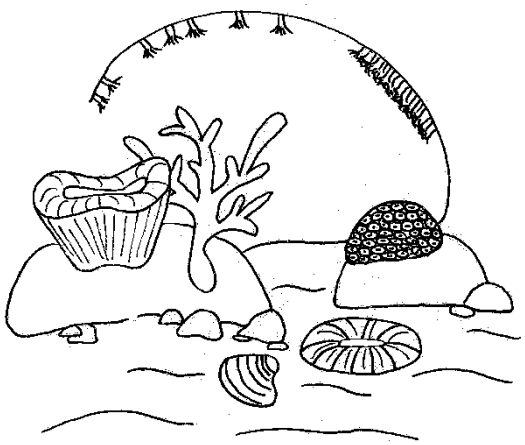

Index

Chapter 1

General introduction

General introduction

The environment plays a key role in growth and development of organisms. There is a strong suggestion that organisms and communities present adaptive and acclimation mechanisms and significant flexibility to respond of environmental change (Buddemeier and Smith 1999). Moreover, many organisms have the ability to express different observable phenotypes in response to changes of biotic and abiotic environmental parameters. This process is referred as phenotypic plasticity, which is the ability of organism to produce a range of relatively fit phenotypes by altering morphology, state, movement, life history or behavior in relation to variations in environmental parameters (Pigliucci 2001; West-Eberhard 2003; DeWitt and Scheiner 2004; Beldade et al. 2011; Gilbert 2012).

Environmental parameters and climate change

Coastal marine systems are arguably among the most ecologically and socio-economically important on the planet, and calcifying marine organisms, such as corals and mollusks are likely to be among the most susceptible organisms to changing environmental parameters, including anthropogenic climate change (Laing et al. 1987; Levitan 1991; DeWitt 1998; Carballo et al. 2006; Harley et al. 2006).

Over the past several centuries, burning of fossil fuels, deforestation, industrialization, cement production, and other land-use changes have become an additional, important component to the climate system through greenhouse gas (mainly CO_2) emissions (Wisshak et al. 2013). The increasing atmospheric carbon dioxide (CO_2) concentration by human activities is driving global climate change, in which the main forces are ocean warming (OW), ocean acidification (OA) and the alteration of seawater physicochemical status (Diaz and Rosenberg 2008; Kroeker et al. 2010; Byrne 2012). Mean sea surface temperatures increased of 0.7°C since the industrial revolution (Feely et al. 2009), and the Intergovernmental Panel of Climate Change

(IPCC) projected a further rise of 1.6-4.3°C by the end of this century (Stocker et al. 2013). Moreover, about 30% of anthropogenic CO_2 is absorbed by oceans (Solomon et al. 2007), causing a decrease of 0.1 pH units from the preindustrial time (Caldeira and Wickett 2003; Langdon and Atkinson 2005; Feely et al. 2012). If anthropogenic CO_2 emission will be not mediated, is projected a further drop of 0.06-0.32 units by the end of this century (Stocker et al. 2013; Caldeira and Wickett 2003; Feely et al. 2009). The extensive absorption of pCO_2 by oceans is triggering a series of chemical reactions that alter the seawater carbonate chemistry. In the first key reaction is formed the carbonic acid (H_2CO_3), which dissociates releasing H^+ ions:

$$CO_2 + H_2O \leftrightarrow H_2CO_3 \leftrightarrow H^+ + HCO_{3-}$$

The second key reaction occurs between free carbonate ions (CO_3^{2-}) and hydrogen ions (H^+), with the bicarbonate ions formation (HCO_{3-}):

$$CO_3^{2-} + H^+ \leftrightarrow HCO_{3-}$$

The combined effect of these two reactions not only causes an increase in acidity, due to rise of hydrogen ion concentration (H^+), but also reduced availability of carbonate ion (CO_3^{2-}) concentration, increasing energetic costs associated with production of calcium carbonate ($CaCO_3$) structures by organisms (Caldeira and Wickett 2003). Moreover, dissolution or precipitation of $CaCO_3$ is linked to the stability of the crystalline structure and the rate of biogenic calcification is, among other factors, determined by the saturation state of seawater (Ω) with respect to $CaCO_3$:

$$\Omega = [Ca^{2+}]*[\ CO_3^{2-}]/K$$

where $[Ca^{2+}]$ is the in situ concentration of calcium ions and K is the stoichiometric solubility product, that is inversely related to temperature (T), so the carbonate saturation Ω increases with increasing T. When $\Omega > 1$ is favored the precipitation of CaCO3, that begins to dissolve when Ω drops below 1 (Hofmann and Schellnhuber 2010).

Calcifying marine organisms (e.g. corals and mollusks) use $CaCO_3$, in the form of calcite or aragonite, as a structural and/or protective material through the biomineralization process (Lowenstam and Weiner 1989). This process occurs in a biological confined environment, under the control of biological macromolecules (Allemand et al. 2011). The structure of marine calcifying organism is a composite of both, inorganic (aragonite or calcyte) and organic components (Wilfert and Peters 1969; Young 1971), the intracrystalline skeletal organic matrix (OM), which is involved in biomineral synthesis playing a major role in biomineralization process (Addadi et al. 1987; Falini et al. 1996, 2009; Puverel et al. 2005). Although several studies was performed to understand the empirical aspects of biomineralization, the fundamental mechanisms and dynamics of skeletal morphogenesis are still only partially understood (Cohen and McConnaughey 2003; Allemand et al. 2011).

Calcifying marine organisms are likely to be among the most susceptible organisms to environmental change (Laing et al. 1987; Levitan 1991; DeWitt 1998; Carballo et al. 2006), showing morphological variations of the skeleton/shell related to bottom topography, sediment characteristics, hydrodynamic processes (Vogel 1996; Seed and Richardson 1999; Casado-Amezua et al. 2013), and especially with T (Laing et al 1987; McNeil et al. 2004; Goffredo et al. 2007, 2008; Doyle 2010; Rodolfo-Metalpa et al. 2011; Watson et al. 2012) and pH (Kleypas et al. 1999, 2006; Ries et al. 2009; Nienhuis et al. 2010; Findlay et al. 2011; Goffredo et al. 2014; Fantazzini et al. 2015; Thomsen et al. 2015).

Effects of temperature and ocean warming

OW alone has already affected the marine species distribution and threatens the survivor of marine species and ecosystems, such as coral reefs (Parmesan and Yohe 2003; Thomas et al. 2004; Perry et al. 2005; Hoegh-Guldberg 2005; Brierley and Kingsford 2009). T is the major environmental factor controlling invertebrate population biology and its increased negatively

affects physiology, developmental rates (Hoegh-Guldberg and Pearse 1995; Gillooly et al. 2002; Clarke 2003; Brierley and Kingsford 2009), growth rates, reproductive output (Baird and Marshall 2002; Linares et al. 2008; Albright and Mason 2013), and increases mass mortality events and disease (Przeslawski et al. 2008; Coma et al. 2009; Garrabou et al. 2009). Moreover, many marine organisms has a symbioses with unicellular dinoflagellate algae (zooxanthellae) makes these animals, including zooxanthellate corals, the most affected by OW, due to the negative effect of high T on photosynthetic machinery of their host zooxanthellae (Lesser 2011). Symbiodinium species through photosynthesis process produces energy, mainly as glucose (Burriesci et al. 2012), and are able to meet up to ~95% of the energy requirement of the coral host (Muscatine et al. 1981, 1984). Increasing T may damage the photosynthetic machinery of Symbiodinium, reducing their photosynthetic efficiency and eventually leading to their expulsion from the coral host and/or the loss of the pigments of the zooxathellae, through a process known as bleaching (Brown 1997; Lesser 2011). Coral bleaching cause a loss of energy and carbon budget of corals and may result in a decrease of coral calcification (Schoepf et al. 2015). Bleached coral can survive to bleaching event recovering new zooxanthellae from water column but, if bleaching event persist in time, the coral will die, increasing the mass mortality events (Brown 1997; Berkelmans et al. 2004). It was experimentally found that T at which corals bleach, slow or block the development of gonads within corals and interrupt a number of other key reproductive processes; even if corals recover from bleaching events, the number of recruits may be affected (Hoegh-Guldberg 1999). The negative effects of increasing T on coral reproduction include a reduction of fecundity, egg quality and fertilization success, and recruitment through effects on early life history processes after fertilization (e.g. embryonic development, larval development, survival, settlement, metamorphosis and post-settlement growth; Albright and Mason 2013; Linares et al. 2008). These studies was carried out mainly on zooxanthellate tropical and subtropical corals. The

few information about sexual reproduction of non-zooxanthellate corals reveals no effect of on reproductive output to increasing T (Airi et al. *submitted*; Marchini 2016; present thesis). The different response to high T among species could be due to their different trophic strategies, suggesting that heterotrophic species seem to be less sensitive to T change than zooxanthellate ones.

Effects of pH and ocean acidification

OA alone has the potential to severely affect physiological and ecological process influencing the performance of marine organisms, with implications for population dynamics, community structure, and ecosystem function (Fabry et al. 2008; Doney et al. 2009; Gaylord et al. 2015). Sexual reproduction represents a crucial process, in the development and persistence of populations through the maintaining genetic diversity, and its reduction threaten the resilience of the species, leading to shifts in size and abundance of populations (Roth et al. 2010; Fiorillo et al. 2013) and allows the populations replenishment after disturbances. Very little information is available regarding the effects of ocean acidification on sexual reproduction in corals, and no one on temperate species. The effects of decreasing pH on coral reproduction, show negative response on sperm motility (Morita et al. 2009; Nakamura and Morita 2012), gametogenesis (Fine and Tchernov 2007; Jokiel et al. 2008), fertilization process (Albright and Mason 2013; Albright et al. 2010; Chua et al. 2013), embryonic development (Medina-Rosas et al. 2012), larval settlement and juvenile growth (Kurihara 2008; Suwa et al. 2010; Albright and Langdon 2011; Nakamura et al. 2011; Doropoulos et al. 2012; Chua et al. 2013; Doropoulos and Diaz-Pulido 2013). Moreover, most results show that increasing pCO_2 may affected calcifying marine organisms through disturbances in acid-base regulation, respiration, metabolism, growth rates, reproduction and calcification (Pörtner 2008; Widdicombe and Spicer 2008; Navarro et al. 2013; Duarte et al. 2014; Gazeau et al. 2014) and mortality rates may increase

(Miles et al. 2007; Kroeker et al. 2010; Appelhans et al. 2012). However, in symbiotic organism with algae, such as zooxanthellate corals, increasing CO_2 could stimulates photosynthesis increasing the overall energy introduced into the system, as found in different taxa (Borowitzka and Larkum 1976; Gao et al. 1993; Riebesell et al. 1993; Zimmerman et al. 1997; Langdon and Atkinson 2005) and possibly stimulate the calcification process (Iglesias-Rodriguez et al. 2008). At the contrary, the non-symbiotic organisms, such as non-zooxanthellate corals, could be negatively affected by decreasing pH; in fact, a drop in pH decreases calcification and may ultimately result in the inability of corals to form a skeleton (Knowlton and Jackson 2008). Actually, the effects of decreasing pH, due to increasing pCO_2, on photosynthetic efficiency in corals, showed ambiguous and contradictory results, and could be modified by a rise in T (Gooding et al. 2009; Findlay et al. 2010), making it difficult to understand how zooxanthellate corals will respond to climate change (Harley et al. 2006; Dupont and Thorndyke 2009; Kurihara 2008; Pörtner 2008; Przeslawski et al. 2008).

Temperature/pH interactions and local stressors

A growing body of evidence confirms that OW and OA are among the most important environmental factors controlling the survival, distribution, growth, physiological performance, behaviour and physiology of diverse marine organisms (Pörtner et al. 2005; Pörtner and Knust 2007; Pörtner 2008; Widdicombe and Spicer 2008; Doney et al. 2009; Dupont and Thorndyke 2013; Dupont and Pörtner 2013). In addition, the diseases and local anthropogenic influences could affect coral health, potentially increasing the effects of global climate changes. The great intensification of coastal populations leads to increased sewage in coastal marine populations, resulting in a great amount of inorganic nutrients, organic compounds and sediments, with deleterious effects on corals (Fabricius 2005; Lamb et al. 2015; Wear and Thurber 2015). A moderate rise in nutrient concentrations can substantially increase

the severity of coral diseases by increasing pathogen fitness and virulence (Bruno et al. 2003; Kim and Harvell 2002). Over fishing, destructive fishing, loss of herbivores and high inorganic nutrient produce an increase in algal abundance on reefs, negatively affecting coral healthy (Hughes and Connell 1999; Hughes et al. 1999; McCook 1999; Knowlton 2001; Aronson et al. 2003; Bellwood et al. 2004). Moreover, fishing tools may injure corals, making them more susceptible to disease (Lamb et al. 2015). These local factors weaken resilience of the ecosystem and work in concert with global climate changes, endangering the future of marine ecosystems.

Mediterranean Sea

Most studies regarding the effect of climate change on biology and ecology on Scleractinian corals have been performed in tropical regions, where many species are widely present and can be easily sampled during scientific dives (Freiwald et al. 2004). Temperate regions, including Mediterranean Sea, have deserved much less attention, probably because of higher difficulty in collecting the study material (Freiwald et al. 2004). However, the magnitude of OW and OA is differing markedly between regions (Stocker et al. 2013; Brierley and Kingsford 2009) and Mediterranean Sea will be one of the regions most affected by the ongoing warming and acidifying trend (Field et al. 2012). Mediterranean Sea is a semi-enclosed mid-latitude ocean basin well ventilated in most parts (Copin-Montegut 1993; Bethoux et al. 1999), characterized by high total alkalinity (~2.6 mmol kg−1) and high carbonate saturation state (Schneider et al. 2007). These conditions, in addition to high solubility of CO_2 at low SST, involve in a great chemical potential to sequester atmospheric CO_2, resulting in relatively larger decreases in seawater pH (Copin-Montegut 1993; Bethoux et al. 1999; Pörtner 2008), making the Mediterranean a potential model of more global patterns to occur in the world's marine biota, and a natural focus of interest for research (Lejeusne et al. 2010).

My research objectives

In effort to contribute to better understand how OW and OA affect the biology of calcifying marine organisms, the studies of this PhD thesis were performed mostly in Mediterranean Sea in natural populations along latitudinal gradient of T and SR and in transplanted and natural populations along a pCO_2 natural gradient. These studies involved zooxanthellate and non-zooxantehllate scleractinian corals to furtherly assess if different trophic strategy produces different sensitivity to environmental change. A comparative study between two zooxanthellate Red Sea corals with different growth form, regarding the effect of high T, low pH and their interaction was performed in aquaria experiment. Moreover, along a latitudinal gradient of T and SR, six populations of a common bivalve clam with great commercial value, were considered as case study of calcifying marine organisms.

Specifically, this PhD thesis has been divided into 3 sections to focus the relationship between:

Section 1. Sexual reproduction and environmental parameters

Aim: Quantifying the reproductive output (gametes abundance, gonadal index and reproductive element size) of:

- *Balanophyllia europaea* (solitary, zooxanthellate) along a latitudinal gradient of T and SR. Chapter 2, published in Plos ONE;
- *B. europaea* living along a natural pCO_2 gradient (only oogenesis). Chapter 3, manuscript *in preparation*;
- *Leptopsammia pruvoti* (solitary, non-zooxanthellate) transplanted along a natural pCO_2 gradient. Chapter 4, manuscript *in preparation*;

Section 2. Ecophysiology and environmental parameters

Aim: Quantifying the photosynthetic efficiency, bleached tissue and mortality rate of *Fungia granulosa* (solitary, zooxanthellate) and *Pocillopora verrucosa* (colonial, zooxanthellate) under experimental T and pCO_2 conditions (abroad period). Chapter 5, manuscript *in preparation*.

Section 3. Biomineralization, skeletal phenotype and environmental parameters

Aims:

- Investigate the role of intra-skeletal organic matrix (OM) in the biomineralization process of *B. europaea*, *L. pruvoti*, *Astroides calycularis* and *Cladocora caespitosa*. Chapter 6, published in Crystal Growth & Design;
- Quantifying the macrostructural (length, height, width, thickness, mass and volume) microstructural (microdensity, bulk density, porosity) and nanostructural shell parameters (shell inorganic phase, crystal atomic disorder, OM) of *Chamelea gallina* along a latitudinal gradient of T and SR. Chapter 7, manuscript *in preparation*;

The present PhD work was conducted in the Marine Science Group at Department of Biological, Geological and Environmental Sciences (BiGeA, University of Bologna, Itlay) under supervision of Dr. Stefano Goffredo; at Chemistry Department "G. Ciamician" (University of Bologna, Italy), in collaboration with Prof. Giuseppe Falini; and at Red Sea Research Center (King Abdullah University of Science and Technologies (KAUST), Saudi Arabia), in collaboration with Prof. Christian Voolstra.

Part of my PhD research concerns the EU FP7-IDEAS ERC project, "Corals and global warming: the Mediterranean versus the Red Sea" (CoralWarm; www.coralwarm.eu), which aims to study the influence of OA and OW on Mediterranean and Red Sea corals.

References

Airi V, Prantoni S, Calegari M, Lisini Baldi V, Levy O, Falini G, Dubinsky Z, Goffredo S (2016) Reproductive output of a non-zooxanthellate Mediterranean coral is unaffected by temperature along an 850 km latitudinal gradient. Sci. Rep. *Submitted*.

Albright R, Mason B, Miller M, Langdon C (2010) Ocean acidification compromises recruitment success of the threatened Caribbean coral *Acropora palmata*. Proc. Natl. Acad. Sci. USA. 107:20400-20404.

Albright R, Langdon C (2011) Ocean acidification impacts multiple early life history processes of the Caribbean coral *Porites astreoides*. Glob. Chang. Biol. 17: 2478-2487.

Albright R, Mason B (2013) Projected near-future levels of temperature and pCO_2 reduce coral fertilization success. PLoS ONE. 8:e56468.

Allemand D, Tambutté È, Zoccola D, Tambutté S (2011) Coral calcification, cells to reefs. In Coral reefs: and ecosystem in transition. Dubinsky Z, Stambler N (eds.). Springer: Dordrecht. 31 p.

Appelhans Y, Thomsen J, Pansch C, Melzner F, Wahl M (2012) Sour times: seawater acidification effects on growth, feeding behaviour and acid–base status of *Asterias rubens* and *Carcinus maenas*. Mar. Ecol. Prog. Ser. 459:85-98.

Aronson RB, Bruno JF, Precht WF, Glynn PW, Harvell CD, Kaufman L, Rogers CS, Shinn EA, Valentine JF (2003). Causes of coral reef degradation. Science. 302:1502-1504.

Baird AH, Marshall PA (2002) Mortality, growth and reproduction in scleractinian corals following bleaching on the Great Barrier Reef. Mar. Ecol. Prog. Ser. 237: 133-141.

Beldade P, Mateus ARA, Keller RA (2011) Evolution and molecular mechanisms of adaptive developmental plasticity. Mol. Ecol. 20: 1347-1363.

Bellwood DR, Hughes TP, Folke C, Nyström M (2004) Confronting the coral reef crisis. Nature. 429:827-833.

Berkelmans R, De'ath G, Kininmonth S, Skirving WJ (2004) A comparison of the 1998 and 2002 coral bleaching events on the Great Barrier Reef: Spatial correlation, patterns, and predictions. Coral Reefs. 23:74-83.

Bethoux JP, Gentili B, Morin P, Nicolas E, Pierre C, Ruiz-Pino D (1999) The Mediterranean Sea: a miniature ocean for climatic and environmental studies and a key for the climatic functioning of the North Atlantic. Prog. Oceanogr. 44:131-46.

Borowitzka MA, Larkum A (1976) Calcification in the green algal Halimeda. III. The sources of inorganic carbon for photosynthesis and calcification and a model of the mechanisms of calcification. J. Exp. Bot. 27:879-893.

Brierley AS, Kingsford MJ (2009) Impacts of climate change on marine organisms and ecosystems. Curr. Biol. 19:R602-R614.

Brown BE (1997) Coral bleaching: Causes and consequences. Coral Reefs. 16:129-138.

Bruno JFPLE, Harvell CD, Hettinger A (2003) Nutrient enrichment can increase the severity of coral diseases. Ecol. Lett. 6.

Buddemeier RW, Smith SV (1999) Coral adaptation and acclimatization: a most ingenious paradox. Am. Zool. 39:1-9.

Burriesci MS, Raab TK, Pringle JR (2012) Evidence that glucose is the major transferred metabolite in dinoflagellate-cnidarian symbiosis. J. Exp. Biol. 215:3467-3477.

Byrne M (2012) Global change ecotoxicology: identification of early life history bottlenecks in marine invertebrates, variable species responses and variable experimental approaches. Mar. Environ. Res. 76:3-15.

Caldeira K, Wickett ME (2003) Oceanography: anthropogenic carbon and ocean pH. Nature. 425:365.

Carballo JL, Avila E, Enríquez S, Camacho L (2006) Phenotypic plasticity in a mutualistic association between the sponge *Haliclona caeulea* and the calcareous macroalga *Jania adherens* induced by transplanting experiments. I: morphological responses of the sponge. Mar. Biol. 148:467-478.

Carte BK (1996) Biomedical potential of marine natural products. Bioscience. 46:271-286.

Casado-Amezua P, Gasparini G, Goffredo S (2013) Phenological and morphological variations in the Mediterranean orange coral *Astroides calycularis* between two distant localities. Zoology. 116:159-167.

Chua CM, Leggat W, Moya A, Baird AH (2013) Temperature affects the early life history stages of corals more than near future ocean acidification. Mar. Ecol. Prog. Ser. 475:85-92.

Clarke A (2003) Costs and consequences of evolutionary temperature adaptation. Trends Ecol. Evol. 18:573-581.

Cohen AL, McConnaughey TA (2003) Geochemical perspectives on coral mineralization. Rev. Mineral. Geochem. 54:151-187.

Coma R, Ribes M, Serrano E, Jiménez E, Salat J, Pascual J (2009) Global warming-enhanced stratification and mass mortality events in the Mediterranean. Proc. Natl. Acad. Sci. USA. 106:6176-6181.

Copin-Montegut C (1993). Alkalinity and carbon budgets in the Mediteranean Sea. Global Biogeochem. Cy. 7:915-925.

DeWitt TJ (1998) Costs and limits of phenotypic plasticity: Tests with predator induced morphology and life history in a freshwater snail. J. Evol. Biol. 11:465-480.

DeWitt TJ, Scheiner SM (2004) Phenotypic plasticity: functional and conceptual approaches. Oxford University Press, Oxford. 247 p.

Diaz RJ, Rosenberg R (2008) Spreading dead zones and consequences for marine ecosystems. Science. 321:926-929.

Doney SC, Fabry VJ, Feely RA, Kleypas JA (2009) Ocean acidification: the other CO_2 problem. Annu. Rev. Mar. Sci. 1:169-192.

Doropoulos C, Ward S, Diaz-Pulido G, Hoegh-Guldberg O, Mumby PJ (2012) Ocean acidification reduces coral recruitment by disrupting intimate larval-algal settlement interactions. Ecol. Lett. 15-338-346.

Doropoulos C, Diaz-Pulido G (2013). High CO_2 reduces the settlement of a spawning coral on three common species of crustose coralline algae. Mar. Ecol. Prog. Ser. 475:93-99.

Doyle S, MacDonald B, Rochette R (2010) Is water temperature responsible for geographic variation in shell mass of *Littorina obtusata* (L.) snails in the Gulf of Maine? J. Exp. Mar. Biol. Ecol. 394:98-104.

Duarte C, Navarro JM, Acuña K, Torres R, Manríquez PH, Lardies MA, Vargas CA, Lagos NA, Aguilera V (2014) Combined effects of temperature and ocean acidification on the juvenile individuals of the mussel *Mytilus chilensis*. J. Sea Res. 85:308-314.

Dupont S, Thorndyke MC (2009) Impact of CO_2-driven ocean acidification on invertebrates' early life-history-what we know, what we need to know, and what we can do? Biogeosci. Discuss. 6:3109-3131.

Dupont S, Thorndyke M (2013) Direct impacts of near-future ocean acidification on sea urchins. Climate Change Perspectives from the Atlantic: Past, Present and Future. 2013:461-485.

Dupont S, Pörtner HO (2013) A snapshot of ocean acidification research. Mar. Biol. 160:1765-1771.

Fabricius KE (2005) Effects of terrestrial runoff on the ecology of corals and coral reefs: review and synthesis. Mar. Pollut. Bull. 50:125-146.

Fabry VJ, Seibel BA, Feely RA, Orr JC (2008) Impacts of ocean acidification on marine fauna and ecosystem processes. ICES J. Mar. Sci. 65:414-432.

Falini G, Albeck S, Weiner S Addadi L (1996) Control of aragonite or calcite polymorphism by mollusk shell macromolecules. Science. 271:67-69.

Falini G, Fermani S, Tosi G, Dinelli E (2009) Calcium carbonate morphology and structure in the presence of seawater ions and humic acids. Cryst. Growth Des. 9:2065-72.

Fantazzini P, Mengoli S, Pasquini L, Bortolotti V, Brizi L, Mariani M, Di Giosia M, Fermani S, Carpaccioni B, Caroselli E, Prada F, Zaccanti F, Levy O, Dubinsky Z, Kaandorp JA, Konglers P, Hammel JU, Dauphin Y, Cuif JP, Weaver JC, Fabricus KE, Wagermaier W, Fratzl P, Falini S and Goffredo S (2015) Gains and losses of coral skeletal porosity changes with ocean acidification acclimatation. N. Comms. 6:7785.

Feely RA, Doney SC, Cooley SR (2009) Ocean acidification: present conditions and future changes in a high-CO_2 world. Oceanography. 4:36-47.

Feely RA, Sabine CL, Byrne RH, Millero FJ, Dickson AG, Wanninkhof R, Murata A, Miller LA, Greeley D (2012) Decadal changes in the aragonite and calcite saturation state of the Pacific Ocean. Global Biogeochemical Cycles. 26 p.

Field CB (ed) (2012) Managing the risks of extreme events and disasters to advance climate change adaptation: special report of the intergovernmental panel on climate change. Cambridge University Press, Cambridge and New York.

Findlay HS, Kendall MA, Spicer JI, Widdicombe S (2010) Post-larval development of two intertidal barnacles at elevates CO_2 and temperature. Mar. Biol. 157:725-735.

Findlay HS, Wood HL, Kendall MA, Spicer JI, Twitchett RJ, Widdicombe S (2011) Comparing the impact of high CO_2 on calcium carbonate structures in different marine organisms. Mar. Biol. Res. 7:565-575.

Fine M, Tchernov D (2007) Scleractinian coral species survive and recover from decalcification. Science. 315:1811-1811.

Fiorillo I, Rossi S, Alva V, Gili JM, López-González PJ (2013) Seasonal cycle of sexual reproduction of the Mediterranean soft coral *Alcyonium acaule* (Anthozoa, Octocorallia). Mar. Biol. 160:719-728.

Freiwald A, Fosså JH, Grehan A, Koslow T, Roberts JM (2004) Cold-water coral reefs. UNEP-WCMC, Cambridge, UK. 84 p.

Gao K, Aruga Y, Asada K, Kiyohara M (1993) Influence of enhanced CO_2 on growth and photosynthesis of the red algae *Gracilaria sp*. and *G. chilensis*. J. Appl. Phycol. 5:563-571.

Garrabou J, Coma R, Bensoussan N, Bally M, Chevaldonné P, Cigliano M, Díaz D, Harmelin JG, Gambi MC, Kersting DK, Ledoux JB (2009) Mass mortality in Northwestern Mediterranean rocky benthic communities: effects of the 2003 heat wave. Glob. Chang. Biol. 15:1090-1103.

Gaylord B, Kroeker KJ, Sunday JM, Anderson KM, Barry JP, Brown NE, Connell SD, Dupont S, Fabricius KE, Hall-Spencer JM, Klinger T (2015) Ocean acidification through the lens of ecological theory. Ecology. 96:3-15.

Gazeau F, Alliouane S, Bock C, Bramanti L, López Correa M, Gentile M, Hirse T, Pörtner HO, Ziveri P (2014) Impact of ocean acidification and warming on the Mediterranean mussel (*Mytilus galloprovincialis*). Front. Mar. Sci. 1:1-2.

Gilbert SF (2001) Ecological developmental biology: developmental biology meets the real world. Dev. Biol. 233:1-12.

Gilbert SF (2012) Ecological developmental biology: environmental signals for normal animal development. Evol. Dev. 14:20-28.

Gillooly JF, Charnov EL, West GB, Savage VM, Brown JH (2002) Effects of size and temperature on developmental time. Nature. 417:70-73.

Goffredo S, Caroselli E, Pignotti E, Mattioli G, Zaccanti F (2007) Variation in biometry and population density of solitary corals with solar radiation and sea surface temperature in the Mediterranean Sea. Mar. Biol. 152:351-361.

Goffredo S, Caroselli E, Mattioli G, Pignotti E, Zaccanti F (2008) Relationship between growth, population structure and sea surface temperature in the temperate solitary coral *Balanophillia europaea* (Scleractinia, Dendrophylliidae). Coral Reefs. 27:623-632.

Goffredo S, Prada F, Caroselli E, Capaccioni B, Zaccanti F, Pasquini L, Fantazzini P, Fermani S, Reggi M, Levy O, Fabricus KE, Dubinsky Z, Falini G (2014) Biomineralization control related to population density under ocean acidification. N. Clim. Change. 4:593-597.

Gooding RA, Harley CDG, Tang E (2009) Elevated water temperature and carbon dioxide concentration increase the growth of a keystone echinoderm. Proc. Natl. Acad. Sci. USA. 106:9316-9321.

Harley CD, Randall Hughes A, Hultgren KM, Miner BG, Sorte CJ, Thornber CS, Rodriguez LF, Tomanek L, Williams SL (2006) The impacts of climate change in coastal marine systems. Ecol. Lett. 9:228-41.

Hoegh-Guldberg O, Pearse JS (1995) Temperature, food availability, and the development of marine invertebrate larvae. Amer. Zool. 35:415-425.

Hoegh-Guldberg O (1999) Climate change, coral bleaching and the future of the world's coral reefs. Mar. Fresh. Res. 50:839-866.

Hoegh-Guldberg O (2005) Low coral cover in a high-CO_2 world. J. Geophys. Res. Oceans. 110.

Hofmann M, Schellnhuber HJ (2010) Ocean acidification: a millennial challenge. Energ. Environ. Sci. 3:1883-1896.

Hughes TP, Connell JH (1999) Multiple stressors on coral reefs: a long-term perspective. Limnol. Oceanogr. 44:932-940.

Hughes T, Szmant AM, Steneck R, Carpenter R, Miller S (1999) Algal blooms on coral reefs: what are the causes? Limnol. Oceanogr. 44:1583-1586.

Iglesias-Rodriguez MD, Halloran PR, Rickaby RE, Hall IR, Colmenero-Hidalgo E, Gittins JR, Green DR, Tyrrell T, Gibbs SJ, von Dassow P, Rehm E (2008) Phytoplankton calcification in a high-CO_2 world. Science. 320:336-340.

Jokiel PL, Rodgers KS, Kuffner IB, Andersson AJ, Cox EF, Mackenzie FT (2008) Ocean acidification and calcifying reef organisms: a mesocosm investigation. Coral Reefs. 27:473-483.

Kim K, Harvell CD (2002) Aspergillosis of sea fan corals: disease dynamics in the Florida Keys. In: The Everglades, Florida Bay, and Coral Reefs of the Florida Keys: An Ecosystem Sourcebook. Porter JW, Porter KG (eds). CRC Press, Boca Raton. 11 p.

Kleypas JA, Buddermeier RW, Archer D, Gattuso JP, Langdon C, Opdyke BN (1999) Geochemical consequences of increased atmospheric carbon dioxide on coral reefs. Science. 284:118-120.

Kleypas JA, Feely RA, Fabry VJ, Langdon C, Sabile CL, Robbins LL (2006) Impacts of ocean acidification on coral reefs and other marine calcifiers: a guide for future research. Report NFS, NOAA, US Geological Survey, NSF. 18:1-88.

Knowlton N (2001) The future of coral reefs. Proc. Natl. Acad. Sci. U. S. A. 98:5419-5425.

Knowlton N, Jackson JB (2008) Shifting baselines, local impacts, and global change on coral reefs. PLoS Biol. 6:e54.

Kroeker KJ, Kordas RL, Crim RN, Singh GG (2010) Meta-analysis reveals negative yet variable effects of ocean acidification on marine organisms. Ecol. Let. 13:1419-1434.

Kroeker KJ, Kordas RL, Crim R, Hendriks IE, Ramajo L, Singh GS, Duarte CM, Gattuso JP (2013) Impacts of ocean acidification on marine organisms: quantifying sensitivities and interaction with warming. Glob. Chang. Biol. 19:1884-1896.

Kurihara H (2008) Effects of CO_2-driven ocean acidification on the early developmental stages of invertebrates. Mar. Ecol. Prog. Ser. 373:275-284.

Laing I, Utting SD, Kilada RWS (1987) Interactive effect of diet and temperature on the growth of juvenile clams. J. Exp. Mar. Biol. Ecol. 113:23-38.

Lamb JB, Williamson DH, Russ GR, Willis BL (2015) Protected areas mitigate diseases of reef-building corals by reducing damage from fishing. Ecology. 96:2555-2567.

Langdon C, Atkinson MJ (2005) Effect of elevated pCO_2 on photosynthesis and calcification of corals and interactions with seasonal change in temperature/irradiance and nutrient enrichment. J. of Geophys. Res. Oceans. 110.

Lejeusne C, Chevaldonné P, Pergent-Martini C, Boudouresque CF, Perez T (2010) Climate change effects on a miniature ocean: the highly diverse, highly impacted Mediterranean Sea. Trends Ecol. Evol. 25:250-260.

Lesser MP (2011) Coral bleaching: causes and mechanisms. In Coral Reefs: An Ecosystem in Transition. Dubinsky Z, Stambler N (eds.) Springer, Netherlands. 14 p.

Levitan DR (1991) Skeletal changes in the test and jaws of the sea urchin *Diadema antillarum* in response to food limitation. Mar. Biol. 111:431-435.

Linares C, Coma R, Zabala M (2008) Effects of a mass mortality event on gorgonian reproduction. Coral Reefs. 27:27-34.

Lowenstam HA, Weiner S (1989) On biomineralization. Oxford University Press, USA.

Marchini C (2016) Reproduction and population structure in temperate and tropical corals in relation to environmental parameters. PhD thesis in Biodiversity end Evolution. University of Bologna, Italy.

McCook LJ (1999) Macroalgae, nutrients and phase shifts on coral reefs: scientific issues and management consequences for the Great Barrier Reef. Coral Reefs. 18:357-367.

McNeil BI, Matear RJ, Barnes DJ (2004) Coral reef calcification and climate change: the effect of ocean warming. Geophys. Res. Lett. 31:L22309.

Medina-Rosas P, Szmant, AM, Whitehead RF (2012) CO_2 enrichment and reduced seawater pH had no effect on the embryonic development of *Acropora palmata* (Anthozoa, Scleractinia). Invertebr. Reprod. Dev. 57:132-141.

Miles H, Widdicombe S, Spicer JI, Hall-Spencer J (2007) Effects of anthropogenic seawater acidification on acid–base balance in the sea urchin *Psammechinus miliaris*. Mar. Poll. Bull. 54:89-96.

Morita M, Suwa R, Iguchi A, Nakamura M, Shimada K, Sakai K, Suzuki A (2009) Ocean acidification reduces sperm flagellar motility in broadcast spawning reef invertebrates. Zygote. 18:103-107.

Muscatine L, McCloskey LR, Marian RE (1981) Estimating the daily contribution of carbon from zooxanthellae to coral animal respiration1. Oceanography. 26.

Muscatine L, Falkowski PG, Porter JW, Dubinsky Z (1984) Fate of photosynthetic fixed carbon in light- and shade-adapted colonies of the symbiotic coral *Stylophora pistillata*. Proc. R. Soc. Lond. B. 222:181-202.

Nakamura M, Ohki S, Suzuki A, Sakai K (2011) Coral larvae under ocean acidification: survival, metabolism, and metamorphosis. PLoS ONE. 6:e14521.

Nakamura M, Morita M (2012) Sperm motility of the scleractinian coral *Acropora digitifera* under preindustrial, current, and predicted ocean acidification regimes. Aquatic Biol. 15:299-302.

Navarro JM, Torres R, Acuña K, Duarte C, Manriquez PH, Lardies M, Lagos NA, Vargas C, Aguilera V (2013) Impact of medium-term exposure to elevated pCO_2 levels on the physiological energetics of the mussel *Mytilus chilensis*. Chemosphere. 90:1242-1248.

Nienhuis S, Palmer AR, Harley CDG (2010) Elevated CO_2 affects shell dissolution rate but not calcification rate in a marine snail. Proc. R. Soc. Lond. B. 277:2553-2558.

Parmesan C, Yohe G (2003) A globally coherent fingerprint of climate change impacts across natural systems. Nature. 421:37-42.

Perry AL, Low PJ, Ellis JR, Reynolds JD (2005) Climate change and distribution shifts in marine fishes. Science. 308:1912-1915.

Pigliucci M (2001) Phenotypic plasticity: beyond nature and nurture. Johns Hopkins University Press, Baltimore, MD. 333 p.

Pörtner HO, Langenbuch M, Michaelidis B (2005) Synergistic effects of temperature extremes, hypoxia, and increases in CO_2 on marine animals: From Earth history to global change. J. Geophys. Res. Oceans. 110.

Pörtner HO, Knust R (2007) Climate change affects marine fishes through the oxygen limitation of thermal tolerance. Science. 315:95-97.

Pörtner H (2008). Ecosystem effects of ocean acidification in times of ocean warming: a physiologist's view. Mar. Ecol. Prog. Ser. 373:203-217.

Przeslawski R, Ahyong S, Byrne M, Woerheide G, Hutchings PA (2008) Beyond corals and fish: the effects of climate change on noncoral benthic invertebrates of tropical reefs. Glob. Chang. Biol. 14:2773-2795.

Puverel S, Tambutté E, Pereira-Mouries L, Zoccola D, Allemand D, Tambutté S (2005) Soluble organic matrix of two Scleractinian corals: partial and comparative analysis. Comp. Biochem. Physiol. B Biochem. Mol. Biol. 141:480-7.

Riebesell U, Wolf-Gladrow DA, Smetacek V (1993) Carbon dioxide limitation of marine phytoplankton growth rates. Nature. 361:249-251.

Ries JB, Cohen AL, McCorkle DC (2009) Marine calcifiers exhibit mixed responses to CO_2 induced ocean acidification. Geology. 37:1131-1134.

Rodolfo-Metalpa R, Houlbrèque F, Tambutté É, Boisson F, Baggini C, Patti FP, Jeffree R, Fine M, Foggo A, Gattuso JP, Hall-Spencer JM (2011) Coral and mollusc resistance to ocean acidification adversely affected by warming. Nat. Clim. Change. 1:308-312.

Roth L, Koksal S, van Woesik R (2010) Effects of thermal stress on key processes driving coral population dynamics. Mar. Ecol. Prog. Ser. 411:73-87.

Schoepf V, Grottoli AG, Levas SJ, Aschaffenburg MD, Baumann JH, Matsui Y, Warner ME (20015) Annual coral bleaching and the long-term recovery capacity of coral. Proc. R. Soc. B. 282:20151887.

Seed R, Richardson CA (1999) Evolutionary traits in *Perna viridis* (Linnaeus) and *Septifer virgatus* (Wiegmann) (Bivalvia: Mytilidae). J. Exp. Mar. Biol. Ecol. 239:273-287.

Schneider A, Wallace DW, Körtzinger A (2007) Alkalinity of the Mediterranean sea. Geophys. Res. Lett. 34.

Solomon S, Qin D, Manning M, Chen Z, Marquis M, et al. (2007) Climate Change 2007: The Physical Science Basis. Contribution of Working Group I to the Fourth Assessment Report of the Intergovernmental Panel on Climate Change. Cambridge and New York, Cambridge University Press. 996 p.

Stocker TF, Qin D, Plattner GK, Tignor M, Allen SK, Boschung J, Nauels A, Xia Y, Bex V, Midgley PM (eds.) IPCC 2013: Summary for Policymakers. In: Climate Change 2013: The Physical Science Basis. Contribution of Working Group I to the Fifth Assessment Report of the Intergovernmental Panel on Climate Change. Cambridge University Press, Cambridge, United Kingdom and New York, NY, USA.

Suwa R, Nakamura M, Morita M, Shimada K, Iguchi A, Sakai K, Suzuki A (2010) Effects of acidified seawater on early life stages of scleractinian corals (Genus Acropora). Fish. Sci. 76:93-99.

Thomas CD, Cameron A, Green RE, Bakkenes M, Beaumont LJ, Collingham YC, Erasmus BF, De Siqueira MF, Grainger A, Hannah L, Hughes L (2004) Extinction risk from climate change. Nature. 427:145-148.

Thomsen J, Haynert K, Wegner KM, Melzner F (2015) Impact of seawater carbonate chemistry on the calcification of marine bivalves. Biogeosciences. 12:4209-4220.

Vogel S (1996) Life in Moving Fluids: The Physical Biology of Flow. Princeton Paperbacks. 469p.

Watson SA, Peck LS, Tyler PA, Southgate PC, Tan KS, Day RW, Morley SA (2012) Marine invertebrate skeleton size varies with latitude, temperature and carbonate saturation: implications for global change and ocean acidification. Global Change Biol. 18:3026-3038.

Wear SL, Thurber RV (2015) Sewage pollution: mitigation is key for coral reef stewardship. Ann. N. Y. Acad. Sci. 1355:15-30.

West-Eberhard MJ (2003) Developmental Plasticity and Evolution. Oxford University Press. 797 p.

Widdicombe S, Spicer JI (2008) Predicting the impact of ocean acidification on benthic biodiversity: What can animal physiology tell us? J. Exp. Mar. Biol. Ecol. 366:187-197.

Wilfert M, Peters W (1969) Vorkommen von chitin bei coelenteraten. Zeitschrift für Morphologie der Tiere. 64:77-84.

Wisshak M, Schönberg CH, Form AU, Freiwald A (2013) Effects of ocean acidification and global warming on reef bioerosion-lessons from a clionaid sponge. Aquatic Biol. 19:111-127.

Young SD (1971) Organic material from scleractinian coral skeletons. I. variation in composition between several species. Comp. Biochem. Physiol. B. 40:113-120.

Zimmerman RC, Kohrs DG, Steller DL, Alberte RS (1997) Impacts of CO_2 enrichment on productivity and light requirements of eelgrass. Plant Physiol. 115:599-607.

Section 1

Sexual reproduction and environmental parameters

Chapter 2

Reproductive efficiency of a Mediterranean endemic zooxanthellate coral decreases with increasing temperature along a wide latitudinal gradient

Published in PLoS ONE

OPEN ACCESS Freely available online

PLOS ONE

Reproductive Efficiency of a Mediterranean Endemic Zooxanthellate Coral Decreases with Increasing Temperature along a Wide Latitudinal Gradient

Valentina Airi[1], Francesca Gizzi[1], Giuseppe Falini[2], Oren Levy[3], Zvy Dubinsky[3], Stefano Goffredo[1]*

1 Marine Science Group, Department of Biological, Geological and Environmental Sciences, Section of Biology, Alma Mater Studiorum – University of Bologna, Bologna, Italy, European Union, **2** Department of Chemistry "G. Ciamician," Alma Mater Studiorum – University of Bologna, Bologna, Italy, European Union, **3** The Mina and Everard Goodman Faculty of Life Sciences, Bar-Ilan University, Ramat-Gan, Israel

Abstract

Investments at the organismal level towards reproduction and growth are often used as indicators of health. Understanding how such energy allocation varies with environmental conditions may, therefore, aid in predicting possible responses to global climatic change in the near future. For example, variations in seawater temperature may alter the physiological functioning, behavior, reproductive output and demographic traits (e.g., productivity) of marine organisms, leading to shifts in the structure, spatial range, and abundance of populations. This study investigated variations in reproductive output associated with local seawater temperature along a wide latitudinal gradient on the western Italian coast, in the zooxanthellate Mediterranean coral, *Balanophyllia europaea*. Reproductive potential varied significantly among sites, where *B. europaea* individuals from the warmest site experienced loss of oocytes during gametogenesis. Most of the early oocytes from warmest sites did not reach maturity, possibly due to inhibition of metabolic processes at high temperatures, causing *B. europaea* to reabsorb the oocytes and utilize them as energy for other vital functions. In a progressively warming Mediterranean, the efficiency of the energy invested in reproduction could be considerably reduced in this species, thereby affecting vital processes. Given the projected increase in seawater temperature as a consequence of global climate change, the present study adds evidence to the threats posed by high temperatures to the survival of *B. europaea* in the next decades.

Citation: Airi V, Gizzi F, Falini G, Levy O, Dubinsky Z, et al. (2014) Reproductive Efficiency of a Mediterranean Endemic Zooxanthellate Coral Decreases with Increasing Temperature along a Wide Latitudinal Gradient. PLoS ONE 9(3): e91792. doi:10.1371/journal.pone.0091792

Editor: Christina A. Kellogg, U.S. Geological Survey, United States of America

Received October 30, 2013; **Accepted** February 13, 2014; **Published** March 11, 2014

Funding: The research leading to these results has received funding from the European Research Council under the European Union's Seventh Framework Programme (FP7/2007–2013)/ERC grant agreement no. 249930 – CoralWarm: Corals and global warming: the Mediterranean versus the Red Sea. The funders had no role in study design, data collection and analysis, decision to publish, or preparation of the manuscript.

Competing Interests: The authors have declared that no competing interests exist.

* E-mail: stefano.goffredo@marinesciencegroup.org

Introduction

Coral reefs, like many other ecosystems, are currently undergoing changes in biodiversity, ecosystem function, and resilience due to rising seawater temperatures acting in synergy with additional environmental pressures [1]. A rise in global average temperature of 0.7°C since the start of the industrial revolution has caused or contributed to significant losses of global coral cover over the past few decades, and oceans are expected to experience a further warming of 1.1–6.4°C within the 21st century [2]. Climatic models [3] predict that the Mediterranean basin will be one of the most impacted regions by the ongoing warming trend [4]. The Mediterranean is already showing rates of seawater warming that exceed threefold those of the global ocean [2,4], making it a potential model for global scenarios to occur in the world's marine biota, and a natural focus of interest for research [5].

Increasing temperatures are having a strong impact on marine systems [6]. Indeed, temperature is the major environmental factor controlling invertebrate development, marine species distributions and recruitment dynamics [7,8]. Seawater temperature increases will likely affect the population biology of coral species by reducing reproductive capacity [9]. The harmful effects of increasing temperature on coral reproduction include reduced individual fecundity, egg quality, lowered fertilization success and reduced recruitment through effects on post-fertilization processes (e.g., embryonic development, larval development, survival, settlement, metamorphosis, and early post-settlement growth) [10,11]. The combined effects of fertilization failure and reduced embryonic development in some coral species are likely to exacerbate ecological impacts of climate change by reducing biodiversity [12]. Several studies assessed the immediate and delayed impacts of environmental change on Mediterranean gorgonian colonies [11–14] including sublethal impacts on reproductive effort [11,15,16,17], but few studies have examined temperate solitary corals. Research focusing on reproductive processes in regions with peculiar physical conditions is urgently needed as a baseline against which to test the effects of climate change on sexual reproduction (e.g. fecundity) [10,18] and organismal performance, that are essential to understand population dynamics of marine organisms [19].

Organismal performance under both "normal" and "stressful" conditions is mainly determined by the energetic status of the individual, which can ultimately affect its fitness (i.e. reproductive output). During prolonged periods of stress, the energy balance of

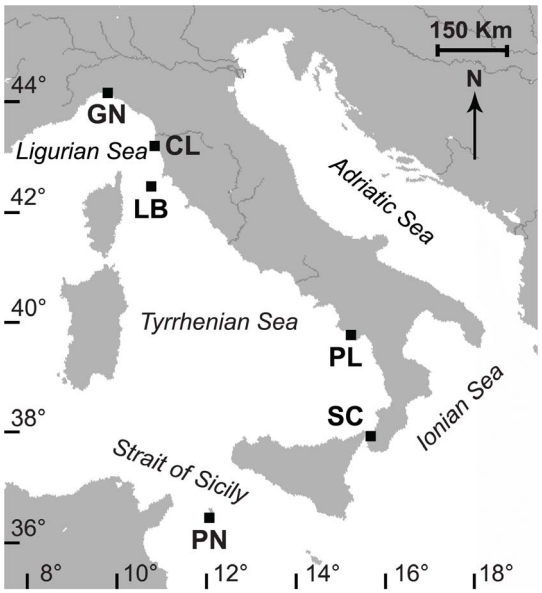

Figure 1. Map of the Italian coastline indicating the sites where corals were collected. Abbreviations and coordinates of the sites in decreasing order of latitude: GN Genova, 44°20′N, 9°08′E; CL Calafuria, 43°27′N, 10°21′E; LB Elba Isle, 42°45′N, 10°24′E; PL Palinuro, 40°02′N, 15°16′E; SC Scilla, 38°01′N, 15°38′E; PN Pantelleria Isle, 36°45′N, 11°57′E.
doi:10.1371/journal.pone.0091792.g001

a coral is negative and the organism is drawing on all biochemical pools, and thus both storage and structural components for energy could be compromised [20]. Shallow water reef corals strongly rely on energy derived from photosynthesis by its symbiotic zooxanthellae [21]. In particular, key processes like gametogenesis [22], larval longevity and settlement [23] are dependent on the availability of stored energy as lipids that are reabsorbed when resources are limited [24]. If metabolic processes involved in recovery from stress deplete lipid reservoirs in oocytes, then fewer resources are available for new egg production [25], significantly affecting gametogenesis.

This study focused on an endemic zooxanthellate Mediterranean scleractinian, *Balanophyllia europaea* (Fig. S1), a simultaneous hermaphrodite and brooding coral [26]. There is growing concern for the future of this endemic species in light of expected seawater warming, since increasing temperature negatively affects *B. europaea* skeletal density [27] (due to increased porosity [28]), population abundance [29], population structure stability [30], growth and calcification [28]. Our specific aim was to quantify the reproductive output of *B. europaea* along a latitudinal gradient of temperature. We expected to find a similar negative response of reproductive output with increasing temperature.

Materials and Methods

Ethics Statement

This study was carried out following the fundamental ethical principles. According to the European normative, there is no active conservation measure for the Mediterranean scleractinian coral studied here (*B. europaea*). The species is not protected in Italy, nor is it subject to any regulations. Thus, no permit was needed to sample specimens. For this study, sampling was limited strictly to the number necessary and performed where the species has high population density to minimize the impact of removing individuals and preserve both the demographic and genetic structure of the natural populations.

Specimens of *B. europaea* came from six sites along a latitudinal gradient, from 44°20′N to 36°45′N (Fig. 1). Coral collection began in June 2010 and ended in November 2012. During this period, 18 samples were taken monthly from five populations (Genova: April 2011-September 2012; Elba: December 2010-May 2012; Palinuro: June 2010-November 2011; Scilla: June 2011-November 2012; Pantelleria: June 2011-November 2012), with a minimum of 15 polyps collected during each excursion. Data from Calafuria population came from a previous study [26] in which samples were collected from July 1997 to October 1998.

Biometric analyses were performed by measuring length (L, maximum axis of the oral disc), width (W, minimum axis of the oral disc) and height (h, oral–aboral axis) of each sampled polyp. The volume (V) of the individual polyp was calculated using the formula [26].

Polyps were post-fixed in Bouin solution. After decalcification in EDTA and dehydration in a graded alcohol series from 80% to 100%, polyps were embedded in paraffin and serial transverse sections were cut at 7 μm intervals along the oral-aboral axis, from the oral to the aboral poles. Tissues were then stained with Mayer's haematoxylin and eosin [26].

Cytometric analyses were made with an optical microscope using the image analyzer NIKON NIS-Elements D 3.2. The maximum and minimum diameters of oocytes in nucleated sections and spermaries were measured and the presence of embryos in the coelenteric cavity was recorded. Spermaries were classified into five developmental stages in accordance with earlier studies on gametogenesis in scleractinians [19,31,32].

Reproductive output was defined through three reproductive parameters: a) *fecundity rate* and *spermary abundance*, both defined as

Table 1. Mean annual solar radiation (W/m^2) and temperature (DT; °C) values of the sampled populations.

Population	Code	DT (°C) mean ± SE	Solar radiation (W/m^2) mean ± SE
Calafuria	CL	17.73±0.16	174.1±1.9
Elba	LB	18.07±0.24	184.9±2.3
Genova	GN	18.13±0.43	156.9±3.2
Scilla	SC	18.73±0.15	205.5±1.8
Palinuro	PL	19.14±0.14	194.6±2.7
Pantelleria	PN	19.69±0.05	218.2±0.5

DT sensors (I-Button DS1921H, Maxim Integrated Products), were placed at the sampling location, at 5–7 m depth in each population. Solar radiation (W/m^2) was collected from MFG satellites. The sites are arranged in order of increasing DT; SE, standard error.
doi:10.1371/journal.pone.0091792.t001

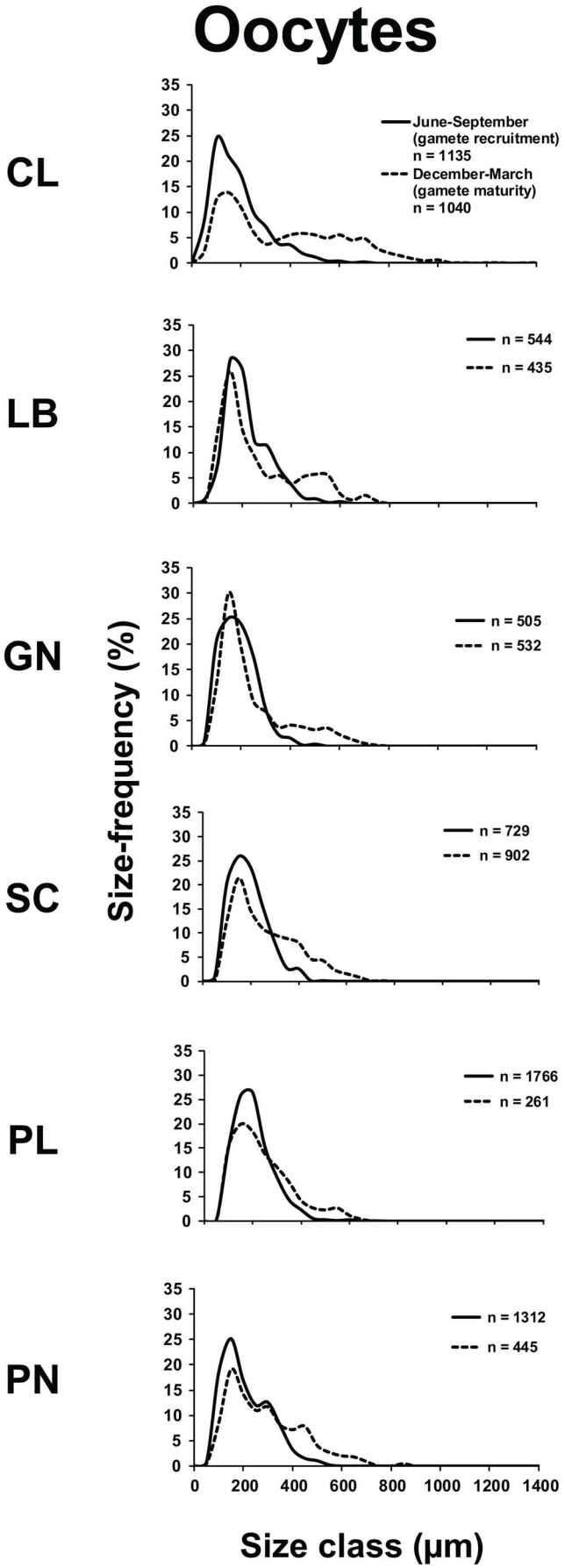

Figure 2. Oocyte size/frequency distribution in the recruitment and maturity periods. Distribution of the oocytes size during gamete recruitment period (solid line) and gamete maturity period (dashed line).
doi:10.1371/journal.pone.0091792.g002

the number of reproductive elements per body volume unit (100 mm^3); b) *"gonadal" index*, defined as the percentage of body volume occupied by germ cells [26]); and c) *reproductive element size*, defined as the average of the maximum and minimum diameter of spermaries and oocytes in nucleated section [26].

Based on the reproductive season [26], gametal development in *B. europaea* was divided in two gamete activity periods. The *gametes recruitment period* [33,34] was defined as the post-fertilization period, between June and September, generally characterized by: 1) a stock of smaller oocytes; 2) the recruitment of new oocytes; and 3) the beginning of spermary development [26]. The *gametes maturity period* [33,34] was defined as the pre-fertilization period taking place between December and March and generally characterized by the presence of larger oocytes and advanced stage of maturation of spermaries [26].

Temperature data (Depth Temperature – DT; °C) came from temperature sensors (I-Button DS1921H, Maxim Integrated Products), placed at the sampling location for each population. Sensors recorded temperatures during the entire experimental period. Sea Surface Temperature data (SST; °C) for each site were recorded hourly from the National Mareographic Network of the Institute for the Environmental Protection and Research (ISPRA, available to http://www.mareografico.it). These data are measured by mareographic stations placed close to the sampling sites using SM3810 manufactured by the Society for the Environmental and Industrial monitoring (SIAP+MICROS). A linear regression was produced between DT and SST data to estimate historical at-depth temperatures. In this study we considered the average DT temperature of the three years preceding the sampling (n = 36 monthly temperatures).

Solar radiation (W/m^2) was collected from the archives of the Satellite Application Facility on Climate Monitoring (CM-SAF/EUMETSAT, available to http://www.cmsaf.eu), using real time data sets based on intersensor calibrated radiances from MFG satellites. Mean annual solar radiation of each site was obtained for the 2.5°-latitude-by-longitude square associated with each of the six sites. As for temperature, also for solar radiation we considered the average of the three years preceding the sampling (n = 36 monthly solar radiation).

Data were checked for normality using a Kolmogorov-Smirnov's test and for variance homoskedasticity using a Levene's test. When assumptions for parametric statistics were not fulfilled, a nonparametric test was used. The Kruskal–Wallis test is a non-parametric alternative to the analysis of variance (ANOVA) and is used to compare groups of means; it is useful for data that do not meet ANOVA's assumptions. The non-parametric Kruskal–Wallis test was used to compare reproductive parameters among study sites. The non-parametric Kolmogorov-Smirnov test was used to compare the size-frequency distribution of reproductive elements between populations and between the two periods. Student's *t* test was used to compare the mean oocytes and spermaries size of populations between periods. Spearman's rank correlation coefficient was used to calculate the significance of the correlations between reproductive and environmental parameters. Spearman's rank correlation coefficient is an alternative to Pearson's correlation coefficient [35]. It is useful for data that are non-normally distributed and do not meet the assumptions of Pearson's correlation coefficient [36]. All analyses were computed using PASW Statistics 17.0.

Table 2. Mean fecundity, gonadal index and diameter of oocytes in each population.

Gametes recruitment period (June – September)					
Population	**N**	**Fecundity (#/100 mm^3) mean ± SE**	**Gonadal Index (%) mean ± SE**	**N**	**Diameter (μm) mean ± SE**
Calafuria	18	161±39	0.22±0.07	1135	166.3±3.3
Elba	6	148±37	0.65±0.17	544	193.7±3.8
Genova	8	168±47	0.27±0.12	505	166.0±3.3
Scilla	9	256±58	0.41±0.13	729	166.7±2.8
Palinuro	10	734±194	1.57±0.38	1766	178.4±1.9
Pantelleria	8	663±240	1.43±0.51	1312	188.2±2.6
Gametes maturity period (December – March)					
Population	**N**	**Fecundity (#/100 mm^3) mean ± SE**	**Gonadal Index (%) mean ± SE**	**N**	**Diameter (μm) mean ± SE**
Calafuria	19	117±38	1.04±0.30	1040	350.3±7.5
Elba	8	175±32	0.79±0.16	435	243.4±7.7
Genova	4	411±183	1.37±0.40	532	222.5±6.2
Scilla	4	602±257	2.72±1.50	902	241.1±4.5
Palinuro	7	112±30	0.39±0.15	261	217.7±7.5
Pantelleria	6	236±106	1.25±0.41	445	265.4±7.1

Mean fecundity, gonadal index and diameter of oocytes in each population for both reproductive periods. The sites are arranged in order of increasing DT; SE, standard error. N, polyp number for fecundity and gonadal index, oocyte number for diameter.

doi:10.1371/journal.pone.0091792.t002

Results

Mean annual solar radiation (W/m^2) and mean annual DT (°C) were significantly different among sites (solar radiation, ANOVA, $p<0.001$; DT, Kruskal-Wallis, $p<0.05$; Table 1; Fig S2).

All populations contained both oocytes and spermaries during both reproductive periods, while embryos were detected only between June and September (gametes recruitment period). The oocyte size/frequency distribution of June-September (gametes recruitment period) was significantly different from that of December-March (gametes maturity period), in all populations (Kolmogorov-Smirnov, $p<0.001$; Fig. 2). Within June and September (gametes recruitment period) most oocytes were smaller than 400 μm, in all populations. In the following season (December-March, gametes maturity period), two distinct oocyte stocks appeared in all populations, characterized respectively by small (immature<400 μm) and large (mature >400 μm) cells (Fig. 2). The mean oocyte size of June-September (gametes recruitment period) was significantly lower than that of December-March (gametes maturity period) in all populations (Student's *t*-test, $p<0.001$; Table 2; Fig. S3).

The distribution of spermary maturation stages in June-September (gametes recruitment period) was significantly different from that in December-March (gametes maturity period), in all populations (Kolmogorov-Smirnov, $p<0.001$; Fig. 3). Each population was characterized, from June to September (gametes recruitment period), by small spermaries, mainly belonging to the earliest maturation stages (stages I and II). In the period December-March (gametes maturity period), all populations were characterized by more advanced maturation stages (mainly stage III; Fig. 3). The mean spermary size of June-September (gametes recruitment period) was significantly lower than that of December-March (gametes maturity period) in all populations (Student's *t*-test, $p<0.001$; Table 3; Fig. 3). In all populations, June-September (gametes recruitment period) was characterized by the presence of embryos in the coelenteric cavity.

Fecundity, gonadal index and oocyte size were significantly different among populations, during June-September (gametes recruitment period) (fecundity, Kruskal–Wallis test, $p<0.01$; gonadal index and oocyte size, Kruskal–Wallis test, $p<0.001$; Tables 2 and S1). In this period, all oocyte reproductive parameters showed positive correlations with both environmental parameters (DT and solar radiation; Table S1; Fig. S4). During December-March (gametes maturity period), the fecundity and oocyte size were significantly different among populations (fecundity, Kruskal–Wallis test, $p<0.05$; diameter, Kruskal–Wallis test, $p<0.001$; Tables 2 and S1). The mean size of oocytes across all populations was negatively correlated with the DT (Table S1; Fig. S5). In the warmest population (Pantelleria island, 19.69±0.05°C; Table 1), the number of mature oocytes at fertilization was three times lower than in the recruitment period, indicating a clear reduction of fecundity during this period (Table 2). In the coldest population (Calafuria, 17.73±0.16°C; Table 1), fecundity was the same during both periods (Table 2).

In both periods, only the spermary size was significantly different among populations (Kruskal–Wallis test, $p<0.001$; Tables 3 and S2) and in both reproductive periods, spermary size was negatively correlated with both DT and solar radiation (Table S2; Fig. S6 and S7).

Discussion

Traditionally, seawater temperature cycles and solar radiation fluctuations have been related to reproductive timing of gamete development, fertilization and planulation [16,37] providing a reliable cue to reset the biological clock and trigger the physiological changes related to oocyte yolk deposition [38] and spermary development [26,39,40]. The effects of changing photoperiod and seawater temperature on gametogenic cycles of anthozoans have been largely overlooked [15,41,42]. The reproductive biology of *B. europaea*, studied at Calafuria, shows a reproductive seasonality induced by annual variation of seawater

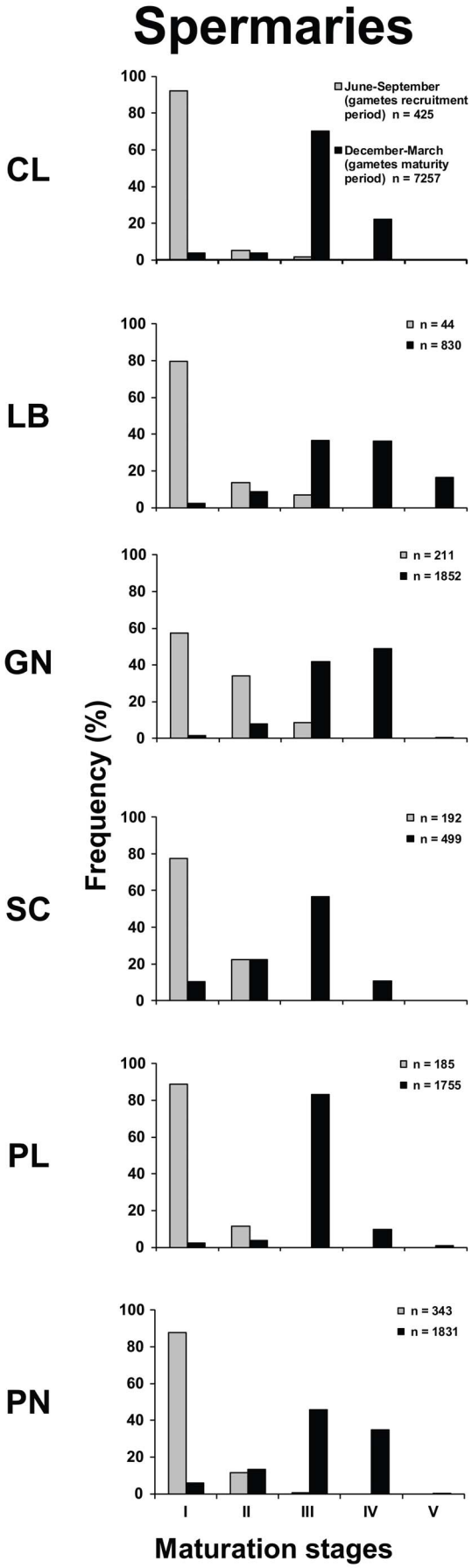

Figure 3. Spermary frequency distribution in the recruitment and maturity periods. Distribution of the maturation stages during gamete recruitment period (gray histogram bars) and gamete maturity period (black histogram bars).
doi:10.1371/journal.pone.0091792.g003

temperature and photoperiod [26]. The same pattern seems to appear in other Mediterranean dendrophylliids like *Leptopsammia pruvoti* [39] and *Astroides calycularis* [40] and in the Mediterranean endemic oculinid *Cladocora caespitosa* [43,44]. A similar periodicity for gamete development and embryonic presence during the recruitment period, suggest an overlap of reproductive seasonality in all populations along the latitudinal gradient by *B. europaea*. In broadcasting scleractinian corals, where temperature dependence leads to location-specific synchronous reproductive times [45], temporal variation in spawning events by corals from different latitudes, over two or more consecutive months, is uncommon [18]. In brooding scleractinians, reproductive cycles are protracted over several months coinciding with environmental seasonality change [46,47].

Specimens from the warmer and more irradiated populations of *B. europaea* generated a significantly greater number of oocytes during the initial stages of gametogenesis (gametes recruitment period). Before fertilization (gametes maturity period), however, individual oocyte number was not related to temperature/irradiance along the gradient, while oocyte size was smaller with increasing temperature (Tables 2 and S1). A reduction of photosynthetic efficiency is documented for several species when temperatures are above optimal [48,49], thereby limiting energetic resources for polyp gametogenesis [9,50]. The onset of gametogenesis (proliferation of germ cells and their differentiation into gametes) may require little energy investment and may, therefore, be less sensitive to selective pressures such as food availability and more reliant on environmental seasonal cycles [51]. In this scenario, warmer populations of *B. europaea* could invest in energetically inexpensive early stages of oogenesis to generate a potential energy resource that would guarantee sufficient metabolic efficiency. On the other hand, the ripening of gametes, especially of oocytes, is an energy consuming process and, therefore, extremely sensitive to selective pressures [51].

Regarding male gametogenesis, during both reproductive periods, the size of spermaries decreased with increasing temperature (Tables 3, S2), while their abundance was not significantly related to environmental parameters. The energetic investment for gametogenesis between males and females is often assumed to differ [52]. For many lower invertebrates, and especially sessile ones, mating effort and parental care are minimal and reproductive output provides a good approximation of the reproductive effort, so most of the energy involved in reproduction is stored in gonads [53]. This "cost of sex" is mainly represented by oogenesis, while the investment of spermary production minimally influences the energetic balance of the organism [52].

For all organisms, energy flow provides an important cost for physiological performance, including maintenance, growth and reproduction, all of which have implications on survival and fitness. Reproductive investment and growth are often used as indicators of health or stress at the organism level (e.g. [54]), and knowledge of how such allocation varies among species or morphological types is crucial for the interpretation of physiological response to environmental factors [53]. Essentially, organisms invest their energy in continuous trade-offs between somatic/skeletal growth and reproduction, which in many species includes the possibility of asexual reproduction [55]. In a changing environment, physiological trade-offs vary through time, reflecting variations in resource availability [56], and the 'energy allocation'

Table 3. Mean abundance, gonadal index and diameter of spermaries in each population.

Gametes recruitment period (June – September)					
Population	**N**	**Abundance (#/100 mm^3) mean ± SE**	**Gonadal Index (%) mean ± SE**	**N**	**Diameter (μm) mean ± SE**
Calafuria	17	140±52	0.010±0.003	425	51.4±1.2
Elba	2	169±106	0.010±0.001	44	54.2±2.8
Genova	1	1463	0.080	211	46.3±1.1
Scilla	6	272±80	0.010±0.004	192	40.7±0.8
Palinuro	6	393±133	0.020±0.006	185	40.0±1.0
Pantelleria	5	760±368	0.030±0.020	343	42.0±0.7
Gametes maturity period (December – March)					
Population	**N**	**Abundance (#/100 mm^3) mean ± SE**	**Gonadal Index (%) mean ± SE**	**N**	**Diameter (μm) mean ± SE**
Calafuria	19	1840±609	1.10±0.40	7257	120.5 ±0.8
Elba	8	595±235	0.47±0.23	830	126.0 ±1.8
Genova	4	2135±1122	1.95±1.51	1852	124.8 ±1.3
Scilla	4	981±561	0.16±0.09	499	81.7 ±1.6
Palinuro	6	1875±1664	0.85±0.80	1755	103.2 ±1.1
Pantelleria	5	2660±2320	0.93±0.25	1831	92.0 ±1.0

Mean abundance, gonadal index and diameter of spermaries in each population for both reproductive periods. The sites are arranged in order of increasing DT; SE, standard error. N, polyps number for abundance and gonadal index, spermaries number for diameter.

doi:10.1371/journal.pone.0091792.t003

explains this partitioning between the various investment options (e.g. growth, sexual reproduction, defense) [57]. For example, the coral *Montipora digitata* under varying light regimes shows an increase of energy allocated to reproduction versus growth at intermediate light levels. In this species the skeletal growth is less susceptible to environmental variations and during periods of resource shortage, energy is preferentially allocated for skeletal growth [57]. *B. europaea* shows a reduction of skeletal density, due to increasing porosity, and especially of pores with larger size, with increasing temperature [28,29,58]. Also its growth and calcification are negatively related to temperature [27,30]. Warmer populations are less stable, showing a progressive reduction in young individuals and reduced population density [29,30]. It has been hypothesized that the decrease in calcification rate [27] and skeletal density [29] in *B. europaea* with increasing temperature could be due to a reduction of energy input available, maybe due to photosynthetic inhibition of the symbionts [29,30]. Populations of *B. europaea* in warmer sites could potentially resorb earlier oocytes adjusting their energetic budget by reallocating the resources destined to oocyte maturity into other vital functions depleted by the negative effect of temperature. Resorption of oocytes is not fully understood, but it is thought that by breaking down the large amount of lipid vesicles in oocytes, energy can be absorbed back into the coral [59]. In the soft coral *Lobophytum compactum*, fecundity is reduced after an induced bleaching event. In this zooxanthellate coral, early oocytes are resorbed to allow development of remaining ones. Energy allocated to reproduction is apparently shifted towards maintaining fewer eggs than normal to ensure that they reach a mature size [37]. The branching coral *Acropora formosa* shows lower survival rate and a resorption of early vitellogenic oocytes after fragmentation, suggesting that there is a trade-off of energy between reproduction and survival [60].

In conclusion, *B. europaea* shows the highest ecological performance in the coldest part of its distribution, characterized by a higher growth coefficient [30], a greater population density [29,61] and a higher efficiency in partitioning the energy budget (this work; [27-30]). On the contrary, populations in warmer regions appear to invest their energy in the initial stages of gametogenesis in order to ensure a sufficient gamete number ready for fertilization in the maturity period. Nevertheless, this effort is not enough to guarantee the same reproductive performance at higher temperatures, as adult populations in warmer sites are less abundant, less stable, and contain fewer young individuals [29,30]. This suggests that increasing temperature may negatively influence post-fertilization life stages, such as larval dispersal, survival and settlement. Depressed organismal condition exhibited by the warmer population could be due to their location near the edge of the species distribution range, where species generally show a lower ecological performance with reduced adaptability to variations in climate [62]. Being endemic to the Mediterranean [63], *B. europaea* has limited potential to respond to seawater warming by migrating northward toward lower temperatures, since the latitudinal range considered covers almost the entire northern distribution of this species [27]. This scenario would indicate a possible reduction in the distribution area of this species, with irrecoverable losses in terms of genetic variability, particularly considering the fragmented genetic structure that characterizes the species [64]. The present study, therefore, confirms the concerns for the future of this endemic species [27–30]. In fact, in a progressively warming Mediterranean, the energetic efficiency of this species could be considerably reduced, affecting vital processes (e.g. growth). Thus, an effective allocation strategy will be crucial for ensuring adaptability to a changing environment.

Supporting Information

Figure S1 Living specimens of *Balanophyllia europaea* photographed at Scilla (South Italy, 38°01′N, 15°38′E). (TIF)

Figure S2 Annual fluctuation of solar radiation and temperature. Mean monthly solar radiation (W/m^2) and temperature (DT; °C) during three years preceding the sampling.

Annual fluctuation referred to January 1995 - December 1997 in the Calafuria population. For the other five populations it referred to January 2009 - December 2011.
(EPS)

Figure S3 Oocyte diameter during recruitment and maturity periods. Monthly size increase of the oocyte diameter during gamete recruitment (gray indicators) and maturity (black indicators) period.
(EPS)

Figure S4 Oocytes. Correlation analyses. Spearman's correlation between reproductive and environmental parameters during gamete recruitment period; N, polyp number for fecundity and gonadal index, oocyte number for diameter; r_s, Spearman's correlation coefficient; p, significance of the correlation test.
(EPS)

Figure S5 Oocytes. Correlation analyses. Spearman's correlation between reproductive and environmental parameters during gamete maturity period; N, polyp number for fecundity and gonadal index, oocyte number for diameter; r_s, Spearman's correlation coefficient; p, significance of the correlation test.
(EPS)

Figure S6 Spermaries. Correlation analyses. Spearman's correlation between reproductive and environmental parameters during gamete recruitment period; N, polyps number for abundance and gonadal index, spermaries number for diameter; r_s, Spearman's correlation coefficient; p, significance of the correlation test.
(EPS)

Figure S7 Spermaries. Correlation analyses. Spearman's correlation between reproductive and environmental parameters during gamete maturity period; N, polyps number for abundance and gonadal index, spermaries number for diameter; r_s, Spearman's correlation coefficient; p, significance of the correlation test.
(TIF)

Table S1 Oocytes. Kruskal-Wallis test and correlation analyses between reproductive and environmental parameters in the sampled populations, in both periods.
(DOC)

Table S2 Spermaries. Kruskal-Wallis test and correlation analyses between reproductive and environmental parameters in the sampled populations, in both periods.
(DOC)

Acknowledgments

We wish to thank M. Ghelia, M. Pisconti, A. Picariello, S. Guerrieri, F. Croci, F. Fasoli, F. Sesso, Centro Immersioni Pantelleria, Il Pesciolino, Bubble Lounge Diving and Submaldive that supplied logistic assistance in the field and collaborated in the underwater activities. We thank F. Sesso also for the picture of a living *B. europaea* specimen. The Scientific Diving School provided scientific, technical, and logistical support. We are grateful to E. Caroselli (University of Bologna), F. Prada (University of Bologna), G. Goodbody-Gringley (Bermuda Institute of Ocean Sciences) for their critical reading and valuable suggestions on the early drafts. Two anonymous reviewers gave comments which improved manuscript quality.

Author Contributions

Conceived and designed the experiments: SG. Performed the experiments: VA FG SG. Analyzed the data: VA FG SG. Contributed reagents/materials/analysis tools: SG. Wrote the paper: VA FG GF OL ZD SG. Gave conceptual advice: GF OL ZD.

References

1. Pandolfi JM, Connolly SR, Marshall DJ, Cohen AL (2011) Projecting coral reef futures under global warming and ocean acidification. Science 333: 418–422.
2. Solomon S, Qin D, Manning M, Chen Z, Marquis M, et al. (2007) Climate Change 2007: The Physical Science Basis. Contribution of Working Group I to the Fourth Assessment Report of the Intergovernmental Panel on Climate Change. Cambridge and New York: Cambridge University Press. 996 p.
3. Parry M (2000) Assessment of potential effects and adaptions for climate change in Europe: The europe acacia project (a concerted action towards a comprehensive climate impacts and adaptions assessment for the European Union). Jackson Environment Institute, University of East Anglia. 320 p.
4. Field CB, Barros V, Stocker TF, Dahe Q (2012) Managing the Risks of Extreme Events and Disasters to Advance Climate Change Adaptation: Special Report of the Intergovernmental Panel on Climate Change. Cambridge and New York: Cambridge University Press. 594 p.
5. Lejeusne C, Chevaldonné P, Pergent-Martini C, Boudouresque CF, Pérez T (2010) Climate change effects on a miniature ocean: the highly diverse, highly impacted Mediterranean Sea. Trends Ecol Evol 25: 250–260.
6. Brierley A, Kingsford M (2009) Impacts of climate change on marine organisms and ecosystems. Curr Biol 19: 602-614.
7. Hoegh-Guldberg OVE, Pearse JS (1995) Temperature, food availability, and the development of marine invertebrate larvae. Am Zool 35: 415–425.
8. Gillooly JF, Charnov EL, West GB, Savage VM, Brown JH (2002) Effects of size and temperature on developmental time. Nature 417: 70–73.
9. Baird AH, Marshall PA (2002) Mortality, growth and reproduction in scleractinian corals following bleaching on the Great Barrier Reef. Mar Ecol Prog Ser 237: 133–141.
10. Albright R, Mason B (2013) Projected near-future levels of temperature and pCO_2 reduce coral fertilization success. PloS One 8: e56468.
11. Linares C, Coma R, Zabala M (2008) Effects of a mass mortality event on gorgonian reproduction. Coral reefs 27: 27–34.
12. Negri AP, Marshall PA, Heyward AJ (2007) Differing effects of thermal stress on coral fertilization and early embryogenesis in four Indo Pacific species. Coral Reefs 26: 759–763.
13. Coma R, Ribes M, Serrano E, Jiménez E, Salat J, et al. (2009) Global warming-enhanced stratification and mass mortality events in the Mediterranean. Proc Natl Acad Sci 106: 6176–6181.
14. Cupido R, Cocito S, Manno V, Ferrando S, Peirano A, et al. (2012) Sexual structure of a highly reproductive, recovering gorgonian population: quantifying reproductive output. Mar Ecol Prog Ser 469: 25–36.
15. Gori A, Linares C, Rossi S, Coma R, Gili JM (2007) Spatial variability in reproductive cycle of the gorgonians *Paramuricea clavata* and *Eunicella singularis* (Anthozoa, Octocorallia) in the Western Mediterranean Sea. Mar Biol 151: 1571–1584.
16. Torrents O, Garrabou J (2011) Fecundity of red coral *Corallium rubrum* (L.) populations inhabiting in contrasting environmental conditions in the NW Mediterranean. Mar Biol 158: 1019–1028.
17. Kipson S, Linares C, Teixidó N, Bakran-Petricioli T, Garrabou J (2012) Effects of thermal stress on the early development stages of a gorgonian coral. Mar Ecol Prog Ser 470: 69–78.
18. Bauman AG, Baird AH, Cavalcante GH (2011) Coral reproduction in the world's warmest reefs: southern Persian Gulf (Dubai, United Arab Emirates). Coral Reefs 30: 405–413.
19. Goffredo S, Radetić J, Airi V, Zaccanti F (2005) Sexual reproduction of the solitary sunset cup coral *Leptopsammia pruvoti* (Scleractinia, Dendrophylliidae) in the Mediterranean. 1. Morphological aspects of gametogenesis and ontogenesis. Mar Biol 147: 485–495.
20. Lesser MP (2013) Using energetic budgets to assess the effects of environmental stress on corals: are we measuring the right things?. Coral Reefs 32: 25–33.
21. Muscatine L (1990) The role of symbiotic algae in carbon and energy flux in reef corals. In: Dubinsky Z, editor. Coral reefs. Ecosystems of the World. New York: Elsiever. vol. 25, pp. 75–87.
22. Henry LA, Hart M (2005) Regeneration from injury and resource allocation in sponges and corals - a review. International review of hydrobiology 90: 125–158.
23. Graham EM, Baird AH, Connolly SR (2008) Survival dynamics of scleractinian coral larvae and implications for dispersal. Coral Reefs 27: 529–539.
24. Weil E, Cróquer A, Urreiztieta I (2009) Yellow band disease compromises the reproductive output of the Caribbean reef-building coral *Montastraea faveolata* (Anthozoa, Scleractinia). Dis Aquat Org 87: 45.
25. Tamelander J (2002) Coral recruitment following a mass mortality event. Ambio 31: 551–557.
26. Goffredo S, Arnone S, Zaccanti F (2002) Sexual reproduction in the Mediterranean solitary coral *Balanophyllia europaea* (Scleractinia, Dendrophylliidae). Mar Ecol Prog Ser 229: 83–94.

27. Goffredo S, Caroselli E, Mattioli G, Pignotti E, Dubinsky Z, et al. (2009) Inferred level of calcification decreases along an increasing temperature gradient in a Mediterranean endemic coral. Limnol Oceanogr 54: 930–937.
28. Caroselli E, Prada F, Pasquini L, Nonnis Marzano F, Zaccanti F, et al. (2011) Environmental implications of skeletal micro-density and porosity variation in two scleractinian corals. Zoology 114: 255–264.
29. Goffredo S, Caroselli E, Pignotti E, Mattioli G, Zaccanti F (2007) Variation in biometry and population density of solitary corals with environmental factors in the Mediterranean Sea. Mar Biol 152: 351–361.
30. Goffredo S, Caroselli E, Mattioli G, Pignotti E, Zaccanti F (2008) Relationships between growth, population structure and sea surface temperature in the temperate solitary coral *Balanophyllia europaea* (Scleractinia, Dendrophylliidae). Coral Reefs 27: 623–632.
31. Goffredo S, Gasparini G, Marconi G, Putignano MT, Pazzini C, et al. (2010) Gonochorism and planula brooding in the Mediterranean endemic orange coral *Astroides calycularis* (Scleractinia: Dendrophylliidae). Morphological aspects of gametogenesis and ontogenesis. Mar Biol Res 6: 421–436.
32. Goffredo S, Marchini C, Rocchi M, Airi V, Caroselli E, et al. (2012) Unusual pattern of embryogenesis of *Caryophyllia inornata* (Scleractinia, Caryophylliidae) in the Mediterranean Sea: Maybe agamic reproduction?. J Morphol 273: 943–956.
33. Korta M, Murua H, Kurita Y, Kjesbu OS (2010) How are the oocytes recruited in an indeterminate fish? Applications of stereological techniques along with advanced packing density theory on European hake (*Merluccius merluccius* L.). Fish Res 104: 56–63.
34. Lowerre-Barbieri SK, Ganias K, Saborido-Rey F, Murua H, Hunter JR (2011) Reproductive timing in marine fishes: variability, temporal scales, and methods. Mar Coast Fish 3: 71–91.
35. Altman DG (1991) Practical statistics for medical research. New York: Chapman & Hall, CRC. 624 p.
36. Potvin C, Roff DA (1993) Distribution-free and robust statistical methods: viable alternatives to parametric statistics?. Ecology 74: 1617–1628.
37. Michalek-Wagner K, Willis BL (2001) Impacts of bleaching on the soft coral *Lobophytum compactum*. I. Fecundity, fertilization and offspring viability. Coral Reefs 19: 231–239.
38. McClintock JB, Watts SA (1990) The effects of photoperiod on gametogenesis in the tropical sea urchin *Eucidaris tribuloides* (Lamarck)(Echinodermata, Echinoidea). J Exp Mar Biol Ecol 139: 175–184.
39. Goffredo S, Airi V, Radetić J, Zaccanti F (2006) Sexual reproduction of the solitary sunset cup coral *Leptopsammia pruvoti* (Scleractinia, Dendrophylliidae) in the Mediterranean. 2. Quantitative aspects of the annual reproductive cycle. Mar Biol 148: 923–931.
40. Goffredo S, Gasparini G, Marconi G, Putignano MT, Pazzini C, et al. (2011) Sexual reproduction in the Mediterranean endemic orange coral *Astroides calycularis* (Scleractinia, Dendrophylliidae). Bull Mar Sci 87: 589–604.
41. Ribes M, Coma R, Rossi S, Micheli M (2007). Cycle of gonadal development in Eunicella singularis (Cnidaria: Octocorallia): trends in sexual reproduction in gorgonians. Inv Biol 126: 307–317.
42. Harrison PL (2011) Sexual reproduction of scleractinian corals. In Coral Reefs: an ecosystem in transition. Springer Netherlands. pp. 59–85.
43. Kružić P, Žuljević A, Nikolić V (2008) Spawning of the colonial coral *Cladocora caespitosa* (Anthozoa, Scleractinia) in the Southern Adriatic Sea. Coral Reefs 27: 337–341.
44. Kersting DK, Casado C, López-Legentil S, Linares C (2013) Unexpected patterns in the sexual reproduction of the Mediterranean scleractinian coral *Cladocora caespitosa*. Mar Ecol Prog Ser 486: 165–171.
45. De Putron SJ, Ryland JS (2009) Effect of seawater temperature on reproductive seasonality and fecundity of *Pseudoplexaura porosa* (Cnidaria, Octocorallia): latitudinal variation in Caribbean gorgonian reproduction. Invertebr Biol 128: 213–222.
46. Fadlallah YH (1983) Sexual reproduction, development and larval biology in scleractinian corals. Coral reefs 2: 129–150.
47. Richmond RH, Hunter CL (1990) Reproduction and recruitment of corals: Comparisons among the Caribbean, the Tropical Pacific, and the Red Sea. Mar Ecol Prog Ser 60: 185–203.
48. Nakamura E, Yokohama Y, Tanaka J (2004) Photosynthetic activity of a temperate coral *Acropora pruinosa* (Scleractinia, Anthozoa) with symbiotic algae in Japan. Phycol Res 52: 38–44.
49. Al-Horani FA (2005) Effects of changing seawater temperature on photosynthesis and calcification in the scleractinian coral *Galaxea fascicularis*, measured with O_2, Ca^{2+} and pH microsensors. Sci Mar 69: 347–354.
50. Rinkevich B (1989) The contribution of photosynthetic products to coral reproduction. Mar Biol 101: 259–263.
51. Ramirez-Llodra E (2002) Fecundity and life-history strategies in marine invertebrates. Adv Mar Biol 43: 87–170.
52. Hayward A, Gillooly JF (2011) The cost of sex: quantifying energetic investment in gamete production by males and females. PloS One 6: e16557.
53. Leuzinger S, Anthony KR, Willis BL (2003) Reproductive energy investment in corals: scaling with module size. Oecologia 136: 524–531.
54. Maltby L (1999) Studying stress: the importance of organism-level responses. Ecol Appl 9: 431–440.
55. Nespolo RF, Halkett F, Figueroa CC, Plantegenest M, Simon JC (2009) Evolution of trade-offs between sexual and asexual phases and the role of reproductive plasticity in the genetic architecture of aphid life histories. Evolution 63: 2402–2412.
56. Fischer B, Dieckmann U, Taborsky B (2011) When to store energy in a stochastic environment. Evolution 65: 1221–1232.
57. Leuzinger S, Willis BL, Anthony KR (2012) Energy allocation in a reef coral under varying resource availability. Mar Biol 159: 177–186.
58. Fantazzini P, Mengoli S, Evangelisti S, Pasquini L, Mariani M, et al. (2013) Time-Domain NMR study of Mediterranean scleractinian corals reveals skeletal-porosity sensitivity to environmental changes. Environ Sci Technol 47: 12679–12686.
59. Lueg JR, Moulding AL, Kosmynin VN, Gilliam DS (2012) Gametogenesis and spawning of *Solenastrea bournoni* and *Stephanocoenia intersepta* in southeast Florida, USA. J Mar Biol 2012.
60. Okubo N, Motokawa T, Omori M (2007) When fragmented coral spawn? Effect of size and timing on survivorship and fecundity of fragmentation in *Acropora formosa*. Mar Biol 151: 353–363.
61. Goffredo S, Mattioli G, Zaccanti F (2004) Growth and population dynamics model of the Mediterranean solitary coral *Balanophyllia europaea* (Scleractinia, Dendrophylliidae). Coral Reefs 23: 433–443.
62. Sagarin RD, Gaines SD, Gaylord B (2006) Moving beyond assumptions to understand abundance distributions across the ranges of species. Trends Ecol Evol 21: 524–530.
63. Zibrowius H (1980) Les Scléractiniaires de la Méditerranée et de l'Atlantique nord-oriental. Mémoires de l'Institut océanographique, Monaco 11.
64. Goffredo S, Mezzomonaco L, Zaccanti F (2004) Genetic differentiation among populations of the Mediterranean hermaphroditic brooding coral *Balanophyllia europaea* (Scleractinia, Dendrophylliidae). Mar Biol 145: 1075–1083.

Chapter 3

Reproductive efficiency of a Mediterranean endemic zooxanthellate coral is unaffected by ocean acidification

Manuscript in preparation

Reproductive efficiency of a mediterranean endemic zooxanthellate coral is unaffected by ocean acidification

Abstract

Increasing of anthropogenic CO_2 in atmosphere, and consequent rise of dissolved CO_2 in oceans, are causing a reduction of seawater pH that will continue to decrease of 0.06-0.32 pH units for the end of this century. Several studies suggests that ocean acidification (OA) will produce negative consequences to many marine organisms. Whereas the effects of OA on corals calcification are well documented, the effects on sexual reproduction are poorly known, and concern only aquaria experiments on tropical corals. A critical question, due to the logistical difficulties of testing the long-term effects, is understand if corals will be able to adapt or acclimate to these changes in seawater chemistry. To assess the long-term effect of OA on oogenesis of temperate zooxanthellate corals *Balanophyllia europaea,* it has been chosen a population that naturally lives along a pCO_2 gradient generated by underwater crater near Panarea Island (Mediterranean Sea, Italy). Oogenesis of *B. europaea* was homogeneous along the pCO_2 gradient, not showing differences in oocytes development, production and morphology. The oogenesis could be maintained unaffected by reallocating additional energy due to increasing of photosynthetic efficiency of zooxanthellae under pCO_2 conditions. Nevertheless, despite the additional energy from zooxanthellae, the population density decrease, probably due to negative effect of increased pCO_2 on early life history stages, suggesting an uncertain future for this species.

Introduction

Rapid uptake of carbon dioxide (CO_2) into the ocean's surface waters, is causing a reduced seawater pH and carbonate ion concentrations (Caldeira and Wickett 2003; Gattuso et al. 1999), producing several important consequences principally on calcifying marine organisms, such as corals (Raven et al. 2005; Hoegh-Guldberg et al. 2007; Kroeker et al. 2010). The ocean acidity has increased by 25–30% (corresponding to 0.1 pH units) since the industrial revolution and is predicted a further increase by 150–200% at the end of the century, equivalent to a drop of 0.3 pH (Stocker et al. 2013). The absorption of CO_2 by water not only produce a drop in pH, but also decrease the availability of free carbonate ions (CO_3^{2-}), essential for the formation of calcareous structures of marine calcifying organisms, including scleractinian corals (Raven et al. 2005; Hofmann et al. 2010).

Laboratory and mesocosm experiments show the negative effects of ocean acidification on calcification, metabolism, survivorship, reproduction, and many other fundamental processes on coral reefs (Stocker et al. 2013; Hoegh-Guldberg et al. 2014), and also accelerates destructive processes including erosion and dissolution of the reef structure (Langdon et al. 2000; Fine and Tchernov 2007). These experiments reproduce the responses of short-term exposure of pCO_2, without reflect natural conditions and the adaptive capability of organism and could overestimate the effects of acidification (Hendriks et al. 2010) due to stress responses (Wood et al. 2008).

Shallow water venting areas provide natural laboratories to assess long-term community responses to ocean acidification (Hall-Spencer et al. 2008; Vizzini et al. 2010; Fabricius et al. 2011; Baggini et al. 2014; Goffredo et al. 2014; Fantazzini et al. 2015; Linares et al. 2015), with the advantage of natural environmental conditions, such as currents, nutrients, light and predators (Meron et al. 2013; Strahl et al. 2015). Several areas characterized by high pCO_2 levels occur worldwide (Tarasov et al. 2005), but many CO_2 vents area are characterized also

by temperature, salinity, total alkalinity, toxic gases and metals variations, which could confound the effects of pCO_2 (Vizzini et al. 2013). Few CO_2 vents are suitable for ocean acidification studies and are localized in Italy (Hall-Spencer et al. 2008; Goffredo et al. 2014; Fantazzini et al. 2015), Papua-New Guinea (Fabricius et al. 2011) and Japan (Inoue et al. 2013). To date, the conducted studies along this CO_2 vent sites display a decrease in population abundance (Hall-Spencer et al. 2008; Fabricius et al. 2011; Goffredo et al. 2014), calcification rate and an increase of carbonate structure dissolution in marine calcifying invertebrates, including corals (Hall-Spencer et al. 2008; Rodolfo-Metalpa et al. 2011; Goffredo et al. 2014). Decreasing pH, due to increasing pCO_2 deeply affects the physiological processes in marine organisms (Harley et al. 2006), causing a reduction in subcellular processes (e.g. protein synthesis and ion exchange; Pörtner et al. 2004) and influencing their physiology, morphology, behaviour, larval dispersal and recruitment (Harley et al. 2006). Overall, some marine organisms could be adapted to a range of ambient CO_2 conditions, e.g. to the high CO_2 concentrations found at underwater volcanic vents.

A population of zooxanthellate scleractinian *Balanophyllia europaea* lives along a pCO_2 gradient generated by underwater volcanic vent, characterized by continuous and localized CO_2 emission (Capaccioni et al. 2007) and located near Panarea Island (Mediterranean Sea, Italy). The low depth and the lack of heated or toxic compounds (Capaccioni et al. 2007; Goffredo et al. 2014), make it a perfect site to investigate the influences of ocean acidification on marine organisms, including *B. europaea*. The gradient is represented by an ambient pH zone (control Site) with comparable values to current environmental conditions of Mediterranean Sea, a low pH zones and a lower pH zones, representing respectively an intermediate and the worse scenarios for the end of this century (Caldeira and Wickett 2003; Stocker et al. 2013). Population density of *B. europaea* significantly decrease along this gradient, until completely disappear in proximity to the vent crater centre (Goffredo et al. 2014).

Sexual reproduction is important for maintaining genetic diversity, influences the community structure (such as population density) and allows the populations replenishment after disturbances. Studying the effects of ocean acidification on coral reproduction is relatively new. Influence of decreasing pH on reproduction of marine invertebrates, such as echinoderms, mollusks and crustaceans was deeply studied in aquarium experiments (Kurihara et al. 2004a,b, 2008; Kurihara and Shirayama 2004a,b; Mayor et al. 2007; Siikavuopio et al. 2007; Havenhand et al. 2008; Kurihara 2008; Havenhand and Schlegel 2009; Byrne et al. 2009, 2010, 2013; Parker et al. 2009; 2010; Ericson et al. 2012; Caldwell et al. 2011; Foo et al. 2012), showing a negative response on fertilization process, especially if sperm concentration is low and limiting (Byrne et al. 2010; Ericson et al. 2010; Reuter et al. 2011; Gonzalez-Bernat et al. 2013), on embryo (Desrosiers et al. 1996) and larval development (Kurihara and Shirayama 2004a,b). Few study investigated the effects of ocean acidification on reproduction of tropical corals, in particular about sperm motility (Morita et al. 2009; Nakamura and Morita 2012), gametogenesis (Fine and Tchernov 2007; Jokiel et al. 2008), fertilization process (Albright et al. 2010; Albright and Mason 2013; Chua et al. 2013), embryonic development (Medina-Rosas et al. 2012) larval settlement and juvenile growth (Kurihara 2008; Suwa et al. 2010; Albright and Langdon 2011; Nakamura et al. 2011; Doropoulos et al. 2012; Chua et al. 2013; Doropoulos and Diaz-Pulido 2013). Most of the research was conducted in tropical corals under laboratory conditions and no one on coral population naturally living along a pCO_2 gradient.

The endemic zooxanthellate Mediterranean scleractinian *B. europaea* (Fig. 1), is a simultaneous hermaphrodite and brooding coral (Goffredo et al. 2002), that lives along a pCO_2 gradient. Previous study on the same *B. europaea* population, show that increasing pCO_2 negatively affect its net calcification rate, due to increased skeletal porosity but no changes in linear extension rate was found (Fantazzini et al. 2015). An increase of photosynthetic

efficiency of coral algae with increasing pCO_2 was registered (*personal observation*), which could represent a further energy available to coral. The aims of this study was describe for the first time the effect of decreasing pH, on oogenesis of a temperate zooxanthellate coral, naturally living along a natural gradient of pCO_2.

Materials and Methods

Study site

Experimental field is located near Panarea Island (Aeolian Archipelago, Sicily, Italy, 38°38′16″N 15°06′37″E; Fig. 1), where an underwater crater (20 x 14 m) at 10 m depth, generates stable continuous column of bubbles contained 98-99% CO_2, 0.2-0.3% N_2, 0.01-0.02% O_2, 0.003-0.005% Ar, 0.001-0.002% CH_4, 0.3-0.6% H_2S by volume, at ambient temperature (Capaccioni et al. 2007; Goffredo et al. 2014). CO_2 dissolution and the effect of acidic dissociation is almost instantaneous and determines a significant lowering of pH and the establishment of the pH gradient.

Carbonate chemistry

Three sampling Sites were selected along the gradient: a control site (Site 1: mean Total Scale pH_{TS} 8.1), located about 34m away from the center of the crater, an intermediate pCO_2 sites (Site 2 mean pH_{TS} 7.9), and a high pCO_2 site (Site 3: mean pH_{TS} 7.7), situated about 9 m from the vents.

pH (NBS scale), temperature (T) and salinity (S) were measured at each Site during several surveys between July 2010 and May 2013 with a multi-parametric probe (600R, YSI Incorporated, USA) and operated by SCUBA divers. Total alkalinity (TA) was measured on water samples collected in each Site using sterile 120 ml syringes (two replicates for each site). Syringe samples were immediately transferred in labelled 100 ml amber glass bottles and fixed with saturated mercuric chloride ($HgCl_2$) to avoid biological alteration, and stored in darkness

at 4°C prior to measurement. TA was measured by Gran titration, using a 702 SM Titrino (Metrohm AG). Measured pH_{NBS} was converted in total scale (TS) using CO2SYS software (Mehrbach et al. 1973; Dickson 1990; Dickson and Millero 1987). Temperature sensors (Thermochron iButton, DS1921G, Maxim Integrated Products, USA) were placed near each Site and recorded depth temperature (T; °C) every three hours from June 2011 to May 2013 and replaced to each field campaign. The pH, T, S and TA were used to calculate other carbonate system parameters using the software CO2SYS with referenced dissociation constant. The study site has stable hydrothermal–chemical properties and only pCO_2 concentration differed significantly across sites (Capaccioni et al. 2007; Goffredo et al. 2014).

Sampling

Ten specimens of *B. europaea* were randomly collected by SCUBA diving in each of the three study Sites along the pH gradient on April 28th 2013. On the basis of previous detailed studies on sexual reproduction of this species, in this period the reproductive cycle present the maximum gonadal development (before the fertilization process), characterized by two stock of oocytes, a small one (< 300 µm) that will be fertilized in the following reproductive year, and a large one (> 300 µm; mature oocytes) that will be fertilized in the same reproductive year (Goffredo et al. 2002; Airi et al. 2014).

Only sexually mature individuals (length > 6 mm) was chosen to limit damage on the natural population, which significantly diminishes along the acidified gradient (Goffredo et al. 2014).

Cyto-Histometric Analysis

Biometric analysis of each polyp was performed by measuring length (L, major axis of the oral disk), width (w, minor axis of the oral disk), and height (h, oral–aboral diameter). The body volume (V) was calculated using the equation: $V = (L/2)*(W/2)*h*\pi$ (Goffredo et al. 2002). Biometric parameters were used to calculate Reproductive Parameters (see paragraph below).

Polyps were post-fixed in Bouin solution. After decalcification in EDTA and dehydration in a graded alcohol series from 80 to 100%, polyps were embedded in paraffin, and serial transverse sections were cut at 7µm intervals along the oral–aboral axis, from the oral to the aboral poles. Tissues were stained with Mayer's hematoxylin and eosin (Goffredo et al. 2002).

Cytometric analysis were made with a light microscope NIKON Eclipse 80i using an image analysis systems: NIKON NIS-Elements D 3.1. The maximum and minimum diameters of oocytes, in nucleated sections, were measured.

Reproductive parameters

Reproductive output were defined through three reproductive parameters: 1*) oocytes abundance* defined as the number of reproductive elements per body volume unit (100 mm^3); 2) *gonadal index*, defined as the percentage of body volume occupied by oocytes; 3) *oocytes size*, defined as the average of the maximum and minimum diameter of oocytes in nucleated section.

Statistical analyses

A one-way permutation multivariate analysis of variance (PERMANOVA, Anderson 2005) based on Euclidean distances was performed to test differences between oocytes distribution among Sites using Primer software.

Levene's test was used to test homogeneity of variance and Shapiro-Wilk test was used for testing normality of distribution, useful when sample size is lower than 2000.

The non-parametric Kruskal-Wallis equality-of-populations rank test was used to compare reproductive parameters among Sites, used when assumptions for parametric statistics were not fulfilled. Spearman's rank correlation coefficient was used to calculate the significance of the correlations between oocytes diameters and pH. Spearman's rank correlation coefficient is an alternative to Pearson's correlation coefficient (Altman 1991). It is useful for data that are

non-normally distributed and do not meet the assumptions of Pearson's correlation coefficient (Potvin and Roff 1993). The analyses were computed using PASW Statistics 22.0.

Results

All polyps analyzed were hermaphrodite, containing both oocytes and spermaries.

The size/frequency distribution of oocytes was homogeneous among Sites (Fig. 2) and all Sites shown two distinct stocks of oocyte, characterized respectively by small (immature, 300 mm) and large (mature, 300 mm) cells (Fig. 2).

No differences in oocytes morphology of early, intermediate and late stages, was found along the pCO_2 gradient (Fig.3).

Oocytes abundance and gonadal index did not show differences among Sites (Tab.2; Fig. 4). Only the oocyte diameters was different (Kruskal-Wallis test, $p < 0.001$) and correlated with pH, but without a clear pattern (Tab.2; Fig. 4).

Discussion

To date, the studies on effect of increasing pCO_2 on gametogenesis of corals are very few and the most are on tropical species expose to aquaria experiments. *Montipora capitata* colonies exposed for 6 months under acidified conditions (+365 µatm pCO_2) did not show a decrease in gamete production (Jokiel et al. 2008). Fine and Tchernov (2007) found a similar trend, reporting normal gametogenesis in *Oculina patagonica* and *Madracis pharencis* after 12 months to exposure to acidified conditions. Population of *B. europaea* born and grew along a natural pCO_2 gradient displayed the same pattern on oogenesis, not showing differences in oocytes timing development, production and morphology among different CO_2 conditions. Despite the statistical differences found in oocytes diameters, the oocytes size seemed not influenced to increasing pCO_2, as showed in Figure 4. A parallel study on spermatogenesis of the same population of *B. europaea* revealed no differences in spermary development,

production and morphology among Sites (Marchini 2016), suggesting that increasing pCO_2 seemed to not affect the reproductive performance of this species. Sexual reproduction is a fundamental process to maintain genetic differences and influences the community structure (such as population density) through several mechanisms, including gamete production. Despite the unchanged gametes production among Sites, population density of *B. europaea* decreases by thrice with increasing proximity to the vent crater centre, dropping to zero in the most acidic zone, where the pH drops to 7.4 (Goffredo et al. 2014).

Sexual reproduction of brooder corals occurs through the release of sperms into the water, followed by internal fertilization inside the oogenetic conspecific coral. Consequently, water chemistry can greatly affect fertilization success. Previous studies show that increased pCO_2 reduced sperm flagellar motility in oysters (Parker et al. 2009), sea urchins (Havenhand et al. 2008; Kurihara 2008) and corals (Morita et al. 2009; Nakamura and Morita 2012), impairs the fertilization success mainly with low sperm concentration (Albright et al. 2010; Albright and Meson 2013). The same spermaries production found in *B. europaea* among Sites, could suggest that decreasing of population density along pCO_2 gradient could be due mainly to negative effect on early life history stages, including larval metabolism, development, settlement, post-settlement growth and survival. Respiration experiments on larvae of tropical coral *Porites astreoides* show larval metabolic rates significantly depressed with increasing pCO_2 (Albright and Langdon 2011). If the decreasing respiration rates contribute to decreased larval motility, the ability of larvae to change their position in water to look for an ideal settlement could be negatively influenced, affecting the population dispersion (Mundy and Babcock 1998; Raimondi and Morse 2000). Acidification negatively affects larval settlement and metamorphosis in three marine bivalves (Talmage and Gobler 2009) and in the caribbean coral, *Acropora palmata*, displaying a decreasing settlement success, as indirect effect of increasing pCO_2 (Albright et al. 2010; Albright and Langdon 2011). Acidification also

negatively affects post-settlement growth and calcification in a several species of scleractinian (Albright et al. 2008, 2010; Kurihara et al. 2008; Cohen et al. 2009; Suwa et al. 2010; Anlauf et al. 2011; Albright and Langdon 2011; de Putron et al. 2011), influencing the new recruits ability for space competition, with consequent increase of post-settlement mortality.

Despite the few knowledges about the effect of low pH on corals sexual reproduction reveal no signal on gametogenesis, many studies on early life history stages of coral show negative effects. Similar negative trend was found on coral calcification. Several evidence indicates that corals calcification is negatively affected to decreasing pH (Gattuso et al. 1998; Leclercq et al. 2002; Marubini et al. 2003; Schneider and Erez 2006; Fine and Tchernov 2007, Crook et al. 2013; Iglesias-Prieto et al. 2014; Fantazzini et al. 2015), and is expected a further decreased of 17–37% by the end of this century, as a result of reduced seawater [CO_3^{2-}] (Kleypas et al. 2006). Atlantic coral *Porites astreoides*, growing in an environment of low pH along the Caribbean coast of the Yucatan Peninsula shows a 35% reduction in the calcification rates respect the corals of the same species living in close proximity under ambient pH condition (Crook et al. 2013). Similar results were found in aquaria experiments (Anthony et al. 2008; de Putron et al. 2011). The calcification rates of tropical corals *Acropora intermedia* and *Porites lobata* exposed to high CO_2 conditions for 8 weeks, was about 40% lower than control conditions (Anthony et al. 2008). Samples of *B. europaea* transplanted along a CO_2 gradient off Ischia (Italy) show a decrease of net calcification rate but a gross calcification significantly increased with increasing of pCO_2, suggesting that the decrease of net calcification rate was the result of increased dissolution rates (Rodolfo-Metalpa et al. 2011). With increasing pCO_2, also the natural population of *B. europaea* reveals a decrease of net calcification rate (Fantazzini et al. 2015), due to decreasing skeletal density, caused by increased porosity, but no changes in linear extension rate was observed (Fantazzini et al. 2015). *B. europaea* could keep linear extension rate constant, to face functional reproductive requests (e.g. the ability to

reach critical size at sexual maturity), at the expense of mechanical strength of the skeletons (Fantazzini et al. 2015).

Another study on the same species transplanted along the same gradient, show that with increasing pCO_2, increase the photosynthetic efficiency of coral algae (*personal observation*), representing a further energy available to coral. *B. europaea* could using this additional energy to compensate the effect of pCO_2 on reproductive potential and linear extension rate, maintain them constant among Sites.

By collecting all the information about the natural population of *B. europaea* and other studies, is possible to deduce that *B. europaea* could compensate the dissolution skeleton rate, due to increasing pCO_2, with increasing skeletal porosity to maintain linear extension rate and reach sexual maturity. The gametogenesis and linear extension rate could be maintained unaffected by reallocating additional energy due to increasing of photosynthetic efficiency. Neverless, despite the additional energy from zooxanthellae, the population density decrease, probably due to negative effect of increased pCO_2 on early life history stages, suggesting an uncertain future for this species.

References

Airi V, Gizzi F, Falini G, Levy O, Dubinsky Z, Goffredo S (2014) Reproductive efficiency of a Mediterranean endemic zooxanthellate coral decreases with increasing temperature along a wide latitudinal gradient. PloS ONE. 9:e91792.

Albright R, Mason B, Langdon C (2008) Effect of aragonite saturation state on settlement and post-settlement growth of *Porites astreoides* larvae. Coral Reefs. 27:485-490.

Albright R, Mason B, Miller M, Langdon C (2010) Ocean acidification compromises recruitment success of the threatened Caribbean coral *Acropora palmata*. Proc. Natl. Acad. Sci. USA. 107:20400-20404.

Albright R, Langdon C (2011) Ocean acidification impacts multiple early life history processes of the Caribbean coral *Porites astreoides*. Global Change Biol. 17: 2478-2487.

Albright R, Mason B (2013) Projected near-future levels of temperature and pCO_2 reduce coral fertilization success. PLoS ONE. 8:e56468.

Altman DG (1991) Practical statistics for medical research. Chapman & Hall, London. 613 p.

Anderson MJ (2005) Permutational multivariate analysis of variance. Department of Statistics, University of Auckland, Auckland. 24 p.

Anlauf H, D'Croz L, O'Dea A (2011) A corrosive concoction: the combined effects of ocean warming and acidification on the early growth of a stony coral are multiplicative. J. Exp. Mar. Biol. Ecol. 397:13-20.

Anthony KR, Kline DI, Diaz-Pulido G, Dove S, Hoegh-Guldberg O (2008) Ocean acidification causes bleaching and productivity loss in coral reef builders. Proc. Natl. Acad. Sci. USA. 105:17442-17446.

Baggini C, Salomidi M, Voutsinas E, Bray L, Krasakopoulou E, Hall-Spencer JM (2014) Seasonality Affects Macroalgal Community Response to Increases in pCO_2. PloS ONE. 9:e106520.

Byrne M, Ho M, Selvakumaraswamy P, Nguyen HD, Dworjanyn SA, Davis AR (2009) Temperature, but not pH, compromises sea urchin fertilization and early development under near-future climate change scenarios. Proc. R. Soc. Lond. B Biol. Sci. 276:1883-1888.

Byrne M, Soars NA, Ho MA, Wong E, McElroy D, Selvakumaraswamy P, Dworjanyn SA, Davis AR (2010) Fertilization in a suite of coastal marine invertebrates from SE Australia is robust to near-future ocean warming and acidification. Mar. Biol. 157:2061-2069.

Byrne M, Gonzalez-Bernat M, Doo S, Foo S, Soars N, Lamare M (2013) Effects of ocean warming and acidification on embryos and non-calcifying larvae of the invasive sea star *Patiriella regularis*. Mar. Ecol. Prog. Ser. 473:235-246.

Caldeira K, Wickett ME (2003) Oceanography: anthropogenic carbon and ocean pH. Nature. 425:365.

Caldwell GS, Fitzer S, Gillespie CS, Pickavance G, Turnbull E, Bentley MG (2011) Ocean acidification takes sperm back in time. Invert. Reprod. Develop. 55:217-221.

Capaccioni B, Tassi F, Vaselli, O, Tedesco D, Poreda R (2007) Submarine gas burst at Panarea Island (southern Italy) on 3 November 2002: A magmatic versus hydrothermal episode. J. Geophys. Res. Solid Earth (1978–2012). 112:B5.

Chua CM, Leggat W, Moya A, Baird AH (2013) Temperature affects the early life history stages of corals more than near future ocean acidification. Mar. Ecol. Prog. Ser. 475:85-92.

Cohen AL, McCorkle DC, de Putron S, Gaetani GA, Rose KA (2009) Morphological and compositional changes in the skeletons of new coral recruits reared in acidified seawater: Insights into the biomineralization response to ocean acidification. Geochem. Geophys. Geosyst. 10.

Crook ED, Cohen AL, Rebolledo-Vieyra M, Hernandez L, Paytan A (2013) Reduced calcification and lack of acclimatization by coral colonies growing in areas of persistent natural acidification. Proc. Natl. Acad. Sci. USA. 110:11044-11049.

de Putron SJ, McCorkle DC, Cohen AL, Dillon AB (2011) The impact of seawater saturation state and bicarbonate ion concentration on calcification by new recruits of two Atlantic corals. Coral Reefs. 30:321-328.

Desrosiers RR, Désilets J, Dubé F (1996) Early developmental events following fertilization in the giant scallop *Placopecten magellanicus*. Can. J. Fish. Aquat. Sci. 53:1382-1392.

Dickson AG, Millero FJ (1987) A comparison of the equilibrium constants for the dissociation of carbonic acid in seawater media. Deep-Sea Res. A. 34:1733-1743.

Dickson AG (1990) Thermodynamics of the dissociation of boric acid in synthetic sea water from 273.15 to 298.15 K. Deep-Sea Res. A. 37:755-766.

Doropoulos C, Ward S, Diaz-Pulido G, Hoegh-Guldberg O, Mumby PJ (2012) Ocean acidification reduces coral recruitment by disrupting intimate larval-algal settlement interactions. Ecol. Lett. 15-338-346.

Doropoulos C, Diaz-Pulido G (2013). High CO_2 reduces the settlement of a spawning coral on three common species of crustose coralline algae. Mar. Ecol. Prog. Ser. 475:93-99.

Ericson JA, Lamare MD, Morley SA, Barker MF (2010) The response of two ecologically important Antarctic invertebrates (*Sterechinus neumayeri* and *Parborlasia corrugatus*) to reduced seawater pH: effects on fertilisation and embryonic development. Mar. Biol. 157:2689-2702.

Ericson JA, Ho MA, Miskelly A, King CK, Virtue P, Tilbrook B, Byrne M (2012) Combined effects of two ocean change stressors, warming and acidification, on fertilization and early development of the Antarctic echinoid *Sterechinus neumayeri*. Polar Biol. 35:1027-1034.

Fabricius KE, Langdon C, Uthicke S, Humphrey C, Noonan S, De'ath G, Okazaki R, Muehllehner N, Glas MS, Lough JM (2011) Losers and winners in coral reefs acclimatized to elevated carbon dioxide concentrations. Nature Clim. Change. 1:165-169.

Fantazzini P, Mengoli S, Pasquini L, Bortolotti V, Brizi L, Mariani M, Di Giosia M, Fermani S, Capaccioni B, Caroselli E, Prada F, Zaccanti F, Levy O, Dubinsky Z, Kaandorp JA, Konglerd P, Hammel JU, Dauphin Y, Cuif JP, Weaver JC, Fabricius KE, Wagermaier W, Fratzl P, Falini G,

Goffredo S (2015) Gains and losses of coral skeletal porosity changes with ocean acidification acclimation. Nat. Commun. 6:7785.

Fine M, Tchernov D (2007) Scleractinian coral species survive and recover from decalcification. Science. 315:1811-1811.

Foo SA, Dworjanyn SA, Poore AG, Byrne M (2012) Adaptive capacity of the habitat modifying sea urchin *Centrostephanus rodgersii* to ocean warming and ocean acidification: performance of early embryos. PLoS ONE. 7:e42497.

Gattuso JP, Frankignoulle M, Bourge I, Romaine S, Buddemeier RW (1998) Effect of calcium carbonate saturation of seawater on coral calcification. Global Planet. Change. 18:37-46.

Gattuso JP, Allemand D, Frankignoulle M (1999) Photosynthesis and calcification at cellular, organismal and community levels in Coral Reefs: A review on interactions and control by carbonate chemistry. Am. Zool. 39:160-183.

Goffredo S, Arnone S, Zaccanti F (2002) Sexual reproduction in the Mediterranean solitary coral *Balanophyllia europaea* (Scleractinia, Dendrophylliidae). Mar. Ecol. Prog. Ser. 229:83-94.

Goffredo S, Prada F, Caroselli E, Capaccioni B, Zaccanti F, Pasquini L, Fantazzini P, Fermani S, Reggi M, Levy O, Fabricius KE (2014) Biomineralization control related to population density under ocean acidification. Nature Clim. Change. 4:593-597.

Gonzalez-Bernat MJ, Lamare M, Uthicke S, Byrne M (2013) Fertilisation, embryogenesis and larval development in the tropical intertidal sand dollar *Arachnoides placenta* in response to reduced seawater pH. Mar. Biol. 160:1927-1941.

Hall-Spencer JM, Rodolfo-Metalpa R, Martin S, Ransome E, Fine M, Turner SM, Rowley SJ, Tedesco D, Buia MC (2008) Volcanic carbon dioxide vents show ecosystem effects of ocean acidification. Nature. 454:96-99.

Harley CD, Randall Hughes A, Hultgren KM, Miner BG, Sorte CJ, Thornber CS, Rodriguez LF, Tomanek L, Williams SL (2006) The impacts of climate change in coastal marine systems. Ecol. Lett. 9:228-241.

Havenhand JN, Buttler FR, Thorndyke MC, Williamson JE (2008) Near-future levels of ocean acidification reduce fertilization success in a sea urchin. Curr. Biol. 18:R651-R652.

Havenhand JN, Schlegel P (2009) Near-future levels of ocean acidification do not affect sperm motility and fertilization kinetics in the oyster *Crassostrea gigas*. Biogeosciences. 6:3009-3015.

Hendriks IE, Duarte CM, Álvarez M (2010) Vulnerability of marine biodiversity to ocean acidification: a meta-analysis. Estuar. Coast. Mar. Sci. 86:157-164.

Hoegh-Guldberg O, Mumby PJ, Hooten AJ, Steneck RS, Greenfield P, Gomez E, Harvell CD, Sale PF, Edwards AJ, Caldeira K, Knowlton N, Eakin CM, Iglesias-Prieto R, Muthiga N, Bradbury RH, Dubi A, Hatziolos ME (2007) Coral Reefs under rapid climate change and ocean acidification. Science. 318:1737-1742.

Hoegh-Guldberg O, Cai R, Poloczanska ES, Brewer PG, Sundby S, Hilmi K, Fabry VJ, Jung S (2014) The Ocean. In: Climate Change 2014: Impacts, Adaptation, and Vulnerability. Part B: Regional Aspects. Contribution of Working Group II to the Fifth Assessment Report of the Intergovernmental Panel on Climate Change. Barros VR, Field CB, Dokken DJ, Mastrandrea MD, Mach KJ, Bilir TE, Chatterjee M, Ebi KL, Estrada YO, Genova RC, Girma B, Kissel ES, Levy AN, MacCracken S, Mastrandrea PR, White LL (eds.) Cambridge University Press, Cambridge, United Kingdom and New York, NY, USA. 76 p.

Hofmann GE, Barry JP, Edmunds PJ, Gates RD, Hutchins DA, Klinger T, Sewell MA (2010) The effect of ocean acidification on calcifying organisms in marine ecosystems: an organism-to-ecoystem perspective. Annu. Rev. Ecol. Evol. Syst. 41:127-147.

Iglesias-Prieto R, Galindo-Martinez CT, Enriquez S, Carricart-Ganivet JP (2014) Attributing reductions in coral calcification to the saturation state of aragonite, comments on the effects of persistent naturals acidification. Proc. Natl. Acad. Sci. USA. 111:E300-E301.

Inoue S, Kayanne H, Yamamoto S, Kurihara H (2013) Spatial community shift from hard to soft corals in acidified water. Nature Clim. Change. 3: 683-687.

Jokiel PL, Rodgers KS, Kuffner IB, Andersson AJ, Cox EF, Mackenzie FT (2008) Ocean acidification and calcifying reef organisms: a mesocosm investigation. Coral Reefs. 27:473-483.

Kleypas JA, Feely RA, Fabry VJ, Langdon C, Sabine CL, Robbins LL (2006) Impacts of Ocean Acidification on Coral Reefs and Other Marine Calcifiers: A Guide for Future Research, report of a workshop held 18-20 April 2005, St. Petersburg, FL, sponsored by NSF, NOAA, and the U.S. Geological Survey. 88 p.

Kroeker KJ, Kordas RL, Crim RN, Singh GG (2010) Meta-analysis reveals negative yet variable effects of ocean acidification on marine organisms. Ecol. Lett. 13:1419-1434.

Kurihara H, Shirayama Y (2004a) Effects of increased atmospheric CO_2 on sea urchin early development. Mar. Ecol. Prog. Ser. 274:161-169.

Kurihara H, Shirayama Y (2004b) Effects of increased atmospheric CO_2 and decreased pH on sea urchin embryos and gametes. Echinoderms: München, Taylor & Francis Group, London, United Kingdom. 5 p.

Kurihara H, Shimode S, Shirayama Y (2004a) Effects of raised CO_2 concentration on the egg production rate and early development of two marine copepods (*Acartia steueri* and *Acartia erythraea*). Marine Poll. Bull. 49:721-727.

Kurihara H, Shimode S, Shirayama Y (2004b) Sub-lethal effects of elevated concentration of CO_2 on planktonic copepods and sea urchins. J. Oceanogr. 60:743-750.

Kurihara H (2008) Effects of CO_2-driven ocean acidification on the early developmental stages of invertebrates. Mar. Ecol. Prog. Ser. 373:275-284.

Kurihara H, Asai T, Kato S, Ishimatsu A (2008) Effects of elevated pCO_2 on early development in the mussel *Mytilus galloprovincialis*. Aquatic Biol. 4:225-233.

Langdon C, Takahashi T, Sweeney C, Chipman D, Goddard J, Marubini F, Aceves H, Barnett H, Atkinson MJ (2000) Effect of calcium carbonate saturation state on the calcification rate of an experimental coral reef. Global Biogeochem. Cy. 14:639-654.

Leclercq N, Gattuso J-P, Jaubert J (2002) Primary production, respiration, and calcification of a coral reef mesocosm under increased CO_2 partial pressure. Limnol. Oceanogr. 47:558-564.

Linares C, Vidal M, Canals M, Kersting DK, Amblas D, Aspillaga E, Cebrián E, Delgado-Huertas A, Díaz D, Garrabou J, Hereu B (2015) Persistent natural acidification drives major distribution shifts in marine benthic ecosystems. Proc. R. Soc. Lond. B Biol. Sci. 282:20150587.

Marchini C (2016) Reproduction and population structure in temperate and tropical corals in relation to environmental parameters. PhD thesis in Biodiversity end Evolution. University of Bologna, Italy.

Marubini F, Ferrier-Page`s C, Cuif JP (2003) Suppression of growth scleractinian corals by decreasing ambient carbonate ion concentration: a cross-family comparison. Proc. R. Soc. Lond. B Biol. Sci. 270:179-184.

Mayor DJ, Matthews C, Cook K, Zuur AF, Hay S (2007) CO_2-induced acidification affects hatching success in *Calanus finmarchicus*. Mar. Ecol. Prog. Ser. 350:91-97.

Medina-Rosas P, Szmant, AM, Whitehead RF (2012) CO_2 enrichment and reduced seawater pH had no effect on the embryonic development of *Acropora palmata* (Anthozoa, Scleractinia). Invertebr. Reprod. Dev. 57:132-141.

Mehrbach C, Culberson CH, Hawley JE, Pytkowicz RM (1973) Measurement of the apparent dissociation constants of carbonic acid in seawater at atmospheric pressure. Limnol. Oceanogr. 18:897-907.

Meron D, Buia MC, Fine M, Banin E (2013) Changes in microbial communities associated with the sea anemone Anemonia viridis in a natural pH gradient. Microb. Ecol. 65:269-276.

Morita M, Suwa R, Iguchi A, Nakamura M, Shimada K, Sakai K, Suzuki A (2009) Ocean acidification reduces sperm flagellar motility in broadcast spawning reef invertebrates. Zygote. 18:103-107.

Mundy CN, Babcock RC (1998) Role of light intensity and spectral quality in coral settlement: implications for depth-dependent settlement?. J. Exp. Mar. Biol. Ecol. 223:235-255.

Nakamura M, Ohki S, Suzuki A, Sakai K (2011) Coral larvae under ocean acidification: survival, metabolism, and metamorphosis. PLoS ONE. 6:e14521.

Nakamura M, Morita M (2012) Sperm motility of the scleractinian coral *Acropora digitifera* under preindustrial, current, and predicted ocean acidification regimes. Aquatic Biol. 15:299-302.

Parker LM, Ross PM, O'Connor WA (2009) The effect of ocean acidification and temperature on the fertilization and embryonic development of the Sydney rock oyster *Saccostrea glomerata* (Gould 1850). Global Change Biol. 15:2123-2136.

Parker LM, Ross PM, O'Connor WA (2010) Comparing the effect of elevated pCO_2 and temperature on the fertilization and early development of two species of oysters. Mar. Biol. 157:2435-2452.

Pörtner HO, Langenbuch M, Reipschläger A (2004) Biological impact of elevated ocean CO_2 concentrations: lessons from animal physiology and earth history. J.Oceanogr. 60:705-718.

Potvin C, Roff DA (1993) Distribution-free and robust statistical methods: viable alternatives to parametric statistics. Ecology. 74:1617-1628.

Raimondi PT, Morse AN (2000) The consequences of complex larval behavior in a coral. Ecology. 81:3193-3211.

Raven J, Caldeira K, Elderfield H, Hoegh-Guldberg O, Liss P, Riebesell U, Shepherd J, Turley C, Watson A (2005) Ocean acidification due to increasing atmospheric carbon dioxide. The Royal Society. 60 p.

Reuter KE, Lotterhos KE, Crim RN, Thompson CA, Harley CD (2011) Elevated pCO_2 increases sperm limitation and risk of polyspermy in the red sea urchin *Strongylocentrotus franciscanus.* Global Change Biol. 17:163-171.

Rodolfo-Metalpa R, Houlbrèque F, Tambutté É, Boisson F, Baggini C, Patti FP, Jeffree R, Fine M, Foggo A, Gattuso JP, Hall-Spencer JM (2011) Coral and mollusc resistance to ocean acidification adversely affected by warming. Nature Clim. Change. 1:308-312.

Schneider K, Erez J (2006) The effect of carbonate chemistry on calcification and photosynthesis in the hermatypic coral *Acropora eurystoma*. Limnol. Oceanogr. 51:1284-1293.

Siikavuopio SI, Mortensen A, Dale T, Foss A (2007) Effect of carbon dioxide exposure on feed intake and gonad growth in green sea urchin, *Strongylocentrotus droebachiensis*. Acquaculture. 266:97-101.

Stocker TF, Qin D, Plattner GK, Tignor M, Allen SK, Boschung J, Nauels A, Xia Y, Bex V, Midgley PM (eds) IPCC 2013: Summary for Policymakers. In: Climate Change 2013: The Physical Science Basis. Contribution of Working Group I to the Fifth Assessment Report of the Intergovernmental Panel on Climate Change. Cambridge University Press, Cambridge, United Kingdom and New York, NY, USA. 1535 p.

Strahl J, Stolz I, Uthicke S, Vogel N, Noonan SHC, Fabricius KE (2015) Physiological and ecological performance differs in four coral taxa at a volcanic carbon dioxide seep. Comp. Biochem. Physiol. A Mol. Integr. Physiol. 184:179-186.

Suwa R, Nakamura M, Morita M, Shimada K, Iguchi A, Sakai K, Suzuki A (2010) Effects of acidified seawater on early life stages of scleractinian corals (Genus Acropora). Fish. Sci. 76:93-99.

Talmage SC, Gobler CJ (2009) The effects of elevated carbon dioxide concentrations on the metamorphosis, size, and survival of larval hard clams (*Mercenaria mercenaria*), bay scallops (*Argopecten irradians*), and Eastern oysters (*Crassostrea virginica*). Limnol. Oceanogr. 54:2072.

Tarasov VG, Gebruk AV, Mironov AN, Moskalev LI (2005) Deep-sea and shallow-water hydrothermal vent communities: Two different phenomena?. Chem. Geol. 224:5-39.

Vizzini S, Tomasello A, Maida GD, Pirrotta M, Mazzola A, Calvo S (2010) Effect of explosive shallow hydrothermal vents on δ13C and growth performance in the seagrass *Posidonia oceanica.* J. Ecol. 98:1284-1291.

Vizzini S, Di Leonardo R, Costa V, Tramati CD, Luzzu F, Mazzola A (2013) Trace element bias in the use of CO_2 vents as analogues for low pH environments: implications for contamination levels in acidified oceans. Estuarine, Coastal and Shelf. Science. 134:19-30.

Wood HL, Spicer JI, Widdicombe S (2008) Ocean acidification may increase calcification rates, but at a cost. Proc. R. Soc. Lond. B Biol. Sci. 275:1767-1773.

Tables

Table 1. Seawater carbonate chemistry for each transplantation Site. The pH, temperature (T), total alkalinity (TA) and salinity (S) were used to calculate all the other parameters using CO2SYS software with dissociation constants. Mean pH values were calculated after conversion of data to hydrogen ion concentrations. Mean values are reported with minimum and maximum values in brackets.

Measured Parameters

Site	pH range (total scale)	T (°C)	TA (µmol kg^{-1})	S (‰)
1	8.07 (7.82-8.45)	20.5 (14.3-26.0)	2438 (2368-2600)	37 (33-38)
2	7.87 (7.54-8.25)	20.7 (14.4-26.0)	2429 (2334-2618)	37 (33-38)
3	7.74 (7.05-8.21)	20.6 (14.4-26.0)	2426 (2343-2610)	37 (34-38)

Calculated Parameters

Site	*pCO_2 (µatm)	*HCO_3^- (µmol kg^{-1})	*CO_3^{2-} (µmol kg^{-1})	*DIC (µmol kg^{-1})	*Ω_{arag}
1	391 (127-780)	1869 (1466-2144)	232 (120-398)	2114 (1867-2291)	3.6 (1.8-6.3)
2	672 (234-1561)	2030 (1664-2264)	163 (68-314)	2214 (1984-2383)	2.5 (1.1-5.0)
3	907 (262-5100)	2073 (1835-2365)	144 (25-243)	2246 (2089-2552)	2.2 (0.4-3.9)

pH (n = 103-110 per Site), T (n = 2580 per Site) was recorded from May to September 2012 and from November 2012 to April 2013. and S (n = 107-110 per Site) were measured in July 2010, September 2010, November 2010, March 2011, June 2011, July-August 2011, November-December 2011, April-May 2012, June 2012 and May 2013. TA (n = 14 per Site) was measured in September 2010, November 2010, March 2011, June 2011, July-August 2011, November-December 2011, April-May 2012, June 2012 and May 2013. pCO2 = carbon dioxide partial pressure; HCO3- = bicarbonate; CO_3^{2-} = carbonate; DIC = dissolved inorganic carbon; Ωarag = aragonite saturation.

Table 2. Mean values ± SE of abundance, gonadal index and diameter of oocytes for each Sites.

Site	pH_{TS}	N_p	Abundance (#/100 mm^3)	Gonadal Index (%)	N_o	Diameter (µm)
1	8.07	7	254 ± 70	1.4 ± 0.3	672	260 ± 6.6
2	7.87	7	177 ± 73	0.9 ± 0.3	426	268 ± 7.8
3	7.74	6	289 ± 89	2.3 ± 0.7	745	290 ± 6.9

N_p = polyp number for abundance and gonadal index, N_o = oocyte number for diameter. SE=standard error.

Tab. 3. Kruskal-Wallis test and correlation analyses between reproductive and environmental parameters in the sampled populations.

Reproductive parameters	K-W	rho_S
Abundance (#/100 mm^3)	NS	-
Gonadal Index (%)	NS	-
Diameter (µm)	***	***

K-W = significance of the Kruskal-Wallis test; rho_s = Spearman's correlation coefficient; *** = $p < 0.001$; NS = not significant.

Figures

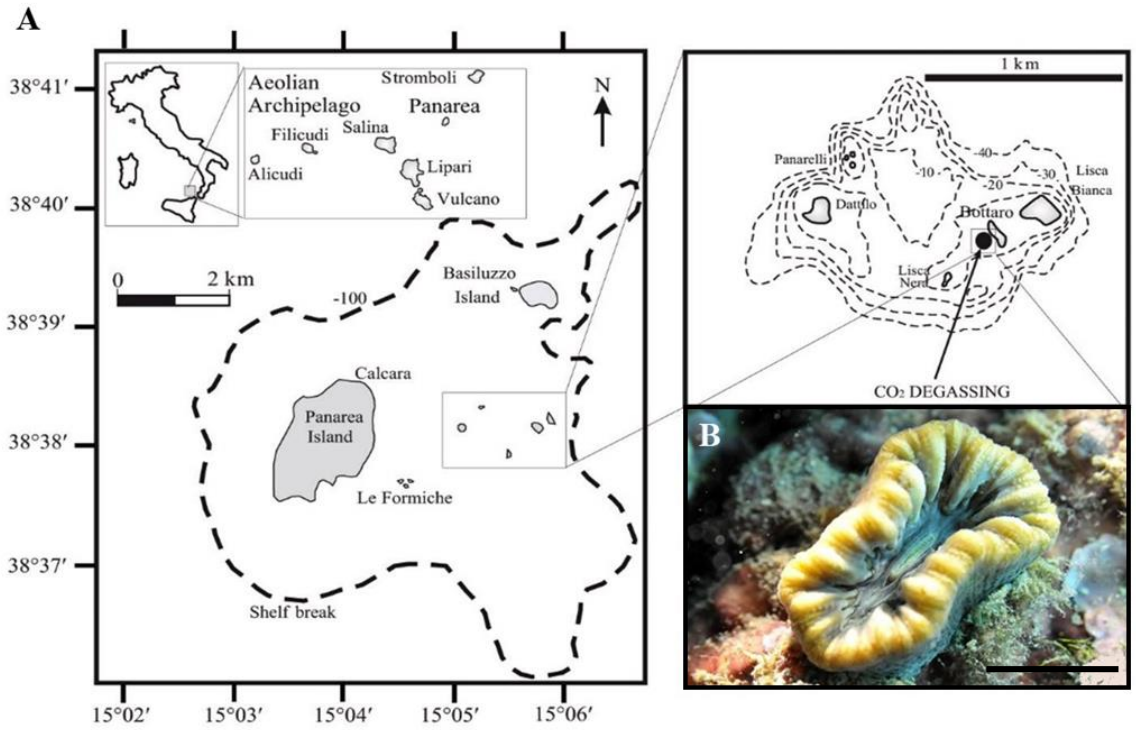

Figure 1. (A) Map of the experimental field. Located off the southwestern coast of Italy, near Panarea Island, there is underwater volcanic vent releasing persistent gaseous emissions (98–99% CO_2 without instrumentally detectable toxic compounds), resulting in a stable pH gradient. Three sites at various distances from the primary vent were initially selected for study. No temperature difference exists among the four study sites throughout the year. (B) Living specimens of *Balanophyllia europaea*, photographed during the day with contracted tentacles. Scale bar = 5 mm.

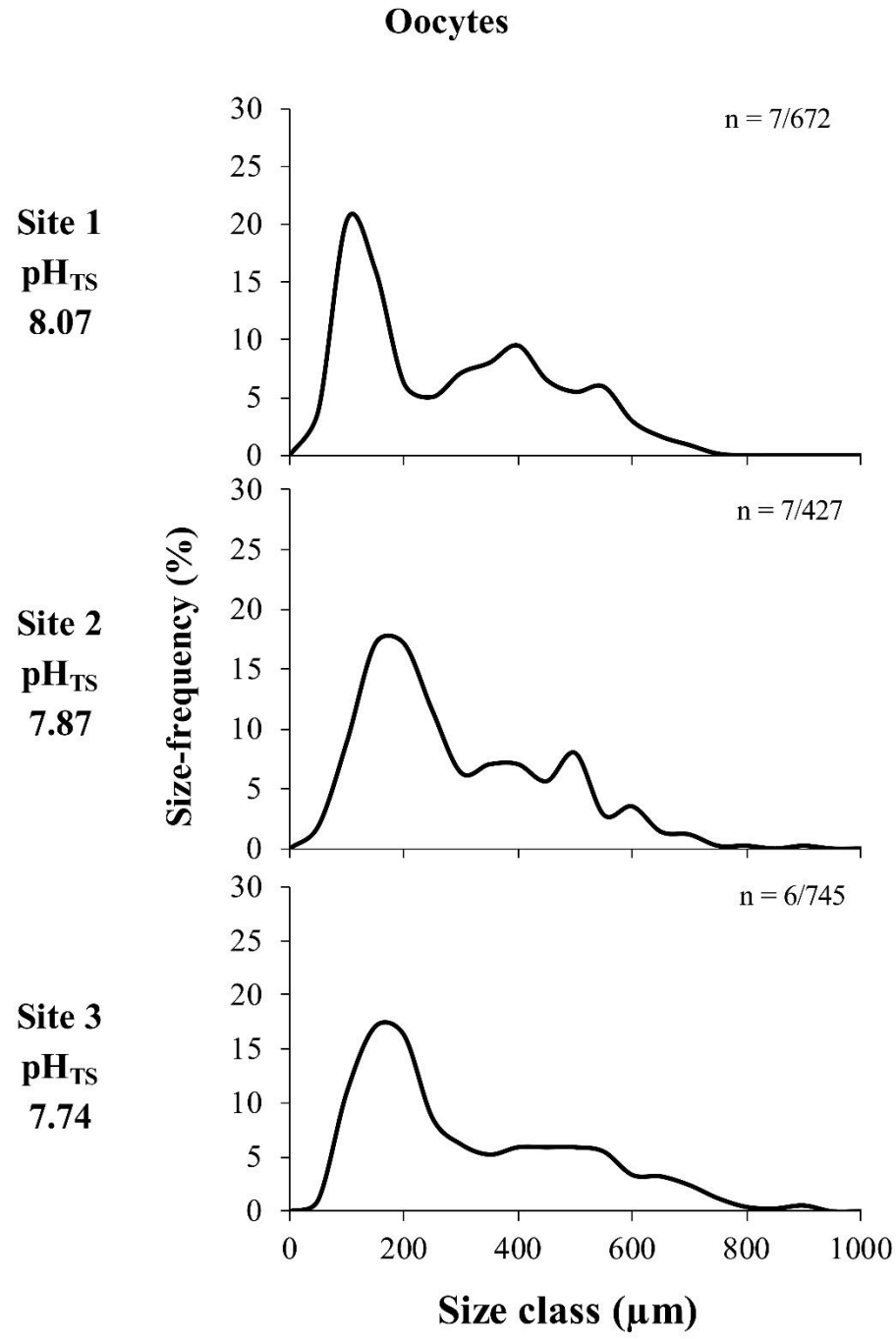

Figure 2. Oocyte size/frequency distribution in the three Sites. N = number polyps/number oocytes

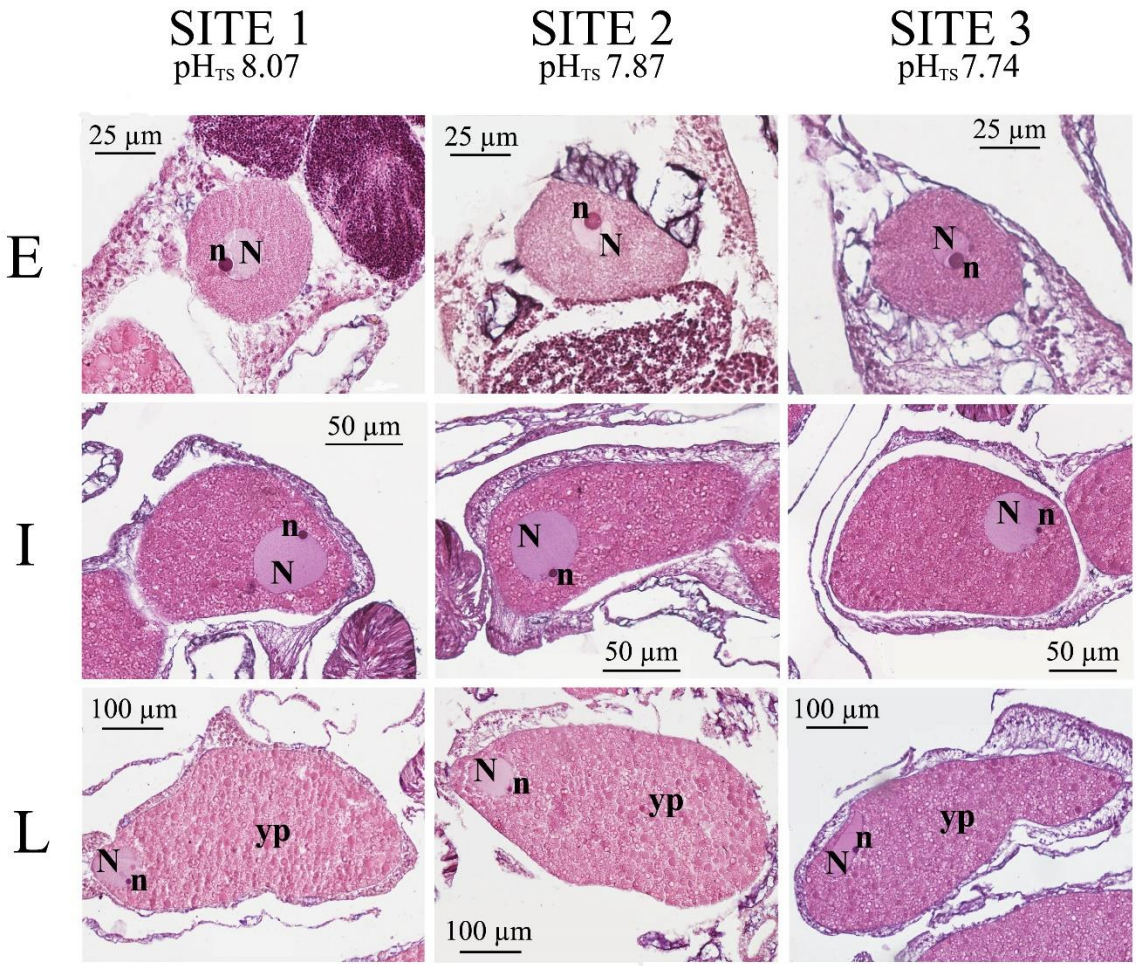

Figure 3. Oogenesis. E = Early stage. Small oocyte characterized by a high nucleus:cytoplasm ratio. The spherical nucleus is located centrally and contains a single nucleolus. I = Intermediate stage. A medium-sized oocytes with cytoplasm still quite homogeneous. The spherical-shaped nucleus has started to migrate toward the cell's periphery. L = Late stage. The nucleus is now located in the outer portion of the oocyte. The ooplasm is full of small yolk plates. N = nucleus; n = nucleolus; yp = yolk plates.

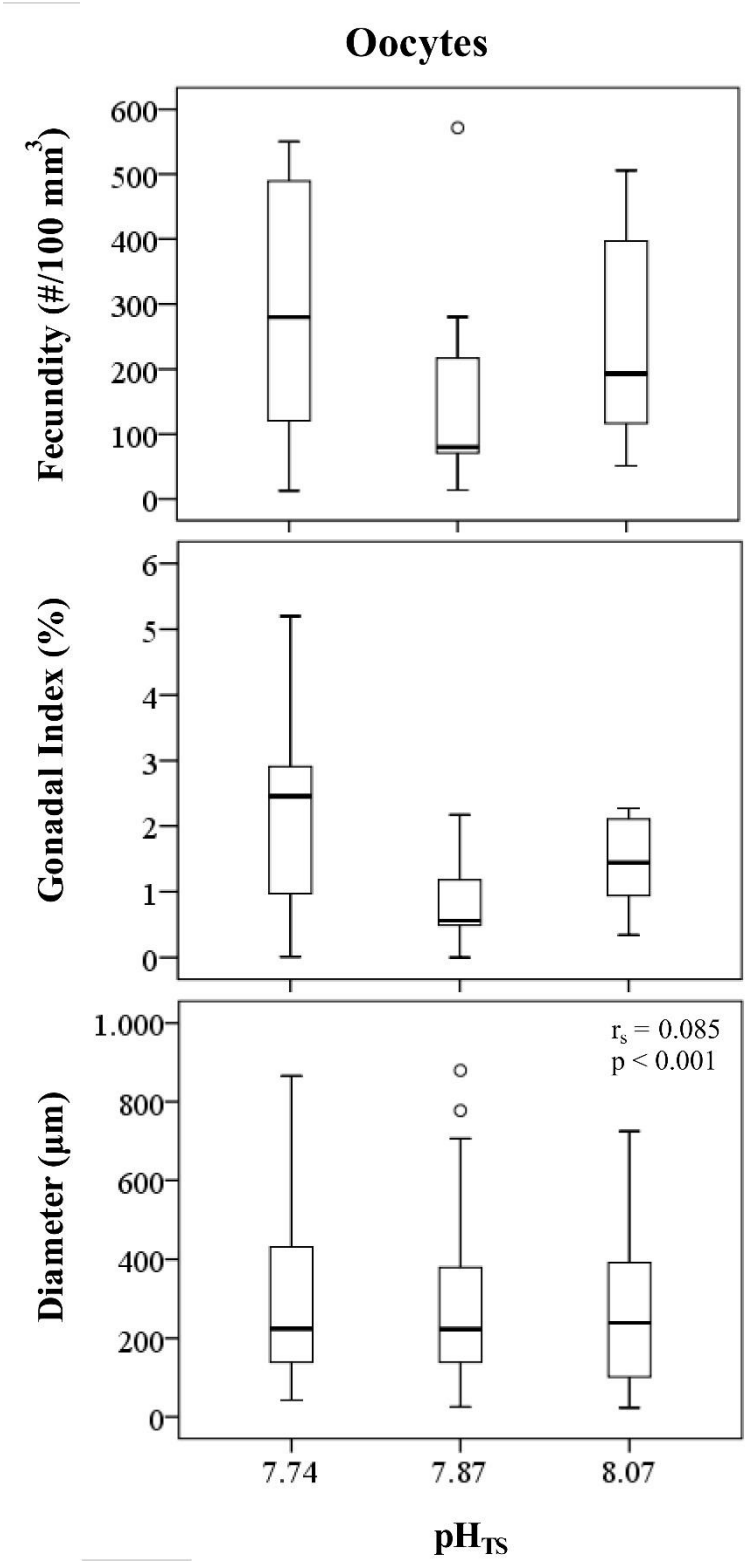

Figure 4. Box plot of oocytes abundance, gonadal index and diameters in the three study sites. Number of samples and mean values for each parameter and Site are reported in Table 2.

Chapter 4

Short-term exposure at CO_2 vent affect spermatogenesis in a temperate non-zooxanthellate coral

Manuscript in preparation

Short-term exposure at CO_2 vent affect spermatogenesis in a temperate non-zooxanthellate coral

Abstract

Anthropogenic carbon dioxide (CO_2) emissions and the resultant ocean acidification (OA) are projected to have extensive consequences for a variety on marine organisms, such as corals. Whereas the effects of OA on coral calcification is well documented, the effects on coral sexual reproduction have still been poorly studied and there are no information about Mediterranean corals. The possible effects of OA on sexual reproduction in the temperate scleractinian *Leptopsammia pruvoti* were studied in samples transplanted along a natural pCO_2 gradient under volcanic underwater crater at Panarea Island (Tyrrhenian Sea, Italy), providing a unique ecosystem naturally exposed to future scenarios of environmental change. Increasing pCO_2 prevent neither the production of germ cells nor the fertilization process, but seems to negatively influence the spermaries production and development, causing a delayed in fertilization and planulation process. The sensitivity of this species may have severe consequences for its reproductive success in a changing world.

Introduction

The absorption of anthropogenic CO_2 by ocean is resulting in decreasing of seawater pH and in changing of ocean chemistry, reducing the availability of carbonate ions (CO_3^{2-}) (Gattuso et al. 1999; Caldeira and Wickett 2003), essentials for the production of calcareous structures of marine organisms, such as corals (Raven et al. 2005; Hoegh-Guldberg et al. 2007; Kroeker et al. 2010). Seawater pH has already decreased by 0.1 pH units since the industrial revolution (Brewer 2009; Doney et al. 2009; Hoegh-Guldberg and Bruno 2010) and if CO_2 emissions are not mediated, the "business as usual" scenario project a further drop to 7.8 pH by the end of the century (Stocker et al. 2013).

Numerous laboratory studies have demonstrated that calcifying algae (Anthony et al. 2008; Kuffner et al. 2008), corals (Schneider and Erez 2006; Anthony et al. 2008) and coral reef communities, including some fishes (Langdon et al. 2000; Andersson et al. 2009; Hofmann et al. 2010), show reduced calcification in seawater with lower pH due to depleted carbonate saturation. Moreover, numerous biological processes and physiological functions independent of calcification may be impacted by decreasing pH (Kurihara 2008; Parker et al. 2009; Todgham and Hofmann 2009; Byrne 2011). Previous studies on ocean acidification confirmed highly variable response and contradictory results that may be partly attributed to different experimental designs, to control of carbonate chemistry or to species-specific responses to decreasing of pH (Hurd et al. 2009; Inoue et al. 2013). To date, most of the studies on ocean acidification have been done under laboratory conditions, losing information on complex natural conditions (Meron et al 2013).

Areas that naturally are enriched with CO_2, such as CO_2 vents can be used as natural laboratories to evaluate the consequences of increase in seawater pCO_2 on marine ecosystems *in situ* (Hall-Spencer et al. 2008; Vizzini et al. 2010; Fabricius et al. 2011; Rodolfo-Metalpa et al. 2011; Goffredo et al. 2014; Fantazzini et al. 2015). This areas have the advantage to be

subjected to natural environmental conditions, such as currents, nutrients, light, etc. (Meron et al. 2013), allowing to study the influence of pH in a natural environment that mime the seawater pH of the future. A volcanic underwater vent near Panarea Island (Sicily, Italy) provides a unique natural environment characterized by continuous and localized CO_2 emission that generate a stable pH from the centre to its periphery. Thanks to the low depth and the lack of heated or toxic compounds (Capaccioni et al. 2007; Goffredo et al. 2014), it represents an ideal area to investigate the influences of ocean acidification on marine organisms, including corals. The pCO_2 gradient is characterized by an ambient pH zone (control Site) with comparable values to current conditions in the temperate surface ocean in the Mediterranean, two low pH zones correspond the nearfuture (2100) scenarios and an extreme low pH zones represent an extreme scenarios of the more distant future (e.g., 2500) (Caldeira and Wickett 2005; Stocker et al. 2013).

Ocean acidification influences the metabolism of marine invertebrates, characterized by a low capacity to compensate for disturbances in extracellular ion and acid-base status, affecting their performances at the level of reproduction and behaviour (Pörtner 2008). Sexual reproduction represents a crucial process in the development and persistence of populations and its reduction threaten the resilience of the species, leading to shifts in size and abundance of populations (Roth et al. 2010; Fiorillo et al. 2013). The effects of ocean acidification on reproduction have been examined by several studies in echinoderm, mollusks and crustaceans (Kurihara and Shirayama 2004a, b; Havenhand et al. 2008; Morita et al. 2009; Parker et al. 2009, 2010; Byrne et al. 2010; Reuter et al. 2011). The few information available regarding the effects of ocean acidification on sexual reproduction was conducted in tropical corals under laboratory conditions (Fine and Tchernov 2007; Jokiel et al. 2008; Holcomb et al. 2010; Morita et al. 2009; Albright 2011, Albright et al. 2010), and no one on natural populations along a CO_2 vents or in temperate species.

This study focused on a solitary, non-zooxanthellate Mediterranean dendrophylliid, *Leptopsammia pruvoti* (Fig. 1), a gonochoric and brooding scleractinian (Goffredo et al. 2005). Previous studies on *L. pruvoti* reported that sea surface temperature and solar radiation did not significantly influence its skeletal bulk density, porosity, population abundance and structure stability, calcification rate and reproduction along an 850-km latitudinal gradient on the west coast of Italy (Goffredo et al. 2007; Caroselli et al. 2011, 2012a, b; Airi et al. *submitted*). This is the first study investigating the effects of environmental pCO_2 on reproductive output of temperate and non-zooxanthellate coral *L. pruvoti,* transplanted along the natural pH gradient.

Materials and Methods

Study site

Experimental field is located near Panarea Island (Aeolian Archipelago, Sicily, Italy, 38°38′16″N 15°06′37″E; Fig. 1), where an underwater crater (20 x 14 m) at 10 m depth, generates stable continuous column of bubbles (CO_2 99%; Capaccioni et al. 2007; Goffredo et al. 2014) at ambient temperature, creating a natural pH gradient. Along the gradient, four sampling Sites were selected: a control Site (Site 1: mean Total Scale pH_{TS} 8.1), located about 34m away from the center of the crater, two intermediate pCO_2 Sites (Site 2 and 3: mean pH_{TS} respectively 7.9 and 7.7), and a high pCO_2 Site (Site 4: mean pH_{TS} 7.4), situated in proximity of the vents.

Carbonate chemistry

pH (NBS scale), temperature (T) and salinity (Sal) were measured at each Site during several surveys between July 2010 and May 2013 with a multi-parametric probe (600R, YSI Incorporated, USA) and operated by SCUBA divers. Total alkalinity (TA) was measured on water samples collected in each Site using sterile 120 ml syringes (two replicates for each site). Water samples were immediately fixed with saturated mercuric chloride ($HgCl_2$) inside to

labelled 100 ml amber glass bottles to avoid biological alteration, and stored in darkness at 4°C. TA was measured by Gran titration, using a 702 SM Titrino (Metrohm AG).

Measured pH_{NBS} was converted in total scale (TS) using CO2SYS software (Mehrbach et al. 1973; Dickson 1990; Dickson and Millero 1987). Temperature sensors (Thermochron iButton, DS1921G, Maxim Integrated Products, USA) were placed near each Site and recorded depth temperature (T; °C) every three hours from June 2011 to May 2013 and replaced to each field campaign. The pH, total alkalinity, salinity and temperature were used to calculate other carbonate system parameters using the software CO2SYS with referenced dissociation constant. The study site has stable hydrothermal–chemical properties and only pCO_2 concentration differed significantly across sites (Capaccioni et al. 2007; Goffredo et al. 2014).

Sampling and field transplantation

During several expeditions (November 2010, March 2011, June 2011, August 2011, December 2011 and June 2012), specimens of *L. pruvoti* of approximately the same size were sampled at ~2 km away from the vent area and transplanted into the four Sites. The same number of corals (4-6) was randomly assigned to each of the four Sites (n=~20 for each expedition). Polyps were glued with a bicomponent epoxy coral glue (Milliput, Wales, UK) onto ceramic tiles and placed upside-down under plastic cages to mimic their natural orientation in overhangs and caves. Corals were subjected to the experimental conditions for ~3 months in different moment of reproductive cycle (Goffredo et al. 2006).

Cyto-Histometric Analysis

Biometric analysis of each polyp was performed by measuring length (L, major axis of the oral disk), width (w, minor axis of the oral disk), and height (h, oral–aboral diameter). The body volume (V) was calculated using the equation: $V = (L/2)*(W/2)*h*\pi$ (Goffredo et al. 2002). Biometric parameters were used to calculate Reproductive Parameters (see paragraph below).

Polyps were post-fixed in Bouin solution. After decalcification in EDTA and dehydration in a graded alcohol series from 80 to 100%, polyps were embedded in paraffin, and serial transverse sections were cut at 7µm intervals along the oral–aboral axis, from the oral to the aboral poles. Tissues were stained with Mayer's hematoxylin and eosin (Goffredo et al. 2006).

Cytometric analysis were made with a light microscope NIKON Eclipse 80i using an image analysis systems: NIKON NIS-Elements D 3.1. The maximum and minimum diameters of oocytes, in nucleated sections, and spermaries, classified into developmental stages in accordance with earlier studies on gametogenesis in scleractinians (Goffredo et al. 2002, 2005, 2011, 2012), were measured. The presence of embryos in the gastrovascular cavity were recorded (Goffredo et al. 2005)

Reproductive parameters

Reproductive output were defined through four reproductive parameters: 1) oocytes and spermaries abundance, both defined as the number of reproductive elements per body volume unit (100 mm^3); 2) gonadal index, defined as the percentage of body volume occupied by germ cells; 3) reproductive element size, defined as the average of the maximum and minimum diameter of spermaries and oocytes in nucleated section; 4) fertility, defined as the number of embryos per body volume unit (100 mm^3).

Based on the reproductive season, the reproductive cycle was characterized by two gamete activity periods (Goffredo et al. 2006). Gonadal development period is characterized by a stock of small oocytes, the recruitment of new oocytes, and the beginning of spermary development (Goffredo et al. 2006). Fertilization period is characterized by two stock of oocytes, a small one (< 350 µm) that will be fertilized in the following reproductive year, and a large one (> 350 µm) that will be fertilized in the same reproductive year. Advanced stage of maturation of spermaries and incubated embryos in celenteric cavity of females were expected to be funded (Goffredo et al. 2006).

Statistical analyses

Kolmogorov-Smirnov's test was used for testing the distribution of size class of oocytes and maturation stage of spermaries among Sites and between the two periods. Student's *t* test was used to compare the mean oocytes and spermaries size of populations between same Sites in different sampling periods. Levene's test was used to test homogeneity of variance and Kolmogorov-Smirnov's test was used for testing normality of distribution. When the sample size was lower than 2000, the Shapiro-Wilk test was used.

The non-parametric Kruskal-Wallis equality-of-populations rank test was used to compare reproductive parameters among Sites, it is used when assumptions for parametric statistics were not fulfilled. A Monte Carlo permutation test (10,000 permutations) was used to estimate the significance of the Kruskal–Wallis test when comparing the mean fertility among Sites, solving problems in the non-parametric test for small samples.

Spearman's rank correlation coefficient was used to calculate the significance of the correlations between reproductive elements diameters and pH. Spearman's rank correlation coefficient is an alternative to Pearson's correlation coefficient (Altman 1991). It is useful for data that are non-normally distributed and do not meet the assumptions of Pearson's correlation coefficient (Potvin and Roff 1993). The analyses were computed using PASW Statistics 22.0.

Results

All polyps resulted gonochoric in both reproductive periods. Sexually inactive individuals, without germ cells, was found in both periods (Tab. 1).

Size/frequency distribution of oocytes was significantly different between gonadal development period and fertilization period, in all Sites (Kolmogorov-Smirnov, $p < 0.05$; Fig. 2). Gonadal development period was characterized by a cohort of small oocytes in all Sites, but the size/frequency distribution was different among Sites (Kolmogorov-Smirnov, $p < 0.05$; Fig.

2). Fertilization period showed most oocytes smaller than 300 µm in all Sites without differences in size/frequency distribution among Sites (Fig. 2). Oocytes abundance and gonadal index did not show differences among Sites in both periods (Tab. 2). In the gonadal development period, the oocytes diameters were different among Sites and correlated with pH, but without a clear signal (Kruskal-Wallis test, $p < 0.001$; Fig. 4). Diameters were homogeneous among Sites in the fertilization period (Tab. 2; Fig. 4).

Maturation stage/frequency distribution of spermaries was different between gonadal development period and fertilization period, in all Sites ($n = 4$; Kolmogorov-Smirnov, $p < 0.001$; Fig. 3). Gonadal development period showed small spermaries in developing stage, with mode in stage III in all Sites, but there was differences in distribution among all Sites (Kolmogorov-Smirnov, $p < 0.05$; Fig. 3). Fertilization period was characterized by advanced maturation stages in all Sites, only the fourth Site, presenting higher frequencies of stage III and IV, resulted different from the others (Kolmogorov-Smirnov, $p < 0.01$; Fig. 3). Spermaries abundance and male gonadal index did not show differences among Sites (Tab. 3), but showed a different distribution trend between periods. In gonadal development period, both male reproductive parameters were characterized by lowest values in the most acidic Site, while during the fertilization period, was the control Site to be characterized by lowest values (Tab. 3; Fig. 5). In both period the diameter of spermaries was different among Sites and increased with decreasing of pH, less clearly during gonadal development period (Kruskal Wallis test, $p < 0.001$; Tab. 3; Fig. 5).

In fertilization period, female polyps containing embryos in the coelenteric cavity were found in all Sites. Fertility was different along the gradient and correlated with pH (Monte Carlo test $p < 0.05$; Tab. 2; Fig. 6).

Discussion

Increasing pCO_2 seemed to hinder neither the production of male and female germ cells, as suggested by the record of oocytes and spermaries in both, gonadal development and fertilization periods, nor the fertilization process, establishing by presence of embryos in female corals during fertilization period, in all Sites.

Spermatogenesis seemed to be more sensitive than oogenesis, showing different response among Sites with increasing pCO_2. This dissimilarity could be due to the timing exposure to experimental condition and to different development and maturation timing of oocytes and spermaries in this species. Male germ cells of *L. pruvoti*, takes approximately 12 months to mature indeed female germ cells need about 24 months (Goffredo et al. 2006). Considering the short-term exposure to experimental condition (3 months), spermatogenesis was influenced for a quarter of its length, instead only an eighth of the oogenesis processes was been exposed to pCO_2.

Despite the statistical differences found in size/frequency distribution of oocytes and in maturation stage/frequency distribution of spermaries among Sites, the development of both, oocytes and spermaries seemed not influenced to increasing pCO_2 in gonadal development period (Fig. 2, 3). During this period, oogenesis did not show a clear signal with increasing pCO_2.

Statistical analysis did not found differences in spermaries abundance and gonadal index among Sites. However, a drop in spermaries abundance and gonadal index in the most acidic Site was observed, suggesting that high pCO_2 level could delay spermaries production. Specimens from this Site could reallocate the energies from spermatogenesis into other vital functions, to face the great stress. Tropical zooxanthellate coral *Montipora capitata* show a normal gametogenesis and gametes production after 6 months under acidified conditions (Jokiel et al. 2008); the same result was found in *Oculina patagonic*a after 12 months (Fine and

Tchernov 2007). Despite the short-term exposure, the spermatogenesis of transplanted *L. pruvoti* seemed start to show a negative influence to increasing acidity. Possibly, under long-term exposure or in a natural population living under pCO_2 conditions, a clearer and stronger influence could be revealed.

During the fertilization period, the discovery of embryos in all Sites proved that the release of sperms in the water column and fertilization process was already started in all Sites. In the control Site only few mature spermaries (V maturation stage) was identified, proving that the release of sperms into water column was started and almost terminated. With increasing pCO_2, the amount of spermaries in the other Sites was greater than control Site and their maturation delayed, showing mature spermaries (V stage) together with earlier maturation stages (III and IV stages). The presence of earlier maturation stages of spermaries in more acidic Sites proved that the most of spermaries was still no mature and their release surely was not completed. Increasing pCO_2 could slow down spermaries development, as found in the green sea urchin, *Strongylocentrotus droebachiensis.* After 60 days under pCO_2 condition, *S. droebachiensis* shows a gonads development 67% less than the control treatment, unable to maintain high gonad growth facing such conditions (Siikavuopio et al. 2007).

During the same period, spermaries abundance and gonadal index were not different among Sites, but they were fallen from previous period (gonadal development period), confirming that the sperms release was started in all Sites (Fig. 5). The differences between periods were maximum in the control Site, characterized by lowest amount of spermaries in fertilization period, providing again that sperms expulsion was started and almost concluded. Increasing pCO_2 could to affect the fertilization process due to limited spermaries production during gonadal development period and a further delayed spermaries development, postponing the sperms release in water column.

Under stress condition event, Mediterranean gorgonian *Paramuricea clavata*, not alters its cycle of gonadal development, but reduce the amount of gonads produced, reallocating the energetic resources from gametogenesis into other vital functions (Linares et al. 2008). When sperm concentration is limited, fertilization strongly depends on chemical cues to activate sperm motility (e.g. Eisenbach 1999, Jantzen et al. 2001). However, increasing pCO_2 alter the seawater carbonate chemistry and could cause a progressive decline of motile sperm in corals, as recently found in *Acropora palmata* and *A. digitifera*, displaying a reduction in sperm motility and consequently in fertilization process in particular with low sperm concentration (Morita et al. 2009; Nakamura and Morita 2012).

The lowest amount of spermaries (Fig. 5) together with lowest fertility observed in control Site (Fig. 6), seemed to prove that not only the sperms release was concluded, but also the planulation processes was almost terminated. In the other Sites the fertilization started, but the probably delay in spermaries development postponed the release of sperms in the water column, delaying the fertilization and consequently postponing the embryos maturation and the planulation process.

Increasing pCO_2 negatively affect embryos growth and development in mollusks (Kurihara 2008; Kurihara and Shirayama 2004a, b), echinoderms (Gonzalez-Bernat et al. 2013) and crustaceans (Arnold et al. 2009) and planulae of coral *Acropora digitifera* under pH condition show smaller size than control (Suwa et al. 2010).

A previous study on calcification of *L. pruvoti* transplanted along the same natural pCO_2 gradient in the same short-time exposure do not show a reduction of calcification in both periods (gonadal development period and fertilization period). Instead, display a drop in calcification in a warmer period, probably due to a synergistic effect between pH and temperature (Prada et al. *submitted*). Is possible assume that in gonadal development period

and fertilization period, a reduction of energy intake intended for reproduction, could be due to a reallocation of energy in favor of the calcification process.

A population of zooxanthellate coral *Balanophyllia europaea*, naturally living along the same pCO_2 gradient at Panarea, shows an equal reproductive output among Sites; both gonadal production and gonadal development seem to be unaffected by increasing acidity (Chapter 3 of this thesis; Marchini 2016). With increasing pCO_2, the same population revealed no changes in linear extension rate, unaltered to the detriment of net calcification rate due to increase in skeletal porosity. To keeps linear extension rate constant, could to face functional reproductive requests (e.g. the ability to reach critical size at sexual maturity), at the expense of mechanical strength of the skeletons (Fantazzini et al. 2015). The same species shows an increase of photosynthetic efficiency of coral algae with increasing pCO_2 (*personal observation*), representing a further energy available to coral. *B. europaea* could to reallocate this additional resource into reproduction and linear extension rate, highlighting a lower sensitivity in *B. europaea* than *L. pruvoti* to increasing ocean acidification. The lack of zooxanthellae involve a lack in additional resources, making *L. pruvoti* negatively affected to increasing pCO_2. Impacts on reproduction and fertilization processes can directly affect size and structure of coral populations, doing hypothesize that environmental changing could affect the long-term survivability of the species. Further study under long-term exposure of pCO_2 are needed to better understand how the natural population will behave in the environment of the future sea.

References

Airi V, Prantoni S, Calegari M, Lisini Baldi V, Levy O, Falini G, Dubinsky Z, Goffredo S (2016) Reproductive output of a non-zooxanthellate Mediterranean coral is unaffected by temperature along an 850 km latitudinal gradient. Sci. Rep. *Submitted.*

Albright R, Mason B, Miller M, Langdon C (2010) Ocean acidification compromises recruitment success of the threatened Caribbean coral *Acropora palmata*. Proc. Natl. Acad. Sci. USA. 107:20400-20404.

Albright R (2011) Reviewing the effects of ocean acidification on sexual reproduction and early life history stages of reef-building corals. J.Mar. Biol. 2011.

Altman DG (1991) Practical statistics for medical research. Chapman & Hall, London. 613 p.

Andersson AJ, Kuffner IB, Mackenzie FT, Jokiel PL, Rodgers KS, Tan A (2009) Net Loss of $CaCO_3$ from a subtropical calcifying community due to seawater acidification: mesocosm-scale experimental evidence. Biogeosciences. 6:1811-1823.

Anthony KR, Kline DI, Diaz-Pulido G, Dove S, Hoegh-Guldberg O (2008) Ocean acidification causes bleaching and productivity loss in coral reef builders. Proc. Natl. Acad. Sci. USA. 105:17442-17446.

Arnold KE, Findlay HS, Spicer JI, Daniels CL, Boothroyd D (2009) Effect of CO_2-related acidification on aspects of the larval development of the European lobster, *Homarus gammarus* (L). Biogeosciences. 6:1747-54.

Brewer PG (2009) A changing ocean seen with clarity. Proc. Natl. Acad. Sci. USA. 106:12213-12214.

Byrne M, Soars NA, Ho MA, Wong E, McElroy D, Selvakumaraswamy P, Dworjanyn SA, Davis AR (2010) Fertilization in a suite of coastal marine invertebrates from SE Australia is robust to near-future ocean warming and acidification. Mar. Biol. 157:2061-2069.

Byrne M (2011) Impact of ocean warming and ocean acidification on marine invertebrate life history stages: vulnerabilities and potential for persistence in a changing ocean. Oceanogr. Mar. Biol. Annu. Rev. 49:1-42.

Caldeira K, Wickett ME (2005) Ocean model predictions of chemistry changes from carbon dioxide emissions to the atmosphere and ocean. J. Geophys. Res. Oceans (1978–2012). 110:C9.

Capaccioni B, Tassi F, Vaselli, O, Tedesco D, Poreda R (2007) Submarine gas burst at Panarea Island (southern Italy) on 3 November 2002: A magmatic versus hydrothermal episode. J. Geophys. Res. Solid Earth (1978–2012). 112:B5.

Caroselli E, Prada F, Pasquini L, Nonnis Marzano F, Zaccanti F, Falini G, Levy O, Dubinsky Z, Goffredo S (2011) Environmental implications of skeletal micro-density and porosity variation in two scleractinian corals. Zoology. 114:255-264.

Caroselli E, Mattioli G, Levy O, Falini G, Dubinsky Z, Goffredo S (2012a) Inferred calcification rate of a Mediterranean azooxanthellate coral is uncoupled with sea surface temperature along an 8° latitudinal gradient. Frontiers Zool. 9:32.

Caroselli E, Zaccanti F, Mattioli G, Falini G, Levy O, Dubinsky Z, Goffredo S (2012b) Growth and demography of the solitary scleractinian coral *Leptopsammia pruvoti* along a sea surface temperature gradient in the Mediterranean Sea. PLoS ONE. 7:e37848.

Dickson AG, Millero FJ (1987) A comparison of the equilibrium constants for the dissociation of carbonic acid in seawater media. Deep-Sea Res. A. 34:1733-1743.

Dickson AG (1990) Thermodynamics of the dissociation of boric acid in synthetic sea water from 273.15 to 298.15 K. Deep-Sea Res. A. 37:755-766.

Doney SC, Fabry VJ, Feely RA, Kleypas JA (2009) Ocean acidification: the other CO_2 problem Annual Review of Marine. Science. 1:169-192.

Eisenbach M (1999) Sperm chemotaxis. Reproduction. 4:56-66.

Fabricius KE, Langdon C, Uthicke S, Humphrey C, Noonan S, De'ath G, Okazaki R, Muehllehner N, Glas MS, Lough JM (2011) Losers and winners in coral reefs acclimatized to elevated carbon dioxide concentrations. Nature Clim. Change 1:165-169.

Fantazzini P, Mengoli S, Pasquini L, Bortolotti V, Brizi L, Mariani M, Di Giosia M, Fermani S, Capaccioni B, Caroselli E, Prada F, Zaccanti F, Levy O, Dubinsky Z, Kaandorp JA, Konglerd P, Hammel JU, Dauphin Y, Cuif JP, Weaver JC, Fabricius KE, Wagermaier W, Fratzl P, Falini G, Goffredo S (2015) Gains and losses of coral skeletal porosity changes with ocean acidification acclimation. Nat. Commun. 6:7785.

Fine M, Tchernov D (2007) Scleractinian coral species survive and recover from decalcification. Science. 315:1811.

Fiorillo I, Rossi S, Alva V, Gili JM, López-González PJ (2013) Seasonal cycle of sexual reproduction of the Mediterranean soft coral *Alcyonium acaule* (Anthozoa, Octocorallia). Mar. Biol. 160:719-728.

Gattuso JP, Allemand D, Frankignoulle M (1999) Photosynthesis and calcification at cellular, organismal and community levels in Coral Reefs: A review on interactions and control by carbonate chemistry. Am. Zool. 39:160-183.

Goffredo S, Arnone S, Zaccanti F (2002) Sexual reproduction in the Mediterranean solitary coral *Balanophyllia europaea* (Scleractinia, Dendrophylliidae). Mar. Ecol. Prog. Ser. 229:83-94.

Goffredo S, Radetić J, Airi V, Zaccanti F (2005) Sexual reproduction of the solitary sunset cup coral *Leptopsammia pruvoti* (Scleractinia, Dendrophylliidae) in the Mediterranean. 1. Morphological aspects of gametogenesis and ontogenesis. Mar. Biol. 147:485-495.

Goffredo S, Airi V, Radetić J, Zaccanti F (2006) Sexual reproduction of the solitary sunset cup coral *Leptopsammia pruvoti* (Scleractinia, Dendrophylliidae) in the Mediterranean. 2. Quantitative aspects of the annual reproductive cycle. Mar. Biol. 148:923-932.

Goffredo S, Caroselli E, Pignotti E, Mattioli G, Zaccanti F (2007) Variation in biometry and population density of solitary corals with solar radiation and sea surface temperature in the Mediterranean Sea. Mar. Biol. 152:351-361.

Goffredo S, Gasparini G, Marconi G, Putignano MT, Pazzini C, Airi V, Zaccanti F (2011) Sexual reproduction in the Mediterranean endemic orange coral, *Astroides calycularis* (Scleractinia, Dendrophylliidae). Bull. Mar. Sci. 87:589-604.

Goffredo S, Marchini C, Rocchi M, Airi V, Caroselli E, Falini G, Levy O, Dubinsky Z, Zaccanti F (2012) Unusual pattern of embryogenesis of *Caryophyllia inornata* (Scleractinia, Caryophylliidae) in the Mediterranean Sea. Maybe agamic reproduction? J.Morphol. 273:943-956.

Goffredo S, Prada F, Caroselli E, Capaccioni B, Zaccanti F, Pasquini L, Fantazzini P, Fermani S, Reggi M, Levy O, Fabricius KE (2014) Biomineralization control related to population density under ocean acidification. Nature Clim. Change. 4:593-597.

Gonzalez-Bernat MJ, Lamare M, Uthicke S, Byrne M (2013) Fertilisation, embryogenesis and larval development in the tropical intertidal sand dollar *Arachnoides placenta* in response to reduced seawater pH. Mar. Biol. 160:1927-1941.

Hall-Spencer JM, Rodolfo-Metalpa R, Martin S, Ransome E, Fine M, Turner SM, Rowley SJ, Tedesco D, Buia MC (2008) Volcanic carbon dioxide vents show ecosystem effects of ocean acidification. Nature. 454:96-99.

Havenhand JN, Buttler FR, Thorndyke MC, Williamson JE (2008) Near-future levels of ocean acidification reduce fertilization success in a sea urchin. Curr. Biol. 18:R651-R652.

Hoegh-Guldberg O, Mumby PJ, Hooten AJ, Steneck RS, Greenfield P, Gomez E, Harvell CD, Sale PF, Edwards AJ, Caldeira K, Knowlton N, Eakin CM, Iglesias-Prieto R, Muthiga N, Bradbury RH, Dubi A, Hatziolos ME (2007) Coral Reefs under rapid climate change and ocean acidification. Science. 318:1737-1742.

Hoegh-Guldberg O, Bruno JF (2010) The impact of climate change on the world's marine ecosystems. Science. 328:1523-1528.

Hofmann GE, Barry JP, Edmunds PJ, Gates RD, Hutchins DA, Klinger T, Sewell MA (2010) The effect of ocean acidification on calcifying organisms in marine ecosystems: an organism-to-ecosystem perspective. Annu. Rev. Ecol. Evol. Syst. 41:127-147.

Holcomb M, McCorkle DC, Cohen AL (2010) Long-term effects of nutrient and CO_2 enrichment on the temperate coral *Astrangia poculata* (Ellis and Solander, 1786). J. Exp. Mar. Biol. Ecol. 386:27-33.

Hurd CL, Hepburn CD, Currie KI, Raven JA, Hunter KA (2009) Testing the effects of ocean acidification on algal metabolism: considerations for experimental designs 1. J. Phycol. 45:1236-1251.

Inoue S, Kayanne H, Yamamoto S, Kurihara H (2013) Spatial community shift from hard to soft corals in acidified water. Nature Clim. Change. 3:683-687.

Jantzen TM, De Nys R, Havenhand JN (2001) Fertilization success and the effects of sperm chemoattractants on effective egg size in marine invertebrates. Mar. Biol. 138:1153-1161.

Jokiel PL, Rodgers KS, Kuffner IB, Andersson AJ, Cox EF, Mackenzie FT (2008) Ocean acidification and calcifying reef organisms: a mesocosm investigation. Coral Reefs. 27:473-483.

Kroeker KJ, Kordas RL, Crim RN, Singh GG (2010) Meta-analysis reveals negative yet variable effects of ocean acidification on marine organisms. Ecol. Lett. 13:1419-1434.

Kuffner IB, Andersson AJ, Jokiel PL, Ku'ulei SR, Mackenzie FT (2008) Decreased abundance of crustose coralline algae due to ocean acidification. Nat. Geosci. 1:114-117.

Kurihara H, Shirayama Y (2004a) Effects of increased atmospheric CO_2 on sea urchin early development. Mar. Ecol. Prog. Ser. 274:161-169.

Kurihara H, Shirayama Y (2004b) Effects of increased atmospheric CO_2 and decreased pH on sea urchin embryos and gametes. Echinoderms: München, Taylor & Francis Group, London, United Kingdom. 5 p.

Kurihara H (2008) Effects of CO_2-driven ocean acidification on the early developmental stages of invertebrates. Mar. Ecol. Prog. Ser. 373:275-284.

Langdon C, Takahashi T, Sweeney C, Chipman D, Goddard J, Marubini F, Aceves H, Barnett H, Atkinson MJ (2000) Effect of calcium carbonate saturation state on the calcification rate of an experimental coral reef. Global Biogeochem. Cy. 14:639-654.

Linares C, Coma R, Zabala M (2008) Effects of a mass mortality event on gorgonian reproduction. Coral Reefs. 27:27-34.

Marchini C (2016) Reproduction and population structure in temperate and tropical corals in relation to environmental parameters. PhD thesis in Biodiversity end Evolution. University of Bologna, Italy.

Mehrbach C, Culberson CH, Hawley JE, Pytkowicz RM (1973) Measurement of the apparent dissociation constants of carbonic acid in seawater at atmospheric pressure. Limnol. Oceanogr. 18:897-907.

Meron D, Buia MC, Fine M, Banin E (2013) Changes in microbial communities associated with the sea anemone *Anemonia viridis* in a natural pH gradient. Microb. Ecol. 65:269-276.

Morita M, Suwa R, Iguchi A, Nakamura M, Shimada K, Sakai K, Suzuki A (2009) Ocean acidification reduces sperm flagellar motility in broadcast spawning reef invertebrates. Zygote. 18:103-107.

Nakamura M, Morita M (2012) Sperm motility of the scleractinian coral *Acropora digitifera* under preindustrial, current, and predicted ocean acidification regimes. Aquatic Biol. 15:299-302.

Parker LM, Ross PM, O'Connor WA (2009) The effect of ocean acidification and temperature on the fertilization and embryonic development of the Sydney rock oyster *Saccostrea glomerata* (Gould 1850). Global Change Biol. 15:2123-2136.

Parker LM, Ross PM, O'Connor WA (2010) Comparing the effect of elevated pCO_2 and temperature on the fertilization and early development of two species of oysters. Mar. Biol. 157:2435-2452.

Pörtner HO (2008) Ecosystem effects of ocean acidification in times of ocean warming: a physiologist's view. Mar. Ecol. Prog. Ser. 373:203-217.

Potvin C, Roff DA (1993) Distribution-free and robust statistical methods: viable alternatives to parametric statistics. Ecology. 74:1617-1628.

Prada F, Caroselli E, Mengoli S, Fantazzini P, Capaccioni B, Pasquini L, Levy O, Weaver JC, Fabricius KE, Dubinsky Z, Falini G, Goffredo S. (2016) Regardless of being solitary or colonial, symbiotic or not symbiotic, ocean warming and acidification synergistically increase coral mortality. Nat. Commun. *Submitted.*

Raven J, Caldeira K, Elderfield H, Hoegh-Guldberg O, Liss P, Riebesell U, Shepherd J, Turley C, Watson A (2005) Ocean acidification due to increasing atmospheric carbon dioxide. The Royal Society. 60 p.

Reuter KE, Lotterhos KE, Crim RN, Thompson CA, Harley CD (2011) Elevated pCO_2 increases sperm limitation and risk of polyspermy in the red sea urchin *Strongylocentrotus franciscanus* Global Change Biol. 17:163-171.

Roth L, Koksal S, van Woesik R (2010) Effects of thermal stress on key processes driving coral population dynamics. Mar. Ecol. Prog. Ser. 411:73-87.

Schneider K, Erez J (2006) The effect of carbonate chemistry on calcification and photosynthesis in the hermatypic coral *Acropora eurystoma.* Limnol. Oceanogr. 51:1284-1293.

Siikavuopio SI, Mortensen A, Dale T, Foss A (2007) Effect of carbon dioxide exposure on feed intake and gonad growth in green sea urchin, *Strongylocentrotus droebachiensis*. Acquaculture. 266:97-101.

Stocker TF, Qin D, Plattner GK, Tignor M, Allen SK, Boschung J, Nauels A, Xia Y, Bex V, Midgley PM (eds) IPCC 2013: Summary for Policymakers. In: Climate Change 2013: The Physical Science Basis. Contribution of Working Group I to the Fifth Assessment Report of the Intergovernmental Panel on Climate Change. Cambridge University Press, Cambridge, United Kingdom and New York, NY, USA. 1535 p.

Suwa R, Nakamura M, Morita M, Shimada K, Iguchi A, Sakai K, Suzuki A (2010) Effects of acidified seawater on early life stages of scleractinian corals (Genus Acropora). Fish. Sci. 76:93-99.

Rodolfo-Metalpa R, Houlbrèque F, Tambutté É, Boisson F, Baggini C, Patti FP, Jeffree R, Fine M, Foggo A, Gattuso JP, Hall-Spencer JM (2011) Coral and mollusc resistance to ocean acidification adversely affected by warming. Nature Clim. Change. 1:308-312.

Todgham AE, Hofmann GE (2009) Transcriptomic response of sea urchin larvae *Strongylocentrotus purpuratus* to CO_2-driven seawater acidification. J. Exp. Biol. 212:2579-2594.

Vizzini S, Tomasello A, Maida GD, Pirrotta M, Mazzola A, Calvo S (2010) Effect of explosive shallow hydrothermal vents on δ13C and growth performance in the seagrass *Posidonia oceanica.* J. Ecol. 98:1284-1291.

Tables

Table 1. Seawater carbonate chemistry for each transplantation Site. The pH, temperature (T), total alkalinity (TA) and salinity (S) were used to calculate all the other parameters using CO2SYS software with dissociation constants. Mean pH values were calculated after conversion of data to hydrogen ion concentrations. Mean values are reported with minimum and maximum values in brackets.

Measured Parameters				
Sites	pH range (total scale)	T (°C)	TA (µmol kg^{-1})	S (‰)
1	8.07 (7.82-8.45)	20.5 (14.3-26.0)	2438 (2368-2600)	37 (33-38)
2	7.87 (7.54-8.25)	20.7 (14.4-26.0)	2429 (2334-2618)	37 (33-38)
3	7.74 (7.05-8.21)	20.6 (14.4-26.0)	2426 (2343-2610)	37 (34-38)
4	7.40 (6.71-8.14)	20.6 (14.4-26.0)	2395 (2329-2518)	37 (34-38)

Calculated Parameters					
Sites	*pCO_2 (µatm)	*HCO_3^- (µmol kg^{-1})	*CO_3^{2-} (µmol kg^{-1})	*DIC (µmol kg^{-1})	*Ω_{arag}
1	391 (127-780)	1869 (1466-2144)	232 (120-398)	2114 (1867-2291)	3.6 (1.8-6.3)
2	672 (234-1561)	2030 (1664-2264)	163 (68-314)	2214 (1984-2383)	2.5 (1.1-5.0)
3	907 (262-5100)	2073 (1835-2365)	144 (25-243)	2246 (2089-2552)	2.2 (0.4-3.9)
4	1944 (306-7231)	2159 (1826-2355)	96 (16-233)	2317 (2070-2613)	1.4 (0.2-3.1)

pH (n = 103-110 per Site), T (n = 2580 per Site) was recorded from May to September 2012 and from November 2012 to April 2013. and S (n = 107-110 per Site) were measured in July 2010, September 2010, November 2010, March 2011, June 2011, July-August 2011, November-December 2011, April-May 2012, June 2012 and May 2013. TA (n = 14 per Site) was measured in September 2010, November 2010, March 2011, June 2011, July-August 2011, November-December 2011, April-May 2012, June 2012 and May 2013. pCO_2 = carbon dioxide partial pressure; HCO_3^- = bicarbonate; CO_3^{2-} = carbonate; DIC = dissolved inorganic carbon; Ωarag = aragonite saturation.

Table 2. Number of polyps (n) analyzed in four sites in gonadal development and gametes maturity periods. For each site has been indicated the reproductive state of analysed polyps.

Gonadal development period					
Site	n	Female	Male	Sexually inactive	Embryogenetic
1	18	7	7	4	0
2	12	5	6	1	0
3	13	8	4	1	0
4	19	4	7	8	0

Fertilization period					
Site	n	Female	Male	Sexually inactive	Embryogenetic
1	17	5	3	9	3
2	18	4	5	9	2
3	14	1	10	3	1
4	14	5	6	3	2

Table 3. Mean abundance, gonadal index and diameter ± SE of oocytes in each Site.

Gonadal development period						
Site	n_p	Abundance (#/mm^3)	Gonadal Index (%)	n_o		Diameter (µm)
1	7	457 ± 20	0.45 ± 0.72	793		138 ± 9
2	5	690 ± 25	0.57 ± 0.58	598		126 ± 9
3	8	455 ± 20	0.88 ± 1.06	791		157 ± 9
4	4	233 ± 17	0.56 ± 1.94	197		163 ± 10

Fertilization period							
Site	n_p	Abundance (#/mm^3)	Gonadal Index (%)	n_{ep}	Fertility (#/mm^3)	n_o	Diameter (µm)
1	5	768 ± 21	0.46 ± 0.62	3	0.6 ± 0.9	410	118 ± 7
2	4	173 ± 15	0.14 ± 0.42	2	14.0 ± 0.9	263	123 ± 7
3	1	728	0.46	1	31.2	164	116 ± 6
4	5	200 ± 15	0.20 ± 0.51	2	26.0 ± 5.0	174	129 ± 8

SE = standard error; n_p = polyps number; n_o = oocytes number; n_{ep} = embryogenetic polyps number.

Table 4. Mean abundance, gonadal index and diameter of spermaries ± SE in each site.

Gonadal development period					
Site	n_p	Abundance (#/mm^3)	Gonadal Index (%)	n_s	Diameter (µm)
1	7	9646 ± 6525	2.1 ± 1.5	7513	79 ± 0.3
2	6	18139 ± 6215	6.3 ± 2.3	10625	95 ± 0.3
3	4	16941 ± 3808	6.5 ± 1.5	7857	96 ± 0.4
4	7	2233 ± 629	0.5 ± 0.2	2324	78 ± 0.6
Fertilization period					
Site	n_p	Abundance (#/mm^3)	Gonadal Index (%)	n_s	Diameter (µm)
1	3	293 ± 108	0.02 ± 0.01	65	47 ± 3
2	5	1167 ± 406	0.08 ± 0.04	579	53 ± 1
3	10	596 ± 190	0.05 ± 0.02	501	55 ± 1
4	6	1353 ± 468	0.20 ± 0.10	732	70 ± 1

SE = standard error. n_p = polyps number; n_s = spermaries number.

Figures

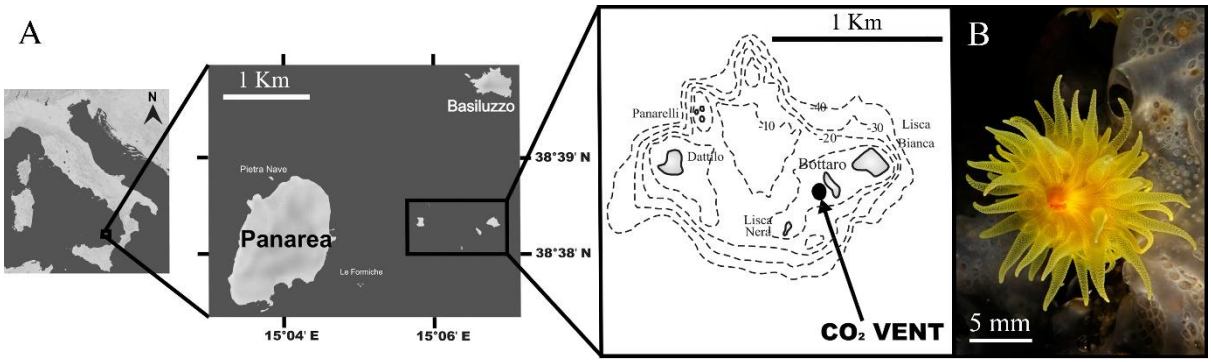

Figure 1. (**A) Study site**. Map of the study site near Panarea Island (Aeolian Archipelago, Italy). An underwater volcanic vent produce continuous emissions of CO_2 (98–99%), resulting in a stable pH gradient. Four sites along the gradient were selected for the study. No temperature difference exists among the four sites throughout the year. **(B**) Living specimen of *L.pruvoti* in Pietranave, photographed by Francesco Sesso.

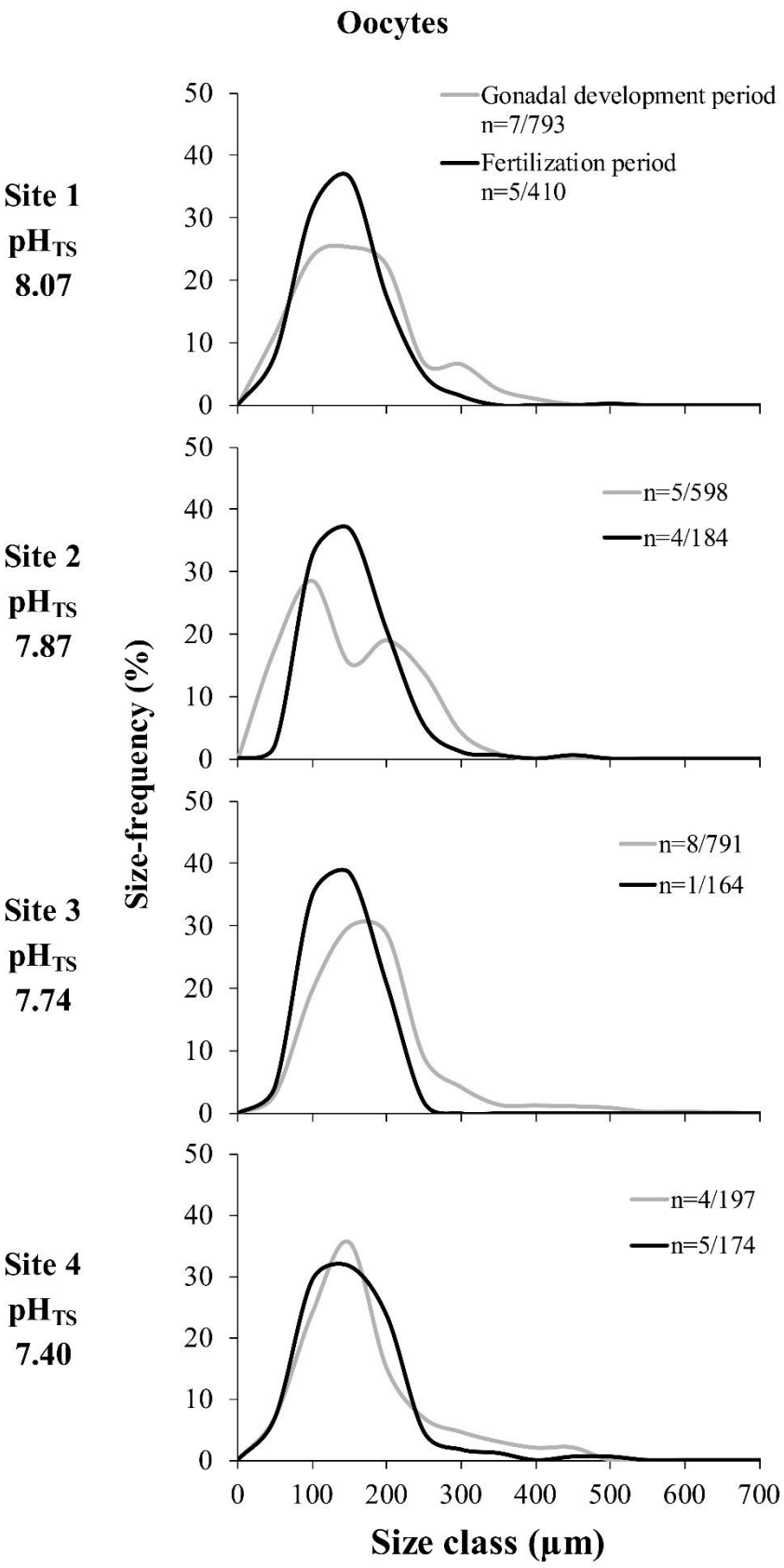

Figure 2. Oocyte size/frequency distribution in the gonadal development and fertilization periods. Distribution of the oocytes size during gonadal development period (dashed line) and fertilization period (solid line). n = number of oocytes.

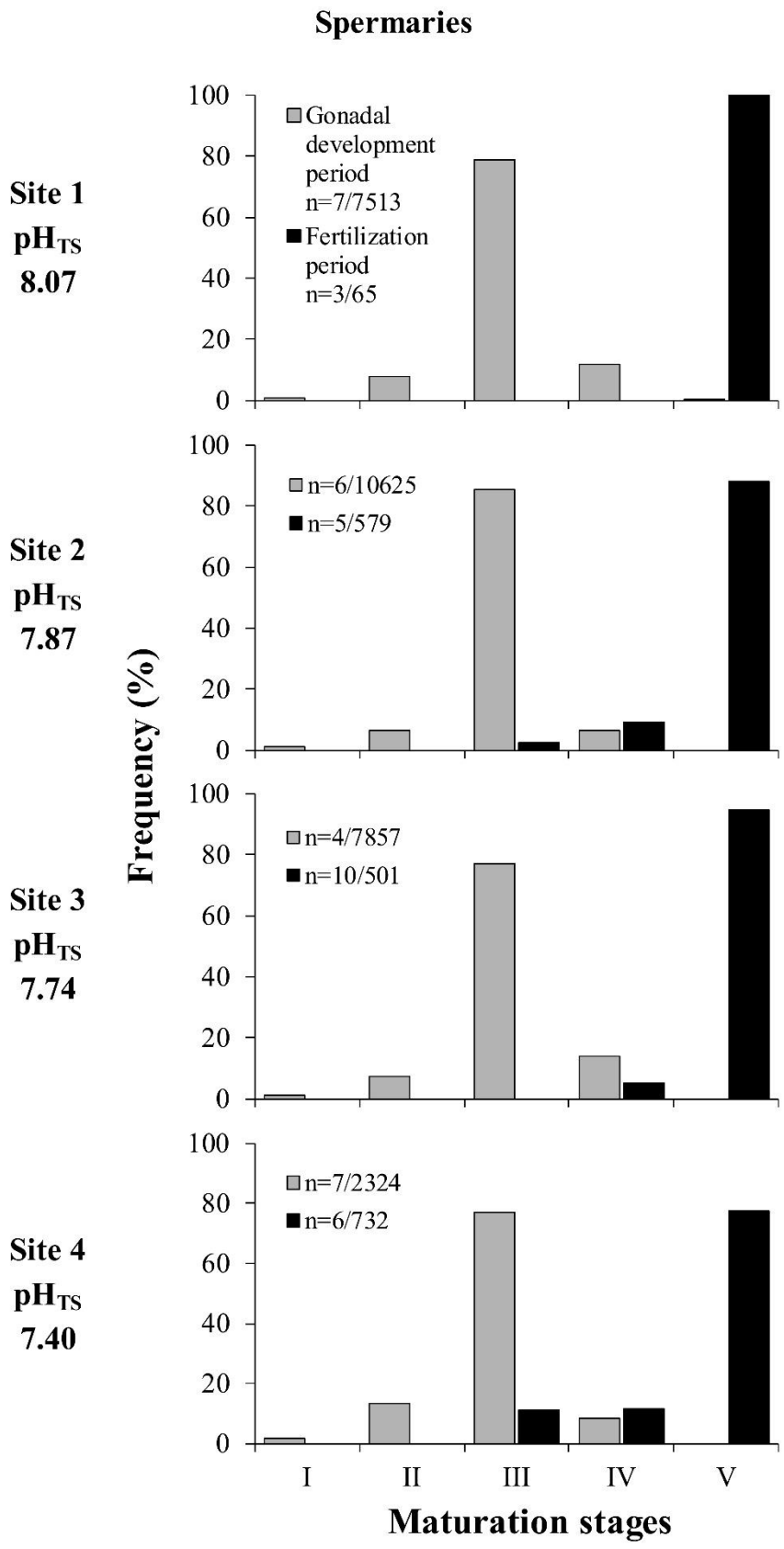

Figure 3. Spermary frequency distribution in gonadal development and fertilization periods. Distribution of five maturation stages of spermaries during gonadal development period (striped histogram bars) and fertilization period (black histogram bars). n = number of spermaries.

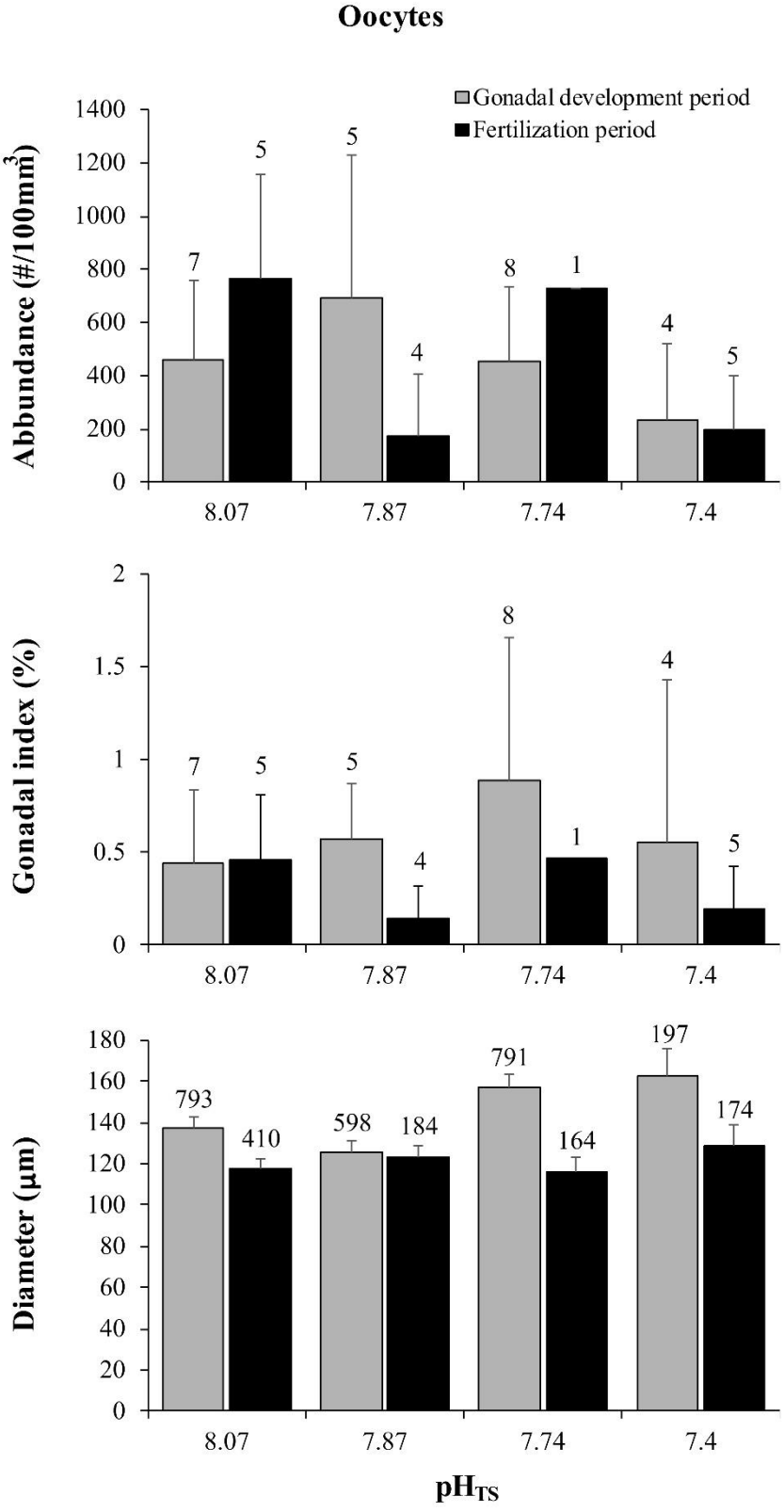

Figure 4. Oocytes. Reproductive parameters in gonadal development and fertilization periods. Mean values ± SE. Abundance, gonadal index and diameter of oocytes in the gonadal development period (striped histogram bars) and fertilization period (black histogram bars). On top of the bars the number of animals (abundance and gonadal index) and number of oocytes (diameter) in each site.

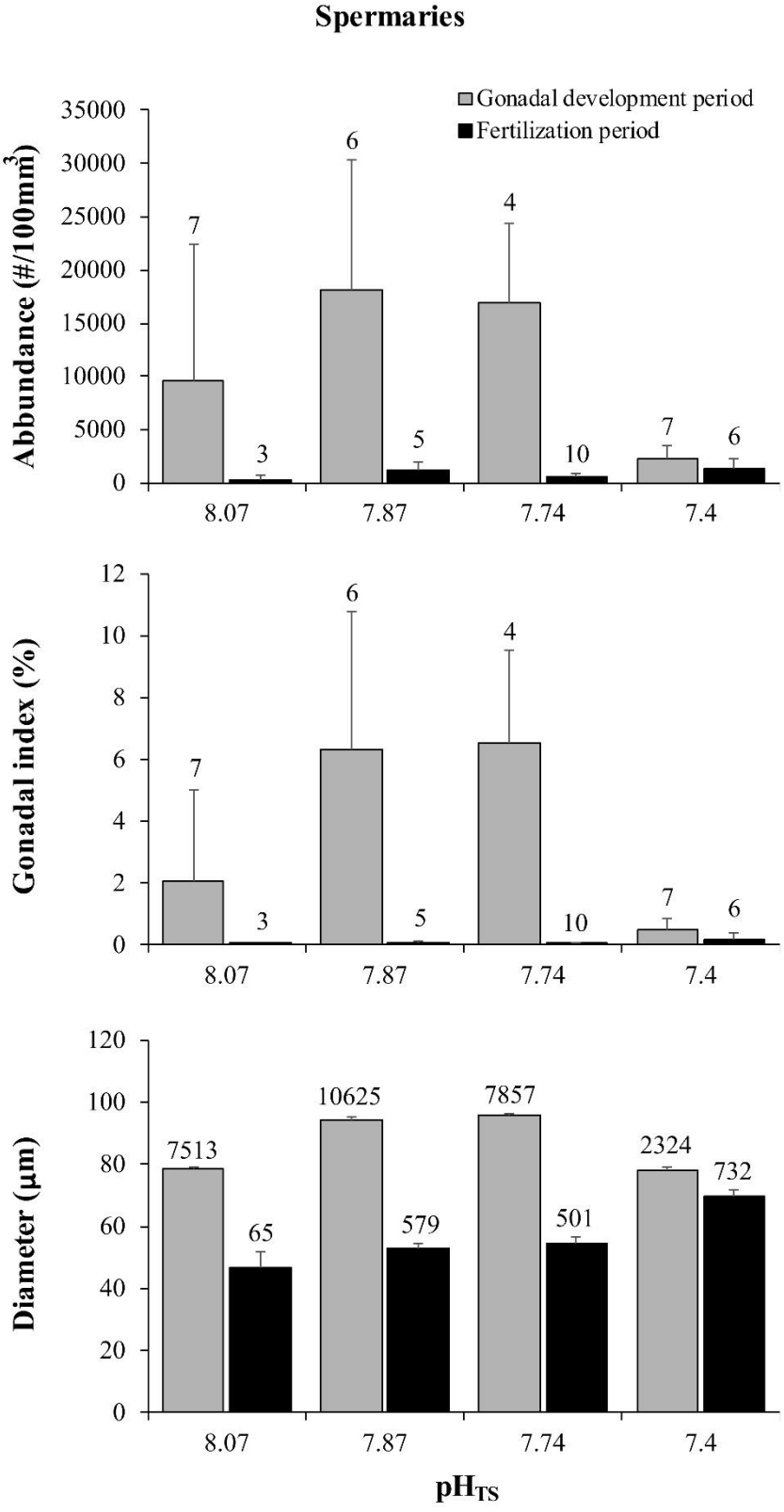

Figure 5. Spermaries. Reproductive parameters in gonadal development and gametes maturity periods. Mean values ± SE. Abundance, gonadal index and diameter of spermaries in the gonadal development (striped histogram bars) and fertilization periods (black histogram bars). On top of the bars the number of animals (abundance and gonadal index) and number of spermaries (diameter) in each site.

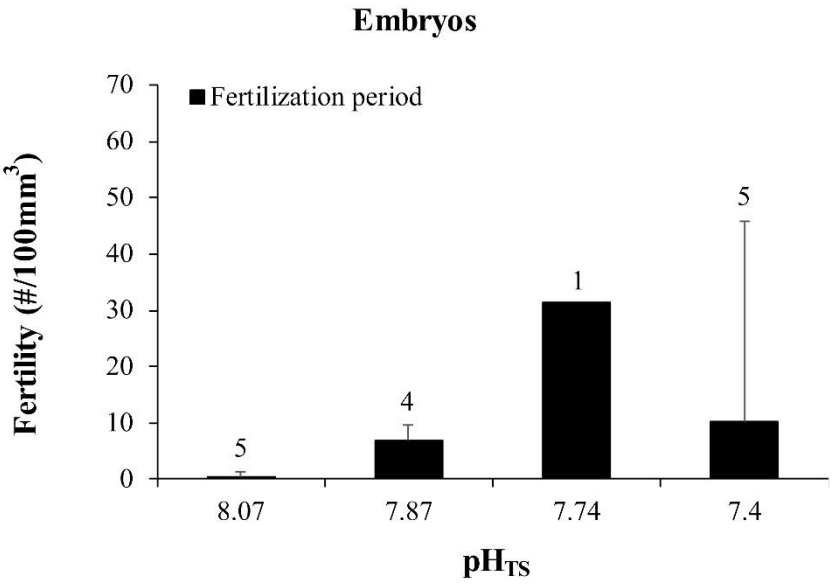

Figure 6. Embryos. Fertility in gonadal development periods. Mean values ± SE. On top of the bars, the number of female found in each site.

Section 2

Ecophysiology and environmental parameters

Chapter 5

Physiology, bleaching and mortality in two tropical corals exposed to pH and temperature levels projected for the end of this century

Manuscript in preparation

Physiology, bleaching and mortality in two tropical corals exposed to pH and temperature levels projected for the end of this century

Abstract

Zooxanthellate corals represent intimate symbioses between coral animals and unicellular photosynthetic dinoflagellates algae (*Symbiodinium sp*.) and are the main builders of the world's shallow-water marine coral reefs. Coral reefs are among the most vulnerable ecosystems to climate changes. The Intergovernmental Panel on Climate Change (IPCC) projected a rise of 1.6-4.3°C and a decrease of 0.06-0.3 pH units for the end of this century. The aim of this study was to test the response of two symbiotic tropical corals, characterized by different growth rates and life strategies, *Fungia granulosa* (solitary) and *Pocillopora verrucosa* (colonial), to a four week exposure to: (C) ambient temperature and ambient pH; (T) high temperature and ambient pH; (pH) ambient temperature and low pH; (T/pH) high temperature and low pH. The high temperature and low pH reflected projected values for the end of this century under the "business-as-usual" IPCC scenario. The solitary coral *F. granulosa* was less sensitive than the colonial coral *P. verrucosa*. However, in all considered parameters (photosynthetic efficiency, bleached tissue and mortality) to increased temperature and/or decreased pH, both species showed raised negative effects with increased exposition time, making them vulnerable to future environmental conditions to the sea, especially if CO_2 emission will be not mitigated.

Introduction

Coral reefs are one of the most productive and biodiverse ecosystems on Earth (Odum and Odum 1955; Connell 1978; Hoegh-Guldberg et al. 2007; Dove et al. 2013). Despite they cover about 0.1–0.5% of the ocean floor (Spalding and Grenfell 1997; Smith 1978; Copper 1994), they provide the habitat for ~25% of the world's marine species (Spalding et al. 2001). Moreover, coral reefs have a great relevance in human society and economy (Hoegh-Guldberg et al. 2007), representing a crucial sources of income and resources through their role in tourism, fishing, building materials and coastal protection (Carte 1996; Moberg and Folke 1999). However, coral reefs are among the most susceptible ecosystems to climate changes (Hoegh-Guldberg 1999, 2007; Fabry et al. 2008; Hofmann et al. 2010; Anthony et al. 2011), and corals are considered to be one of the most vulnerable groups, greatly influenced by the biological and physical factors of their environment (Kleypas 1999; Nakamura et al. 2004; Al-Horani 2005; Orr et al. 2005; Bramanti et al. 2013; Reyes-Nivia et al. 2013).

The increasing atmospheric carbon dioxide (CO_2) concentration by human activities is driving global climate change, altering the physicochemical status of the seawater (Diaz and Rosenberg 2008; Kroeker et al. 2010; Byrne 2012). Mean sea temperatures increased of 0.7°C since the industrial revolution (Feely et al. 2009), and climate models projected a rise of 1.6-4.3°C by the end of this century (Stocker et al. 2013). Moreover, about 30% of atmospheric CO_2 is absorbed by the oceans (Solomon et al. 2007), causing decreased of both, seawater pH and free carbonate ion (CO_3^{2-}; Raven et al. 2005) essential for corals to produce their calcium carbonate ($CaCO_3$) skeletons (Raven et al. 2005; Hofmann et al. 2010). Since the industrial revolution has already registered a drop of 0.1 pH units in seawater (Caldeira and Wickett 2003; Orr et al. 2005; Raven et al. 2005; Hoegh-Guldberg et al. 2007; Doney et al. 2009; Pelejero et al. 2010; Feely et al. 2012) and, if the current rate of anthropogenic CO_2 emissions will be not mediated, is projected a further decrease of 0.3 units by the end of this century (IPCC 2013).

It is becoming increasingly certain that ocean acidification and ocean warming will affect marine ecosystems (Reaka-Kudla 1997; Kleypas et al. 1999; Hoegh-Guldberg et al. 2007), influencing a variety of physiological and biological processes of several marine organisms (Kroeker et al. 2010, 2013; Dupont and Thorndyke 2013; Dupont and Pörtner 2013; McCoy and Kamenos 2015), and their population dynamics, community structure and ecosystem function (Doney et al. 2009; Gaylord et al. 2015).

Ocean acidification is a potential threat to marine ecosystems due to its effect on physiology and ecology of marine species (Kroeker et al. 2013) and are expected severe impacts mainly on calcifying marine organisms due to its negative effects on calcification process. Experimental studies show that high pCO_2 levels may affect also respiration, acid–base regulation, metabolism, growth rates, sensory systems, survivorship, reproduction, and many other fundamental processes on coral reefs (Fabry et al. 2008; Pörtner 2008; Widdicombe and Spicer 2008; Byrne 2011; Navarro et al. 2013; Duarte et al. 2014; Gazeau et al. 2014). Moreover, decreasing seawater pH accelerates destructive processes including erosion and dissolution of the reef structure, reducing the coastal protection (Carte 1996).

Temperature is the major environmental factor controlling marine species distributions and recruitment dynamics (Gillooly et al. 2002) and its increased directly affects physiological functions and developmental rates (Clarke 2003; Brierley and Kingsford 2009), reducing growth rates and reproductive output (McClanahan et al. 2009), and increasing mass mortality events and disease (Coma et al. 2009; Garrabou et al. 2009; Przeslawski et al. 2008). Moreover, the main concern to increasing temperature is the breakdown of the symbiosis between scleractinian corals and unicellular dinoflagellate algae of the genus Symbiodinium (zooxanthellae), through a process known as bleaching (Brown 1997; Lesser 2011). Symbiodinium species are exceptionally efficient utilisers of light energy (Brodersen et al. 2014), producing photosynthate, principally in the form of glucose (Burriesci et al. 2012), and

are able to meet up to ~95% of the energy requirement of the coral host (Muscatine et al. 1981, 1984). Increasing temperature may damage the photosynthetic machinery in Symbiodinium, reducing their photosynthetic efficiency and eventually leading to their expulsion from the coral host (Lesser 2011). Loss of zooxanthellae can starve the coral, and if bleaching event persist time, it will lead to death of the coral, increasing coral mortality events (Brown 1997; Berkelmans et al. 2004).

Ocean warming and acidification are occurring simultaneously and previous studies show that the effects of increased temperature could be exacerbate or mitigate by a rise in pCO_2 (Gooding et al. 2009; Findlay et al. 2010; Harvey et al. 2013). Biological response to rising temperature and decreasing pH varies greatly among species, making it difficult to understand how zooxanthellate corals will respond to climate change (Harley et al. 2006; Dupont and Thorndyke 2009; Kurihara 2008; Pörtner 2008; Przeslawski et al. 2008).

Laboratory conditions allows to investigate about increasing temperature and decreasing pH in dissociate way from other environmental parameters, and permit to test singularly or in combination the parameters, control them and register accurately their values.

Little is known about interactive effects of elevated temperature and low pH on the photosynthetic efficiency and bleaching of tropical corals. Here, we report on a 4-week study that compared photosynthesis, bleaching, and mortality responses of two zooxanthellate tropical coral species in response to increasing temperature and decreasing pH, separately and combined. This study focused on two zooxanthellate tropical corals, *Fungia granulosa* and *Pocillopora verrucosa*, characterized by the same trophic strategy but different growth form (respectively, solitary and colonial). Using 12 tanks experimental system, we manipulated temperature and/or pCO_2 levels to expose these species under "business as usual" projections of IPCC for the end of this century. This work will increase information about how

zooxanthellate tropical corals characterized by different growth forms, will respond to the future climate change.

Materials and methods

Ethics statement

The reefs sampled in this study do not fall under any legislative protection or special designation as a marine/environmental protected area. The Saudi Coastguard Authority issued sailing permits to the sites that include coral collection. Both species, *Fungia granulosa* and *Pocillopora verrucosa* are both listed on the ICUN Red List (http://www.iucnredlist.org/details/133197/0; http://www.iucnredlist.org/details/133183/0). Corals were sampled in accordance with ethical standards for the care and use of invertebrate animals.

Coral collection

Thirty-six specimens of *Fungia granulosa* and nine colonies of *Pocillopora verrucosa* were collected in a range of 10-12 m depth at Al-Fahal reef, about 13 km off the Saudi Arabian coast in the Central Red Sea (22° 15.100' N, 38° 57.386' E). Collected samples of *F. granulosa* and *P. verrucosa* were visually healthy polyps of equivalent size classes (<6 cm length and <10 cm length, respectively) and *F. granulosa* were completely unattached to substrate. After collection, each colony of *P. verrucosa* was cut in four micro colonies, and glued with a bicomponent epoxy coral glue (Aqua Medic Reef Construct, USA) onto ceramic basis (2 cm diameter). Specimens of both taxa were labelled and located in twelve identically equipped 65 l aquaria, set up at the bottom of the aquaria with the apex in front of the artificial light source and recovered for two weeks under controlled conditions. The experimental setup was located in the laboratory of Coastal and Marine Resources Core Lab (CMOR) at King Abdullah University of Science and Technologies (KAUST).

Experimental setup

The CO_2 tanks were located in a temperature-controlled room (20°C). Two levels of CO_2 concentration (ambient and elevated pCO_2, corresponding to increased pH) and 2 levels of temperature (ambient and elevated T) were selected as corresponded to IPCC projections for the end of this century (Stocker et al. 2013). The experimental setup included a control (3 aquaria) and 3 treatment (3 replicates aquaria for each): (1) ambient T + ambient pH, (2) high T + ambient pH, (3) ambient T + low pH, (4) high T + low pH (see Table 1 for mean values of each level of each factor used in the experiments).

Experimental T were maintained constant using aquarium titanium heaters (300W, Schego, Germany) placed in water baths connected to electronic controllers (± 0.5°C accuracy). pH was lowered by bubbling independently pure CO_2 gas in a 65 l additional tanks for each pH treatment (Fig. 1) through CO_2 reactor (aqualine, Aqua Medic, Germany) connected with little pump. A centralised microprocessor (AT-Control system, Aqua Medic, Germany) continuously monitored pH values through a probe located in the support aquaria and adjusted pH by opening/closing the electronic shut off valve gas (M-ventil Standard, Aqua Medic, Germany) in connection with CO_2 tanks (Fig.1).

Water chemistry parameters of T (°C), pH, Salinity (ppm) and Dissolved oxygen (DO, mg/l) were measured in all aquaria of each treatment throughout the experiment once a day using a Professional Plus (Pro Plus) Multiparameter Instrument YSI (Tab. 1). Corals received a constant irradiance of 180 ± 10 μmol photons m^{-2} s^{-1} (photoperiod was 12 h:12h light:dark) using six neon aqualine T5 (2 blue, 2 white 10 K and two white 15 K, Aquamedic, Germany) and were fed once a week.

Each aquaria held 3 specimens of *F. granulosa* (n = 9 for each treatment) and 3 micro colonies of *P. verrucosa* (n = 9 for each treatment). Each micro colony resulting from the same colony was placed in each treatment to guarantee the same genetic differences.

Photosynthetic efficiency measurements.

Photosynthetic efficiency (effective quantum yield $\Delta F/F_{m'}$ and maximum quantum yield F_v/F_m) of zooxanthellae host were measured using a DIVING-PAM fluorometer (Walz, Germany) (n = 8 for each species and each treatment) respectively, at the end of the 2°,3° and 4° week and 2° and 4° week under the experimental conditions.

Ambient light level at the aquarium room was <10 μmol photon m^{-2} s^{-1} and did not substantially affect the coral $\Delta F/F_{m'}$, that was measured at 16:00, while F_v/F_m was measured after 11 hours of dark adaptation, at 8:00 in the morning. During measurements, the 8 mm optical fibre was maintained perpendicular to the coral's surface using a black-jacket at a fixed distance of 5 mm to guarantee correct distance of the optical fiber to the coral.

Bleaching and mortality measurements

Bleaching (percentage of bleached tissue) and mortality (number of dead corals/colonies) were registered during and at the end of the experiment in both species. To measure coral bleaching, a colour reference chart was used and coral mortality was recognize by watching samples.

Statistical analysis

Levene's test was used to test homogeneity of variance and Shapiro-Wilk test was used for testing normality of distribution, useful when sample size is lower than 2000, in all parameters analyzed. A two samples *t*-test was used to highlight similarities and differences of sea water parameters among treatments. One-way analysis of variance (ANOVA) was used to test the significance of the differences inside each treatment among measurement replication over time. The non-parametric Kruskal-Wallis equality-of-populations rank test was used to compare photosynthetic measurement, % bleaching tissue and mortality among treatment, used when assumptions for parametric statistics were not fulfilled. A general linear model (GLM) with best model selection was used to verify if the differences between photosynthetic efficiency,

tissue bleached and mortality was due to aquaria effect and/or aquaria parameters (temperature and pH). The analyses were computed using PASW Statistics 22.0.

Results

Mean aquaria parameters (T, pH, Sal and DO) was homogeneous among three aquaria (a, b, c) from the same treatment, in all treatments (Tab. 1). Using the average of three aquaria for each treatment, T and pH varied significantly among treatment (Kruskal-Wallis test, $p < 0.001$; Tab. 2). In particular, T was homogeneous between control (C) and pH treatment (pH) and between temperature treatment (T) and temperature/pH treatment (T/pH), but was different between the two couples (test t, $p < 0.001$; Tab. 2). pH was homogeneous between C and T and between pH and T/pH, but was different between the two couples (test t, $p < 0.001$; Tab. 2). Sal and DO were homogeneous among treatments (Tab. 2).

Mean effective quantum yield ($\Delta F/F_{m'}$) and maximum quantum yield ($F_v/F_{m'}$) were significantly different among treatment in all registered time and in both species (Kruskal-Wallis test, $p < 0.05$; Tab. 3, 4; Fig. 2). In *F. granulosa*, the effective quantum yield and maximum quantum yield in C treatment, T treatment and pH treatment were homogeneous in time (Tab. 3). Only the interaction treatment (T/pH), showed differences between the first and the last measured value in both parameters (Tab. 3; ANOVA, $p < 0.01$). *P. verrucosa* showed differences in effective quantum yield and in maximum quantum yield in all treatment among the measurement in time (Tab. 4; Kruskal-Wallis test or ANOVA, $p < 0.05$), except for the maximum quantum yield in pH treatment, which was homogeneous between the first and last measured value (Tab. 4). In both species, the detected differences in photosynthetic efficiency was explained by temperature (GLM, $p < 0.05$), and in *F. granulosa* only the effective quantum yield was explained also by pH.

Samples of *F. granulosa* showed bleached tissue in both temperature treatments (T and T/pH), after more than 2 weeks of exposure (first recording - November 15th). Bleaching tissue showed a little increase in both treatments at the end of the experiments (Tab. 5; Fig. 3). In this species, bleached tissue was homogeneous among treatments in the first three measurement, but was different in the last two measurements (Kruskal-Wallis test, $p < 0.001$; Tab. 5; Fig. 3). *P. verrucosa* exhibited bleached tissue from the first measurement (2 weeks of exposure – November 8th) and showed a significant increased during the experiments in all treatments (Tab. 5; Fig. 3). Significant differences in tissue bleached were found among treatments during all registered data (Kruskal-Wallis test, $p < 0.01$; Tab. 5; Fig. 3). The differences identified in bleached tissue were explained by temperature in both species (GLM, $p < 0.05$).

Mortality was registered only in *P. verrucosa* and increased in differential way among treatment during the experiment (Tab. 6; Fig. 4).

GLM did not show a relationship between the differences found in photosynthetic efficiency, tissue bleached and mortality with the aquaria replicates in both species and all treatments.

Discussion

Ocean warming and acidification are two of the major threats that tropical coral reefs are facing during this century. Previous study revealed that key life functions in corals, such as photosynthesis, are affected by increasing temperature (Nakamura et al. 2004; Al-Horani 2005) and decreasing pH due to increasing pCO_2 (Orr et al. 2005; Kleypas 1999). The aim of this study was to test the response of two symbiotic tropical corals to a four week exposure to: (C) ambient temperature (29.2 ± 0.1°C) and ambient pH (8.1 ± 0.003); (T) high temperature (32.5 ± 0.1°C) and ambient pH (8.1 ± 0.004); (pH) ambient temperature (29.3 ± 0.1°C) and low pH (7.8 ± 0.009); (T/pH) high temperature (32.4 ± 0.2°C) and low pH (7.8 ± 0.03). These conditions are similar to actual values and to IPCC projections for the end of this century.

Aquaria salinity, dissolved oxygen and light did not differ among treatments, therefore differences in temperature and/or pH provided the most likely explanation for the differences observed in photosynthetic efficiency, bleaching tissue and mortality.

F. granulosa showed constant values during the experiment in both, effective and maximum quantum yield in C treatment, suggesting that this species was fully adapted to such conditions. This species did not show differences in T and pH treatments during the experiment in both photosynthetic parameters, suggesting a great resistance to increasing temperature and decreasing pH, separately. Instead, *F. granulosa* seemed to be affected by synergistic interaction between high temperature and low pH, showing a reduction of photosynthetic efficiency of both parameters in interaction treatment (T/pH) at the end of the experiment.

P. verrucosa showed differences in both, effective and maximum quantum yield in C treatment in the course of the experiment, probably due to higher stress level than *F. granulosa*, during sampling and the fragmentation in micro colonies. Anyway, both photosynthetic parameters was significantly different among treatments, showing the effects of temperature and/or pH.

2 weeks after the start of the experiment (first measurement – November 8th) the effective quantum yield of *F. granulosa* was different among treatments, due to higher mean values found in pH treatment. Decreasing pH, due to increasing pCO_2 increases the photosynthesis of microalgae (Riebesell et al. 1993), macroalgae (Borowitzka and Larkum 1976; Gao et al. 1993) and seaweeds (Zimmerman et al. 1997). Specimens of *Porites compressa* and *Montipora verrucosa (capitata)* exposed to increasing pCO_2 show higher photosynthetic efficiency, supporting the hypothesis that elevated pCO_2 may stimulates photosynthesis also in corals (Langdon and Atkinson 2005). Actually, the effects of decreasing pH, due to increasing pCO_2, on photosynthetic efficiency in corals, show ambiguous results. Host photosynthetic efficiency could increase (Langdon and Atkinson 2005), be not affected

(Langdon et al. 2003; Reynaud et al. 2003; Schneider and Erez 2006; Marubini et al. 2008; Rodolfo-Metalpa et al. 2010; Takahashi and Kurihara 2013; Enochs et al. 2014) or negative affected (Anthony et al. 2008) at the level of pCO_2 expected for the end of the century. Differential response among corals would be linked to response phylotype-specific of host Symbiodinium exposed to elevated pCO_2, as showed in Brading et al. (2011).

In both species, temperature seemed to be the main cause of the found differences in effective quantum yield ($\Delta F/F_{m'}$) and maximum quantum yield ($F_v/F_{m'}$) among treatments. Several study show negative effect of high temperature on photosynthesis. Scleractinian coral *Montastrea annularis* reduce photosynthesis after 6 h of exposure to elevated temperature (Porter et al. 1999). A decrease in the photosynthetic efficiency due to high temperature was observed also in *Stilophora pistillata, Montastrea cavernosa, Agaricia lamarcki, A. agaricites* and *Siderastrea radians* (Fitt and Warner 1995; Warner et al. 1996), and in heat-stressed zooxanthellae in culture (Iglesias-Prieto 1995; Iglesias-Prieto et al. 1992). High temperature has been considered to adversely affect the zooxanthellae hosts (Lasker et al. 1984; Glynn et al. 1985; Gates et al. 1992), damaging their photosynthetic apparatus, which could lead to bleaching (Fitt and Warner 1995; Jones et al. 1998; Warner et al. 1996, 1999; Fitt et al. 2001; Jones and Hoegh-Guldberg 2001).

The decline of photosynthetic efficiency found in *F. granulosa* and in *P. verrucosa*, was accompanied by increase in bleached tissue in both species. Several studies show that bleached corals have low values of maximum quantum yield (Fv/Fm; Fitt and Warner 1995; Warner et al. 1996, 1999; Jones et al. 2000; Bhagooli and Hidaka 2002) and numerous studies from both, the laboratory and field, indicates that coral bleaching is mainly attributed to elevated temperature (Hoegh-Guldberg and Smith 1989; Glynn and D'Croz 1990; Jokiel and Coles 1990; Glynn 1993; Hoegh-Guldberg and Salvat 1995; Brown 1997; Hoegh-Guldberg 1999). *F. granulosa* showed bleached tissue only in two temperature treatments (T and T/pH),

reaching 7% and 11% of bleached tissue at the end of the experiment respectively in T treatment and interaction treatment (T/pH). *P. verrucosa* seemed more affected by bleaching, showing high percentage in all treatments, with higher values in both temperature treatments (T and T/pH), that reached 100% bleached micro colonies in the interaction treatment (T/pH) at the end of the experiment. Coral bleaching has been attributed also to other factors, such as high irradiance and high CO_2 levels (Glynn et al. 1992; Gleason and Wellington 1993; Fournie et al. 2012). The effect of light could be excluded in this experiment because all treatments received the same constant irradiance of 180 ± 10 μmol photons m^{-2} s^{-1}. Field studies on coral bleaching have reported differences in bleaching susceptibility among coral species. Differences sensitivity of species in this experiment found in bleaching tissue rates, could explained by different growing rates of two species: *F. granulosa* is characterized by slow growing rates (Chadwick-Furman et al. 2000), respect the fast growing rates of *P. verrucosa* (Brown and Suharsono 1990). In the Indo-Pacific region, faster growing rates in corals (e.g. pocilloporid and acroporid) seems to be more severely affected by bleaching than slower growing species (e.g. poritid and faviid; Brown and Suharsono 1990).

Another difference between the two species was in the mortality rates. In contrast to *F. granulosa*, which did never show mortality, micro colonies of *P. verrucosa* started to die from the second week under experimental condition (November 11th) in T, pH and interaction (T/pH) treatments. At the end of the experiment, all treatments showed high mortality rate, reaching 100% of micro colonies died in the interaction treatments (T/pH). During this experiment, *F. granulosa*, by remaining alive, was more able than *P. verrucosa* to resist to high temperature and/or low pH conditions. The differential susceptibility of corals could be linked to their tissue thickness (Loya et al. 2001). *F. granulosa* is a solitary scleractinian coral characterized by large biomass and a completely covered skeleton with high tissue thickness, its energy reserves may help to compensate the stress to the changing environmental conditions. On the opposite, the

colonial coral *P. verrucosa* displays a lower tissue thickness (Ziegler et al. 2014), making this species more exposed and consequently more vulnerable to external environmental conditions.

The species-specific differences in susceptibility found in this study may have long-term consequences for the species composition of the community. Despite *F. granulosa* was less affect to increased temperature and/or decreased pH than *P. verrucosa*, both species showed increased negative effects with increasing exposition time, making both species vulnerable to environmental change, in particular if the CO_2 emissions will be not mitigate. Laboratory studies contribute to highlight knowledge about the effect of climate change on marine organisms and help to identify the species particularly susceptible to future environmental conditions.

References

Al-Horani FA (2005) Effects of changing seawater temperature on photosynthesis and calcification in the scleractinian coral *Galaxea fascicularis*, measured with O_2, Ca^{2+} and pH microsensors. Sci. Mar. 69:347-354.

Anthony KR, Kline DI, Diaz-Pulido G, Dove S, Hoegh-Guldberg O (2008) Ocean acidification causes bleaching and productivity loss in coral reef builders. Proc. Natl. Acad. Sci. USA. 105:17442-17446.

Anthony K, Kleypas JA, Gattuso JP (2011) Coral reefs modify their seawater carbon chemistry-implications for impacts of ocean acidification. Global Change Biol. 17:3655-3666.

Bhagooli R, Hidaka M (2002) Physiological responses of the coral *Galaxea fascicularis* and its algal symbiont to elevated temperatures. Galaxea JCRS. 4:33-42.

Bhagooli R, Hidaka M (2003) Comparison of stress susceptibility of in hospite and isolated zooxanthellae among five coral species. J. Exp. Mar. Biol. Ecol. 291:181-197.

Beardall J, Beer S, Raven JA (1998) Biodiversity of marine plants in an era of climate change: Some predictions based on physiological performance. Bot. Mar. 41:113-123.

Berkelmans R, De'ath G, Kininmonth S, Skirving WJ (2004) A comparison of the 1998 and 2002 coral bleaching events on the Great Barrier Reef: Spatial correlation, patterns, and predictions. Coral Reefs. 23:74-83.

Borowitzka MA, Larkum A (1976) Calcification in the green algal Halimeda. III. The sources of inorganic carbon for photosynthesis and calcification and a model of the mechanisms of calcification. J. Exp. Bot. 27:879-893.

Brading P, Warner ME, Davey P, Smith DJ, Achterberg EP, Suggett D (2011) Differential effects of ocean acidification on growth and photosynthesis among phylotypes of Symbiodinium (Dinophyceae). Limnol. Oceanogr. 56:927-938.

Bramanti L, Movilla J, Guron M, Calvo E, Gori A, Dominguez-Carrió C, Grinyó J, Lopez-Sanz A, Martinez-Quintana A, Pelejero C, Ziveri P (2013) Detrimental effects of ocean acidification on the economically important Mediterranean red coral (*Corallium rubrum*). Global Change Biol. 19:1897-1908.

Brierley AS, Kingsford MJ (2009) Impacts of climate change on marine organisms and ecosystems. Curr. Biol. 19:R602-R614.

Brodersen KE, Lichtenberg M, Ralph PJ, Kühl M, Wangpraseurt D (2014) Radiative energy budget reveals high photosynthetic efficiency in symbiont-bearing corals. J. R. Soc. Interface. 11:20130997.

Brown BE (1997) Coral bleaching: Causes and consequences. Coral Reefs. 16:129-138.

Brown BE, Suharsono (1990) Damage and recovery of coral reefs affected by El Niño related seawater warming in the Thousand Islands, Indonesia. Coral Reefs. 8:163-170.

Burriesci MS, Raab TK, Pringle JR (2012) Evidence that glucose is the major transferred metabolite in dinoflagellate–cnidarian symbiosis. J. Exp. Biol. 215:3467-3477.

Byrne M (2011) Impact of ocean warming and ocean acidification on marine invertebrate life history stages: vulnerabilities and potential for persistence in a changing ocean. Oceanogr. Mar. Biol. Annu. Rev. 49:1-42.

Byrne M (2012) Global change ecotoxicology: identification of early life history bottlenecks in marine invertebrates, variable species responses and variable experimental approaches. Mar. Environ. Res. 76:3-15.

Caldeira K, Wickett ME (2003) Anthropogenic carbon and ocean pH. Nature. 425:365.

Carte BK (1996) Biomedical potential of marine natural products. Bioscience. 46:271-286.

Chadwick-Furman NE, Goffredo S, Loya Y (2000) Growth and population dynamic model of the reef coral *Fungia granulosa* Klunzinger, 1879 at Eilat, northern Red Sea. J. Exp. Mar. Biol. Ecol. 249:199-218.

Clarke A (2003) Costs and consequences of evolutionary temperature adaptation. Trends Ecol. Evolut. 18:573-581.

Coma R, Ribes M, Serrano E, Jiménez E, Salat J, Pascual J (2009) Global warming-enhanced stratification and mass mortality events in the Mediterranean. Proc. Natl. Acad. Sci. USA. 106:6176-6181.

Connell JH (1978) Diversity in tropical rain forests and coral reefs. Science. 199:1302-1310.

Copper P (1994) Ancient reef ecosystem expansion and collapse. Coral Reefs. 13:3-11.

Diaz RJ, Rosenberg R (2008) Spreading dead zones and consequences for marine ecosystems. Science. 321:926-929.

Doney SC, Fabry VJ, Feely RA, Kleypas JA (2009) Ocean acidification: the other CO_2 problem. Ann. Rev. Mar. Sci. 1:169-192.

Dove S, Klinea DI, Pantosa O, Anglyd FE, Tysond GW, Hoegh-Guldberg O (2013) Future reef decalcification under a business-as-usual CO_2 emission scenario. Proc. Natl. Acad. Sci. USA. 110:15342–15347.

Duarte C, Navarro JM, Acuña K, Torres R, Manríquez PH, Lardies MA, Vargas CA, Lagos NA, Aguilera V (2014) Combined effects of temperature and ocean acidification on the juvenile individuals of the mussel *Mytilus chilensis*. J. Sea Res. 85:308-314.

Dupont S, Thorndyke MC (2008) Ocean acidification and its impact on the early life-history stages of marine animals. CIESM Workshop Monographs. 36:89-97.

Dupont S, Thorndyke MC (2009) Impact of CO_2-driven ocean acidification on invertebrates' early life-history-what we know, what we need to know, and what we can do? Biogeosci. Discuss. 6:3109-3131.

Dupont S, Pörtner HO (2013) A snapshot of ocean acidification research. Mar. Biol. 160:1765-1771.

Enochs IC, Manzello DP, Carlton R, Schopmeyer S, Van Hooidonk R, Lirman D (2014) Effects of light and elevated pCO_2 on the growth and photochemical efficiency of *Acropora cervicornis*. Coral Reefs. 33:477-485.

Fabry VJ, Seibel BA, Feely RA, Orr JC (2008) Impacts of ocean acidification on marine fauna and ecosystem processes. J. Mar. Sci. 65:414-432.

Feely RA, Doney SC, Cooley SR (2009) Ocean acidification: present conditions and future changes in a high-CO_2 world. Oceanography. 4:36-47.

Feely RA, Sabine CL, Byrne RH, Millero FJ, Dickson AG, Wanninkhof R, Murata A, Miller LA, Greeley D (2012) Decadal changes in the aragonite and calcite saturation state of the Pacific Ocean. Global Biogeochem. Cy. 26 p.

Findlay HS, Kendall MA, Spicer JI, Widdicombe S (2010) Post-larval development of two intertidal barnacles at elevates CO_2 and temperature. Mar. Biol. 157:725-735.

Fitt WK, Warner ME (1995) Bleaching patterns of four species of Caribbean reef corals. Biol. Bull. 189:298-307.

Fitt WK, Brown BE, Warner ME, Dunne RP (2001) Coral bleaching: interpretation of thermal tolerance limits and thermal thresholds in tropical corals. Coral Reefs. 20:51-65.

Fournie JW, Vivian DN, Yee SH, Courtney LA, Barron MG (2012) Comparative sensitivity of six scleractinian corals to temperature and solar radiation. Dis. Aquat. Organ. 99:85-93.

Gao K, Aruga Y, Asada K, Kiyohara M (1993) Influence of enhanced CO_2 on growth and photosynthesis of the red algae *Gracilaria* sp. and *G. chilensis*. J. Appl. Phycol. 5:563-571.

Garrabou J, Coma R, Bensoussan N, Bally M, Chevaldonné P, Cigliano M, Díaz D, Harmelin JG, Gambi MC, Kersting DK, Ledoux JB (2009) Mass mortality in Northwestern Mediterranean rocky benthic communities: effects of the 2003 heat wave. Global Change Biol. 15:1090-1103.

Gates RD, Baghdasarian G, Muscatine L (1992) Temperature stress causes host cell detachment in symbiotic cnidarians: implications for coral bleaching. Biol. Bull. 182:324-332.

Gaylord B, Kroeker KJ, Sunday JM, Anderson KM, Barry JP, Brown NE, Connell SD, Dupont S, Fabricius KE, Hall-Spencer JM, Klinger T (2015) Ocean acidification through the lens of ecological theory. Ecology. 96:3-15.

Gazeau F, Alliouane S, Bock C, Bramanti L, López Correa M, Gentile M, Hirse T, Pörtner HO, Ziveri P (2014) Impact of ocean acidification and warming on the Mediterranean mussel (*Mytilus galloprovincialis*). Front. Mar. Sci. 1:1-2.

Gillooly JF, Charnov EL, West GB, Savage VM, Brown JH (2002) Effects of size and temperature on developmental time. Nature. 417:70-73.

Gleason DF, Wellington GM (1993) Ultraviolet radiation and coral bleaching. Nature. 365:836-838.

Glynn PW, Peters EC, Muscatine L (1985) Coral tissue microstructure and necrosis: relation to catastrophic coral mortality in Panama. Dis. Aquat. Organ. 1:29-37.

Glynn PW, D'croz L (1990) Experimental evidence for high temperature stress as the cause of El Niño-coincident coral mortality. Coral Reefs. 8:181-191.

Glynn PW, Imai R, Sakai K, Nakano Y, Yamazato K (1992) Experimental responses of Okinawan (Ryukyu Islands, Japan) reef corals to high sea temperature and UV radiation. In: Proceedings of the Seventh Coral Reef Symposium, Guam. Richmond R (ed.) University of Guam. 10 p.

Glynn PW (1993) Coral reef bleaching: ecological perspectives. Coral Reefs. 12:1-7.

Gooding RA, Harley CDG, Tang E (2009) Elevated water temperature and carbon dioxide concentration increase the growth of a keystone echinoderm. Proc. Natl. Acad. Sci. USA. 106:9316-9321.

Harley CD, Randall Hughes A, Hultgren KM, Miner BG, Sorte CJ, Thornber CS, Rodriguez LF, Tomanek L, Williams SL (2006) The impacts of climate change in coastal marine systems. Ecol. Lett. 9:228-241.

Harvey BP, Gwynn-Jones D, Moore PJ (2013) Meta-analysis reveals complex marine biological responses to the interactive effects of ocean acidification and warming. Ecol. Evol. 3:1016-1030.

Hoegh-Guldberg O, Smith GJ (1989) The effect of sudden changes in temperature, light and salinity on the population density and export of zooxanthellae from the reef corals *Stylophora pistillata* Esper and *Seriatopora hystrix* Dana. J. Exp. Mar. Biol. Ecol. 129:279-303.

Hoegh-Guldberg O, Salvat B (1995) Periodic mass-bleaching and elevated sea temperatures: bleaching of outer reef slope communities in Moorea, French Polynesia. Oceanograph. Lit. Rev. 12:1124.

Hoegh-Guldberg O (1999) Climate change, coral bleaching and the future of the world's coral reefs. Mar. Freshwater Res. 50:839-866.

Hoegh-Guldberg O, Mumby PJ, Hooten AJ, Steneck RS, Greenfield P, Gomez E, Harvell CD, Sale PF, Edwards AJ, Caldeira K, Knowlton N (2007) Coral reefs under rapid climate change and ocean acidification. Science. 318:1737–1742.

Hofmann GE, Barry JP, Edmunds PJ, Gates RD, Hutchins DA, Klinger T, Sewell MA (2010) The effect of ocean acidification on calcifying organisms in marine ecosystems: an organism-to-ecoystem perspective. Annu. Rev. Ecol. Evol. Syst. 41:127-147.

Iglesias-Prieto R (1995) The effects of elevated temperature on the photosynthetic responses of symbiotic dinoflagellates. Photosynthesis: From Light to Biosphere. 4:793-796.

Iglesias-Prieto R, Matta JL, Robins WA, Trench RK (1992) Photosynthetic response to elevated temperature in the symbiotic dinoflagellate *Symbiodinium microadriaticum* in culture. Proc. Natl. Acad. Sci. USA. 89:10302-10305.

Jokiel PL, Coles SL (1990) Response of Hawaiian and other Indo-Pacific reef corals to elevated temperature. Coral Reefs. 8:155-162.

Jones RJ, Hoegh-Guldberg O, Larkum AW, Schreiber U (1998) Temperature-induced bleaching of corals begins with impairment of the CO_2 fixation mechanism in zooxanthellae. Plant Cell Environ. 21:1219-1230.

Jones RJ, Ward S, Amri AY, Hoegh-Guldberg O (2000) Changes in quantum efficiency of Photosystem II of symbiotic dinoflagellates of corals after heat stress, and of bleached corals sampled after the 1998 Great Barrier Reef mass bleaching event. Mar. Freshwater Res. 51:63-71.

Jones RJ, Hoegh-Guldberg O (2001) Diurnal changes in the photochemical efficiency of the symbiotic dinoflagellates (Dinophyceae) of corals: photoprotection, photoinactivation and the relationship to coral bleaching. Plant Cell Environ. 24:89-99.

Kleypas JA (1999) Geochemical consequences of increased atmospheric carbon dioxide on coral reefs. Science. 284:118-120.

Kroeker KJ, Kordas RL, Crim RN, Singh GG (2010) Meta-analysis reveals negative yet variable effects of ocean acidification on marine organisms. Ecol. Lett. 13:1419-1434.

Kroeker KJ, Kordas RL, Crim R, Hendriks IE, Ramajo L, Singh GS, Duarte CM, Gattuso JP (2013) Impacts of ocean acidification on marine organisms: quantifying sensitivities and interaction with warming. Global Change Biol. 19:1884-1896.

Kurihara H (2008) Effects of CO_2-driven ocean acidification on the early developmental stages of invertebrates. Mar. Ecol. Prog. Ser. 373:275-284.

Langdon C, Broecker WS, Hammond DE, Glenn E, Fitzsimmons K, Nelson SG, Peng TH, Hajdas I, Bonani G (2003) Effect of elevated CO_2 on the community metabolism of an experimental coral reef. Global Biogeochem. Cy. 17.

Langdon C, Atkinson MJ (2005) Effect of elevated pCO_2 on photosynthesis and calcification of corals and interactions with seasonal change in temperature/irradiance and nutrient enrichment. J. Geophys. Res. Oceans. 110.

Lasker HR, Peters EC, Coffroth MA (1984) Bleaching of reef coelenterates in the San Blas Islands, Panama. Coral Reefs. 3:183-190.

Lesser MP (2011) Coral bleaching: causes and mechanisms. In Coral Reefs: An Ecosystem in Transition. Dubinsky Z, Stambler N (eds.) Springer, Netherlands. 14 p.

Loya Y, Sakai K, Yamazato K, Nakano Y, Sambali H, Van Woesik R (2001) Coral bleaching: the winners and the losers. Ecol. Lett. 4:122-131.

Marubini F, Ferrier-Pagès C, Furla P, Allemand D (2008) Coral calcification responds to seawater acidification: a working hypothesis towards a physiological mechanism. Coral Reefs. 27:491-499.

McClanahan TR, Castilla JC, White AT, Defeo O (2009) Healing small-scale fisheries by facilitating complex socio-ecological systems. Rev. Fish Biol. Fish. 19:33-47.

McCoy SJ, Kamenos NA (2015) Coralline algae (Rhodophyta) in a changing world: Integrating ecological, physiological, and geochemical responses to global change. J. Phycol. 51:6-24.

Moberg F; Folke C (1999) Ecological goods and services of coral reef ecosystems. Ecol. Econom. 29:215-233.

Muscatine L, McCloskey LR, Marian RE (1981) Estimating the daily contribution of carbon from zooxanthellae to coral animal respiration. Oceanography. 26.

Muscatine L, Falkowski PG, Porter JW, Dubinsky Z (1984) Fate of photosynthetic fixed carbon in light- and shade-adapted colonies of the symbiotic coral *Stylophora pistillata*. Proc. R. Soc. Lond. B Biol. Sci. 222:181-202.

Nakamura E, Yokohama Y, Tanaka J (2004) Photosynthetic activity of a temperate coral *Acropora pruinosa* (Scleractinia, Anthozoa) with symbiotic algae in Japan. Phycol. Res. 52:38-44.

Navarro JM, Torres R, Acuña K, Duarte C, Manriquez PH, Lardies M, Lagos NA, Vargas C, Aguilera V (2013) Impact of medium-term exposure to elevated pCO_2 levels on the physiological energetics of the mussel *Mytilus chilensis*. Chemosphere. 90:1242-1248.

Odum HT, Odum EP (1955) Trophic structure and productivity of a windward coral reef community on Eniwetok Atoll. Ecol. Monograph. 25:291-320.

Orr JC, Fabry VJ, Aumont O, Bopp L, Doney SC, Feely RA, Gnanadesikan A, Gruber N, Ishida A, Joos F, Key RM (2005) Anthropogenic ocean acidification over the twenty-first century and its impact on calcifying organisms. Nature. 437:681-686.

Pelejero C, Calvo E, Hoegh-Guldberg O (2010) Paleo-perspectives on ocean acidification. Trends Ecol. Evolut. 25:332-344.

Porter JW, Lewis SK, Porter KG (1999) The effect of multiple stressors on the Florida Keys coral reef ecosystem: A landscape hypothesis and a physiological test. Limnol. Oceanogr. 44:941-949.

Pörtner H (2008). Ecosystem effects of ocean acidification in times of ocean warming: a physiologist's view. Mar. Ecol. Prog. Ser. 373:203-217.

Przeslawski R, Ahyong S, Byrne M, Woerheide G, Hutchings PA (2008) Beyond corals and fish: the effects of climate change on noncoral benthic invertebrates of tropical reefs. Global Change Biol. 14:2773-2795.

Raven J, Caldeira K, Elderfield H, Hoegh-Guldberg O, Liss P, Riebesell U, Shepherd J, Turley C, Watson A (2005) Ocean acidification due to increasing atmospheric carbon dioxide. The Royal Society, London, UK. 60 p.

Reaka-Kudla ML (1997) The global biodiversity of coral reefs: a comparison with rain forests. In: Biodiversity II: understanding and protecting our biological resources. Reaka-Kudla ML, Wilson DE, Wilson EO (eds.) Joseph Henry Press, Washington, DC. 83 p.

Reyes-Nivia C, Diaz-Pulido G, Kline D, Gulderg O, Dove S (2013) Ocean acidification and warming scenarios increase microbioerosion of coral skeletons. Global Change Biol. 19:1919-1929.

Reynaud S, Leclercq N, Romaine-Lioud S, Ferrier-Pagés C, Jaubert J, Gattuso JP (2003) Interacting effects of CO_2 partial pressure and temperature on photosynthesis and calcification in a scleractinian coral. Global Change Biol. 9:1660-1668.

Riebesell U, Wolf-Gladrow DA, Smetacek V (1993) Carbon dioxide limitation of marine phytoplankton growth rates. Nature. 361:249-251.

Rodolfo-Metalpa R, Martin S, Ferrier-Pagès C, Gattuso JP (2010) Response of the temperate coral *Cladocora caespitosa* to mid-and long-term exposure to pCO_2 and temperature levels projected for the year 2100 AD. Biogeosciences. 7:289-300.

Smith SV (1978) Coral-reef area and the contributions of reefs to processes and resources of the world's oceans. Nature. 273:225-226.

Schneider K, Erez J (2006) The effect of carbonate chemistry on calcification and photosynthesis in the hermatypic coral *Acropora eurystoma*. Limnol. Oceanogr. 51:1284-1293.

Solomon S, Qin D, Manning M, Chen Z, Marquis M, et al. (2007) Climate Change 2007: The Physical Science Basis. Contribution of Working Group I to the Fourth Assessment Report of the Intergovernmental Panel on Climate Change. Cambridge and New York, Cambridge University Press. 996 p.

Spalding MD, Grenfell AM (1997) New estimates of global and regional coral reef areas. Coral Reefs. 16:225-230.

Spalding MD, Ravilious C, Green EP (2001) World Atlas of Coral Reefs. University of California Press, Berkeley. 427 p.

Stocker TF, Qin D, Plattner GK, Tignor M, Allen SK, Boschung J, Nauels A, Xia Y, Bex V, Midgley PM (eds.) IPCC 2013: Summary for Policymakers. In: Climate Change 2013: The Physical Science Basis. Contribution of Working Group I to the Fifth Assessment Report of the Intergovernmental Panel on Climate Change. Cambridge University Press, Cambridge, United Kingdom and New York, NY, USA. 1535 p.

Takahashi A, Kurihara H (2013) Ocean acidification does not affect the physiology of the tropical coral *Acropora digitifera* during a 5-week experiment. Coral Reefs. 32:305-314.

Warner ME, Fitt WK, Schmidt GW (1996) The effects of elevated temperature on the photosynthetic efficiency of zooxanthellae in hospite from four different species of reef coral: a novel approach. Plant Cell Environ. 19:291-299.

Warner ME, Fitt WK, Schmidt GW (1999) Damage to photosystem II in symbiotic dinoflagellates: a determinant of coral bleaching. Proc. Natl. Acad. Sci. USA. 96:8007-8012.

Widdicombe S, Spicer JI (2008) Predicting the impact of ocean acidification on benthic biodiversity: What can animal physiology tell us?. J. Exp. Mar. Biol. Ecol. 366:187-197.

Ziegler M, Roder CM, Büchel C, Voolstra CR (2014) Limits to physiological plasticity of the coral *Pocillopora verrucosa* from the central Red Sea. Coral Reefs. 33:1115-1129.

Zimmerman RC, Kohrs DG, Steller DL, Alberte RS (1997) Impacts of CO_2 enrichment on productivity and light requirements of eelgrass. Plant Physiol. 115:599-607.

Tables

Table 1. Seawater parameters for each aquaria from each treatment.

Treatment	Aquaria	T (°C)	pH	Sal (ppm)	DO (mg l^{-1})
C	**a**	29.2 ± 0.2	8.1 ± 0.01	42.9 ± 0.2	5.1 ± 0.03
	b	29.2 ± 0.2	8.1 ± 0.01	42.9 ± 0.2	5.1 ± 0.03
	c	29.2 ± 0.2	8.1 ± 0.01	42.9 ± 0.2	5.1 ± 0.03
	K-W	NS	NS	NS	NS
T	**a**	32.4 ± 0.3	8.1 ± 0.005	42.8 ± 0.1	5.1 ± 0.02
	b	32.6 ± 0.2	8.1 ± 0.004	42.9 ± 0.2	5.1 ± 0.03
	c	32.5 ± 0.2	8.1 ± 0.010	42.8 ± 0.2	5.1 ± 0.03
	K-W	NS	NS	NS	NS
pH	**a**	29.2 ± 0.2	7.8 ± 0.02	42.8 ± 0.1	5.1 ± 0.03
	b	29.4 ± 0.2	7.8 ± 0.02	42.8 ± 0.1	5.1 ± 0.02
	c	29.3 ± 0.1	7.8 ± 0.02	42.8 ± 0.1	5.1 ± 0.03
	K-W	NS	NS	NS	NS
T/pH	**a**	32.3 ± 0.3	7.8 ± 0.05	42.8 ± 0.2	5.1 ± 0.04
	b	32.4 ± 0.3	7.8 ± 0.05	42.9 ± 0.2	5.1 ± 0.05
	c	32.5 ± 0.4	7.8 ± 0.05	42.9 ± 0.2	5.1 ± 0.05
	K-W	NS	NS	NS	NS

Mean value ± CI (95%) for temperature (T), pH, Salinity (Sal), Dissolved Oxygen (DO) of each aquaria (a, b, c) from each treatment. C = control, T = temperature treatment, pH = pH treatment, T/pH = interactive temperature/pH treatment. N = 39 for each aquaria and parameters. NS = not significant, Kruskal-Wallis equality-of-populations rank test.

Table 2. Mean seawater parameters for each treatment.

Treatment	T (°C)	pH	Sal (ppm)	DO (mg/l)
C	29.2 ± 0.1	8.1 ± 0.003	42.9 ± 0.1	5.1 ± 0.02
T	32.5 ± 0.1	8.1 ± 0.004	42.8 ± 0.1	5.1 ± 0.02
pH	29.3 ± 0.1	7.8 ± 0.009	42.8 ± 0.1	5.1 ± 0.02
T/pH	32.4 ± 0.2	7.8 ± 0.03	42.9 ± 0.1	5.1 ± 0.03
K-W	***	***	NS	NS

Mean value of three replica aquaria ± CI (95%) for temperature (T), pH, Salinity (Sal), Dissolved Oxygen (DO) of each treatment. C = control, T = temperature treatment, pH = pH treatment, T/pH = interactive temperature/pH treatment. N = 108 for each treatment and parameters. *** = $p < 0.001$, NS = not significant, Kruskal-Wallis equality-of-populations rank test.

Table 3. Effective quantum yield and maximum quantum yield in *Fungia granulosa*.

Fungia granulosa

Treatment	ΔF/Fm'						
	N	8 Nov	N	15 Nov	N	23 Nov	K-W/ANOVA
Control	9	0.67 ± 0.01	9	0.67 ± 0.01	6	0.66 ± 0.01	0.148 NS
T	9	0.66 ± 0.02	9	0.64 ± 0.02	6	0.60 ± 0.03	0.067 NS
pH	9	0.69 ± 0.01	9	0.69 ± 0.01	6	0.70 ± 0.01	0.877 NS
T/pH	9	0.66 ± 0.01	9	0.66 ± 0.01	6	0.60 ± 0.02	0.002 **
K-W		0.011 *		0.003 **		0.002 **	

Fungia granulosa

Treatment	Fv/Fm' (180)				
	N	11 Nov	N	21 Nov	ANOVA
Control	9	0.70 ± 0.01	6	0.69 ± 0.01	0.097 NS
T	9	0.68 ± 0.02	6	0.64 ± 0.04	0.084 NS
pH	9	0.72 ± 0.01	6	0.72 ± 0.02	0.527 NS
T/pH	9	0.69 ± 0.01	6	0.65 ± 0.02	0.001 ***
K-W		0.001 ***		0.001 ***	

Mean value ± CI (95%) of.effective quantum yield (ΔF/Fm') and maximum quantum yield (Fv/Fm') in each treatment during and at the end of the experiment. C = control, T = temperature treatment, pH = pH treatment, T/pH = interactive temperature/pH treatment. N = number of samples for each measurement. On 21st November one sample of *F. granulosa* from each aquaria was withdrawn for another study. * = $p < 0.05$, ** = $p < 0.01$, *** = $p < 0.001$, NS = not significant, Kruskal-Wallis equality-of-populations rank test and ANOVA.

Table 4. Effective quantum yield and maximum quantum yield in *Pocillopora verrucosa.*

Pocillopora verrucosa

Treatment	ΔF/Fm'						
	N	8 Nov	N	15 Nov	N	23 Nov	K-W/ANOVA
Control	9	0.56 ± 0.02	8	0.49 ± 0.04	7	0.39 ± 0.08	0.002 **
T	9	0.49 ± 0.05	8	0.38 ± 0.07	4	0.25 ± 0.07	0.001 ***
pH	9	0.56 ± 0.05	8	0.46 ± 0.07	7	0.35 ± 0.06	0.001 ***
T/pH	9	0.50 ± 0.04	8	0.38 ± 0.05	0	-	0.02 **
K-W/ANOVA		0.066 NS		0.031 *		0.001 ***	

Pocillopora verrucosa

Treatment	Fv/Fm' (180)				
	N	11 Nov	N	21 Nov	ANOVA
Control	9	0.52 ± 0.05	8	0.40 ± 0.08	0.020 **
T	8	0.46 ± 0.06	7	0.27 ± 0.05	0.001 ***
pH	8	0.49 ± 0.07	8	0.40 ± 0.06	0.802 NS
T/pH	8	0.50 ± 0.05	4	0.21 ± 0.04	0.001 ***
K-W/ANOVA		0.357 NS		0.004 **	

Mean value ± CI (95%) of.effective quantum yield (ΔF/Fm') and maximum quantum yield (Fv/Fm') in each treatment during and at the end of the experiment. C = control, T = temperature treatment, pH = pH treatment, T/pH = interactive temperature/pH treatment. N = number of samples for each measurement. * = $p < 0.05$, ** = $p < 0.01$, *** = $p < 0.001$, NS = not significant, Kruskal-Wallis equality-of-populations rank test and ANOVA.

Table 5. Percentage of bleaching tissue in *Fungia granulosa* and *Pocillopora verrucosa.*

Fungia granulosa

Treatment	Bleached tissue (%)									
	N	8 Nov	N	11 Nov	N	15 Nov	N	21 Nov	N	23 Nov
C	9	0.0	9	0.0	9	0.0	6	0.0	6	0.0
T	9	0.0	9	0.0	9	1.1 ± 2.1	6	6.7 ± 6.5	6	6.7 ± 6.5
pH	9	0.0	9	0.0	9	0.0	6	0.0	6	0.0
T/pH	9	0.0	9	0.0	9	1.1 ± 2.1	6	10 ± 5.1	6	11.7 ± 3.2

Pocillopora verrucosa

Treatment	Bleached tissue (%)									
	N	8 Nov	N	11 Nov	N	15 Nov	N	21 Nov	N	23 Nov
C	9	18.8 ± 2.0	9	31.1 ± 4.5	9	40.0 ± 8.0	9	60.0 ± 8.5	9	63.3 ± 9.0
T	9	30.0 ± 6.2	9	51.1 ± 8.4	9	60.0 ± 7.5	9	87.8 ± 4.0	9	92.2 ± 4.3
pH	9	20.0 ± 3.3	9	42.2 ± 8.8	9	44.4 ± 8.8	9	65.5 ± 8.4	9	71.1 ± 8.2
T/pH	9	28.9 ± 3.1	9	46.7 ± 8.5	9	57.8 ± 7.0	9	95.6 ± 1.8	9	100

Mean value ± CI (95%) of percentage tissue bleached in each treatment during and at the end of the experiment. C = control, T = temperature treatment, pH = pH treatment, T/pH = interactive temperature/pH treatment. N = number of samples for each record.

Table 6. Percentage of polyp mortality in *Pocillopora verrucosa.*

Pocillopora verrucosa

Treatment	Polyp mortality (%)									
	N	8 Nov	N	11 Nov	N	15 Nov	N	21 Nov	N	23 Nov
C	0/9	0	0/9	0	1/9	11	1/9	11	2/9	22
T	0/9	0	1/9	11	1/9	11	2/9	22	5/9	55
pH	0/9	0	1/9	11	1/9	11	1/9	11	2/9	22
T/pH	0/9	0	1/9	11	1/9	11	5/9	55	9/9	100

Percentage values of polyp mortality in each treatment during and at the end of the experiment. C = control, T = temperature treatment, pH = pH treatment, T/pH = interactive temperature/pH treatment. N = number of dead samples/total sample number for each treatment.

Figures

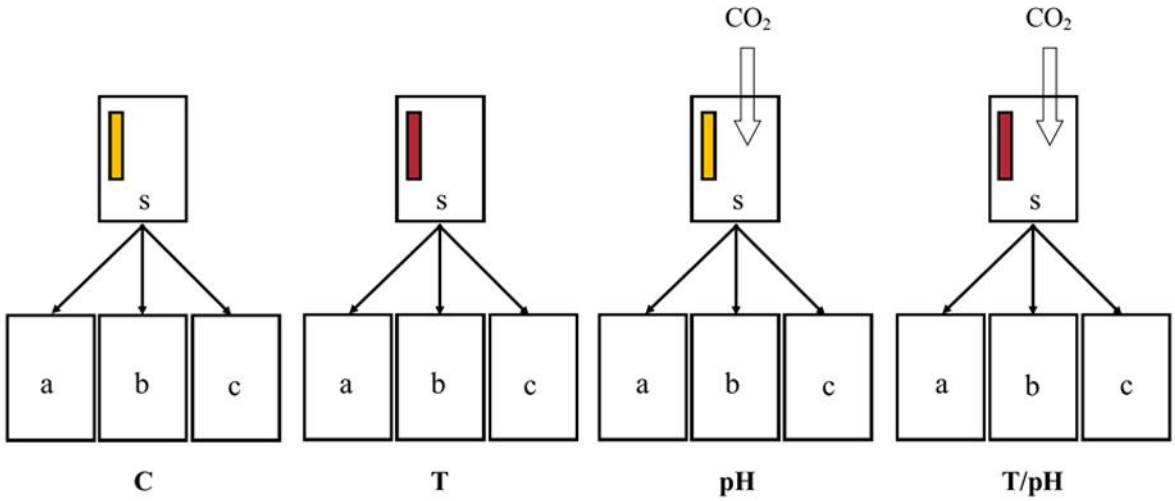

Figure 1. Aquaria setup. Each treatment (C = control, T = temperature treatment, pH = pH treatment and T/pH = temperature/pH treatment) had three replicates aquaria (a, b, c) and one support aquarium (s). Heathers were represented by yellow bars (ambient temperature, 29°C) and red bars (high temperature, 32°C) in the support aquaria. White arrows represented bubbling CO_2. Sea water circulation was from support aquaria, where water became warm and/or enriched of CO_2 in the treatments, to three replicates aquaria, where were the samples of both species (n = 3 for each aquaria and species). Support aquaria did not host the samples.

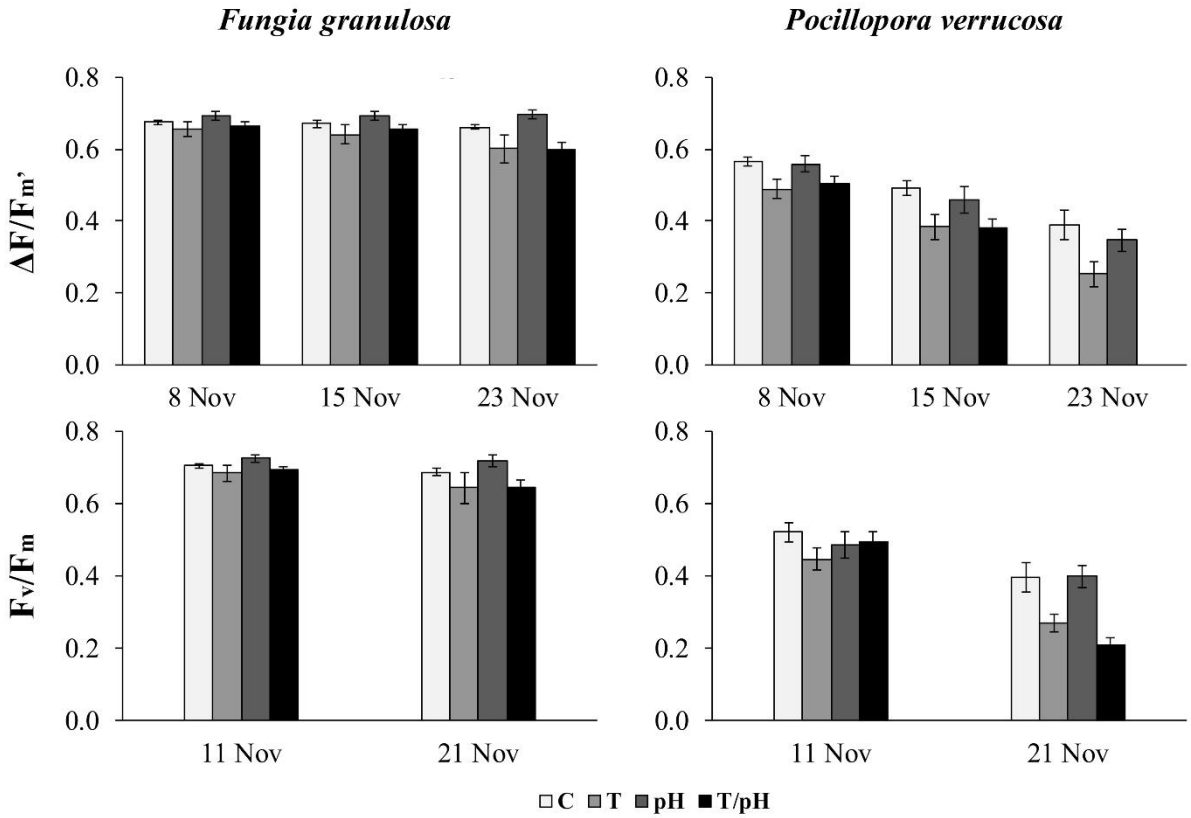

Figure 2. Effective quantum yield ($\Delta F/F_{m'}$) and maximum quantum yield ($F_v/F_{m'}$). Mean value ± CI (95%) collected by Diving PAM during and at the end of the experiment in both species. The experiment started on 26 October and ended on 23 November (4 weeks). Samples number and mean values for each treatment are listed in Table 3 and 4.

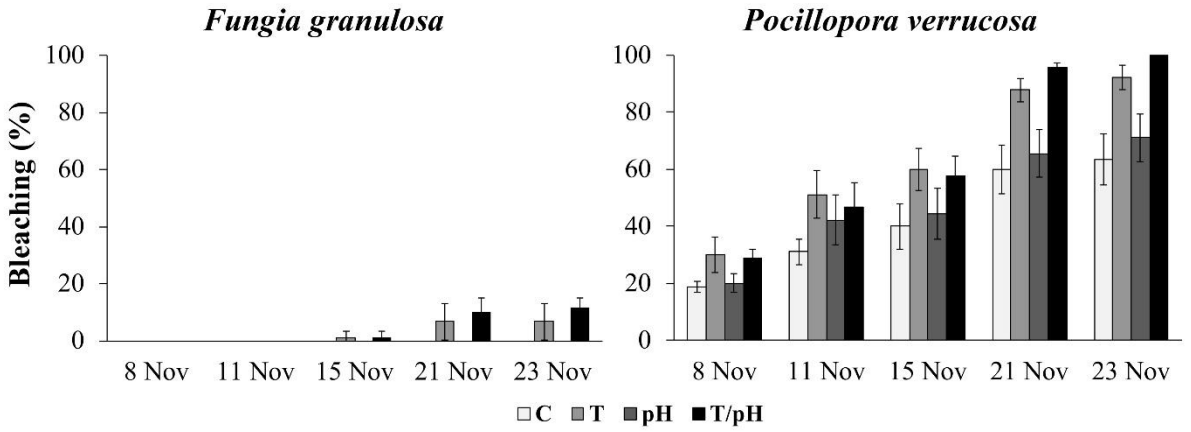

Figure 3. Coral tissue bleaching percentage. Mean value ± CI (95%) of registered bleaching tissue during and at the end of the experiment in both species. Samples number and mean values for each treatment are listed in Table 5.

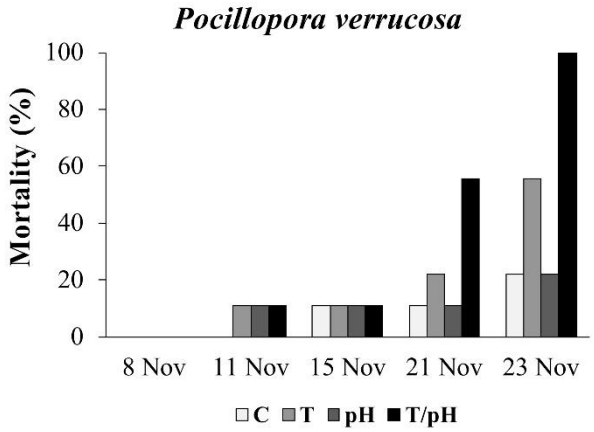

Figure 4. Coral mortality in *Pocillopora verrucosa*. Mean value of registered mortality during and at the end of the experiment in *Pocillopora verrucosa*. *Fungia granulosa* did never show polyp mortality during and at the end of the experiment. Samples number are listed in Table 6.

Section 3

Biomineralization, skeletal phenotype and environmental parameters

Chapter 6

Biomineralization in Mediterranean corals: the role of the intraskeletal organic matrix

Published in Crystal Growth & Design

CRYSTAL GROWTH & DESIGN

Article

pubs.acs.org/crystal

Biomineralization in Mediterranean Corals: The Role of the Intraskeletal Organic Matrix

Michela Reggi,[†] Simona Fermani,[†] Valerio Landi,[†] Francesca Sparla,[‡] Erik Caroselli,[§] Francesca Gizzi,[§] Zvy Dubinsky,[∥] Oren Levy,[∥] Jean-Pierre Cuif,[⊥] Yannicke Dauphin,[⊥] Stefano Goffredo,*[,§] and Giuseppe Falini*[,†,#]

[†]Dipartimento di Chimica "Giacomo Ciamician", via Selmi 2, [‡]Dipartimento di Farmacia e Biotecnologie, Via S. Donato 15, [§]Dipartimento di Scienze Biologiche, Geologiche e Ambientali, Sezione di Biologia, via Selmi 3, Alma Mater Studiorum - Università di Bologna, 40100 Bologna, Italy

[∥]The Mina and Everard Goodman Faculty of Life Sciences, Bar-Ilan University, Ramat-Gan 52900, Israel

[⊥]Université Paris-Sud, Orsay, Bat. 504, UMR IDES, F-91405 Orsay, France

[#]Centro Interdipartimentale di Ricerca per le Scienze Ambientali, Sede di Ravenna - Università di Bologna, via S. Alberto 163, 48100 Ravenna, Italy

Supporting Information

ABSTRACT: The precipitation of calcium carbonate was carried out in the presence of the intraskeletal organic matrix (OM) extracted from Mediterranean corals. They were diverse in growth form and trophic strategy, *Balanophyllia europaea* and *Leptopsammia pruvoti*—solitary corals, only the first zooxanthellate coral—and *Cladocora caespitosa* and *Astroides calycularis*—colonial corals, only the first zooxanthellate coral. The results showed that, although the OM marked differences among species, the diverse influence over the calcium carbonate precipitation was evident only for *B. europaea*. This OM was the most prone to favor the precipitation of aragonite in the absence of magnesium ions, according to overgrowth and solution precipitation experiments. In artificial seawater, where magnesium ions were present, this OM, as well the one from *A. calycularis*, precipitated mainly a form of amorphous calcium carbonate different from that obtained with SOM from *L. pruvoti* or *C. caespitosa*. The amorphous calcium carbonate from *B. europaea* was the most stable upon heating up to 100 °C and was the one that mainly converted into aragonite instead of magnesium calcite after heating at 300 °C. All this indicated a higher control of *B. europaea* OM over the calcium carbonate polymorphism than the other species. The influence of SOMs over precipitate morphology turned out to be also species related. In conclusion, this comparative study has shown that the influence of OM on *in vitro* precipitation of calcium carbonate was not related to the coral ecology, solitary vs colonial and zooxanthellate vs nonzooxanthellate, and suggested that the coral control over biomineralization process was species specific and encoded in coral genes.

INTRODUCTION

Scleractinian corals represent the biggest source of biogenic calcium carbonate[1,2] and are among the fastest marine mineralizing organisms.[3] In corals the calcification process occurs in a biological confined environment, under the control of biological macromolecules.[4] This is confirmed by the observation that, although coral skeleton morphology can be affected by habitat conditions,[5−7] the change always remains within the species-specific "vocabulary" controlled by the DNA of the organism.[8−10]

The skeleton of corals is a composite structure with both inorganic (aragonite) and organic components.[11,12] The merging of data from several investigations[13,14] has revealed that the actual growth unit of the skeleton is a few micrometers-thick mineralizing growth layer synchronically increasing the "sclerodermites", forming a given skeletal unit (e.g., a septum). The mineralizing growth layer simultaneously increases the two distinct mineralizing areas that have been extensively described from a structural point of view. At the growth edge of any structural components (e.g., septal spines) a granular and porous nanocrystalline phase (randomly oriented) forms the initial skeletal framework (also the earliest appearing mineralized elements after larval metamorphosis, according to Vandermeulen and Watabe[15]). These early mineralizing zones (EMZ), usually called "center of calcification", are laterally reinforced by deposition of a second structural layer made of dense, large, acicular crystals: the fibers.[16]

Organic components, referred to as organic matrix (OM), are involved in biomineral synthesis and become entrapped in the skeleton.[17−20] The composition of coral OM compounds

Received: March 13, 2014
Revised: June 9, 2014
Published: July 7, 2014

   dx.doi.org/10.1021/cg5003572 | Cryst. Growth Des. 2014, 14, 4310−4320

can be determined only after skeleton decalcification processes. On the basis of the studies performed by Young[12] and Constantz and Weiner[21] proteins and glycosaminoglycans but also sulfated polysaccharides[14,22] and lipids[23] are consistently found in the skeletons of many species covering the whole taxonomic scleractinian diversity (ref 9 and references therein). These molecules have a different role in the biomineral synthesis according to diverse biomineralization models. In physicochemical models, involving a liquid layer with chemical properties called calcifying fluid,[24] the OM acts as a support for calcium carbonate-oriented crystallization.[2] In these models crystal growth occurs through a primarily inorganic process, which involves a coral-controlled transcellular ion transport to the calcifying fluid (ref 9 and references therein). A recent model of ionic transport shows a direct and rapid seawater transport to the calcification site.[25] In contrast to physicochemical models, Clode and Marshall[26] have suggested a molecular model in which calcification occurs within a gel secreted at the interface between the calicoblastic cells and the skeleton. According to this model the glycoproteins form an architectural framework bearing the sites for development of the mineral phase.[27] In this model, OM interacts with the growing crystal changing its shape.[28−30] More recently, attention was drawn on the potential role of OM as carriers of the mineral precursors, which are possibly in an amorphous status. In this view, the OM became trapped along the boundary grains of the final crystal during the transition from the amorphous to the crystalline phase.[10,30]

Many aspects of the OM role in the dynamics of skeleton formation of corals are enigmatic.[4] It has been recently shown, by *in vitro* studies, that the OM from different corals species influences polymorphism and morphology of calcium carbonate. Goffredo et al.[31] showed that the intraskeletal OM from Mediterranean zooxanthellate solitary coral, *Balanophyllia europaea*, can favor the precipitation of aragonite and that a transient phase of amorphous calcium carbonate (ACC) stabilized by lipids is involved. The influence of coral intraskeletal OM molecules in the precipitation of calcium carbonate was proved also for the tropical species *Acropora digitifera*, *Lophelia pertusa*, and *Montipora caliculata*.[10] Moreover, an important recent study has shown that four highly acidic proteins, derived from the expression of genes obtained from the common coral *Stylophora pistillata* can spontaneously catalyze the precipitation of calcium carbonate *in vitro* from seawater.[32]

This study deepened the investigations using the OM from skeletons of *Leptopsammia pruvoti* (solitary, nonzooxanthellate), *Balanophyllia europaea* (solitary, zooxanthellate), *Astroides calycularis* (colonial, nonzooxanthellate), and *Cladocora caespitosa* (colonial, zooxanthellate). These Mediterranean coral species were chosen because they represent the combination among different growth forms and trophic strategies. Solitary corals are single autonomous individuals (polyps), while colonial corals are modular organisms constituted by cloned polyps living in close connection (physical and physiological) one to each other. Symbiosis determines the synthesis of molecules essential to the biomineralization process,[33] such as precursors for the OM.[9,34−36] The first link between photosynthesis and calcification was found by Kawaguti and Sakumoto;[37] they pointed out that calcification rate is higher in the light than in the dark.[9] It was also shown that in the presence of light the calcification rate is higher in zooxanthellate corals than in nonzooxanthellate corals.[38] However, from a general point of view, it is clear that coral calcification is not dependent on the presence of symbionts[39,40] and non-zooxanthellate corals have an efficient calcification as well. Moreover, tissues that calcify at the highest rates, or which initiate calcification, do not possess zooxanthellae.[9,41,42] It was also shown that photosynthesis increases calcification rate because it fixes CO_2 and increases the skeleton surface pH.[43−45]

The main goals of this study are (a) to evaluate whether the intraskeletal OM from different coral species shows a different capability to govern the formation and stability of calcium carbonate precipitates; (b) to infer possible relationships between the organism ecology (growth form and trophic strategy) and its OM capabilities.

MATERIALS AND METHODS

Coral Skeletons. The samples of *L. pruvoti*, *B. europaea*, *C. caespitosa* from Calafuria and *A. calycularis* from Palinuro (Italian coast, North-Western Mediterranean Sea) were randomly collected by scuba diving at 16, 6, and 9 m depth, respectively, between 1 July 2010 and 25 February 2012. Coral skeletons were cleaned, ground, and analyzed by X-ray powder diffraction using a powder diffractometer (PanAnalytical X'Pert Pro equipped with X'Celerator detector) with Cu Kα radiation. Thermogravimetric analysis (TGA) was performed to estimate the OM content in the coral skeleton using an SDT Q600 instrument (TA Instruments). These analyses were carried out as previously reported.[10]

Extraction of the Organic Matrix. The soluble (SOM) and the insoluble (IOM) OM fractions were extracted through decalcification using a 0.1 M CH_3COOH solution as previously reported.[10] The whole OM (*w*OM) was obtained using the same procedure without the separation step between SOM and IOM.

Characterization of the OM. The polyacrylamide gel electrophoresis (SDS-PAGE) of SOM was performed on 12.5% polyacrylamide gel, according to a reported procedure[10] that implies the use of strong fixative agents. The PAS (Periodic Acid Schiff) stain was performed to detect glycoprotein.

Amino acid analysis (AAA) was conducted by a chromatographic technique using an amino acid analyzer, according to a reported procedure.[10] The average protein pI of all the OM fractions was calculated from the amino acid analyses of all the species, following the method described in Sillero and Ribeiro.[46]

Aliquots of OM fractions and *w*OM were analyzed by Fourier transform infrared spectroscopy (FTIR) using a FTIR Nicolet 380 Thermo Electron Corporation working in the range of wavenumbers 4000−400 cm^{-1} at a resolution of 2 cm^{-1}. The statistical analysis of amino acid data and FTIR spectra was carried out with the Mann−Whitney test.

Calcium Carbonate Overgrowth Experiments. Transversal sections of coral skeletons, placed in a microplate for cellular culture (MICROPLATE 24 well with Lid, IWAKI) or in a Petri dish (d = 3.2 cm), were overlaid with 750 or 3360 μL of 10 mM $CaCl_2$ solution, respectively, according to previous experiments.[10] A 30 × 30 × 50 cm^3 crystallization chamber was used. Two 25 mL beakers half-full of $(NH_4)_2CO_3$ (Carlo Erba) covered with Parafilm with 10 holes and two Petri dishes (d = 8 cm) full of anhydrous $CaCl_2$ (Fluka) were put inside the chamber. The crystallization time was 4 days. At the end of the precipitation process the transversal sections were lightly rinsed with milli-Q water (resistivity 18.2 MΩ cm at 25 °C; filtered through a 0.22 μm membrane), dried, and examined by scanning electron microscopy (SEM).

Calcium Carbonate Crystallization Experiments. The same crystallization chamber utilized for overgrowth experiments, containing $(NH_4)_2CO_3$ and anhydrous $CaCl_2$, was used. Microplates for cellular culture containing a round glass coverslip in each well were used. In each well, 750 μL of 10 mM $CaCl_2$ solutions ($CaCl_2 \cdot 2H_2O$, Merck) or of modified (increased of 10 times the Ca^{2+} and Mg^{2+} concentration) artificial seawater (ASW)[47], were poured. In the first sets of experiments, OM fractions, separately or together, were added

dx.doi.org/10.1021/cg5003572 | Cryst. Growth Des. 2014, 14, 4310−4320

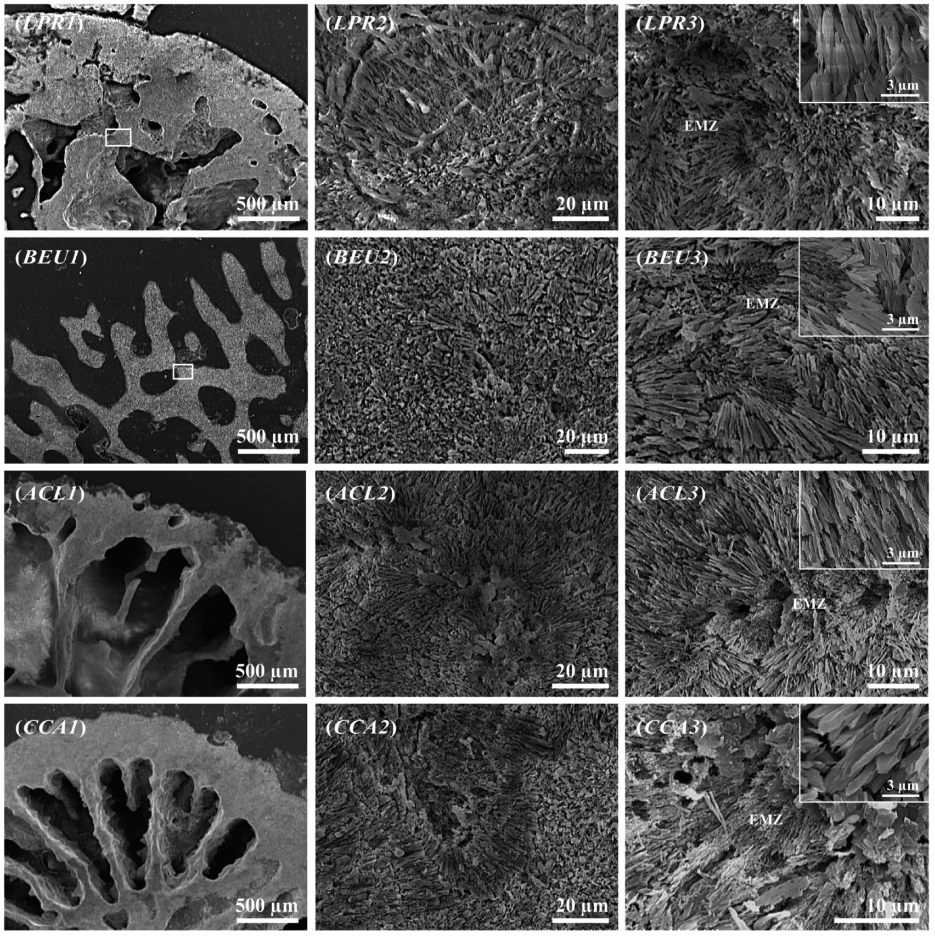

Figure 1. SEM pictures at increasing magnifications (1−3) of sections of coral skeleton of *L. pruvoti* (*LPR*), *B. europaea* (*BEU*), *A. calycularis* (*ACL*) and *C. caespitosa* (*CCA*) after etching. The pictures with suffix 3 show early mineralization zones (EMZ) surrounded by fibers, which are shown in the insets at higher magnifications.

to 750 μL of 10 mM $CaCl_2$ solution. Eight μL (for *L. pruvoti* and *A. calycularis*) or 20 μL (for *B. europaea* and *C. caespitosa*) of a solution obtained dissolving lyophilized SOM in water (17.5 mg/mL) were added to the solution. This quantity was chosen by keeping in consideration SOM concentration in the skeleton.[10,31] In other wells 0.5 mg of IOM were added to 750 μL of 10 mM $CaCl_2$ solution. SOM and the IOM (*e*OM) were added in the last wells. In the second set of experiments the whole OM (*w*OM) was added to 750 μL of 10 mM $CaCl_2$ solution and to ASW. The quantity of *w*OM added was 0.4 and 0.2 mg, respectively. The experiment proceeded for 4 days. The obtained crystals were washed three times with milli-Q water and then analyzed. All the experiments were conducted at room temperature. The crystallization trials of calcium carbonate in the different conditions were replicated starting from different batches of OM fractions.

Characterization of $CaCO_3$ Precipitates. FTIR spectra of samples in KBr disks were collected at room temperature by using a FTIR Nicolet 380 Thermo Electron Corporation working in the range of wavenumbers 4000−400 cm^{-1} at a resolution of 2 cm^{-1} according to a reported procedure.[10]

Atomic absorption measurements of calcium and magnesium were carried out with a PerkinElmer AAnalyst 100 flame and graphite furnace (HGA 800) spectrometer equipped with a Zeeman effect background corrector, and an automatic data processor. A 20-μL volume sample solution obtained by precipitated dissolution in 0.1 M HNO_3, was injected by an auto sampler. A multi-element hollow cathode lamp of analytes was used as a radiation source. Three measurements were carried out for each sample.

Thermal Treatment of $CaCO_3$ Precipitates. The samples that showed the presence of ACC in the precipitate from ASW solution with *w*OMs were heated at 105° for 18, 36, and 72 h.[48] At the end the same samples were heated at 300 °C for 8 h. FTIR spectra were collected after each thermal treatment.

Microscopic Observations. A Leica microscope equipped with a digital camera was used for optical microscope observations of $CaCO_3$ precipitates. SEM observations were conducted using a scanning electronic microscope Phenom microscope (FEI) or a Hitachi FEG 6400 scanning electron microscope after sample coating with gold.

RESULTS

Skeletal Structures of Corals. Scanning electron microscope images of septum cross sections showed the typical textural pattern of the coral skeleton (Figure 1): the EMZ was composed of small rounded granules, and fibers are produced with a patterned growth. EMZs are more sensitive to acidic etching than the fibers[49] and thus appear rich with cavities. Size and spatial distribution of EMZs and fibers vary upon species. In *L. pruvoti* and *B. europaea* the EMZs were observed as shallow cavities from which fibers radially extend having in *L. pruvoti* a smaller diameter and a less compact structure than in *B. europaea* (Figure 1 *LPR*1−3 and *BEU*1−3). In *A. calycularis* in the EMZs were observed as granular particles that cover the fiber tips. In *A. calycularis* and *C. caespitosa* the cavities are deep and episodically aligned parallel to the long axis of the septa and

dx.doi.org/10.1021/cg5003572 | *Cryst. Growth Des.* 2014, 14, 4310−4320

Table 1. Summary of the *in Vitro* Calcium Carbonate Crystallization Experiments[a] in the Presence of Organic Matrix (OM) Extracted from *L. pruvoti*, *B. europaea*, *A. calycularis*, and *C. caespitosa*

	OM composition			$CaCO_3$ overgrowth		$CaCO_3$ precipitation				
medium				10 mM $CaCl_2$		10 mM $CaCl_2$				ASW
species		SOM[e]	IOM[e]	C	A	SOM (C)	IOM (C)	*e*OM (C, A)[g]	*w*OM (C, A)[g]	*w*OM (ACC[h], MgC, A)
LPR *sol. azo.*	2.5 ± 0.1[b]	*p* (=)	*p* (=)	s. cryst.	needle bundles (1−3)[f]	db., s. ag.	cr. ag.	s. ag.	**cr. ag.**, s. ag.	nanoparticles[I]
	0.3[c]	*s* (−)	s (+)	{10.4}		(s. m. layers)	{10.4} {10.8}	(ag. nano p.)	(ag. nano p.)	2D struct.
	−[d]	*l* (=)	l (=)	(7−29)[f]		(5−57)[f]	(12−72)[f]	(5−32)[f]	(3−28)[f]	ACC1 (19.8 ± 0.5)
BEU *sol. zoo.*	2.9 ± 0.1[b]	*p* (=)	*p* (=)	**s. cryst.**	prisms (0.3−1)[f]	db., s. ag.	cr. ag.	flat. ag.[g]	**cr. ag.**, flat. ag.	nanoparticles
	1.5[c]	*s* (−)	*s* (+)	**{10.4}{hk.0}**		(add. part.)	{10.4}{10.8}	(ag. nano p.)	(ag. nano p.)	3D struct.
	+[d]	*l* (=)	*l* (=)	(6−33)[f]		(2−20)[f]	(16−53)[f]	(3−10)	(38−124)[f]	ACC2 (20.3 ± 0.6)
ACL *col. azo.*	2.7 ± 0.1[b]	*p* (=)	*p* (=)	s. cryst.	fused prisms (2−5)[f]	db., s. ag.	s. cr.	ag.	**cr. ag.**, ag.	nanoparticles
	0.2[c]	*s* (−)	*s* (+)	{10.4}		(add. part.)	{10.4} {10.8}	(ag. nano p.)	(ag. nano p.)	3D struct.
	+[d]	*l* (−)	*l* (+)	(10−50)[f]		(4−40)[f]	(4−21; 113−139)[f]	(37−68)	(7−24; 54−106)[f]	ACC2 (19.4 ± 0.5)
CCA *col. zoo.*	2.5 ± 0.1[b]	*p* (=)	*p* (=)	**s. cryst.**	fused prisms (1−4)[f]	db., s. ag.	cr. ag.	s. ag.	**cr. ag.**, s. ag.	nanoparticles
	0.3[c]	*s* (−)	*s* (+)	**{10.4} {*hk*0}**		(ag. nano p.)	{10.4}{10.8}	(ag. nano p.)	(ag. nano p.)	2D struct.
	−[d]	l (−)	l (+)	(4−28)[f]		(7−10)[f]	(26−85)[f]	(3−16)[f]	(10−42)[f]	ACC1 (19.6 ± 0.5)

[a]The main features of the OM fractions are also reported. [b]Mass percentage of OM entrapped in the skeleton. [c]Mass ratio between SOM and IOM. This data showed a great variability from one experiment to another, and the median value is reported. [d]Relative content of acidic amino acid between SOM and IOM: (+) indicates higher and (−) indicates lower. [e]*p*, *s*, and *l* indicate protein, sugars, and lipids, respectively, and their relative content between SOM and IOM is evaluated as higher (+), equal (=), or lower (−). [f]Indicates the range of dimension of the particles (in μm). [g]Only in the presence of BEU was the precipitation of aragonite observed. [h]Two forms of ACC were observed, having the FTIR ν_2 band at 868 cm^{-1} (ACC1) and 871 cm^{-1} (ACC2). In parentheses the magnesium content with respect to calcium as mol percentage is reported. [I]The presence of few elongated rhombohedral single crystals and aggregates of needle-like crystals (only BEU) was observed. When indicated, the errors are reported as standard deviations.

dx.doi.org/10.1021/cg5003572 | Cryst. Growth Des. 2014, 14, 4310−4320

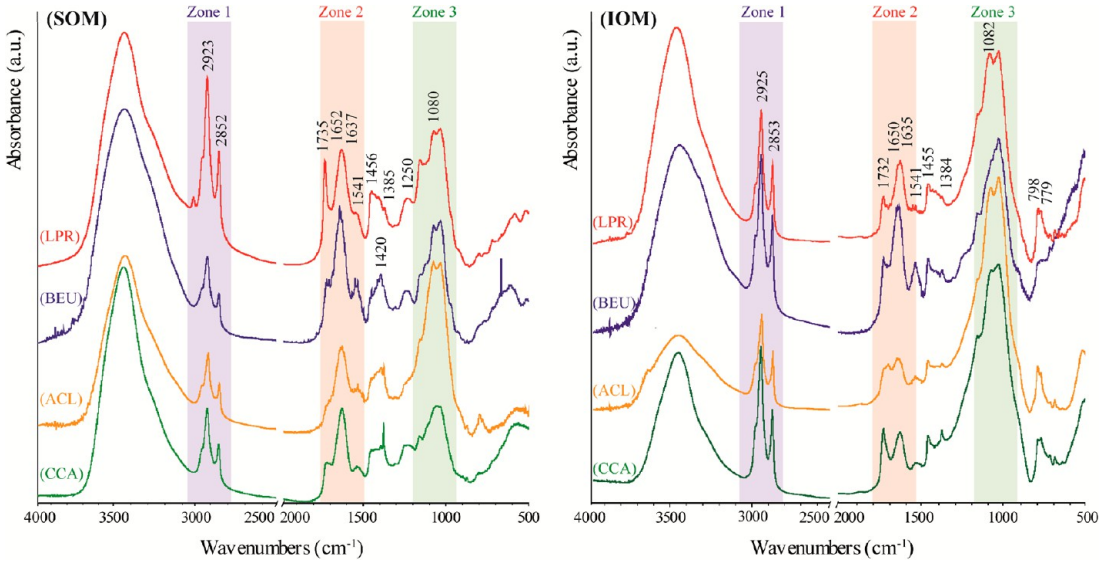

Figure 2. FTIR spectra of intraskeletal soluble (SOM) and insoluble (IOM) organic matrix from aragonitic skeleton of *L. pruvoti* (LPR), *B. europaea* (BEU), *A. calycularis* (ACL), and *C. caespitosa* (CCA). The wavenumbers of the main absorption bands are indicated. The three marked zones define diagnostic regions of functional groups, which could be mainly associated with the presence of lipids (zone 1), protein and polysaccharides (zone 2), and polysaccharides (zone 3).

the fibers are similar to those of *B. europaea* (Figure 1 *ACL*1−3 and *CCA*1−3).

Studies on the Intraskeletal OM. In *L. pruvoti*, *B. europaea*, *A. calycularis*, and *C. caespitosa* the mineral skeleton hosting the OM was expected to be of pure aragonite (Figure SI1 in the Supporting Information [SI]); however, in the insoluble residue obtained after decalcification, few silica needles were observed, constantly in *A. calycularis* and rarely in the other species (Figure SI2 in SI). The presence of this impurity, which was not possible to remove, was considered not influencing the calcium carbonate precipitation assays. The skeleton TGA showed a first weight loss (bounded water) in the range 150−220 °C followed by a second one (OM pyrolysis) between 280 and 450 °C (Figure SI3 in SI).[50] The overall weight loss was 3.4 ± 0.1, 3.9 ± 0.1, 3.5 ± 0.1, and 3.4 ± 0.1% (*w*/*w*) in *L. pruvoti*, *B. europaea*, *A. calycularis*, and *C. caespitosa*, respectively (Table1, OM composition). After extraction the OM separated in SOM and IOM fractions; the median amount of IOM was higher than that of SOM in all species, except in *B. europaea* (Table 1, OM composition).

The OM fractions were analyzed by FTIR, SDS-PAGE, and AAA. Table SI1 in SI summarizes the observations from the FTIR spectra of SOM and IOM (n = 6) and in Figure 2 the most representative spectra are shown. In SOM and IOM the same absorption bands were detected with different relative intensities (according to refs 8, 10, and 31). To estimate the relative amounts of the main molecular components of the OM from the FTIR spectra, three zones (1−3) were defined (Figure 2, Table SI3 in SI).[10] In the zone 1 (3000−2800 cm^{-1}) the bands were related to fatty acids or to molecules bearing alkylic chain regions, in the zone 2 (1750−1500 cm^{-1}) were located the bands associated to proteins (and some sugars), and in the zone 3 (1100−950 cm^{-1}) bands linked to polysaccharides.[51] The integrated intensities of the bands in zones 1 and 3 were normalized to that of zone 2 (Table SI3 in SI). Then a Mann−Whitney test was carried out to check for significant differences between SOM and IOM. In all the species SOM showed a lower absorption than IOM in the zone 3, and only in *A. calycularis* and *C. caespitosa* in the zone 1. Comparing OM fractions among all the species, the absorption of IOM from *A. calycularis* is the highest.

SDS-PAGE observations (Figure 3) of SOMs showed many bands gathered around 45 and 30 kDa in *L. pruvoti* and bands

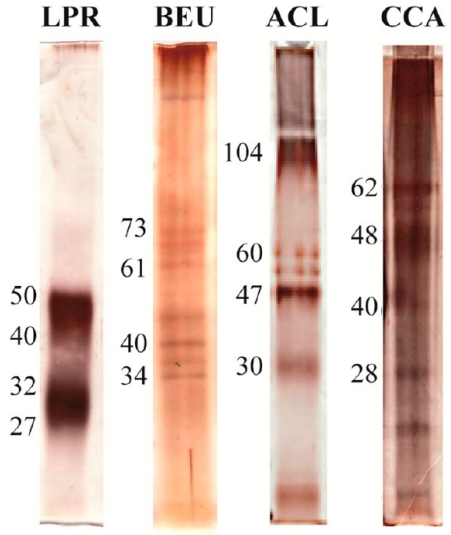

Figure 3. SDS-PAGE of intracrystalline soluble organic matrix extracted from aragonitic skeleton of *L. pruvoti* (LPR), *B. europaea* (BEU), *A. calycularis* (ACL), and *C. caespitosa* (CCA). The side numbers indicate the molecular weight (kDa) of silver stain marked bands.

clustered in two groups having molecular masses from ∼40 to 34 kDa and from 73 to 60 kDa[31] in *B. europaea*. In *A. calycularis* and *C. caespitosa* many bands distributed from ∼104 to 30 kDa and from 62 to 28 kDa, respectively, were revealed.

The AAA from SOM and IOM was reported in Table SI2 in SI. SOM was characterized by a content of aspartic (and asparagine) higher than that in IOM. The content of hydrophobic residues was always higher in IOM (33−50 mol

dx.doi.org/10.1021/cg5003572 | *Cryst. Growth Des.* 2014, 14, 4310−4320

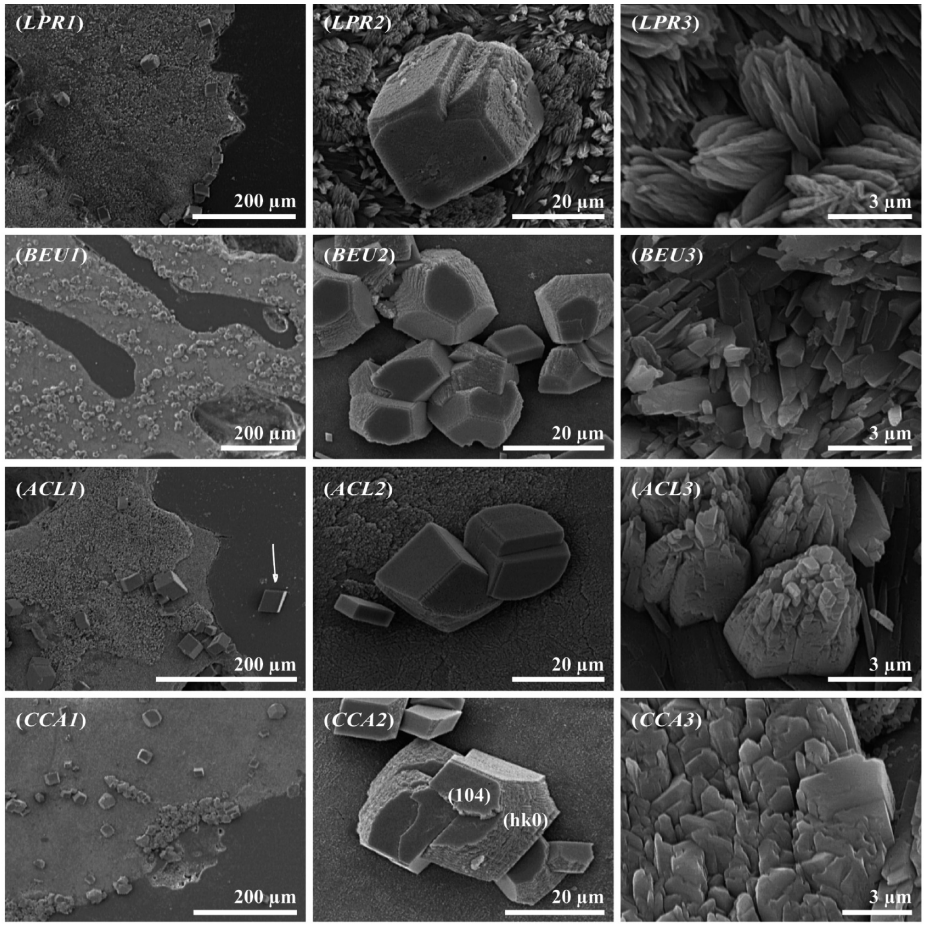

Figure 4. SEM pictures at increasing magnifications (1−3) of sections of coral skeleton of *L. pruvoti* (*LPR*), *B. europaea* (*BEU*), *A. calycularis* (*ACL*), and *C. caespitosa* (*CCA*) after calcium carbonate overgrowth experiments. A new layer of crystals with aragonite typical morphology grew on the skeleton surfaces in all the species (magn. 3). On these new layers more or less smoothed calcite crystals were observed (magn. 2) that in some cases they showed additional {*hk*0} faces to the rhombohedral {10.4}. Outside the skeletons sections only rhombohedra of calcite precipitated (*ACL1*, indicated by the arrow).

%) than in SOM (24−34 mol %). The calculated average protein pI[46] shows that OMs were acidic, and IOM was less acidic than the SOM within a species (Figure SI4 in SI).

Overgrowth of $CaCO_3$ onto Coral Skeleton Sections. The results of the calcium carbonate overgrowth experiments on skeleton cross sections are illustrated in Figure 4. Surfaces normal to the oral−aboral axis and close to the growing tips were used. The overgrowth occurred in a 10 mM calcium chloride solution under diffusion of ammonium carbonate vapors. Calcium carbonate crystals were observed on the skeleton cross section and outside it (on the surface of the embedding resin). On the resin only calcite crystals appearing almost as perfect {10.4} faced rhombohedra (see Figure 4 *ACL1* on the right) were observed. The crystals with the typical morphology of aragonite were observed only on the surface of the skeletons. They appeared as bundles of needle-like crystals in *L. pruvoti* and as single hexagonal prisms in *B. europaea*, the bundles were about 3 μm in diameter, while the needle-like crystals and the single prisms had an average diameter smaller than 1 μm. In *A. calycularis* and *C. caespitosa* the hexagonal prisms observed on *B. europaea* were coherently fused in big prisms having a diameter usually above 4 μm. On the coral skeleton calcite crystals were also observed, and they exhibited additional {*hk*0} faces to {10.4} ones, which were wider in those grown on the skeleton of *B. europaea* and *C. caespitosa* (Figure 4 *CCA2* and *BEU2*) than in those on the *A. calycularis* and *L. pruvoti* skeletons (Figure 4 *ACL2* and *LPR2*).

Precipitation in the Presence of OM Fractions. A first set of $CaCO_3$ precipitation trials was carried out from 10 mM $CaCl_2$ solutions containing the OM fractions. Without OM only the deposition of rhombohedral crystals of calcite was observed. The presence of OM fractions induced an inhibition of the precipitation and a reduction of the average particle sizes, as a monotone function of the additive concentration. On the basis of a set of preliminary studies and previous similar experiments[10,31] a SOM concentration of 185 μg/mL was used for *L. pruvoti* and *A. calycularis* and 455 μg/mL for *B. europaea* and *C. caespitosa*, while 666 μg/mL of IOM were dispersed in the calcium chloride solution.

The reported results are the trends observed from six precipitations trials (see Experimental Section and Table SI4 in SI). In the presence of SOM, aggregates having the shape of dumbbell and sphere were always observed (Figure 5 SOM). These particles (5−69 μm) showed surfaces formed by stacked multilayers (Figure 5 SOM *LPR*, inset) in the presence of *L. pruvoti* SOM, while with *B. europaea* and *A. calycularis* SOMs they showed (4−20 μm and 4−80 μm, respectively) smooth surfaces and were copresent with aggregates having various shapes (Figure 5 SOM *BEU* and *ACL*, inset). In the presence of *C. caespitosa* SOM the dumbbells and spherical shaped

dx.doi.org/10.1021/cg5003572 | *Cryst. Growth Des.* 2014, 14, 4310−4320

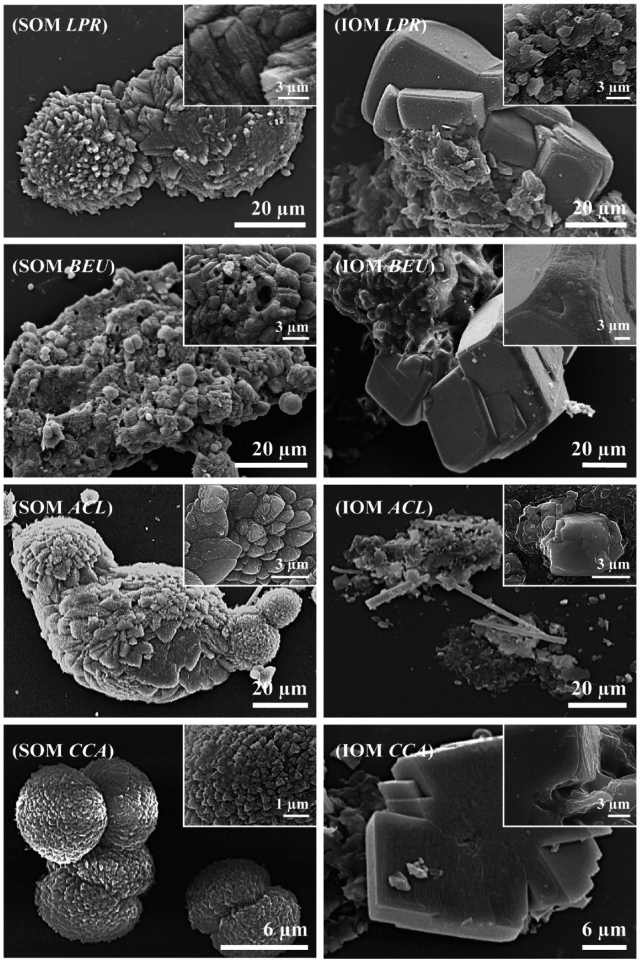

Figure 5. SEM pictures of particles obtained from precipitation experiments of $CaCO_3$ from 10 mM $CaCl_2$ solutions in the presence of OM fractions. In the first and second columns are shown particles obtained in the presence of soluble (SOM) or insoluble (IOM) organic matrix, respectively. In the rows are shown, from top to bottom, particles obtained in the presence of *L. pruvoti* (LPR), *B. europaea* (BEU), *A. calycularis* (ACL), and *C. caespitosa* (CCA). In the insets are reported high magnification pictures of the particles. The calcite crystals on IOMs show truncation of rhombohedral {104} corners and edges (probably the presence of small {108} and {*hk*0} faces). These pictures are the most representative of the populations of observed particles.

aggregates (7−80 μm) appeared formed by the association of submicrometer particles (Figure 5 SOM *CCA*, inset). The FTIR spectra of these precipitates showed the characteristic absorption bands of calcite plus those due to the SOM (Figure SI5 SOM [in SI]). In the presence of dispersed IOM, which sometime floated at the air/solution interface, the formation of mineral particles was observed both on the matrix surface and outside it. On the IOMs framework, from all the species, calcite crystals grew, showing truncation of rhombohedral corners and edges (Figure 5 IOM and insets). On *A. calycularis* IOM only a few calcium carbonate particles were observed, together with the needle-like silica contaminants (see Materials and Methods section). On *L. pruvoti*, *C. caespitosa*, and *B. europaea* IOM, and outside it, the calcite crystals assembled showing overlapping edges (Figure 5 IOM *LPR*, IOM *BEU*). The FTIR spectra showed only the presence of the absorption bands of calcite, with those of IOM (Figure SI5 IOM [in SI]).

When the *e*OM was used (Figure 6 *e*OM and inset) few aggregates formed by small particles (submicrometer size)

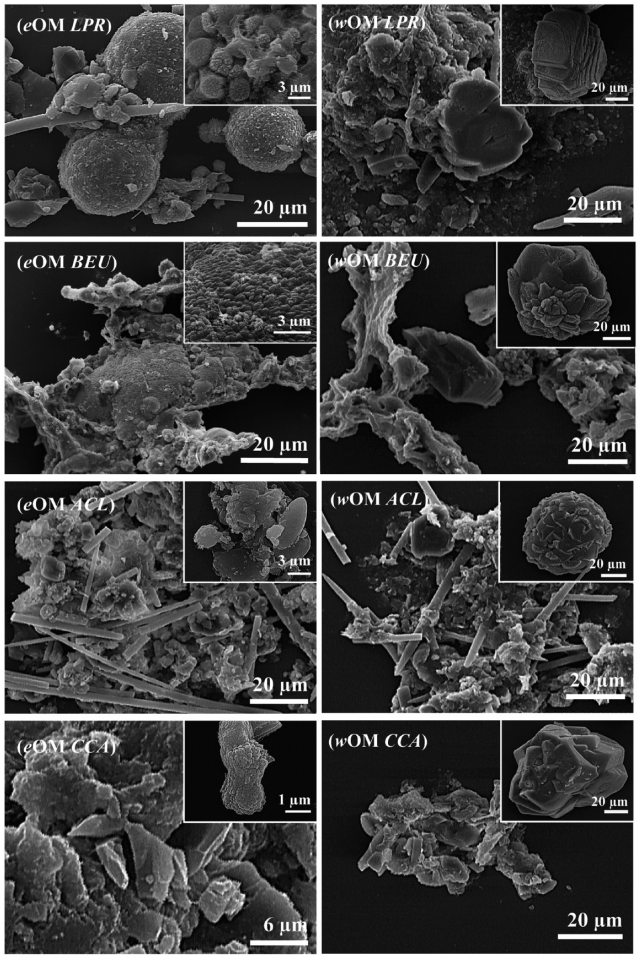

Figure 6. SEM pictures of particles obtained from precipitation experiments of $CaCO_3$ from 10 mM $CaCl_2$ solutions in the presence of the entire organic matrix (*e*OM) or the whole organic matrix (*w*OM). The *e*OM and *w*OM were extracted from *L. pruvoti* (LPR), *B. europaea* (BEU), *A. calycularis* (ACL), and *C. caespitosa* (CCA). In the picture ACL needle-like silica spicules are present. In the insets are reported high magnification images of representative features of the associated particles. These pictures are the most representative of the populations of observed particles.

precipitated; this observation effect was prominent for *A. calycularis*. In the presence of *L. pruvoti*, *B. europaea*, and *C. caespitosa* *e*OM, the surface of the IOM was covered by aggregates of submicrometer units having a rough surface. In addition, crystals, like those precipitated in the presence of SOM, were observed around the IOM, particularly for *C. caespitosa* (Figure 6 *e*OM *CCA* inset). In the presence of *A. calycularis* *e*OM few aggregates with shape changing from one experiment to another were observed (the most representative in Figure 6 *e*OM *ACL*). The FTIR spectra of these materials (Figure SI5 *e*OM [in SI]) showed the absorption bands of calcite, except for *B. europaea* where the aragonite bands were observed as well (as reported in ref 31).

Precipitation in the Presence of the Whole OM. A second set of $CaCO_3$ precipitation trials, in which the *w*OM was added into a 10 mM $CaCl_2$ solution or into an ASW[47] solution (Figure 6, Table 1 and Table SI4 in SI), was carried

dx.doi.org/10.1021/cg5003572 | *Cryst. Growth Des.* 2014, 14, 4310−4320

out. The experiments were carried out using 0.25 or 0.5 mg/mL of *w*OM, but the latter inhibited the precipitation over 4 days.

From the 10 mM $CaCl_2$ solution containing *w*OM precipitated $CaCO_3$ particles (Figure 6 *w*OM) similar to those observed in the presence of *e*OM (Figure 6 *e*OM) but showing morphological features closer to those observed in the presence of the respective IOM (Figure 5 IOM).

From the precipitation in ASW, aggregates having the shapes of peanut, dumbbell, and spherulite and formed by submicrometer-sized elongated rhombohedral crystals and needle-like crystals were observed (Figure 7 ASW). These aggregates were formed of magnesium calcite and aragonite (Figure 8a). The addition of the *w*OM to the ASW produced the massive precipitation of spherical submicrometer particles (Figure 7 ASW + *w*OM) and of few elongated rhombohedral crystals and needle-like crystals (only BEU). The aggregation of the submicrometer particles was species specific. They appeared as forming long chains associated in a two-dimensional network for *L. pruvoti* and *C. caespitosa*, while for *B. europaea* and *A. calycularis* three-dimensional architectures were generated. The FTIR spectra showed the presence of the typical absorption bands of ACC.[52] The presence of ACC was also verified by X-ray powder diffraction (Figure SI7 in SI). The diffraction pattern of the precipitates obtained in the presence of *w*OM showed only diffraction peaks due to the presence of halite and a very weak broad peak at about 29.7°. From ASW, diffraction peaks owing to aragonite and magnesium calcite were observed. Despite these observations the presence of traces of hydrated forms of calcium carbonate could not be excluded. ACC was further investigated by FTIR experiments upon thermal treatment of the precipitates (Figure 8 and Table SI5 in SI). The ν_3 and ν_2 showed a different position and profile bands after the thermal treatments. In the ACC obtained from *L. pruvoti* and *C. caespitosa* the ν_2 band was at 868 cm^{-1}, and in the ones from *B. europaea* and *A. calycularis* the band was at 871 cm^{-1}. Upon thermal treatment at 105 °C for 18 h for all the ACC the ν_2 band was at 871 cm^{-1}, and after 76 h this band moved to 875 cm^{-1} for all the samples, the same value showing in the precipitate formed from ASW without OM. When the same samples were thermally treated for 8 h at 300 °C they all showed the ν_2 band at 877 cm^{-1}. Moreover, a second band at 860 cm^{-1} clearly appeared in the precipitate obtained from *B. europaea*, analogous to that obtained from pure ASW, and was present as a shoulder in *A. calycularis* precipitate. The profile of the ν_3 band showed three main maxima centered at 1431, 1466, and 1480 cm^{-1}. By thermal treatment the maximum at 1431 cm^{-1} strengthened, while the one at 1480 cm^{-1} weakened. This change in intensities was more difficult in *B. europaea* that in the other species. The analysis of the absorption band at about 3300 cm^{-1}, due to the OH groups stretching, did not reveal any clear trend. This difficulty can be ascribed to the diverse contributions (e.g., water solvatation, carbohydrates) to this band and the presence of moisture. In the precipitates from the ASW the Mg/Ca molar ratio was measured by the atomic absorption spectroscopy ($n = 6$). These were 19.8 ± 0.5, 20.3 ± 0.6, 19.4 ± 0.5, and 19.6 ± 0.5 in *L. pruvoti*, *B. europaea*, *C. caespitosa*, and *A. calycularis*, respectively, while in the absence of OM it was 5.1 ± 0.1 (Table 1).

DISCUSSION

The precipitation of aragonite in corals occurs in a confined environment in a seawater-like fluid that contains biomineralizing (macro)molecules.[25,53] The understanding of the role of seawater ions (mainly magnesium) and of biomineralizing macromolecules in the *in vivo* calcification process lays objective difficulties, although terrific results were achieved.[54] The *in vitro* mineral precipitation in the presence of OM components represents an alternative approach. This assay has the disadvantage, and limitation, that only intraskeletal macromolecules upon an extraction process are considered. However, the assay was validated by a plethora of studies that have proved that the intraskeletal macromolecules were effective modifiers

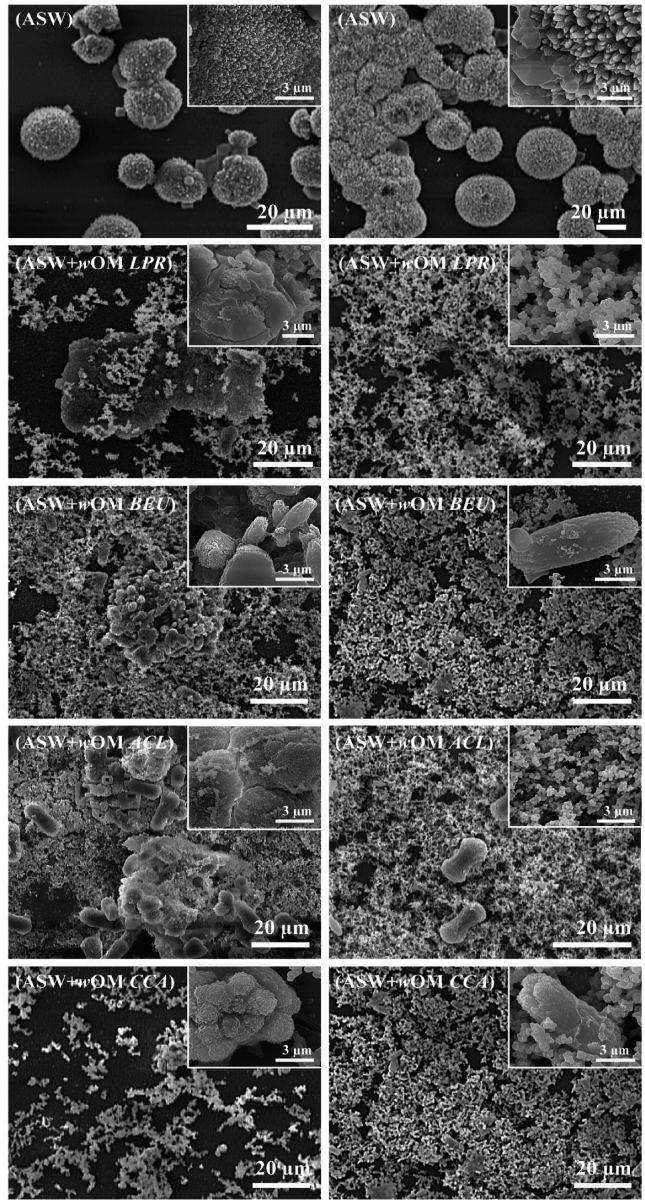

Figure 7. SEM pictures of particles obtained from precipitation experiments of $CaCO_3$ from artificial seawater (ASW) in the presence of the whole organic matrix (*w*OM), after the synthesis (left), and after the thermal treatment at 300 °C for 12 h (right). The spherical nanoparticles (2nd–4th row) were made of ACC before the thermal treatment and of magnesium calcite after the thermal treatment. In the presence of the *w*OM from *B. europaea*, aragonite coformed with magnesium calcite. The *w*OM was extracted from *L. pruvoti* (LPR), *B. europaea* (BEU), *A. calycularis* (ACL), and *C. caespitosa* (CCA). These pictures are the most representative of the populations of observed particles.

dx.doi.org/10.1021/cg5003572 | *Cryst. Growth Des.* 2014, 14, 4310–4320

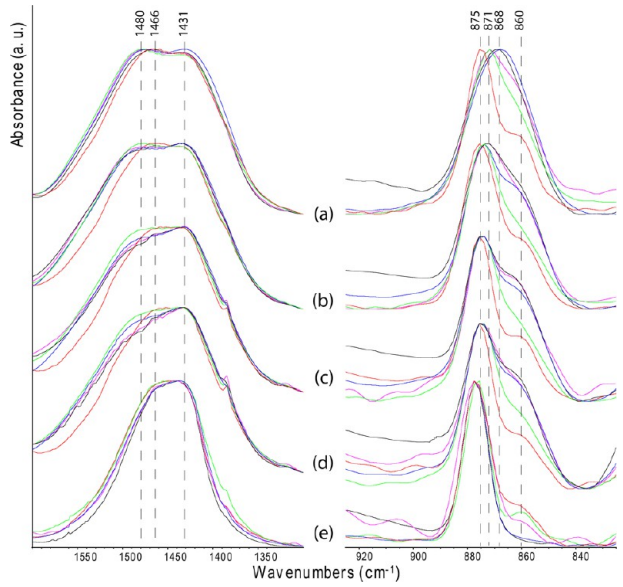

Figure 8. FTIR spectra of calcium carbonate precipitated from artificial seawater in the presence of the whole organic matrix (*w*OM), which was extracted from *L. pruvoti* (blue), *B. europaea* (green), *A. calycularis* (magenta), and *C. caespitosa* (black). The spectra from calcium carbonate precipitated from artificial seawater in the absence of *w*OM are also reported (red). Only the diagnostic ranges from 800 to 900 cm^{-1} and 1300 to 1600 cm^{-1} are shown (see SI for the entire FTIR spectra). (a) Spectra collected without any thermal treatment of the samples. (b–d) Spectra collected after a thermal treatment of the samples at 105 °C for 18 h (b), 36 h (c), and 72 h (d). (e) Spectra collected after a thermal treatment of the samples at 300 °C for 12 h.

of the nucleation and growth processes of minerals deposited by organisms.[54−56] Until few years ago this assay was almost ignored in the study of the biomineralization of corals. Recently, few *in vitro* studies have shown that the intraskeletal OM of corals influenced the aragonite precipitation.[10,31,32] Scleractinian corals, differently from many other marine calcifiers, show diverse growth forms (solitary vs colonial) and trophic strategies (zooxanthellate vs nonzooxanthellate). The presence of zooxanthellae was reported to have an influence on the calcification process.[9,42] A study on the OM amino acid composition showed differences between different species with different trophic strategies in the content of acidic residues.[35] Here, the study of the composition of OMs from the corals *L. pruvoti*, *B. europaea*, *A. calycularis*, and *C. caespitosa* showed the absence of any clear correlation among coral ecology (growth form or trophic strategy) and OM content, mass ratio between SOM and IOM, protein features, and macromolecule distribution (Table 1). An emerging feature was the high mass ratio SOM/IOM (1.5) in *B. europaea* (Table 1), a non-unique behavior since in *Acropora digitifera* a ratio of about 5 was observed.[10] Overgrowth experiments showed that aragonite formed on the surface of all coral skeletons. This effect, which could be due to secondary nucleation events, brought to the growth of crystals having species specific size and texture. On the skeleton of the zooxanthellate species, *B. europaea* and *C. caespitosa*, the overgrowth of numerous calcite crystals having a modified morphology was also observed. This can be related with the release in solution of molecules able to interact specifically with the {*hk*0} faces of calcite.[28] The band's distribution revealed by SDS-PAGE seemed to exclude that this effect was related to the presence of a significant amount of low-molecular weight molecules more easily released from the skeleton, keeping in consideration that some molecules could be not stained or fixed by the gel.[57] The calcium carbonate precipitation experiments in the presence of SOM, IOM, and the *e*OM gave results in agreement to what is observed for other coral species.[10,31] The SOM molecules were strong modifiers of the morphology of the calcite particles. These changes in morphology were due either to the aggregation of modified single-crystalline units of calcite, as in case of *L. pruvoti*, *A. calycularis*, and *C. caespitosa*, or to the assembly of submicrometer particles, as for *B. europaea*. The presence of IOM lightly affected the precipitation of calcite, and the crystals were slightly modified from their rhombohedral morphology, suggesting the limited release of IOM molecules in solution, favored by the crystallization conditions (pH and ionic strength).[10,31] According to reported data[10,31] the *e*OM effect on the precipitation was dominated by the SOM fraction, except for *B. europaea* where the copresence of SOM and IOM allowed the precipitation of aragonite together with calcite in a Mg-ion-free $CaCl_2$ solution, where usually calcite precipitated.[31] The favored precipitation of aragonite by OM molecules has been observed also for *Stylophora pistillata*,[32] but these experiments were carried out in seawater where the presence of magnesium ions (Mg/Ca molar ratio equal to 5) favors the precipitation of aragonite. The trials in which the *w*OM was used instead of *e*OM were performed to exclude possible artifacts associated with the separation process between SOM and IOM (e.g., reaggregation and reprecipitation). The results with *w*OM were in line with those obtained using *e*OM, but the morphological effects were more similar to those observed in the presence of IOM, suggesting that in the *w*OM a lower content of SOM was present with respect to the *e*OM.

More information with respect to what is already known was obtained from precipitation experiments in ASW using the *w*OM. In fact, previously described experiments showed that *w*OM behaved similarly to *e*OM, and it was definitely more representative of the OM entrapped in the skeleton. These two OMs differed for the extraction mode. In the *e*OM experiments the soluble and insoluble organic matrices were separated during the extraction process and then used together; with the *w*OM extracted in one step. The fact that these two procedures gave materials having similar functions in the precipitation of calcium carbonate indicated that (i) the activity of soluble and insoluble fractions was not affected by the extraction process and that (ii) the interaction between soluble and insoluble fractions was a reversible process. The use of ASW was in line with recent researches showing direct seawater transport to the calcifying site in corals.[25] The presence of magnesium ions in the extracytoplasmic calcifying fluid, at the nucleation site of corals, has been also reported.[47,58,59] The addition of *w*OM to ASW induced the precipitation of almost only ACC instead of aragonite and Mg-calcite, as revealed by the FTIR and X-ray diffraction analyses. ACC appeared in two forms having different FTIR spectra and thermal stabilities. The thermally less stable form of ACC, which precipitated in the presence of *w*OM from *L. pruvoti* and *C. caespitosa*, converted in the one more stable, which precipitated in the presence of *w*OM from *B. europaea* and *A. calycularis*, upon heating at 105 °C for 18 h. According to Radha et al.[60] a hydrated ACC transformed with aging or heating into a less hydrated form, crystallizing with time as calcite or aragonite. Two ACC forms, anhydrous ACC and hydrated ACC containing about 1 mol of water that persists for longer time periods, exist in biogenic sources.[61]

dx.doi.org/10.1021/cg5003572 | *Cryst. Growth Des.* 2014, 14, 4310−4320

Thus, we could infer that in our experiment the ACC thermally less stable forms (probably the hydrated ACC) converted to less hydrated, or anhydrous, ones upon heating (the complexity of the material did not allow accurate thermal analyses). The less hydrated ACC showed a different behavior when subject to a further heating process. It converted to poor crystalline Mg calcite in the presence of *w*OM from *L. pruvoti*, *A. calycularis*, and *C. caespitosa*, while the one from *B. europaea* formed Mg calcite and aragonite (Table SI5 in SI). This polymorphic selectivity in the solid-state crystallization of the ACC was attributed to the *w*OM, since the same heating profile was used, excluding effects due to the annealing rate.[62] Moreover, an increase in the crystallinity of Mg-calcite was observed after annealing.[48] The existence of two forms of ACC, which had a diverse binding strength, was reported as precursors of diverse crystalline phases.[63]

The wet transition from ACC to specific crystalline phases was reported to rely on the Mg/Ca molar ratio and the presence of additives in the precipitating solution.[64−67] In particular it was observed that in conditions of the Mg/Ca molar ratio >4 the transition from ACC to aragonite[64] occurred through monohydrocalcite at transition phase[67] in times shorter (<4 days) than those used in this study. This strongly indicated a stabilization of the ACC by the *w*OM; indeed in its absence, the ACC precipitation was not observed.

It has been reported that the formation and stability of different hydrated ACC forms have been ascribed to the copresence of Mg ions and OM from diverse mineralized tissues.[52,68] However, our data suggest that *w*OM plays a primary role in the ACC formation. Here, the *w*OM stabilization of two forms of ACC was not related to the content of Mg^{2+} hosted in ACC, being the same in all the precipitates (Table 1). Moreover, the coprecipitation of ACC with crystalline phases was observed also in the absence of magnesium ions.

The stabilization of ACC by *w*OM suggested that also coral biomineralization followed a crystallization pathway involving the formation of a transient form, as reported for foraminifera, mollusks, and echinoderms.[30] This agreed with recent observations on growing corals that reported the presence of transient granules that convert to aragonite fibers.[16] However, the presence of ACC was not detected in coral recruits.[69]

CONCLUSIONS

In conclusion, this research added three important observations to the study on *in vitro* precipitation of calcium carbonate: (i) the capability of OM to affect morphology and polymorphism was not related to the coral growth form or trophic strategy; (ii) in simulated seawater the OM stabilized the formation of diverse forms of ACC which converted species specifically in aragonite or magnesium calcite upon thermal treatment; (iii) *B. europaea* showed distinguished *in vitro* biomineralization features. Under overgrowth and solution precipitation experiments, its OM was the most prone to favor the precipitation of aragonite in the absence of magnesium ions; under thermal treatments, its ACC was unique, with being the most stable, and was the only one that partially converted to aragonite instead of magnesium calcite. These features suggested a stronger control of *B. europaea* OM over the mineral phases and a higher independence from crystallization environment compared to the other species. The reasons for the peculiar behavior of the OM from *B. europaea* were unknown. However, this species is distinguished also for its ecological properties, being the only one able to tolerate the effects of ocean acidification.[70]

ASSOCIATED CONTENT

Supporting Information

Experimental details on the X-ray powder pattern, FTIR spectra, TGA analyses, amino acid analyses, aliphatic index, and isoelectric point. This material is available free of charge via the Internet at http://pubs.acs.org.

AUTHOR INFORMATION

Corresponding Authors

*E-mail: s.goffredo@unibo.it. Telephone: +39 051 20994244.
*E-mail: giuseppe.falini@unibo.it. Telephone: +39 051 2099484.

Author Contributions

G.F., S.G., J.-P.C, Y.D, and Z.D. conceived and designed the project. M.R, V.L., F.S., and Y.D. carried out the experiments. All the authors contributed to data analysis, scientific discussion, and the writing of the paper. All authors have given approval to the final version of the manuscript.

Notes

The authors declare no competing financial interest.

ACKNOWLEDGMENTS

The research leading to these results has received funding from the European Research Council under the European Union's Seventh Framework Programme (FP7/2007-2013)/ERC Grant Agreement No. [249930-CoralWarm: Corals and global warming: the Mediterranean versus the Red Sea; www.CoralWarm.eu]. G.F. and S.F. thank CIRC-MSB for support. S.G. thanks S. Branchini, S. Guerrieri, and M. Marinozzi for help in collecting the samples. We thank Gianni Neto for the underwater picture of *A. calycularis*.

REFERENCES

(1) Spalding, M. D.; Ravilious, C.; Green, E. P. *World Atlas of Coral Reefs*; University of California Press: Berkeley, 2001; pp 424.
(2) Cohen, A. L.; McConnaughey, T. A.; Dove, P. M.; Weiner, S.; Yoreo, J. J. Geochemical perspectives on coral mineralization. *Biominer., Rev. Miner. Geochim.* **2003**, 151−187.
(3) Marshall, A. T.; Clode, P. *Coral Reefs* **2004**, *23*, 218−224.
(4) Allemand, D.; Tambutté, È.; Zoccola, D.; Tambutté, S. Coral calcification, cells to reefs. In *Coral reefs: and ecosystem in transition*; Dubinsky, Z., Stambler, N, Eds.; Springer: Dordrecht, 2011; pp 119−150.
(5) Jokiel, P. F. *J. Exp. Mar. Biol. Ecol.* **1978**, *35*, 87−97.
(6) Jokiel, P. F.; Coles, S. L. *Coral Reefs* **1990**, *8*, 155−162.
(7) Kuffner, I. B.; Andersson, A. J.; Jokiel, P. L.; Rodgers, K. S.; Mackenzie, F. T. *Nature Geosci.* **2008**, *1*, 114−117.
(8) Cuif, J.-P.; Lecointre, G.; Perrin, C.; Tillier, A.; Tillier, S. *Zool. Scr.* **2003b**, *32*, 459−473.
(9) Tambutté, S.; Holcomb, M.; Ferrier-Pagès, C.; Reynaud, S.; Tambutté, É.; Zoccola, D.; Allemand, D. *J. Exp. Mar. Biol. Ecol.* **2011**, *408*, 58−78 (and references therein)..
(10) Falini, G.; Reggi, M.; Fermani, S.; Sparla, F.; Goffredo, S.; Dubinsky, Z.; Levi, O.; Dauphin, Y.; Cuif, J.-P. *J. Struct. Biol.* **2013**, *183*, 226−238.
(11) Wilfert, M.; Peters, W. *Z. Morph. Tiere* **1969**, *64*, 77−84.
(12) Young, S. D. *Comp. Biochem. Physiol.* **1971**, *40B*, 113−120.
(13) Cuif, J.-P.; Dauphin, Y. *Paläont. Z.* **1998**, *72*, 257−270.
(14) Cuif, J.-P.; Dauphin, Y.; Doucet, J.; Salome, M.; Susini, J. *Geochim. Cosmochim. Acta* **2003a**, *67*, 75−83.
(15) Vandermeulen, J. H.; Watabe, N. *Mar. Biol.* **1973**, *23*, 47−57.

(16) van de Locht, R.; Verch, A.; Saunders, M.; Dissard, D.; Rixen, T.; Moya, A.; Kroger, R. *J. Struct. Biol.* **2013**, *183*, 57−65.
(17) Addadi, L.; Moradian, J.; Shay, E.; Maroudas, N. G.; Weiner, S. *Proc. Natl. Acad. Sci. U.S.A.* **1987**, *84*, 2732−2736.
(18) Falini, G.; Albeck, S.; Weiner, S.; Addadi, L. *Science* **1996**, *271*, 67−69.
(19) Falini, G.; Fermani, S.; Tosi, G.; Dinelli, E. *Cryst. Growth. Des.* **2009**, *9*, 2065−2072.
(20) Puverel, S.; Tambutté, É.; Periera-Mouriès, L.; Zoccola, D.; Allemand, D.; Tambutté, S. *Comp. Biochem. Physiol.* **2005**, *150B*, 10−22.
(21) Constantz, B.; Weiner, S. *J. Exp. Zool* **1988**, *248*, 253−258.
(22) Dauphin, Y. *Int. J. Biol. Macromol.* **2001**, *28*, 293−304.
(23) Farre, B.; Cuif, J.-P.; Dauphin, Y. *Zoology* **2010**, *113*, 250−257.
(24) McConnaughey, T. A.; Whelan, J. F. *Earth Sci. Rev.* **1997**, *42*, 95−117.
(25) Gagnon, A. C.; Adkins, J. F.; Erez, J. *Earth Planet. Sci. Lett.* **2012**, *329*−*330*, 150−161.
(26) Clode, P. L.; Marshall, A. T. *Tissue Cell* **2002**, *34*, 187−198.
(27) Addadi, L.; Joester, D.; Nudelman, F.; Weiner, S. *Chem.—Eur. J.* **2006**, *12*, 981−987.
(28) Addadi, L.; Weiner, S. *Angew. Chem., Int. Ed. Engl.* **1992**, *31*, 153−169.
(29) Didymus, J. M.; Oliver, P.; Mann, S. *Chem. Soc., Faraday Trans.* **1993**, *89*, 2891−2900.
(30) Weiner, S.; Addadi, L. *Annu. Rev. Mater. Res.* **2011**, *41*, 21−40.
(31) Goffredo, S.; Vergni, P.; Reggi, M.; Caroselli, E.; Sparla, F.; Levy, O.; Dubinsky, Z.; Falini, G. *PLoS One* **2011**, *6*, e22338.
(32) Mass, T.; Drake, J. L.; Haramaty, L.; Kim, J. D.; Zelzion, E.; Bhattacharya, D.; Falkowski, P. G. *Curr. Biol.* **2013**, *23*, 1126−1131.
(33) Muscatine, L.; Cerchiarini, F. *Biol. Bull.* **1969**, *137*, 506−523.
(34) Johnson, I. S. *Int. Rev. Cytol.* **1980**, *67*, 171−214.
(35) Cuif, J.-P.; Dauphin, Y.; Freiwald, A.; Gautret, P.; Zibrowius, H. *Comp. Biochem. Physiol. A* **1999**, *123*, 269−278.
(36) Muscatine, L.; Goiran, C.; Land, L.; Jaubert, J.; Cuif, J.-P.; Allemand, D. *Proc. Natl. Acad. Sci. U.S.A.* **2005**, *102*, 1525−1530.
(37) Kawaguti, S.; Sakumoto, D. *Bull. Natl. Inst. Ocean Taiwan* **1948**, *4*, 65−70.
(38) Gattuso, J. P.; Allemand, D.; Frankignoulle, M. *Am. Zool.* **1999**, *39*, 160−183.
(39) Goreau, T. F. *Biol. Bull.* **1959**, *106*, 59−75.
(40) Gautret, P.; Cuif, J.-P.; Freiwald, O. *Facies* **1997**, *36*, 189−194.
(41) Pearse, V. B.; Muscatine, L. *Biol. Bull.* **1971**, *141*, 350−363.
(42) Tambutté, É.; Allemand, D.; Zoccola, D.; Meibom, A.; Lotto, S.; Caminiti, N.; Tambutté, S. *Coral Reefs* **2007**, *26*, 517−529.
(43) Marshall, A. T.; Clode, P. *J. Exp. Biol.* **2002**, *205*, 2107−2113.
(44) Al-Horani, F. A.; Al-Moghrabi, S. M.; De Beer, D. *Mar. Biol.* **2003**, *142*, 419−426.
(45) Al-Horani, F. A. *Sci. Mar.* **2005**, *69*, 347−354.
(46) Sillero, A.; Ribeiro, J. *Anal. Biochem.* **1989**, *179*, 319−325.
(47) Kester, D. R.; Duedall, I. W.; Connors, D. N.; Pytkowicz, R. M. Preparation of artificial seawater. *Limnol. Oceanogr.* **1967**, *12*, 176−179.
(48) Xu, X.; Han, J. T.; Kim, do H.; Cho, K. *J. Phys. Chem. B* **2006**, *110*, 2764−2770.
(49) Cuif, J.-P.; Dauphin, Y. *J. Struct. Biol.* **2005**, *150*, 319−331.
(50) Cuif, J.-P.; Dauphin, Y.; Berthet, P.; Jegoudez, J. *Geochem. Geophys. Geosyst.* **2004**, *5*, Q11011.
(51) Parker, F. S. *Applications of Infrared, Raman, and Resonance Raman Spectroscopy in Biochemistry*; Plenum Press: New York, 1983.
(52) Addadi, L.; Raz, S.; Weiner, S. *Adv. Mater.* **2003**, *15*, 959−970.
(53) Venn, A. A.; Tambutté, É.; Holcomb, M.; Laurent, J.; Allemand, D.; Tambutté, S. *Proc. Natl. Acad. Sci. U.S.A.* **2013**, *110*, 1634−1639.
(54) Mann, S. *Biomineralization. Principles and Concepts in Bioinorganic Materials Chemistry*; Oxford University Press: New York, 2001; Vol. *198*.
(55) Weiner, S.; Dove, P. An Overview of Biomineralization Processes and the Problem of the Vital Effect. Dove, P. M., Weiner, S., Yoreo, J. J., Eds.; In *Biominer., Rev. Miner. Geochim.* **2003**, 1−29.
(56) Meldrum, F. C.; Coelfen, H. *Chem. Rev.* **2008**, *108*, 4332−4342.
(57) Gotliv, B.-A.; Addadi, L.; Weiner, S. *Eur. J. Chem. Biol.* **2003**, *4*, 522−529.
(58) Holcomb, M.; Cohen, A. L.; Gabitov, R. I.; Hutter, J. L. *Geochim. Cosmochim. Acta* **2009**, *73*, 4166−4179.
(59) Tambutté, É.; Tambutté, S.; Segonds, N.; Zoccola, D.; Venn, A. A.; Erez, J.; Allemand, D. *Proc. Biol. Sci.* **2012**, *7*, 19−27.
(60) Radha, A. V.; Forbes, T. Z.; Killian, C. E.; Gilbert, P. U. P. A.; Navrotsky, A. *Proc. Natl. Acad. Sci. U.S.A.* **2010**, *107*, 816438−16443.
(61) Raz, S.; Hamilton, P. C.; Wilt, F. H.; Weiner, S.; Addadi, L. *Adv. Funct. Mater.* **2003**, *13*, 480−486.
(62) Noel, E. H.; Kim, Y.-Y.; Charnock, J. M.; Meldrum, F. C. *CrystEngComm* **2013**, *15*, 697−705.
(63) Gebauer, D.; Gunawidjaj, P. N.; Ko, J. Y. P.; Bacsi, Z.; Aziz, B.; Liu, L.; Hu, Y.; Bergström, L.; Tai, C.-W.; Sham, T.-K.; Edén, M.; Hedin, N. *Angew. Chem.* **2010**, *122*, 9073−9075.
(64) Zhang, Z.; Xie, Y.; Xun, X.; Pan, H.; Tang, R. *J. Cryst. Growth* **2012**, *343*, 62−67.
(65) Raiteri, P.; Gale, J. D. *J. Am. Chem. Soc.* **2010**, *132*, 17623−17634.
(66) Lam, R. S. K.; Charnock, J. M.; Lennie, A.; Meldrum, F. C. *CrystEngComm* **2007**, *9*, 1226−1236.
(67) Loste, E.; Wilson, R. M.; Seshadric, R.; Meldrum, F. C. *J. Cryst. Growth* **2003**, *254*, 206−218.
(68) Politi, Y. *Chem. Mater.* **2010**, *22*, 161−166.
(69) Clode, P. L.; Lema, K.; Saunders, M.; Weiner, S. *Coral Reefs* **2011**, *30*, 1−8.
(70) Goffredo, S.; Prada, F.; Caroselli, E.; Pasquini, L.; Fantazzini, P.; Fermani, S.; Reggi, M.; Levy, O.; Fabricius, K. E.; Dubinsky, Z.; Falini, G. *Nat. Clim. Change* **2014**, *4*, 593−597.

Chapter 7

Relationship between phenotype and environment in calcifying organisms: the case study of shell morphology in the clam *Chamelea gallina* from the Adriatic Sea

Manuscript in preparation

Relationship between phenotype and environment in calcifying organisms: the case study of shell morphology in the clam *Chamelea gallina* from the Adriatic Sea

Abstract

Phenotype can express different morphologies in response to biotic or abiotic environmental influences. Mollusks are particularly sensitive to different environmental parameters, showing shell morphology variation with several environmental factors. Many studies focused on macroscale shell morphology variations in response to environmental parameters, but few studies concern shell variations at the different scale level along environmental gradients. Here, we investigate shell features at the macro, micro and nanoscale, in populations of the commercially important clam *Chamelea gallina* along a latitudinal gradient (~400 km) of temperature and solar radiation in the Adriatic Sea (Italian cost). Six populations of shells having the same length was analyzed. Shells from the warmest and the most irradiated population were about 30% lighter, due to thinner shell and with different aspect ratio. They were also more porous and showed to greater fragility. However, no variation was observed in shell polymorphism (100% aragonite) or in shell parameters at the nanoscale level, indicating no effects of environmental parameters on the composition and crystallography of biomineralized shell. Because of the importance of this species as commercial resource in Adriatic Sea, the experimentally quantified and significant variation of weight and fragility in *C. gallina* shells along the latitudinal gradient has economic implication for fishery producing different economical yield for fishermen and consumers along Adriatic coastline.

Introduction

Organisms are able to modulate their developmental trajectory and to alter gene-expression patterns in response to abiotic environmental cues (such as temperature or photoperiod) or biotic (such as those emanating from predators, conspecifics or food; Gilbert 2001, 2012). Environmental "alteration" influences the organism, producing a not pathological phenotype, appropriate for that environment (Langerhans et al. 2007; Costa et al. 2008; Zieritz and Aldridge 2009; Gilbert 2012). An enduring puzzle in evolutionary biology is to understand how individuals and populations adjust to changing environments (Lorenzi et al. 2015). Intraspecific phenotypic variation is believed to arise from divergent selection pressures between different environments (Schluter 2000 and references therein), from environment-independent phenotype generation, as well as from potentially non-adaptive effects of the environment on phenotype (Schluter 2000; West-Eberhard 2003). Thus, a particular environment can elicit different phenotypes from the same genotype (Gilbert 2001). The ability of organisms to produce different phenotypes under different environmental parameters in natural populations is a critical issue to understand how species might face future changes (Pigliucci 1996).

Phenotype plasticity is the ability of an organism to produce a range of relatively fit phenotypes, by altering morphology, movement, behavior or rate of biological activity in response to fluctuations in environmental parameters (Pigliucci 2001; West-Eberhard 2003; DeWitt and Scheiner 2004; Beldade et al. 2011; Gilbert 2012). Considering the existing effects of anthropogenic activities on the environment, organisms exhibiting higher phenotypic plasticity might adapt better to broad scale disturbances, such as climate change (Pigliucci et al. 2006; Charmantier et al. 2008).

Calcifying marine organisms (e.g. corals, echinoderms and mollusks) are likely to be among the most susceptible organisms to changing environmental parameters (Laing et al. 1987; Levitan 1991; DeWitt 1998; Carballo et al. 2006) and show morphological variations of the skeleton/shell related to bottom topography, sediment characteristics, hydrodynamic processes (Vogel 1996; Seed

and Richardson 1999; Casado-Amezua et al. 2013), and especially pH (Kleypas et al. 1999, 2006; Ries et al. 2009; Nienhuis et al. 2010; Findlay et al. 2011; Goffredo et al. 2014; Fantazzini et al. 2015; Thomsen et al. 2015) and temperature (Laing et al 1987; McNeil et al. 2004; Goffredo et al. 2007, 2008; Doyle 2010; Rodolfo-Metalpa et al. 2011; Watson et al. 2012).

Calcifying marine organisms make extensive use of calcium carbonate ($CaCO_3$), one of the most abundant minerals in nature, as a structural and/or protective material through the biomineralization process (Lowenstam and Weiner 1989). It is well known that the intracrystalline skeletal organic matrix (OM) plays a major role in biomineralization and such as in all biominerals, mollusk shells also contain OM that rarely exceeds 5% by weight of the total shell (Currey and Taylor 1974; Currey and Kohn 1976; Carter 1980; Palmer1983; Currey 1990). Mollusks are able to exert an exquisite biological control on the biomineralization process by determining which type of calcium carbonate polymorph precipitate through the control of intraskeletal macromolecules (Addadi and Weiner 1992; Falini et al. 1996). Morphology, mineralogy and chemistry of biologically formed calcium carbonate skeletons are largely dependent on both biology and environmental surroundings, with structural proteins and enzymes that act as keys to controlling internal conditions and that respond to external environmental parameters (Falini et al. 1996; Rahman and Shinko 2011). To study the effect of solar radiation (SR) and sea surface temperature (SST), latitudinal gradients are useful natural laboratory, allowing to examine long-term effects on populations of the same species, adapted to different environmental conditions.

Latitude is the main factor influencing variation in SR and SST (Kain 1989). Studying populations of the same species dislocated along a latitudinal gradient can provide precious information on the effects of temperature and solar radiation in a natural environments (Goffredo et al. 2007, 2008, 2009, 2015; Jansen et al. 2007; Márquez and Van Der Molen 2011; Caroselli et al. 2012a, b, 2015, 2016a, b; Airi et al. 2014). Several studies on bivalves were performed along a latitudinal gradients, focusing on biodiversity (Crame 2000, 2002; Rex et al. 2000; Roy et al. 2000a),

growth rate, body size and lifespan (MacDonald and Thompson 1988; Hummel et al. 1998; Roy et al. 2000b).

Mollusk shell morphology is particularly sensitive to environmental parameters, varying in relation to depth (Claxon et al. 1998), shore level (Franz 1993), tidal level (Dame 1972), current (Fuiman et al. 1999), wave exposure (Hinch and Bailey 1988), bottom type, sediment (Newell and Hidu 1982; Claxton et al. 1998), pH (Watson et al. 2012) and temperature (Watson et al. 2012). The quagga mussel *Dreissena bugensis* shows plasticity in shell morphology in relation to depth: deep ones presents more laterally flattened shell and ovular in shape than those from shallow water habitats (Dermott and Munawar 1993; Claxton et al. 1998). The clam *Mya arenaria* from sandy bottoms shows a longer and narrower shape, compared to a rounder shape when grown in gravel (Newell and Hindu 1982). Shell shape of limpet *Lottia gigantea* changes as a function of inter-tidal zonation and related environmental factors, such as resistance to desiccation, thermal stress and wave impact, by developing high spiraled and heavily ridges shells which may reduce the likelihood of reaching elevated body temperatures (Denny and Blanchette 2000; Harley et al. 2009). The growth in length and height of the shells of cockle, *Cerastoderma edule*, ceased in winter when mean water temperatures fell to 5 °C (Jones 1979). Bivalve growth is little affected by water temperature variations between 10° and 20 °C, but decreases when the temperature is less than 10 °C or more than 20 °C (Bayne et al. 1976). The observed phenotypic plasticity in many marine calcifying organisms in relation to environmental parameters (Trussell and Etter 2001; Chelazzi and Vannini 2013), makes them potentially ideal models for studying such plastic responses and associated trade-offs in the face of global climate change.

The clam *Chamelea gallina* (Linnaeus 1758) is a common infaunal bivalve in the Mediterranean Sea, where it inhabits well-sorted fine sand biocoenosis at 3-7 m depth (Picard 1965) and has a considerable economical relevance for fishery (Froglia 1989; Ramón and Richardson 1992). In the 1970s the development of clam fishery based on hydraulic dredges led to an over-

exploitation of the resource with a dramatic decrease in clam population density associated with a reduction in the number of clams over 25 mm long, the minimum legal marketable size, although the maximum length recorded for this species is about 50 mm (Froglia 1989). In Italy, in the late 1970s the fishery yielded 80,000-100,000 metric tons while actually it doesn't exceed 20,000 metric tons (Romanelli et al. 2009). Recently, there is growing concern for the survival of bivalve communities because large inter-annual fluctuations in stock abundance, periodic recruitment failure and irregular mortality events threaten the biological and economic sustainability of this fishery, especially in the Adriatic Sea (Ramón and Richardson 1992; Del Piero and Fornaroli 1998; Del Piero et al. 1998; Froglia 2000; Romanelli et al. 2009). Thus, studies on this species are of critical importance for developing appropriate management strategies for one of the most important economic sectors of southern EU countries. FAO reports a mean annual total catch of about 60,000 tonnes (2004-2013) in Atlantic, Mediterranean and Black Sea, with the largest catches in Italy (22,000 t) and Turkey (33,000 t).

Water temperature has a dominant role in shell growth of *C. gallina* (Ramón and Richardson 1992; Froglia 2000; Keller et al. 2002; Moschino and Marin 2006). Temperatures below 10 °C strongly slow or inhibit shell growth (Froglia 2000), whereas values above 28 °C reduce energy absorption and increase energy expenditure via respiration, thus suppressing shell growth (Ramón and Richardson 1992; Moschino and Marin 2006). Calcification of *C. gallina* seems to be related to temperature and food conditions, showing widely spaced growth bands during winter-spring, while narrow growth increments are deposited in summer-autumn (Ramón and Richardson 1992).

Several studies have been reported on aspect ratio shell variations in response to environmental variables (Newell and Hidu 1982; Beukema and Meehan 1985; Claxton et al. 1998; Fuiman et al. 1999; Nagarajan et al. 2006; Krapivka et al. 2007; Doyle et al. 2010; Morley et al. 2010; Valladares et al. 2010; Sepúlveda and Ibáñez 2012; Watson et al. 2012; Briones et al. 2014), however few studies comparatively analyzed shell features at the micro and nanoscale level along

environmental gradients (Prezant et al. 1988; Tan Tiu 1988; Nishida et al. 2012; Fitzer et al. 2014; Milano et al. 2015). The present study aimed to investigate the shell morphology phenotypic response to the environment of *C. gallina* at the diverse scales, from the macroscale to the nanoscale in six populations along a latitudinal gradient.

Materials and methods

Ethics Statement

This study was carried out following the fundamental ethical principles. According to the European normative that regulate minimum fishing size of *Chamelea gallina* (25 mm, Council Regulation (EC) No 1967/2006), for this study only clams of commercial size with minimum length of 25 mm were collected. Thus, no permit was needed to sample specimens. Sampling was limited strictly to the number necessary and performed where the species has high population density to minimize the impact of removing individuals and preserve both the demographic and genetic structure of the natural populations.

Collection and processing of specimens

Between August 2013 and April 2015, specimens of *C. gallina* were collected from six sites along a latitudinal gradient in the Adriatic Sea from 45°42'N to 41°55'N (Fig.1). Latitude is closely related to the variation of the two environmental parameters considered in this study: temperature and solar radiation (Kain 1989). Clams were sampled for each site using hydraulic dredges on soft bottoms in the subtidal zone at 3-7 m depth.

For each collected clam, the bivalve flesh was removed with a scalpel and the shell was cleaned with a toothbrush and washed with distilled water. The right and left valves were then separated, labeled and dried at 37 °C for one night to remove any moisture that may affect measurements.

Shell biometric parameters

Clam shell length (maximum distance on the anterior-posterior axis), width (maximum distance on the dorsal-ventral axis; Fig. 2) were obtained with ImageJ software after data capture of shell shape with a scanner. Height (maximum distance on the lateral axis) and thickness (Fig. 2) of the valve were measured with a pair of calipers (± 0.05 mm) and dry shell mass was measured using an analytical balance (± 0.0001 g). Volume and shell density parameters were measured by means of the buoyant weight techniques (Davies 1989), using a density determination kit Ohaus Explorer Pro balance (±0.0001 g; Ohaus Corp., Pine Brook, NJ, USA). Only clams of commercial size (25-30 mm) were used in this study. Measurements required for calculating shell parameters were:

ρ	density of the fluid medium (in this case, double distilled water: 0.99823 g cm^{-3} at 20 °C and 1 atm)
DW	dry weight of the shell
BW	buoyant weight of the shell = weight of the shell minus weight of the water displaced by it. To obtain this measurement, shells were placed in a desiccator connected to a mechanical vacuum pump for about 1 h in order to suck out all of the water and air from the pores (Barnes and Devereux 1988). Still under vacuum conditions, the dry shells were soaked by gradually pouring distilled water inside the desiccator. The shell was then slowly lowered onto the underwater weighing pan, ensuring that no air bubbles adhered to its surface. The buoyant weight measurements were repeated three times and the average was considered for statistical analysis. This simple and nondestructive method has been widely used with great success to examine various calcifying organisms, such as corals (Davies 1989; Ammar et al. 2005; Shi et al. 2009; Caroselli et al. 2011), marine mollusks (Nishii 1965;

Palmer 1982; Hoegh-Guldberg 1997) and barnacles (Darling and Wilbur 1993).

SW — saturated weight of the shell = weight of the shell plus weight of the water enclosed in its pores. The shell was taken out of the water, quickly blotted with a paper towel to remove surface water, and weighed in air three times, making sure that no water droplets were left on the weighing platform, which would lead to an overestimation.

$V_{MATRIX} = \frac{DW-BW}{\rho}$ — matrix volume = volume of the shell, excluding the volume of its pores.

$V_{PORES} = \frac{SW-DW}{\rho}$ — pore volume = volume of the pores in the shell.

$V_{TOT} = V_{MATRIX} + V_{PORES}$ — total volume = volume of the shell including its pores.

Additionally, the following skeletal parameters were calculated:

Micro-density (matrix density) = DW/V_{MATRIX}

Bulk-density = DW/V_{TOT}

Porosity = $(V_{PORES}/V_{TOT}) \times 100$

Shell mechanical properties

To test for shell resistance to fracture, compression tests were conducted on a universal testing machine equipped with a force transducer (Instron: 2519-105) of 1 kN maximum capacity. Thirty shell samples were randomly selected from each population and were brought to fracture strength using a 3 mm diameter pinhead indenter at a downward speed of 1.5 mm min^{-1}. The Young's modulus and the required force to fracture (Maximum load, kN) were recorded using the software Instron (Series IX).

Ten samples from each population were randomly selected and used for the following analyses. The valves were treated with a sodium hypochlorite solution (commercial) for three days to completely remove any trace of external skeletal organic tissue, and with a 1 M sodium hydroxide solution for one day to hydrolyze residual proteic materials from the shell surface. Then, samples were rinsed with distilled water and dried at room temperature for one day. Subsequently, the left valve was sectioned with a dremel (300 series, Dremel System) from the umbo to the ventral margin. One half of each shell was finely ground in a mortar to obtain a homogenous powder to be used for chemical analyses. A transversal section of about 3 mm in width was cut from the mid remaining shell for scanning electron microscope (SEM) observations (Fig. 10a).

Diffractometric measurements

To obtain qualitative information about shell mineral composition, X-ray powder diffraction (XRD) analyses were performed on five specimens randomly selected for each populations, preparing a thin, compact layer of powdered sample in a silica background signal free holder. Diffractograms for each sample were collected using an X'Celerator detector fitted on a PANalytical X'Pert Pro diffractometer, using Cu-Kα radiation generated at 40 kV and 40 mA. The data were collected within the 2θ range from 10° to 60° with a step size (Δ2θ) of 0.02° and a counting time of 1200 s. Fixed anti-scatter and divergence slits of 1/2° were used with 10 mm beam mask and all scans were carried out in 'continuous' mode. The XRD patterns were analyzed using the X'Pert HighScore Plus software (PANalytical) and the full width at half maximum (FWHM) was measured for one of the main peaks (A111) of each diffractogram.

Fourier transform infrared spectroscopy (FTIR) analyses were performed on the same samples used for XRD, to obtain information about the mineral phase. FTIR analyses were carried out using a FTIR Nicolet 380 Spectrometer (Thermo Electron Corporation) working in the range of wave-numbers 4000–400 cm^{-1} at a resolution of 2 cm^{-1}. Sample disks were obtained mixing a small amount (1 mg) of finely ground sample with 100 mg of KBr and applying a pressure of 670.2 MPa

to the mixture using a hydraulic press. In FTIR spectroscopy, calcium carbonate has four active vibrational modes: ν_1, ν_2, ν_3 and ν_4 bands. For each spectrum, characteristic calcium carbonate active vibrational modes ν_2, ν_3 and ν_4 bands were identified and their intensities were determined. To compare atomic order among the six populations, the intensity of the ν_2 and ν_4 bands were normalized to the ν_3 band and then graphed. To understand if there were differences in the atomic order within crystals, the plotted curves of *C. gallina* were compared with grinding curve of other calcifying marine organisms (*Balanophillia europaea, Protula tubularia, Vermetus triqueter*; Sabbioni 2012), and geogenic and synthetic aragonite (Suzuki et al. 2011).

Evaluation of Organic Matrix (OM) Content

Thermogravimetric analysis (TGA) was performed to estimate the organic matrix (OM) content of each shell, using an SDT Q600 instrument (TA Instruments). Powdered samples (5-10 mg) from 5 to 10 valves for each site were placed in a ceramic crucible. The analyses were performed under a nitrogen flow with a first heating ramp from 30 to 120°C at 10°C min^{-1} heating rate, an isothermal at 120° for 5 min, and a second heating ramp from 120 to 600°C, at 10°C min^{-1} heating rate.

Textural analyses

Scanning electron microscopy (SEM) observations were carried out on a subset of individuals from Chioggia and Capoiale (characterized respectively by lower and higher SST values), to obtain representative information on the textural characteristics of *C. gallina* shell. Skeletal features were investigated on the transversal valve sections. Each section was etched with an acetic acid solution (1% v/v) for 1 minute to remove debris and artifact from cutting. Samples were coated with a gold layer (5 nm) and analyzed with a SEM Hitachi s4000.

Environmental parameters

Solar radiation (SR, W m^{-2}) and sea surface temperature (SST, °C) data were obtained for each site from the Euro-Mediterranean Center on Climate Change (CMCC http://oceanlab.cmcc.it/afs/) data

banks. Mean annual SR and SST were calculated from daily values measured from July 2011 to June 2015 (number of daily values = 1447 for each site), to enclose almost entirely the lifespan of two-three years of each sample.

Statistical analyses

Levene's test was used for testing homogeneity of variance and Kolmogorov-Smirnov's test was used for testing normality of variance for both environmental and shell parameters. One-way analysis of variance (ANOVA) was used to test the significance of the differences among sites for environmental variables and shell parameters. When assumptions for parametric statistics were not fulfilled, the non-parametric Kruskal-Wallis equality-of-populations rank test was used instead. Student's t test was used to compare the mean right and left valves shell parameters (length, width, height, thickness, mass, volume, micro-density, bulk-density and porosity) in each site. Spearman's rank correlation coefficient was used to calculate the significance of the correlations between shell parameters and environmental parameters. Spearman's rank correlation coefficient is an alternative to Pearson's correlation coefficient (Altman 1991). It is useful for data that are non-normally distributed and do not meet the assumptions of Pearson's correlation coefficient (Potvin and Roff 1993). All analyses were computed using PASW Statistics 22.0 (Apache Computer Software Foundation, Forest Hill, USA).

Results

SR and SST both varied among sites (Kruskal–Wallis test, df = 5, and $p < 0.001$; Tab. 1) and correlated negatively with latitude (Fig. 3). The Monfalcone site, located in the Gulf of Trieste, has a higher SST than typically expected for this latitude (Stravisi 2003).

Clam biometric parameters (length, height, width, mass and volume) and shell parameters (micro-density, bulk-density and porosity) were homogeneous between left and right valves, thus data from both valves were pooled for following analyses. Since only commercial size 25-30 mm

was considered in this study, shell length was homogeneous among populations. Shell biometric data (except length) were significantly different among sites, thus correlations analyses between SR or SST and clam parameters were performed (Tab. 2, 3, 4). Biometric parameters (width, height, mass and volume) and shell parameters (micro-density, bulk-density and porosity), were different among populations and correlated negatively with SR and SST, except the height, which did not correlate with SST (Tab. 4; Fig. 4). Micro-density did not correlate with SR or SST, while bulk-density and porosity, correlated negatively and positively, respectively, with both SR and SST (Tab. 4; Fig. 5). All parameters were more highly correlated with SR than with SST (Fig. 4, 5).

Mechanical analyses showed differences among sites for Young's modulus and maximum force to fracture (Tab. 5), and correlated negatively with SR and SST (Fig. 6).

The analysis of the inorganic phase was obtained from the results of XRD and FTIR data. Both techniques showed that clam shells from all populations were composed of pure aragonite and no other mineral phase was detected (Fig. 7, 8). Full width at half maximum (FWHM) calculated for the main peak of each diffractogram was homogeneous among populations (Tab. 6). In FTIR spectra defined peaks at 1482 cm^{-1} (ν_3) 859 cm^{-1} (ν_2) and 713 cm^{-1} (ν_4) typical of aragonite were identified in all samples (Tab. 6; Fig. 8). The peak height was calculated and the height ratios ν_4/ν_3 vs. ν_2/ν_3 were plotted and fitted and the results were all observed as points of a curve (Fig. 9). The curve was compared with other curves obtained from different marine calcifying organisms (Phyla: Cnidaria, Anellida and Mollusca) and from geogenic and synthetic aragonite (Fig. 9; Suzuki et al. 2011). The curve formed from *C. gallina* was displaced between those from geogenic and synthetic aragonite, along with the other biogenic aragonite samples (Fig. 9).

The content of intra-skeletal OM, as weight percentage, was measured by TGA. It was below 2% in all samples and homogeneous among populations (Tab. 7).

The SEM observations revealed that the shell cross section (Fig. 10a) showed two distinct layers of aragonite crystals. The outer one (Fig. 10c) is composed of lamellar fibers showing

preferential spatial organization, aligned along the same elongation direction. They showed an average thickness of 0.5 mm. The inner layer (Fig. 6e) presented a spherulitic texture with no preferential spatial organization of the crystallites having an average thickness of 0.3 mm. Throughout the length of the shell sections the layers showed variations in thikness, but the inner layer was always thinner than the outer one. The two layers are separated by a central transition zone (Fig. 10d) in which the aragonite fibers lose their textural order, in favor of the granular composition that evolves in the spherulitic layer. These layers are distinguishable (Fig 10a, b, c, d, e) at low and intermediate magnifications. At higher magnifications, at the nanoscale level, differences between the outer and inner layer were no longer observable through SEM, as both the lamellar and spherulitic textures showed the same nanoparticle substructure (Fig. 10f, g, h). Mineral grains throughout the whole section showed a size range around 200 nm in both layers and within the transition zone.

Discussion

The main aim of this study was to investigate the effect of SR and SST on shell features at macro, micro and nanoscale levels, in natural population of the common clam *C. gallina* along a latitudinal gradient in the Western Adriatic Sea, as a case study to gain further insight on the relationship between phenotype and environment in calcifying marine organisms.

Shells of the same length of *C. gallina* showed negative effect with increased SR and SST, presenting lighter, more oval shaped, more porous and more fragile valves in warmest and more irradiated populations. Several studies show that shells of many mollusks species seems to be affected by latitudinal changes due to decreasing SST (Vermeij 1993; Trussell 2000; Trussell and Smith 2000; Trussell and Etter 2001; Sepúlveda and Ibáñez 2012; Watson et al. 2012). At low SST, $CaCO_3$ is less saturated and more soluble, increasing energetic costs of shell deposition (Clarke 1993). Another explanation concerns the effect of low SST on biological processes, directly reducing growth (Heilmayer et al. 2004) and development (Peck et al. 2006, 2007). *C. gallina* is negatively affected by high SST and high SR, showing opposite latitudinal trend respect to precedent studies. A possible

explanation for different response could due to effect of elevated temperature on its physiology. The high temperature seems to reduce energy absorption and increases energy expenditure via respiration in *C. gallina*, negatively affecting energy balance and thus growth, as showed in specimens from the northern Adriatic Sea and the eastern coast of Spain (Ramón and Richardson 1992; Moschino and Marin 2006). A drop in metabolism was recorded in the snail *Littorina saxatilis* exposed to elevated temperatures, with negative consequences in growth and fitness (Sokolova and Pörtner 2001). Moreover, oxygen depletion due to high temperature may produce detrimental effects on physiological performance of clams, as observed in the bivalve *Ruditapes decussatus* (Sobral and Widdows 1997a, b). *C. gallina* seems to be relatively low tolerant to high temperature in comparison with other bivalve species, showing a great influence in the overall physiological responses and a heavy stress conditions when exposed to high temperatures, demonstrating that temperature could be a tolerance limit for this species (Moschino and Marin 2006).

Despite *C. gallina* is an infaunal bivalve, all parameters of this species seemed to be stronger correlated with SR than SST. SR have no direct effect on the species, but the SR latitudinal gradient could be related to other abiotic and/or biotic parameters not investigated in this study. For example, the results observed in *C. gallina* shell variation could be due to local environmental pressures, such as nutrients and predators. Phytoplankton distribution in Adriatic Sea is characterized by the relative influence of northern Italian rivers and by influence of Mediterranean waters on the southern Italian coasts, showing a generally decreasing trend of nutrient concentration from North to South (Zavatarelli et al. 1998). The norther Adriatic influenced by Italian rivers, was marked by low phytoplankton community diversities but high nutrient concentrations; while, the southern Adriatic influenced by Mediterranean waters exhibited high community diversities but low nutrient concentrations (Zavatarelli et al. 1998). The lower presence of plankton density in southern Adriatic, could cause feeding deficits and consequently a reduction of available energy for clam to invest in

shell construction, which could explain the reduction in weight, thickness and the higher porosity and fragility of shells.

Differences found in SST and SR along the gradient could also influence the type and/or density of predators. Predation is an important factor associated with morphological plasticity in bivalves, which can exhibit induced responses based on the capture techniques of the predators (Reimer and Tedengren 1996; Reimer and Harms-Ringdahl 2001; Beadman et al. 2003; Caro and Castilla 2004). Bivalves principal defense is their strong calcareous shell (Gutiérrez et al. 2003), and among the shell characteristics, thickness is the most influential factor for shell strength, thus the increased of shell bivalve thickness can reduce successful of many predators (Reimer and Tedengren 1996; Leonard et al. 1999; Smith and Jennings 2000; Caro and Castilla 2004; Nagarajan et al. 2006). The blue mussel *Mytilus edulis* exposed to high predation density shows thicker and more robust shell than those not exposed to intense predation (Leonard et al. 1999). Similar results, showing an increase in shell thickness in response to predators, was found in several gastropods species (Appleton and Palmer 1988; Palmer 1990; Trussell 1996, 2000; Leonard et al. 1999; Trussell and Nicklin 2002). Experimental works on gastropods show that shell thickening in response to predators could be partly due to avoidance behavior, resulting in lower food intake and lower growth rates and partly due to direct result of increased shell deposition in the presence of predators (Appleton and Palmer 1988; Palmer 1990). Phenotypic changes found in *C. gallina* could occur by genetic or plasticity changes, as found in other mollusk (Trussel and Etter 2001), and could be explained by SST variation, nutrient concentration and/or density of predators along the latitudinal gradient.

Moreover, shell porosity and thickness are closely connected to Young's modulus (Wainwright et al. 1976). Increased porosity with increasing SR and SST, decreased *C. gallina* shell stiffness (Young's modulus), while reduced thickness lowers shell load to fracture. Resistance to breakage generally increases as the square of shell thickness (Vermeij 1993), and the breaking resistance doubles with an increase of 41% in thickness, thus providing a good return in shell strength

for each unit of shell thickening (Watson et al. 2012). Thus, the warmest and more irradiated populations of *C. gallina* showed a reduction in shell stiffness and load to fracture, modifying the shell resistance with an increase in fragility and damage susceptibility, affecting the survival of the species. Because of the importance of this species as commercial resource in Adriatic Sea, variation in *C. gallina* shells could have economic implication for fishery. More porous and fragile shells, found in warmest and more irradiated populations, are less resistance to breakage and could be more damages during the catch with hydraulic dredges, with a bigger amount of clams discarded from the trade. This could mean a bigger catch effort for fishermen with a loss in economic yield and a gain for consumers, with an increase in edible material per kilogram.

In addition, the less weighty mass due to thin and porous shells in the southern populations, could require a major number of clams to obtain the same quantitative in kilogram than Northern populations. However, the northern populations could allocate a higher energy fraction to reinforce their shells at the expense of lower somatic growth (Valladares et al. 2010). Contrarily, the warmer and more irradiated populations could use most of their assimilated energy in somatic growth, compensating negative aspect of shell variations with an increase in edible mass per catch and per kilogram, with a potential positive economical yield both for consumers and fishermen. Further analysis on edible animals may necessary to understand if environmental parameters can affect their size.

All populations of *C. gallina* showed the same inorganic phase along the latitudinal gradient of SR and SST, displaying entirely aragonitic shells, as seen in other mollusks (Kennedy et al. 2008; Foster et al. 2009; Yang et al. 2011; Sabbioni 2012). The production of an aragonitic skeleton is also common in other calcifying organisms such as scleractinian corals (Weiner et al. 1983; Higuchi et al. 2014) and sclerosponges (Simpson 1984). The majority of bivalve shells usually present different layers composed of both calcite and aragonite (the density of calcite being 7% lower than that of aragonite; Currey and Taylor 1974; Currey and Kohn 1976; Carter 1980; Palmer 1983; Currey 1990; Falini et al. 1996), which tend to form a number of recurrent patterns occurring in discrete shell layers (Kennedy et al. 2008; Clarkson 2009).

The grinding curve methodology can be used to distinguish the aragonite crystals with different extents of atomic disorder (Suzuki et al. 2011). Data from different grindings of *C. gallina* samples plotted in a graph revealed that the atomic order of the aragonite crystals does not vary among populations along the SR an SST gradient. Different grindings of *C. gallina* were compared to grinding curves of other calcifying marine organisms (Cnidaria, *Balanophillia europaea,* Anellida *Protula tubularia,* and Molluska *Vermetus triqueter)* all showing aragonite as a component of their inorganic phase (Sabbioni 2012), and to fitted curves for geogenic and synthetic aragonite (Fig. 5; Suzuki et al. 2011). The most ordered crystals are the geogenic aragonite crystals, and the least ordered at the atomic level are the synthetic aragonite crystals (Suzuki et al. 2011). Biogenic aragonite crystal samples from these three phyla have different degrees of atomic disorder; all the curves are located between the synthetic and geogenic aragonite samples indicating in all samples an intermediate atomic order. Data from *C. gallina* resulted to be located between the synthetic and geogenic aragonite curves and was positioned closest to the curve obtained from *V. triqueter*, indicating similar aragonite atomic disorder between these two mollusk species, (Suzuki et al. 2011), and no influence on behalf of the environment at the nano-scale level.

Most mollusk classes (Cephalopoda, Gastropoda, Bivalvia) show characteristically layered shell structures (Dauphin and Denis 2000). Aragonite crystals in particular can occur as prismatic, foliated, columnar nacre, sheet nacre, crossed lamellar, complex crossed lamellar, as well as homogeneous granular structures (Currey and Taylor 1974; Kennedy et al. 2008; Barthelat et al. 2009). It is common for bivalves to present a layer of sheet nacre (Cartwright et al. 2009), but this is absent in *C. gallina*. Valves of *C. gallina* were characterized by two different aragonite structures: an external lamellar layer and an internal spherulitic layer, separated by a transition zone. While the thickness of the two layers varied along the shell section, the outer layer was always thicker than the inner one, in all analyzed samples. Nano-particles composing both fibers and granules of the two layers, analyzed at high magnifications, were similar in shape and size and showed a spherical form

of approximately 200 nm in diameter throughout the whole valve section, indicating no difference between the aragonite "building blocks" at the nanoscale level.

The homogeneous amount of OM among populations was supported by the result found at the microscale, where the shell parameters of microdensity (density of the calcium carbonate crystals that compose the shell) did not change along the gradient. The amount of OM present in *C. gallina* shells is below 2% in weight, an equivalent result to that obtained from other mollusk *V. triqueter*, in previous studies (Sabbioni 2012). The presence of OM within biomineral skeletons has long been recognized (Lowenstam and Weiner 1989; Falini et al. 1996) and investigations have mostly focused on the biochemistry of intraskeletal compounds, with respect to their possible role in the biomineralization process (Young 1971; Constantz and Weiner 1988; Reggi et al. 2014). Little information is known on varying OM content in relation to environmental parameters.

As indicated by all micro and nanoscale analyses, the mineral distribution remained the same in all analyzed samples, as does the quantity of OM, indicating that the "building blocks" produced by the biomineralization process are substantially unaffected by the SR and SST variations among the different populations along the latitudinal gradient. Also the organization, morphology and packing of the constituent mineral crystals were the same along the gradient. The unaffected mineralogy in *C. gallina* is possibly due to the exquisite control of biological macromolecules in mollusk mineralization (Lowenstam and Weiner 1989; Falini et al. 1996).

Differences found in shell parameters of the clam *C. gallina* along the latitudinal gradient could be the outcome of the phenotypic plasticity or a genetic adaptation of the populations subjected to different environmental parameters. Environmental parameters could directly affect shell morphology, such as temperature, or indirectly, influencing nutrient concentration and/or predators density. Shell morphology of the most irradiated and warmest populations was characterized by lighter, thinner, more porous and fragile shells, affecting the survival of the species. At the same time, populations of *C. gallina* did not show significant variations of microstructural parameters at the

microscale and nanoscale level. The type of calcium carbonate polymorph, the atomic order of the mineral skeletal phase and the percentage of organic matrix content were unaltered along the latitudinal gradient, indicating no effects of SR and SST on the biomineralization of the clam shells.

References

Addadi L, Weiner S (1992) Control and design principles in biological mineralization. Angew. Chem. Int. Ed. Engl. 31:153-169.

Airi V, Gizzi F, Falini G, Levy O, Dubinsky Z, Goffredo S (2014) Reproductive efficiency of a Mediterranean endemic zooxanthellate coral decreases with increasing temperature along a wide latitudinal gradient. PloS ONE. 9:e91792.

Altman DG (1991) Practical statistics for medical research. New York: Chapman & Hall, CRC. 624 p.

Ammar MS, Mohammed TA, Mahmoud MA (2005) Skeletal density (strength) of some corals in an actively flooding and a non flooding site, south Marsa Alam, Red Sea, Egypt. J. Egypt. Germ. Soc. Zool. 46:125-139.

Appleton RD, Palmer AR (1988) Water-borne stimuli released by predatory crabs and damaged prey induce more predator resistant shells in a marine gastropod. Proc. Natl. Acad. Sci. USA. 85:4387-4391.

Barnes DJ, Devereux MJ (1988) Variations in skeletal architecture associated with density banding in the hard corals Porites. J. Exp. Mar. Biol. Ecol. 121:37-54.

Barthelat F, Rim JE, Espinosa D (2009) A review on the structure and mechanical properties of mollusk shells – perspectives on synthetic biomimetic materials. In: Applied Scanning Probe Methods XIII, Springer Berlin Heidelberg. 27 p.

Bayne BL, Widdows J, Thompson RJ (1976) Physiological integrations. In: Marine mussels: their ecology and physiology. Bayne BL (Ed.), Cambridge University Press, Cambridge. 38 p.

Beadman H, Caldow R, Kaiser M, Willows R (2003) How to toughen up your mussels: using mussel shell morphological plasticity to reduce predation losses. Mar. Biol. 142:487-494.

Beldade P, Mateus ARA, Keller RA (2011) Evolution and molecular mechanisms of adaptive developmental plasticity. Mol. Ecol. 20:1347-1363.

Beukema JJ, Meehan BW (1985) Latitudinal variation in linear growth and other shell characteristics of *Macoma balthica*. Mar. Biol. 90:27-33.

Briones C, Rivadeneira MM, Fernández M, Guiñez R (2014) Geographical variation of shell thickness in the mussel *Perumytilus purpuratus* along the southeast Pacific coast. Biol. Bull. 227:221-31.

Carballo JL, Avila E, Enríquez S, Camacho L (2006) Phenotypic plasticity in a mutualistic association between the sponge *Haliclona caeulea* and the calcareous macroalga *Jania adherens* induced by transplanting experiments. I: morphological responses of the sponge. Mar. Biol. 148:467-478.

Caro A, Castilla J (2004) Predator-inducible defences and local intrapopulation variability of the intertidal mussel *Semimytilus algosus* in central Chile. Mar. Ecol. Prog. Ser. 276:115-123.

Caroselli E, Prada F, Pasquini L, Marzano FN, Zaccanti F, Falini G, Levy O, Dubinsky Z, Goffredo S (2011) Environmental implications of skeletal micro-density and porosity variation in two scleractinian corals. Zoology. 114:255-264.

Caroselli E, Mattioli G, Levy O, Falini G, Dubinsky Z, Goffredo S (2012a) Inferred calcification rate of a Mediterranean azooxanthellate coral is uncoupled with sea surface temperature along an 8° latitudinal gradient. Front. Zool. 9:32.

Caroselli E, Zaccanti F, Mattioli G, Falini G, Levy O, Dubinsky Z, Goffredo S (2012b) Growth and demography of the solitary scleractinian coral *Leptopsammia pruvoti* along a sea surface temperature gradient in the Mediterranean Sea. PLoS ONE. 7:e37848.

Caroselli E, Nanni V, Levy O, Falini G, Dubinsky Z, Goffredo S (2015) Latitudinal variations in biometry and population density of a Mediterranean solitary coral. Limnol. Oceanogr. 60:1356-1370.

Caroselli E, Brambilla V, Ricci F, Mattioli G, Levy O, Falini G, Dubinsky Z, Goffredo S (2016a) Inferred calcification rate of a temperate azooxanthellate caryophylliid coral along a wide latitudinal gradient. Coral Reefs. *In press*.

Caroselli E, Ricci F, Brambilla V, Mattioli G, Levy O, Falini G, Dubinsky Z, Goffredo S (2016b) Relationships between growth, population dynamics, and environmental parameters in the solitary non-zooxanthellate scleractinian coral *Caryophyllia inornata* along a latitudinal gradient in the Mediterranean Sea. Coral Reefs. *In press*.

Carter JG (1980) Environmental and biological controls of bivalve shell mineralogy and microstructure. In: Skeletal Growth of Aquatic Organisms. Rhoads DC, Lutz RA (Eds.) Plenum, New York. 44 p.

Cartwright JHE, Checa AG, Escribano B, Saint-Diaz C (2009) I. Proc. Natl. Acad. Sci. USA. 106:10499-10504.

Casado-Amezua P, Gasparini G, Goffredo S (2013) Phenological and morphological variations in the Mediterranean orange coral *Astroides calycularis* between two distant localities. Zoology. 116:159-167.

Charmantier A, McCleery HR, Cole RL, Perrins C, Kruuk EBL, Sheldon CB (2008) Adaptive phenotypic plasticity in response to climate change in a wild bird population. Science. 320:800-803.

Chelazzi G, Vannini M (2013) Behavioral adaptation to intertidal life. Springer. Vol. 151.

Claxton WT, Wilson AB, Mackie GL, Boulding EG (1998) A genetic and morphological comparison of shallow and deepwater populations of the introduced dreissenid bivalve *Dreissena bugensis.* Can. J. Zool. 76:1269-1276.

Clarke A (1993) Temperature and extinction in the sea: a physiologist's view. Paleobiology. 19:499-518.

Clarkson E (2009) Invertebrate palaeontology and evolution. John Wiley & Sons. 451 p.

Constantz B,Weiner S (1988) Acidic macromolecules associated with the mineral phase of scleractinian coral skeletons. J. Exp. Zool. 248:253-258.

Costa C, Aguzzi J, Menesatti P, Antonucci F, Rimatori V, Mattoccia M (2008) Shape analysis of different populations of clams in relation to their geographical structure. J. Zool. 276:71-80.

Crame JA (2000) Evolution of taxonomic diversity gradients in the marine realm: evidence from the composition of Recent bivalve faunas. Paleobiology. 26:188-214.

Crame JA (2002) Evolution of taxonomic diversity gradients in the marine realm: a comparison of Late Jurassic and Recent bivalve faunas. Paleobiology. 28:184-207.

Currey JD (1990) Biomechanics of mineralized skeletons. In: Skeletal Biomineralization: Patterns, Processes and Evolutionary Trends, vol. 1. Carter JG (Ed.) Van Nostrand-Reinhold, New York. 14 p.

Currey JD, Taylor JD (1974) The mechanical behavior of some molluskan hard tissues. J. Zool. 173:395-406.

Currey JD, Kohn AJ (1976) Fatigue fracture in the crossed-lamellar structure of Conus shells. J. Mater. Sci. 11:1615-1623.

Dame RF (1972) Comparison of various allometric relationships in intertidal and subtidal American oysters. Fish. Bull. 70:1121-1126.

Darling MS, Wilbur KM (1993) A method for measuring growth in living barnacles (Crustacea: Cirripedia). J. Mar. Biol. Assoc. UK. 73:723-726.

Dauphin Y, Denis A (2000) Structure and composition of the aragonitic crossed lamellar layers in six species of Bivalvia and Gastropoda. Comp. Biochem. Physiol. Part A Mol. Integr. Physiol. 126:367-377.

Davies PS (1989) Short-termgrowth measurements of corals using an accurate buoyant weighing technique. Mar. Biol. 101:389-395.

Del Piero D, Fornaroli D (1998) Situazione dello stock di *Chamelea gallina* (L.) nel compartimento marittimo di Venezia (1984/1995). Biol. Mar. Medit. 5:393-403.

Del Piero D, Fornaroli D, Balzo M (1998) Situazione dello stock di *Chamelea gallina* (L.) nel Golfo di Trieste dal 1984 al 1995. Biol. Mar. Medit. 5:382-392.

Denny MW, Blanchette CA (2000) Hydrodynamics, shell shape, behavior and supervisorship in the owl limpet *Lottia gigantean*. J. Exp. Biol. 203:2623-2639.

Dermott R, Munawar M (1993) Invasion of Lake Erie offshore sediments by *Dreissena*, and its ecological implications. Can. J. Fish. Aquat. Sci. 50:2298-2304.

DeWitt TJ (1998) Costs and limits of phenotypic plasticity: Tests with predator induced morphology and life history in a freshwater snail. J. Evol. Biol. 11:465-480.

DeWitt TJ, Scheiner SM (2004) Phenotypic plasticity: functional and conceptual approaches. Oxford University Press, Oxford. 247 p.

Doyle S, MacDonald B, Rochette R (2010) Is water temperature responsible for geographic variation in shell mass of *Littorina obtusata* (L.) snails in the Gulf of Maine*?* J. Exp. Mar. Biol. Ecol. 394:98-104.

Falini G, Albeck S, Weiner S Addadi L (1996) Control of aragonite or calcite polymorphism by mollusk shell macromolecules. Science. 271:67-69.

Fantazzini P, Mengoli S, Pasquini L, Bortolotti V, Brizi L, Mariani M, Di Giosia M, Fermani S, Carpaccioni B, Caroselli E, Prada F, Zaccanti F, Levy O, Dubinsky Z, Kaandorp JA, Konglers P, Hammel JU, Dauphin Y, Cuif JP, Weaver JC, Fabricus KE, Wagermaier W, Fratzl P, Falini S and Goffredo S (2015) Gains and losses of coral skeletal porosity changes with ocean acidification acclimatation. N. Comms. 6:7785.

Findlay HS, Wood HL, Kendall MA, Spicer JI, Twitchett RJ, Widdicombe S (2011) Comparing the impact of high CO_2 on calcium carbonate structures in different marine organisms. Mar. Biol. Res. 7:565-575.

Fitzer SC, Vittert L, Bowman A, Kamenos NA, Phoenix VR, Cusack M (2015) Ocean acidification and temperature increase impact mussel shell shape and thickness: problematic for protection?. Ecol. evol. 5:4875-84.

Foster LC, Allison N, Finch AA, Andersson C (2009) Strontium distribution in the shell of the aragonite bivalve *Arctica inslandica*. Geochem. Geophys. Geosyst. 10:Q03003.

Franz DR (1993). Allometry of shell and body weight in relation to shore level in the intertidal bivalve *Geukensia demissa* (Bivalvia: Mytilidae). J. Exp. Mar. Biol. Ecol. 174:193-207.

Froglia C (1989) Clam fisheries with hydraulic dredges in the Adriatic Sea. In: Marine invertebrates fisheries: their assessment and management. Caddy JF (Ed.) J. Wiley, New York. 27 p.

Froglia C (2000) Il contributo della ricerca scientifica alla gestione della pesca dei molluschi bivalvi con draghe idrauliche. Biol. Mar. Mediterr. 7:71-82.

Fuiman LA, Gage JD, Lamont PA (1999) Shell morphometry of the deep sea protobranch bivalve *Ledella pustulosa* in the Rockall Trough, North-East Atlantic. J. Mar. Biol. Ass. U. K. 79:661-671.

Gilbert SF (2001) Ecological developmental biology: developmental biology meets the real world. Dev. Biol. 233:1-12.

Gilbert SF (2012) Ecological developmental biology: environmental signals for normal animal development. Evol. Dev. 14:20-28.

Goffredo S, Caroselli E, Pignotti E, Mattioli G, Zaccanti F (2007) Variation in biometry and population density of solitary corals with solar radiation and sea surface temperature in the Mediterranean Sea. Mar. Biol. 152:351-361.

Goffredo S, Caroselli E, Mattioli G, Pignotti E, Zaccanti F (2008) Relationship between growth, population structure and sea surface temperature in the temperate solitary coral *Balanophillia europaea* (Scleractinia, Dendrophylliidae). Coral Reefs. 27:623-632.

Goffredo S, Caroselli E, Mattioli G, Pignotti E, Dubinsky Z, Zaccanti F (2009) Inferred level of calcification decreases along an increasing temperature gradient in a Mediterranean endemic coral. Limnol. Oceanogr. 54:930-937.

Goffredo S, Prada F, Caroselli E, Capaccioni B, Zaccanti F, Pasquini L, Fantazzini P, Fermani S, Reggi M, Levy O, Fabricus KE, Dubinsky Z, Falini G (2014) Biomineralization control related to population density under ocean acidification. N. Clim. Change. 4:593-597.

Goffredo S, Mancuso A, Caroselli, Prada F, Dubinsky Z, Falini G, Levy O, Fantazzini P, Pasquini L (2015) Skeletal mechanical proprieties of Mediterranean corals along a wide latitudinal gradient. Coral Reefs. 34:121-132.

Gutiérrez JL, Jones CG, Strayer DL, Iribarne OO (2003) Mollusks as ecosystem engineers: the role of shell production in aquatic habitats. Oikos. 101:79-90.

Harley CDG, Denny MW, Mach KJ, Miller LP (2009) Thermal stress and morphological adaptations in limpets. Func. Ecol. 23:292-301.

Heilmayer O, Brey T, Pörtner HO (2004) Growth efficiency and temperature in scallops: a comparative analysis of species adapted to different temperatures. Funct. Ecol. 18:641-647.

Higuchi T, Fujimura H, Yuyama I, Harii S, Agostini S, Oomori T (2014) Biotic control of skeletal growth by scleractinian corals in aragonite-calcite seas. PLoS ONE. 9:e91021.

Hinch SG, Bailey RC (1988) Within- and among- lake variation in shell morphology of the freshwater clam *Elliptio complanata* (Bivalvia: Unionidae) from south-central Ontario lakes. Hydrobiologia. 157:27-32.

Hoegh-Guldberg O (1997) Effect of nutrient enrichment in the field on the biomass, growth and calcification of the giant clam, *Tridacna maxima*. Mar. Biol. 129:635-642.

Hummel H, Bogaards R, Bek T, Polishchuk L, Sokolov K, Amiard-Triquet C, Bachelet G, Desprez M, Naumov A, Strelkov P, Dahle S (1998) Growth in the bivalve *Macoma balthica* from its northern to its southern distribution limit: a discontinuity in North Europe because of genetic adaptations in Arctic populations? Comp. Biochem. Physiol. A. 120:133-141.

Jansen JM, Pronker AE, Kube S, Sokolowski A, Sola JC, Marquiegui MA, Schiedek D, Bonga SW, Wolowicz M, Hummel H (2007) Geographic and seasonal patterns and limits on the adaptive response to temperature of European Mytilus spp. and *Macoma balthica* populations. Oecologia. 154:23-34.

Jones AM (1979) Structure and growth of a high-level population of *Cerastoderma edule* (Lamellibranchiata). J. Mar. Biol. Ass. U.K. 59:277-287.

Kain JM (1989) The seasons in the subtidal. Br. Phycol. J. 24:203-215.

Keller N, Del Piero D, Longinelli A (2002) Isotopic composition, growth rates and biological behavior of *Chamelea gallina* and *Callista chione* from the Gulf of Trieste (Italy). Mar. Biol. 140:9-15.

Kennedy WJ, Taylor JD, Hall A (2008) Environmental and biological controls on bivalve shell mineralogy. Biol. Rev. 44:499-530.

Kleypas JA, Buddermeier RW, Archer D, Gattuso JP, Langdon C, Opdyke BN (1999) Geochemical consequences of increased atmospheric carbon dioxide on coral reefs. Science. 284:118-120.

Kleypas JA, Feely RA, Fabry VJ, Langdon C, Sabile CL, Robbins LL (2006) Impacts of ocean acidification on coral reefs and other marine calcifiers: a guide for future research. Report NFS, NOAA, US Geological Survey, NSF. 18:1-88.

Krapivka S, Toro JE, Alcapán AC, Astorga M, Presa P, Pérez M, Guiñez R (2007) Shell-shape variation along the latitudinal range of the Chilean blue mussel *Mytilus chilensis* (Hupe 1854). Aquacult. Res. 38:1770-1777.

Laing I, Utting SD, Kilada RWS (1987) Interactive effect of diet and temperature on the growth of juvenile clams. J. Exp. Mar. Biol. Ecol. 113:23-38.

Langerhans RB, Chapman LJ, DeWitt TJ (2007) Complex phenotype-environment associations revealed in an East African cyprinid. J. Evol. Biol. 20:1171-81.

Leonard GH, Bertness MD, Yund PO (1999) Crab predation, waterborne cues, and inducible defenses in the blue mussel, *Mytilus edulis*. Ecology. 80:1-4.

Levitan DR (1991) Skeletal changes in the test and jaws of the sea urchin *Diadema antillarum* in response to food limitation. Mar. Biol. 111:431-435.

Lorenzi T, Chisholm RH, Desvillettes L, Hughes BD (2015) Dissecting the dynamics of epigenetic changes in phenotype-structured populations exposed to fluctuating environments. J. Theor. Biol. 386:166-176.

Lowenstam HA, Weiner S (1989) On biomineralization. Oxford University Press, USA. 324 p.

Márquez F, Van Der Molen S (2011) Intraspecific shell-shape variation in the razor clam *Ensis macha* along the Patagonian coast. J. Molluscan. Stud. 77:123-128.

MacDonald BA, Thompson RJ (1988) Intraspecific variation in growth and reproduction on latitudinally differentiated populations of the giant scallop *Placopecten magellanicus* (Gmelin). Biol. Bull. 175:361-371.

Milano S, Schöne BR, Witbaard R (2015) Changes of shell microstructural characteristics of *Cerastoderma edule* (Bivalvia) - A novel proxy for water temperature. Palaeogeogr. Palaeoclimatol. Palaeoecol.

McNeil BI, Matear RJ, Barnes DJ (2004) Coral reef calcification and climate change: the effect of ocean warming. Geophys. Res. Lett. 31:L22309.

Morley SA, Clark MS, Peck LS (2010) Depth gradients in shell morphology correlate with thermal limits for activity and ice disturbance in Antarctic limpets. J. Exp. Mar. Biol. and Ecol. 390:1-5.

Moschino V, Marin MG (2006) Seasonal changes in physiological responses and evaluation of "well-being" in the Venus clam *Chamelea gallina* from the Northern Adriatic Sea. Comp. Bioch. Physiol. 145A:433-440.

Nagarajan R, Lea SE, Goss-Custard JD (2006) Seasonal variations in mussel, *Mytilus edulis* L. shell thickness and strength and their ecological implications. J. Exp. Mar. Biol. Ecol. 339:241-250.

Newell CR, Hidu H (1982) The effects of sediment type on growth rate and shell allometry in the soft shelled clam *Mya arenaria*. L. J. Exp. Mar. Biol. Ecol. 65:285-295.

Nienhuis S, Palmer AR, Harley CDG (2010) Elevated CO_2 affects shell dissolution rate but not calcification rate in a marine snail. Proc. R. Soc. Lond. B. 277:2553-2558.

Nishida K, Ishimura T, Suzuki A, Sasaki T (2012) Seasonal changes in the shell microstructure of the bloody clam, *Scapharca broughtonii* (Mollusca: Bivalvia: Arcidae). Palaeogeogr. Palaeoclimatol. Palaeoecol. 363:99-108.

Nishii T (1965) Examination of the underwater weight used for measuring the growth of pearl oyster, *Pinctada martensii*. Bull. Natl. Pearl. Res. Lab 10:1264-1282.

Palmer AR (1982) Growth in marine gastropods: A non-destructive technique for independently measuring shell and body weight. Malacologia. 23:63-73.

Palmer AR (1983) Relative cost of producing skeletal organic matrix versus calcification: evidence from marine gastropods. Mar. Biol. 75:287-292.

Palmer AR (1990) Predator size, prey size, and the scaling of vulnerability: hatchling gastropods vs. barnacles. Ecology. 1:759-775.

Peck LS, Convey P, Barnes DKA (2006) Environmental constraints on life histories in Antarctic ecosystems: tempos, timings and predictability. Biol. Rev. 81:75-109.

Peck LS, Powell DK, Tyler PA (2007) Very slow development in two Antarctic bivalve molluscs, the infaunal clam, *Laternula elliptica* and the scallop *Adamussium colbecki*. Mar. Biol. 150:1191-1197.

Picard J (1965) Recherche qualitative sur les biocoenoses marines des substrats meubles dragables de la region Marseillaise. Rec. Trav. Sta. mar. Endoume. 52:1-160.

Pigliucci M (1996) How organisms respond to environmental changes: from phenotypes to molecules (and vice versa). Trends Ecol. Evol. 11:168-163.

Pigliucci M (2001) Phenotypic plasticity: beyond nature and nurture. Johns Hopkins University Press, Baltimore, MD. 333 p.

Pigliucci M, Murren CJ, Schlichting CD (2006) Phenotypic plasticity and evolution by genetic assimilation. J. exp. Boil. 209:2362-2367.

Potvin C, Roff DA (1993) Distribution-free and robust statistical methods: viable alternatives to parametric statistics? Ecology. 74:1617-1628.

Prezant RS, Tan Tiu A, Chalermwat K (1988) Shell microstructure and color changes in stressed *Corbicula fluminea*. Veliger. 31:236-243.

Rahman MA, Shinko R (2011) Biocalcification of corals and their response to global climate change. Bionature 2011: The Second International Conference on Bioenvironment, Biodiversity and Renewable Energies. 4 p.

Ramón M, Richardson CA (1992). Age determination and shell growth of *Chamelea gallina* (Bivalvia: Veneridae) in the western Mediterranean. Mar. Ecol. Prog. Ser. 89:15-23.

Reggi M, Fermani S, Landi V, Sparla F, Caroselli E, Gizzi F, Dubinsky Z, Levi O, Cuif JP, Dauphin Y, Goffreso S, Falini G (2014) Biomineralization in Mediterranean corals: the role of the intraskeletal organic matrix. Cryst. Growth Des. 14:4310-4320.

Reimer O, Tedengren M (1996) Phenotypical improvement of morphological defences in the mussel *Mytilus edulis* induced by exposure to the predator *Asterias rubens*. Oikos. 75:383-390.

Reimer O, Harms-Ringdahl S (2001) Predator-inducible changes in blue mussels from the predator-free Baltic Sea. Mar. Biol. 139:959-965.

Rex MA, Stuart CT, Coyne G (2000) Latitudinal gradients of species richness in the deep-sea benthos of the North Atlantic. Proc. Natl. Acad. Sci. USA. 97:4082-4085.

Ries JB, Cohen AL, McCorkle DC (2009) Marine calcifiers exhibit mixed responses to CO_2 induced ocean acidification. Geology. 37:1131-1134.

Rodolfo-Metalpa R, Houlbrèque F, Tambutté É, Boisson F, Baggini C, Patti FP, Jeffree R, Fine M, Foggo A, Gattuso JP, Hall-Spencer JM (2011) Coral and mollusc resistance to ocean acidification adversely affected by warming. Nat. Clim. Change. 1:308-312.

Romanelli M, Cordisco CA, Giovanardi O (2009) The long term decline of the *Chamelea gallina* L. (Bivalvia: Veneridae) clam fishery in the Adriatic Sea: is a synthesis possible? Acta Adriat. 50:171-205.

Roy K, Jablonski D, Valentine JW (2000a) Dissecting latitudinal diversity gradients: functional groups and clades of marine bivalves. Proc. R. Soc. B. Biol. Sci. 267:293-299.

Roy K, Jablonski D, Martien KK (2000b) Invariant size-frequency distributions along a latitudinal gradient in marine bivalves. Proc. Natl. Acad. Sci. USA. 97:13150-13155.

Sabbioni L (2012) Influence of global warming on marine calcifying organisms. MS Thesis, Department of Chemistry "G. Ciamician", University of Bologna, Bologna.

Schluter D (2000) The ecology of adaptive radiation. Oxford University Press, Oxford. 292 p.

Seed R, Richardson CA (1999) Evolutionary traits in *Perna viridis* (Linnaeus) and *Septifer virgatus* (Wiegmann) (Bivalvia: Mytilidae). J. Exp. Mar. Biol. Ecol. 239:273-287.

Sepúlveda RD, Ibáñez CM (2012) Clinal variation in the shell morphology of intertidal snail *Acanthina monodon* in the Southeastern Pacific Ocean. Mar. Bio. Res. 8:363-372.

Shi Q, Zhao MX, Zhang QM, Yu KF, Chen TR, Li S, Wang HK (2009) Estimate of carbonate production by scleractinian corals at Luhuitou fringing reef, Sanya, China. Chin. Sci. Bull. 54:696-705.

Simpson TL (1984) The cell biology of sponges. Springer Science & Business Media. 661 p.

Smith LD, Jennings JA (2000) Induced defensive responses by the bivalve *Mytilus edulis* to predators with different attack modes. Mar. Biol. 136:461-469.

Sobral P, Widdows J (1997a) Influence of hypoxia and anoxia on the physiological responses of the clam *Ruditapes decussatus* from southern Portugal. Mar. Biol. 127:455-461.

Sobral P, Widdows J (1997b) Effects of elevated temperatures on the scope for growth and resistance to air exposure of the clam *Ruditapes decussatus* (L.), from southern Portugal. Sci. Mar. 61:163-171.

Sokolova IM, Pörtner HO (2001) Physiological adaptations to high intertidal life involve improved water conservation abilities and metabolic rate depression in *Littorina saxatilis*. Mar. Ecol. Prog. Ser. 224:171-186.

Stravisi L (2003) Meteorological characteristics of the Gulf of Trieste. University of Trieste.

Suzuki M, Dauphin Y, Addadi L, Weiner S (2011) Atomic order of aragonite crystals formed by mollusks. Cryst. Eng. Comm. 13:6780-6786.

Tan Tiu A (1988) Temporal and spatial variation of shell microstructure of *Polymesoda caroliniana* (Bivalvia: Heterodonta). Am. Malacol. Bull. 6:199-206.

Thomsen J, Haynert K, Wegner KM, Melzner F (2015) Impact of seawater carbonate chemistry on the calcification of marine bivalves. Biogeosciences. 12:4209-4220.

Trussell GC (1996) Phenotypic plasticity in an intertidal snail: the role of a common crab predator. Evolution. 50:448-454.

Trussell GC (2000) Predator-induced plasticity and morphological trade-offs in latitudinally separated populations of *Littorina obtusata*. Evol. Ecol. Res. 2:803-822.

Trussell GC, Smith LD (2000) Induced defenses in response to an invading crab predator: an explanation of historical and geographic phenotypic change. Proc. Natl. Acad. Sci. USA. 97:2123-2127.

Trussell GC, Etter RJ (2002) Integrating genetic and environmental forces that shape the evolution of geographic variation in a marine snail. Genetica. 114:103.

Trussell GC, Nicklin MO (2002) Cue sensitivity, inducible defense, and trade-offs in a marine snail. Ecology. 83:1635-1647.

Valladares A, Manríquez G, Suárez-Isla BA (2010) Shell shape variation in populations of *Mytilus chilensis* (Hupe 1854) from southern Chile: a geometric morphometric approach. Mar. Biol. 157:2731-2738.

Vermeij GJ (1993) A natural history of shells. Princeton University Press, New Jersey. 207 p.

Vogel S (1996) Life in Moving Fluids: The Physical Biology of Flow. Princeton Paperbacks. 469 p.

Yang W, Kashani N, Li XW, Zhang GP, Meyers MA (2011) Structural characterization and mechanical behavior of a bivalve shell (*Saxidomus purpuratus*). Mater. Sci. Eng. C. 31:724-729.

Young SD (1971) Organic material from scleractinian coral skeletons. I. variation in composition between several species. Comp. Biochem. Physiol. B. 40:113-120.

Wainwright SA, Biggs WD, Curry JD, Gosline JM (1976) Mechanical design in organisms. Edward Arnold, London. 429 p.

Watson SA, Peck LS, Tyler PA, Southgate PC, Tan KS, Day RW, Morley SA (2012) Marine invertebrate skeleton size varies with latitude, temperature and carbonate saturation: implications for global change and ocean acidification. Global Change Biol. 18:3026-3038.

Weiner S, Traub W, Lowenstam HA (1983) Organic matrix in calcified exoskeletons. In: Biomineralization and biological metal accumulation. Westbroek P, De Jong EW (eds.) Springer Netherlands. 19 p.

West-Eberhard MJ (2003) Developmental Plasticity and Evolution. Oxford University Press. 797 p.

Zavatarelli M, Raicich F, Bregant D, Russo A, Artegiani A (1998) Climatological biogeochemical characteristics of the Adriatic Sea. J. Mar. Syst. 18:227-263.

Zieritz A, Aldridge DC (2009) Identification of ecophenotypic trends within three European freshwater mussel species (Bivalvia: Unionoida) using traditional and modern morphometric techniques. Biol. J. Linn. Soc. 98:814-825.

Tables

Table 1. Environmental parameters. Mean annual values ± SE for solar radiation (SR) and sea surface temperature (SST) from 2011 to 2014, of the sites. n = number of collected data; SE = standard error.

Code	Latitude (°)	n	SR (W m^{-2})		SST (°C)	
			mean	Range	mean	Range
MO	45.7	1447	159.4 (2.5)	154.4 - 164.4	16.96 (0.19)	16.58 - 17.35
CH	45.2	1447	160.8 (2.5)	155.8 - 165.7	16.47 (0.19)	16.09 - 16.84
GO	44.8	1447	163.8 (2.6)	158.7 - 168.8	16.54 (0.19)	16.17 - 16.92
CE	44.2	1447	165.2 (2.5)	160.2 - 170.2	17.05 (0.20)	16.65 - 17.45
SB	43.1	1447	172.4 (2.5)	167.4 - 177.4	17.90 (0.19)	17.52 - 18.28
CA	41.9	1447	180.4 (2.6)	175.4 - 185.5	18.60 (0.17)	18.27 - 18.93

Values for each population, in decreasing order of latitude: MO (Monfalcone), CH (Chioggia), GO (Goro), CE (Cesenatico), SB (San Benedetto), CA (Capoiale).

Table 2. Shell parameters. Macroscale level. Mean ± CI (95%) of biometric parameters at each site. n = number of samples. CI = 95% confidence interval

Code	n	Lenght (mm)	Height (mm)	Width (mm)	Thickness (mm)	Mass (g)	Volume (cm3)
MO	40	26.85 (0.40)	22.28 (0.27)	7.41 (0.13)	1.58 (0.07)	2.15 (0.07)	0.77 (0.03)
CH	40	26.14 (0.41)	21.45 (0.32)	6.39 (0.09)	1.28 (0.06)	1.66 (0.07)	0.59 (0.02)
GO	40	26.06 (0.47)	21.29 (0.39)	6.69 (0.13)	1.25 (0.07)	1.59 (0.08)	0.57 (0.03)
CE	40	26.52 (0.49)	21.49 (0.39)	6.47 (0.15)	1.13 (0.06)	1.57 (0.09)	0.56 (0.03)
SB	40	26.39 (0.45)	21.71 (0.32)	6.44 (0.11)	1.14 (0.06)	1.52 (0.07)	0.54 (0.02)
CA	40	26.40 (0.51)	21.42 (0.42)	6.13 (0.12)	1.07 (0.04)	1.41 (0.08)	0.51 (0.03)

Populations are arranged in order of decreasing latitude: MO (Monfalcone), CH (Chioggia), GO (Goro), CE (Cesenatico), SB (San Benedetto), CA (Capoiale).

Table 3. Shell parameters. Microscale level. Mean ± CI (95%) of microdensity, bulk density and apparent porosity of the sites in decreasing order of latitude. n = number of samples; CI = 95% confidence interval.

Code	n	Microdensity (g cm^{-3})	Bulkdensity (g cm^{-3})	Apparent porosity (%)
MO	40	2.80 (0.010)	2.72 (0.010)	2.86 (0.149)
CH	40	2.82 (0.010)	2.72 (0.012)	3.30 (0.317)
GO	40	2.81 (0.012)	2.70 (0.013)	3.87 (0.261)
CE	40	2.81 (0.003)	2.70 (0.011)	4.04 (0.342)
SB	40	2.82 (0.006)	2.70 (0.008)	3.98 (0.343)
CA	40	2.80 (0.004)	2.68 (0.008)	4.20 (0.312)

Populations are arranged in order of decreasing latitude: MO (Monfalcone), CH (Chioggia), GO (Goro), CE (Cesenatico), SB (San Benedetto), CA (Capoiale).

Table 4. Shell and environmental parameters. Kruskal-Wallis test and correlation analyses between biometric and shell parameters and environmental parameters in the sampled populations.

Shell parameter	K-W	SR (W m^{-2}) r_s	SST (°C) r_s
Lenght (mm)	NS	-	-
Height (mm)	***	*	NS
Width (mm)	***	***	***
Thickness (mm)	***	***	***
Mass (g)	***	***	***
Volume (cm3)	***	***	***
Microdensity (g/cm3)	***	NS	NS
Bulkdensity (g/cm3)	***	***	***
Apparent porosity (%)	***	***	***

K-W = Kruskal-Wallis equality-of-populations rank test, NS = not significant, *** = $p < 0.001$. r_s = Spearman's determination coefficient, NS = not significant, * = $p < 0.05$, *** = $p < 0.001$.

Table 5. Shell mechanical properties. Mean ± CI (95%) of Young's modulus and maximum load (kN) mean value for each population. n = number of samples; CI = 95% confidence interval.

Code	n	Young's modulus	Maximum Load (kN)
MO	14	2.50 (0.54)	0.13 (0.02)
CH	30	2.80 (0.16)	0.15 (0.01)
GO	28	2.35 (0.18)	0.11 (0.01)
CE	21	2.61 (0.13)	0.13 (0.02)
SB	28	2.30 (0.19)	0.11 (0.02)
CA	20	2.18 (0.29)	0.09 (0.01)

Values for each population, in decreasing order of latitude: MO (Monfalcone), CH (Chioggia), GO (Goro), CE (Cesenatico), SB (San Benedetto), CA (Capoiale).

Table 6. Microstructural parameters. Mean ± CI (95%) of XRD, full width at half maximum (FWHM) and FTIR, mean peak height values. n = number of samples; CI = 95% confidence interval. ν_2, ν_3 and ν_4 = characteristic calcium carbonate active vibrational modes.

Code	n	FWHM	ν_2/ν_3	ν_4/ν_3
MO	5	0.170 (0)	0.386 (0.014)	0.095 (0.005)
CH	5	0.180 (0)	0.345 (0.009)	0.058 (0.012)
GO	5	0.180 (0.006)	0.401 (0.014)	0.102 (0.015)
CE	5	0.172 (0.004)	0.388 (0.009)	0.100 (0.008)
SB	5	0.174 (0.005)	0.352 (0.014)	0.090 (0.007)
CA	5	0.188 (0.004)	0.369 (0.011)	0.075 (0.005)

Values for each population, in decreasing order of latitude: MO (Monfalcone), CH (Chioggia), GO (Goro), CE (Cesenatico), SB (San Benedetto), CA (Capoiale).

Table 7. Microstructural parameters. Mean ± CI (95%) of OM percentage weight loss for each population of *C. gallina*. n = number of samples; CI = 95% confidence interval.

Code	n	OM (%)
MO	10	1.95 (0.09)
CH	10	1.86 (0.11)
GO	5	1.83 (0.16)
CE	5	1.93 (0.16)
SB	5	1.72 (0.13)
CA	10	1.97 (0.08)

Values for each population, in decreasing order of latitude: MO (Monfalcone), CH (Chioggia), GO (Goro), CE (Cesenatico), SB (San Benedetto), CA (Capoiale).

Figures

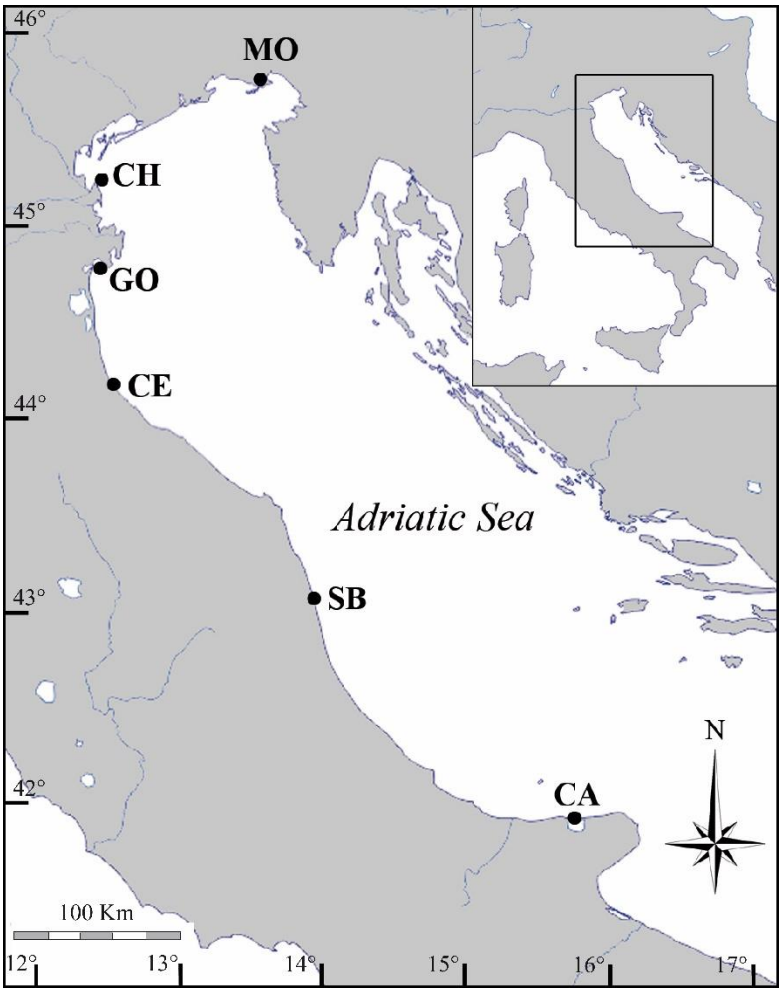

Figure 1. Map of the Adriatic coastline indicating the sites where the clams were collected. Abbreviations and coordinates of the sites in decreasing order of latitude: MO, Monfalcone 45°42′N, 13°14′E; CH, Chioggia 45°12′N, 12°19′E; GO, Goro 44°47′N, 12°25′E; CE, Cesenatico 44°11′N, 12°26′E; SB, San Benedetto 43°5′N, 13°51′E; CA, Capoiale 41°55′N, 15°39′E.

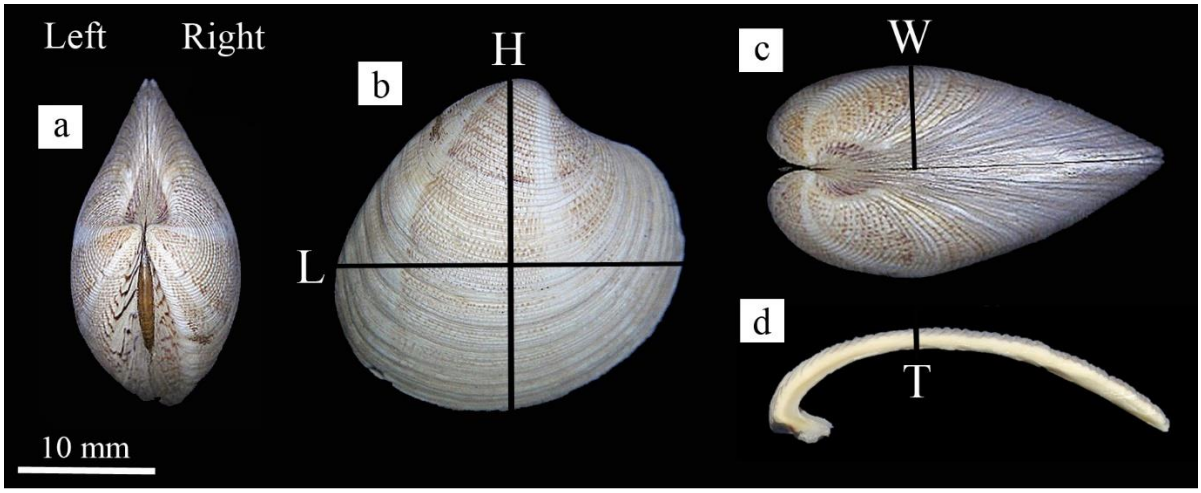

Figure 2. Shell parameters. a) Frontal orientation; by placing the umbo upwards can be distinguished the valve left from the right one; b) Lateral orientation, L = length, H = height; c) cross-sectional orientation, W = width; d) cross-section, T = thickness.

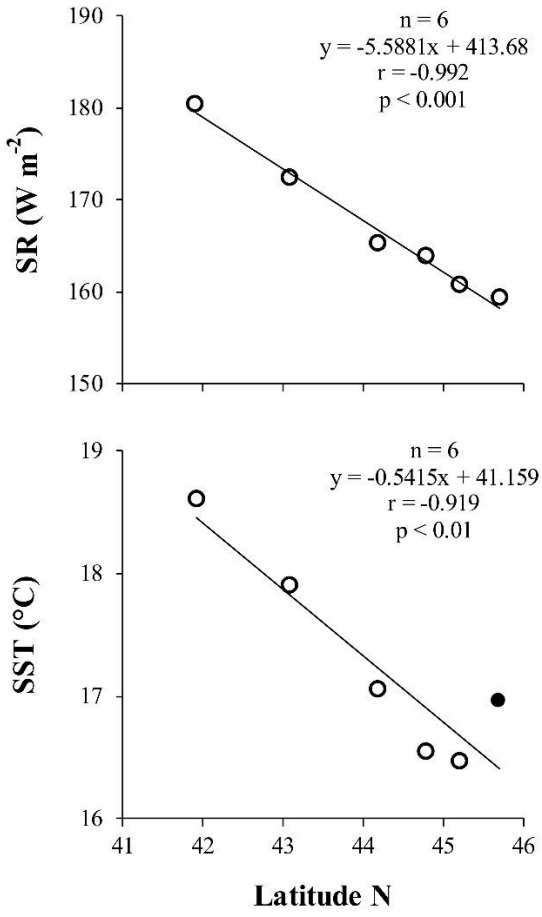

Figure 3. Relationship between environmental parameters (mean annual SR and SST) and the latitude of study sites along the coast of Italy. The black dot indicates the site of Monfalcone, which was characterized by higher temperature than expected at its latitude. n = number of stations; r = Pearson's correlation coefficient.

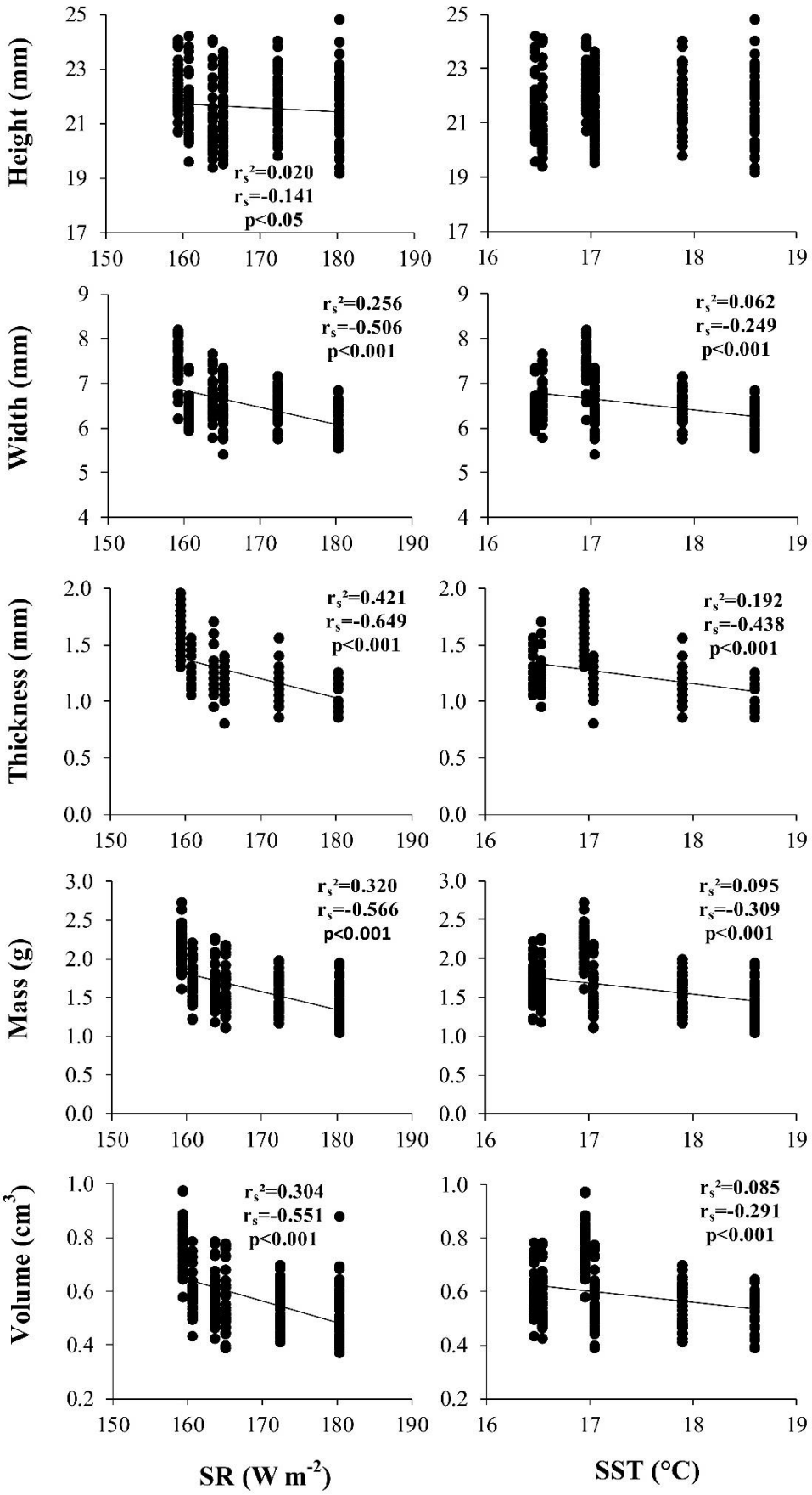

Figure 4. Variation in the biometric parameters of *C. gallina* with environmental variables (SR and SST). r_s = Spearman's determination coefficient.

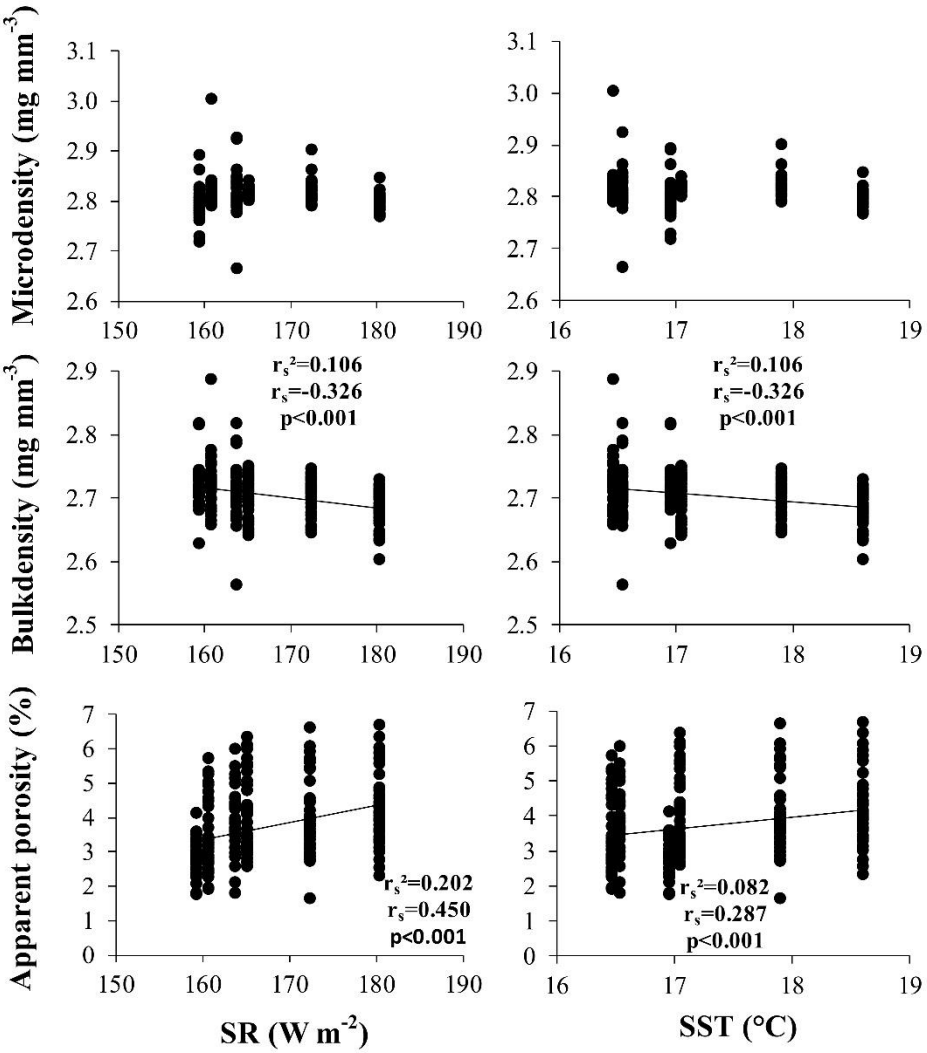

Figure 5. Variation in the shell parameters of *C. gallina* with environmental variables (SR and SST). r_s = Spearman's determination coefficient. n = 40 in each population.

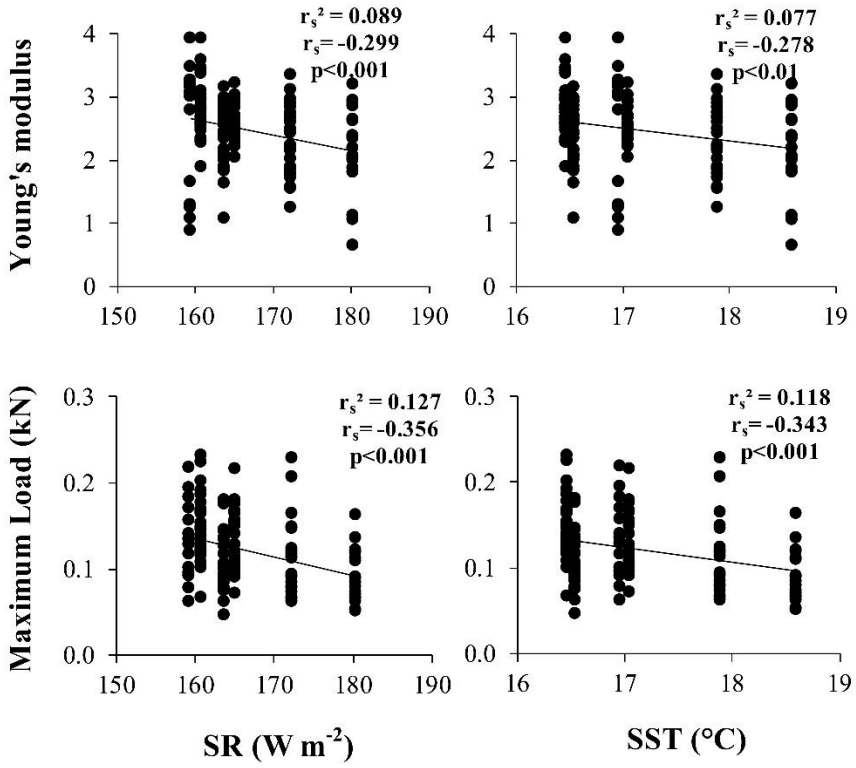

Figure 6. Variation in mechanical properties of *C. gallina* with environmental variables (SR and SST). r_s = Spearman's determination coefficient. n = 141 in each graph.

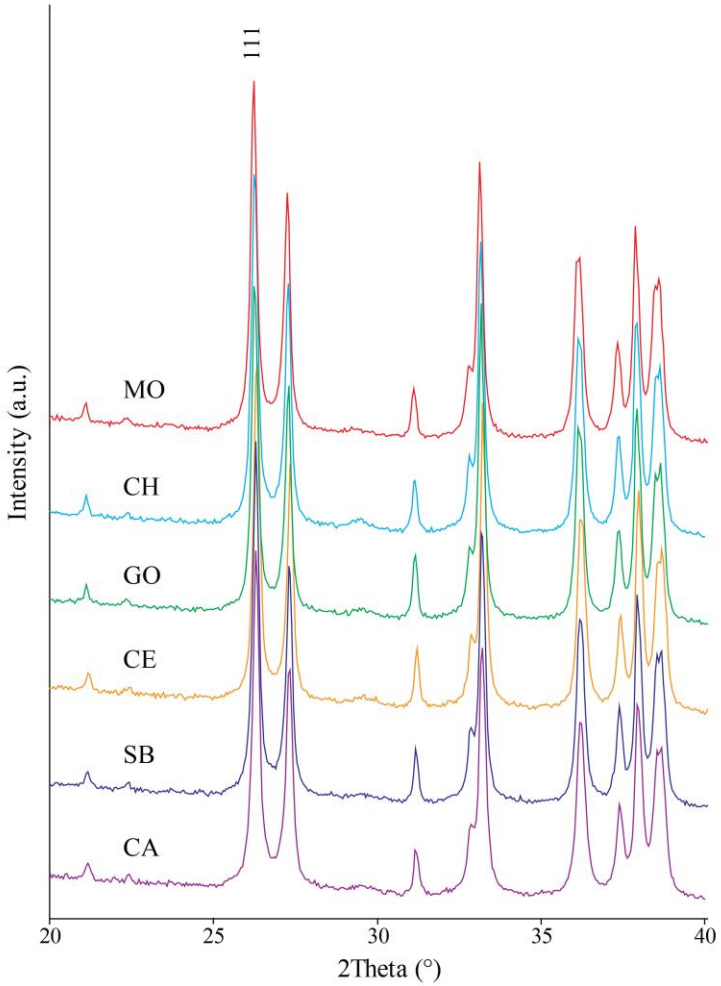

Figure 7. X-ray powder diffraction patterns (XRD) from ground shells of *C. gallina*. A representative diffractogram is shown for each population, in decreasing order of latitude: MO (Monfalcone), CH (Chioggia), GO (Goro), CE (Cesenatico), SB (San Benedetto), CA (Capoiale). For better readability the Miller index is indicated only for the first peak, all peaks are representative of aragonite. Diffractograms are offset to increase readability.

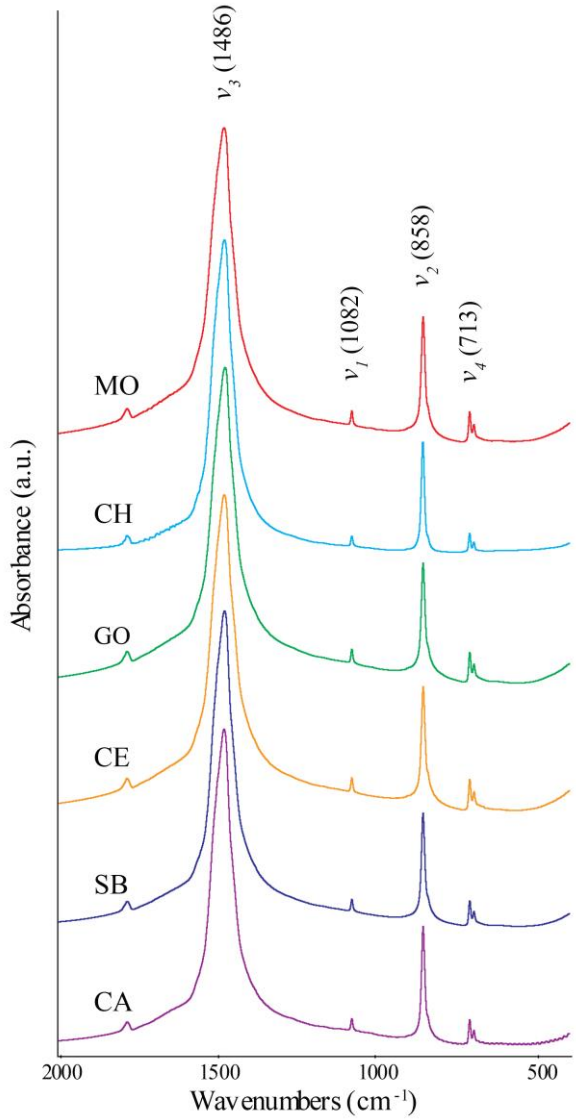

Figure 8. FTIR spectra from ground shells of *C. gallina*. A representative spectra is shown for each population, in decreasing order of latitude: MO (Monfalcone), CH (Chioggia), GO (Goro), CE (Cesenatico), SB (San Benedetto), CA (Capoiale). Wavenumbers of the main absorption bands are indicated, all absorption bands are indicative of aragonite. Spectra are offset to increase readability.

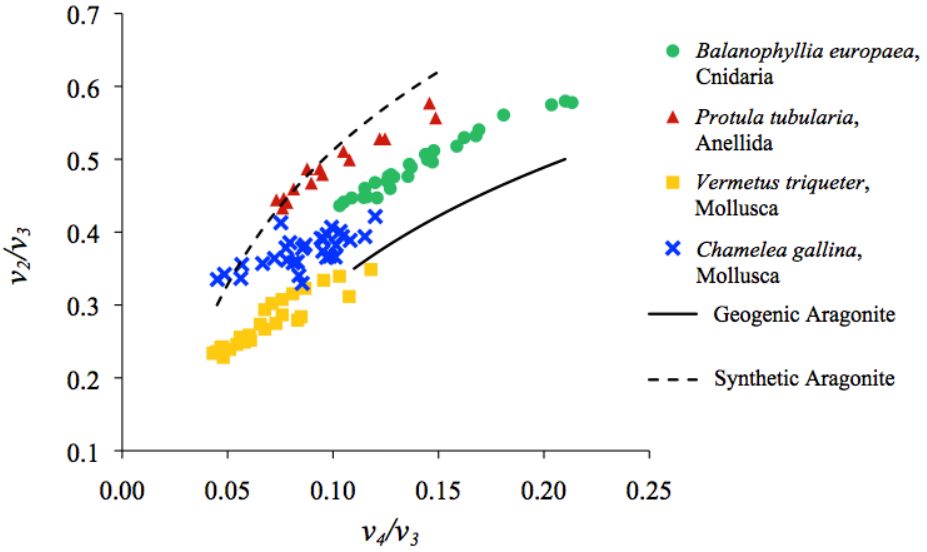

Figure 9. Combined plots of the v_4/v_3 vs. v_2/v_3 peak heights of *C. gallina* from this study, *B. europaea*, *P. tubularia* and *V. triqueter* (Sabbioni 2012) and fitted curves of the v_4/v_3 vs. v_2/v_3 peak heights of geogenic and synthetic aragonite (Suzuki 2011).

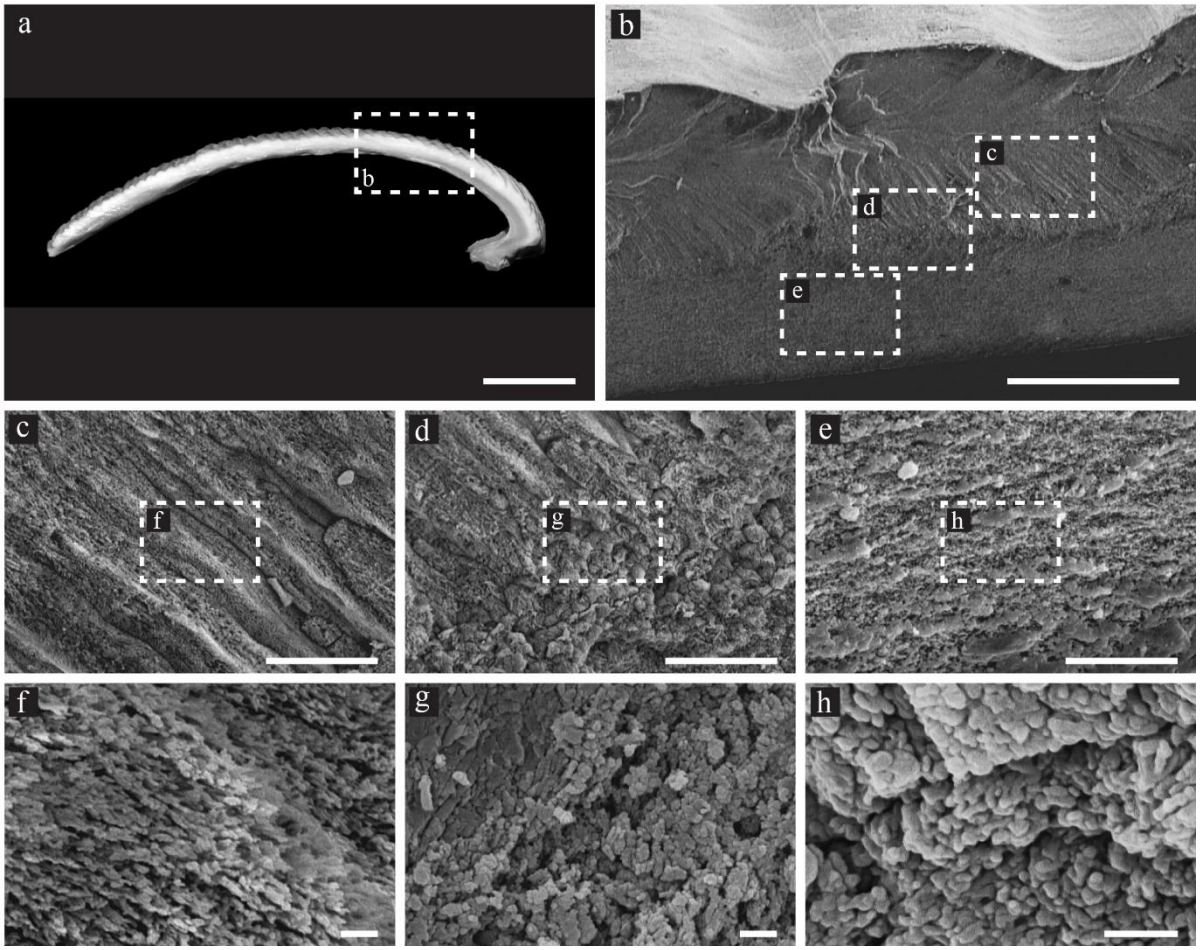

Figure 10. SEM imaging. Skeletal morphology of *C. gallina* from macroscale to nanoscale. Images are representative of all observed valves. (a, b) Low magnification images of the entire valve section. a) Scale bar 5 mm. b) Scale bar 0.5 mm. (c, d, e) Outer layer, transition layer and inner layer, respectively. Scale bar 30 μm. (f, g, h) Outer layer, transition layer and inner layer, respectively. The arrow indicates the presence of OM. Scale bar 1 μm. Outlined rectangles indicate areas of interest subject to higher magnifications in subsequent images.

Chapter 8

Conclusion

Conclusion

The studies described in this dissertation demonstrate that near future ocean warming (OW) and ocean acidification (OA) have the potential to affect sexual reproduction, physiology and growth of calcifying marine organisms. The implications of high temperature (T), solar radiation (SR) and carbon dioxide partial pressure (pCO_2) on each of the biological parameters examined are discussed below.

Section 1. Sexual reproduction and environmental parameters

The effects of increasing T, SR and pCO_2 on sexual reproduction was performed on two Mediterranean scleractinian corals, characterized by different trophic strategy, along natural gradients. The effects of T and SR on reproductive output of solitary zooxanthellate coral *Balanophyllia europaea* was studied in six populations located along a latitudinal gradient in the western coast of Italy (Mediterranean Sea). The warmer and more irradiated populations of *B. europaea* produced a significantly greater number of oocytes during the initial stages of gametogenesis (gametes recruitment period) than the colder populations, but before the fertilization process (gametes maturity period) the amount of oocytes in these populations declined, and gametogenesis was homogeneous along the gradient. The warmer and more irradiated populations seemed to spend more energy in the initial stages of gametogenesis in order to guarantee a sufficient number of gametes for the fertilization process. During this period (before the fertilization), the amount of oocytes was homogeneous among sites, but contrary to expectations, the warmer populations are less abundant, less stable, and contain fewer young individuals (Goffredo et al. 2007, 2008), suggesting that increasing T may negatively influence also the post-fertilization life stages such as larval dispersal, survival and settlement. The zooxanthellate species *B. europaea* seemed more sensitive to increasing T and SR than the non-zooxanthellate solitary coral *Leptopsammia pruvoti*, previously studied along the same latitudinal gradient in the Tyrrhenian Sea (Mediterranean

Sea, Italy; Airi et al. *submitted*). The reproductive output of *L. pruvoti* was homogeneous among populations in both periods, confirming the results of previous studies on population density, growth and population structure stability, all unaffected by temperature (Goffredo et al. 2007; Caroselli et al. 2011, 2012a, b).

A possible explanation for different responses found between the two species concern their different trophic strategy. The zooxanthellate corals have a symbiosis with unicellular algae (Symbiodinium sp.) that produce energy through photosynthesis process and are able to meet up to ~95% of the energy requirement of the coral host (Muscatine et al. 1981, 1984). Increasing temperature may damage the photosynthetic machinery of Symbiodinium, reducing their photosynthetic efficiency and consequently the amount of energy to coral host. Most of the early oocytes from warmer sites did not reach maturity, possibly due to inhibition of metabolic processes at high T, leading *B. europaea* to reabsorb a greater amount of oocytes in order to reallocate the energy resources into other vital functions. *L. pruvoti* seems less sensitive to increasing T probably due to the absence of symbionts, and consequently the lack of an inhibition of host physiological processes (Goffredo et al. 2007).

To better understand the effect of environmental parameters on coral sexual reproduction, further studies on oogenesis of *B. europaea* and on gametogenesis of *L. pruvoti* were performed along a natural pCO_2 gradient produced by an underwater crater vents located near Panarea Island (Mediterranean Sea, Italy). The studies were performed on a population of *B. europaea* naturally living along the gradient (long-term experiment) and on a population of *L. pruvoti* transplanted along the same gradient (short-term experiment).

With decreasing pH, due to increasing pCO_2, *B. europaea* showed no differences in oocytes reproductive parameters in natural populations grown along the gradient. Same results was find on spermatogenesis (Marchini 2016), confirming that gametogenesis of *B. europaea* seemed unaffected by increase in pCO_2. At the contrary, despite short-term experiment, increasing pCO_2 seemed to

affect spermatogenesis and consequently fertilization process of *L. pruvoti*. During the gonadal development period, the amount of spermaries of the most acidic Site showed lowest values, suggesting a negative effect of pH on spermaries production. During the fertilization period, a delay of spermaries development in the most acidic Site was detected. Contrary to the previous period, the control Site exhibited the lowest values of abundance and gonadal index than the other Sites, probably due to the low number of residual mature spermaries after the fertilization process. Indeed, the control Site showed lower values of fertility than the experimental Sites. These results confirmed a delay in the fertilization process in the acidic Sites, in which fertilization started, but was not completed. In the control Site, the fertilization process appeared complete and the planulation process was almost terminated. With increasing pCO_2, *B. europaea* appeared to be less sensitive than *L. pruvoti*, probably due to increase of photosynthetic efficiency of coral algae under high pCO_2 (*personal observation*), representing a further energy available to coral. *B. europaea* could to reallocate this additional resource into reproduction, while in *L. pruvoti* the lack of zooxanthellae involve in a lack of additional resources, making this species more sensitive to increasing pCO_2. Further study under long-term exposure of pCO_2 are needed to better understand how the natural population will behave in the environment of the future sea. Further study on interaction between increasing T and pCO_2 are needed to better understand how zooxanthellate and non-zooxanthellate corals will respond to both, OW and OA.

Section 2. Ecophysiology and environmental parameters

The effects of increasing T, pCO_2 and their interaction on photosynthesis, bleaching tissue and mortality, was performed in aquaria experiment on two Red Sea zooxanthellate scleractinians characterized by different growth form. The solitary species *Fungia granulosa* was less sensitive to experiment treatments than the colonial *Pocillopora verrucosa*. *F. granulosa* did not show negative effects in photosynthetic efficiency, suggesting a great resistance to increasing T and decreasing pH,

separately. However, it seemed to be affected by synergistic interaction between high T and low pH, showing a reduction of photosynthetic efficiency at the end of the experiment. Bleached tissue was registered only in T and interaction treatments (T/pH), reaching respectively 7% and 11% of bleached tissue at the end of the experiment. During the entire experiment, coral mortality was no recorded in this species.

P. verrucosa was more sensitive to experimental conditions, showing a reduction in photosynthetic efficiency, and an increase in bleached tissue and coral mortality in all treatments. Again, the interaction treatment (T/pH) registered strongest effect reaching 100% bleached tissue and 100% coral mortality at the end of the experiment. The differential susceptibility of corals could be due to their tissue thickness (Loya et al. 2001). *F. granulosa* is a solitary scleractinian coral characterized by large biomass and a completely covered skeleton with high tissue thickness, its energy reserves may help to compensate the stress to the changing environmental conditions. On the opposite, the colonial coral *P. verrucosa* is characterized by lower tissue thickness (Ziegler et al. 2014), making this species more exposed and consequently more vulnerable to external environmental conditions. Anyway, both species showed increased negative effects with increasing exposition time, making together vulnerable to environmental changes to the future.

Section 3. Biomineralization, skeletal phenotype and environmental parameters

Coral calcification is one of the major treats affected by climate changes (Hoegh-Guldberg et al. 2014). The fundamental mechanisms and dynamics of skeletal morphogenesis are still only partially understood (Allemand et al. 2011), in particular the role of organic matrix (OM) is still unclear. To investigate the role of intra-skeletal OM in coral biomineralization process, four Mediterranean species characterized by different trophic strategy and/or growth form was selected: *B. europaea* (solitary, zooxanthellate), *L. pruvoti* (solitary, non-zooxanthellate), *Cladocora caespitosa* (colonial, zooxanthellate) and *Astroides calycularis* (colonial, non-zooxanthellate). The comparative study

showed that the ability of OM in *in vitro* crystallization experiments to influence morphology and polymorphism was not related to the coral ecology and suggested that the coral control over the biomineralization process was species specific and encoded in coral genes. *B. europaea* OM was the most prone to favor the precipitation of aragonite in the absence of magnesium ions, while only calcite precipitated in the other examined species. The calcium carbonate ($CaCO_3$) precipitation starting by an artificial seawater solution revealed that the presence of OM inhibits the crystallization, favoring the precipitation of amorphous calcium carbonate (ACC). Under thermal treatments, the ACC of *B. europaea* was the most stable and only in this species was partially converted to aragonite instead of magnesium calcite. These features suggested a stronger control of *B. europaea* OM over the mineral phases, and a higher independence from the crystallization environment compared to the other species. Thanks to greater independence from the chemical environment, *B europaea* under high pCO_2, could maintain unchanged the amount of energy used in the biomineralization process, and invest the greatest amount of available energy (due to increased photosynthetic efficiency) on gametogenesis.

The relationship between the environmental parameters and growth was also performed in an animal model more complex than phylum Cnidaria. The effects of increasing T and SR on shell morphology at the macro, micro and nanoscale level was performed in six natural populations of the commercially important clam *Chamelea gallina,* located along a latitudinal gradient in the Adriatic Sea (Mediterranean Sea, Italy). The more irradiated and warmer populations was characterized by thinner, more porous and more fragile shell than the others populations, affecting the survival of the species to high T and SR. A possible explanation regards the effect of high T on *C. gallina* physiology. Elevated T reduce energy absorption and increase energy expenditure via respiration, negatively affecting energy balance and thus growth (Ramón and Richardson 1992; Moschino and Marin 2006). A further explanation concerns local environmental pressures, such as nutrients and predators due to SR gradient. The southern sites are characterized by lower plankton density

(Zavatarelli et al. 1998), which could cause feeding deficits and consequently a reduction of available energy for clam to invest in shell construction. Moreover, it is not possible to exclude the influence of T and SST on type/density of predators that can induce changes in bivalves shell morphology (Leonard et al. 1999). However, the shell composition was the same in all populations (100 % aragonite), and the amount of OM and shell parameters at micro and nano scale level were homogeneous among populations, suggesting no influence of T and SR on the crystallography of biomineralized shell building blocks. Because of the importance of this species as commercial resource in Adriatic Sea, more porous and fragile shells found in more irradiated and warmer populations could have great economic implication for fishery.

General conclusion

Global environmental change, led by the current dramatic rise in sea surface T and pCO_2, is expected to have a great impact on marine ecosystems and mainly on calcifying marine organisms. The symbiosis with zoxanthellae seemed to play one of key roles in determining the effect of OW and OA. In fact, the photosynthesis of zooxanthellae may be inhibited at high T, but may increase under high pCO_2, determining different response among species. Symbiont organisms seemed more sensitive to increasing T but more resistant to increase pCO_2 while the non-symbiont seemed behave on the contrary. The future oceans changes will lead increasing of both, T and pCO_2, and severely will affect most of marine species, zooxanthellate or not. There is a need to further investigate the ability of marine calcifying organisms to acclimatize and/or adapt to prolonged exposure of high T and pCO_2 together, as well as the possibility of taxonomic differences in sensitivity. Focusing efforts on the protection and cultivation of more adaptable species may improve the effectiveness of marine calcifying organisms preservation and restoration efforts.

References

Airi V, Prantoni S, Calegari M, Lisini Baldi V, Levy O, Falini G, Dubinsky Z, Goffredo S (2016) Reproductive output of a non-zooxanthellate Mediterranean coral is unaffected by temperature along an 850 km latitudinal gradient. Sci. Rep. *Submitted*.

Allemand D, Tambutté È, Zoccola D, Tambutté S (2011) Coral calcification, cells to reefs. In Coral reefs: and ecosystem in transition. Dubinsky Z, Stambler N (eds.) Springer: Dordrecht. 31 p.

Caroselli E, Prada F, Pasquini L, Marzano FN, Zaccanti F, Falini G, Levy O, Dubinsky Z, Goffredo S (2011) Environmental implications of skeletal micro-density and porosity variation in two scleractinian corals. Zoology. 114:255-264.

Caroselli E, Mattioli G, Levy O, Falini G, Dubinsky Z, Goffredo S (2012a) Inferred calcification rate of a Mediterranean azooxanthellate coral is uncoupled with sea surface temperature along an 8° latitudinal gradient. Front. Zool. 9:32.

Caroselli E, Zaccanti F, Mattioli G, Falini G, Levy O, Dubinsky Z, Goffredo S (2012b) Growth and demography of the solitary scleractinian coral *Leptopsammia pruvoti* along a sea surface temperature gradient in the Mediterranean Sea. PLoS ONE. 7:e37848.

Goffredo S, Caroselli E, Pignotti E, Mattioli G, Zaccanti F (2007) Variation in biometry and population density of solitary corals with solar radiation and sea surface temperature in the Mediterranean Sea. Mar. Biol. 152:351-361.

Goffredo S, Caroselli E, Mattioli G, Pignotti E, Zaccanti F (2008) Relationship between growth, population structure and sea surface temperature in the temperate solitary coral *Balanophillia europaea* (Scleractinia, Dendrophylliidae). Coral Reefs. 27:623-632.

Hoegh-Guldberg O, Cai R, Poloczanska ES, Brewer PG, Sundby S, Hilmi K, Fabry VJ, Jung S (2014) The Ocean. In: Climate Change 2014: Impacts, Adaptation, and Vulnerability. Part B: Regional Aspects. Contribution of Working Group II to the Fifth Assessment Report of the Intergovernmental Panel on Climate Change. Barros VR, Field CB, Dokken DJ, Mastrandrea MD, Mach KJ, Bilir TE, Chatterjee M, Ebi KL, Estrada YO, Genova RC, Girma B, Kissel ES, Levy AN, MacCracken S, Mastrandrea PR, White LL (eds.) Cambridge University Press, Cambridge, United Kingdom and New York, NY, USA. 76 p.

Leonard GH, Bertness MD, Yund PO (1999) Crab predation, waterborne cues, and inducible defenses in the blue mussel, *Mytilus edulis*. Ecology. 80:1-4.

Loya Y, Sakai K, Yamazato K, Nakano Y, Sambali H, Van Woesik R (2001) Coral bleaching: the winners and the losers. Ecol. Lett. 4:122-131.

Marchini C (2016) Reproduction and population structure in temperate and tropical corals in relation to environmental parameters. PhD thesis in Biodiversity end Evolution. University of Bologna, Italy.

Moschino V, Marin MG (2006) Seasonal changes in physiological responses and evaluation of "well-being" in the Venus clam *Chamelea gallina* from the Northern Adriatic Sea. Comp. Bioch. Physiol. 145A:433-440.

Muscatine L, McCloskey LR, Marian RE (1981) Estimating the daily contribution of carbon from zooxanthellae to coral animal respiration1. Oceanography. 26.

Muscatine L, Falkowski PG, Porter JW, Dubinsky Z (1984) Fate of photosynthetic fixed carbon in light-and shade-adapted colonies of the symbiotic coral *Stylophora pistillata*. Proc. R. Soc. Lond. B. 222:181-202.

Ramón M, Richardson CA (1992). Age determination and shell growth of *Chamelea gallina* (Bivalvia: Veneridae) in the western Mediterranean. Mar. Ecol. Prog. Ser. 89:15-23.

Zavatarelli M, Raicich F, Bregant D, Russo A, Artegiani A (1998) Climatological biogeochemical characteristics of the Adriatic Sea. J. Mar. Syst. 18:227-263.

Ziegler M, Roder CM, Büchel C, Voolstra CR (2014) Limits to physiological plasticity of the coral *Pocillopora verrucosa* from the central Red Sea. Coral Reefs. 33:1115-1129.

Acknowledgements

The majority of this research has been funded by the European Research Council under the European Union's Seventh Framework Programme (FP7/2007-2013) / ERC grant agreement n° 249930 – CoralWarm: Corals and global warming: the Mediterranean versus the Red Sea.

I would like to thank my supervisor Stefano Goffredo for all his advice and for encouraging me constantly to strive for improvement. I acknowledge Prof. Giuseppe Falini for helping me to rediscover the charm of chemistry. A special thanks to Prof. Christian Voolstra for his economic and intellectual support and for allowing me to carry out the research at the King Abdullah University of Science and Technology (KAUST). I would like to thank The Marine Science Group (www.marinesciencegroup.org) and Scientific Diving School (www.sdseducational.org) that supplied scientific, technical, logistical support and underwater activities. Thanks to M. Ghelia, M. Pisconti, A. Picariello, S. Guerrieri, F. Croci, F. Fasoli, F. Sesso, Centro Immersioni Pantelleria, Il Pesciolino, Bubble Lounge Diving, Eolo Sub and Submaldive for supplying logistic assistance in the field. Thanks to Gianni Neto and Francesco Sesso for the pictures. Thanks to all the people at Voolstra Lab, for helping me and supporting me during this period abroad. I would like to thank all the students that helped me during my Ph.D., in chronological order: Valentina, Luca, Ludovica, Maria Giulia, Ginevra and Francesco. I acknowledge all the staff at MSG, in particular Valentina for her support and advice during these years, Michela for sharing elements of her chemistry knowledge, Arianna for her “Fanese” support, Fiorella, always available to help out, Simone for his passion for smiles, Chiarina for making work fun, and many thanks to Erik, he knows why.
Most importantly, thanks to my super family for their endless support. I did it! Yo!